

**GHR SST**  
GROUP FOR HIGH RESOLUTION  
SEA SURFACE TEMPERATURE

# Proceedings

22<sup>nd</sup> international GHR SST Science Team Meeting

7-11 June 2021



Copyright 2021© Group for High Resolution Sea Surface Temperature (GHRST)

This copyright notice applies only to the overall collection of papers: authors retain their individual rights and should be contacted directly for permission to use their material separately. Editorial correspondence and requests for permission to publish, reproduce or translate this publication in part or in whole should be addressed to the GHRST Project Office. The papers included comprise the proceedings of the meeting and reflect the authors' opinions and are published as presented. Their inclusion in this publication does not necessarily constitute endorsement by GHRST or the co-organisers.



This report has been edited by the GHRST project office.

The GHRST Project Office is funded by the European Union Copernicus Programme and is hosted by the Danish Meteorological Institute, Lyngbyvej 100, 2100 Copenhagen (DK)

Follow us on Twitter: <https://twitter.com/ghrsst>

Website: <https://www.ghrsst.org/>

Zenodo: <https://zenodo.org/communities/ghrsst>

## Welcome to the 22nd GHRSSST Science Team meeting

Anne O'Carroll

---

Science Team Chair  
EUMETSAT

The 22<sup>nd</sup> International Science Team meeting of the Group for High Resolution Sea-Surface Temperature (GHRSSST XXII) was held online from 7 to 11 June 2021.

The provision of high quality SST data from a broad satellite constellation has continued, with particular advances towards the continuity of microwave SST with AMSR-3 planned for launch by JAXA in 2023/2024 on the Global Observation Satellite for Greenhouse gases and water cycle. An online meeting addressing Science to Operations was held for the Copernicus Imaging Microwave Radiometer (CIMR) mission planned for 2029, with contributions on bridging the gap between the scientific measurements made by the CIMR mission and preparation to operational services and scientific applications.

There are exciting times ahead with further launches of several Sea Surface Temperature capable and specific missions coming up in the next few years, all adding valuable observations to the constellation. These include GOES-T, JPSS-2, MTG I1, Metop-SG A1, Sentinel-3C/D, FY-3E, FY-4B, plus others.

We have an interesting agenda for the week covering sessions on *the Coastal margin and the Arctic; Spatio-temporal variation and extreme events; Calibration, validation and product assessment; Algorithms and Computing and Products*. Highlights include: *high-latitude SST progress; hearing about the retrieval of SST from INSAT 3D/3DR; validation and trends in Korean coastal waters; progress towards climate records of SST; analysis ready data applications; and the new release of NOAA STAR OceanView*.

There will be live discussions on the Task Teams progress with dedicated Zoom sessions each day, focusing on a few Task Teams at a time, supplemented by the Moodle forum and discussions. We will also have a dedicated session on GHRSSST priorities. This will address GHRSSST's user driven priorities as presented in our OceanObs19 white paper, covering: improving data quality in the Arctic, Improving coastal SST data quality; and improving SST feature resolution. We will also have a panel discussion on the needs of coupled ocean atmosphere NWP and how can GHRSSST respond to this. GHRSSST participated to last month's 2<sup>nd</sup> International Operational Satellite Oceanography Symposium (OSOS), where coupled model and Numerical Weather Prediction needs were considered. The third panel discussion will address further questions raised by the Science Team on considerations of machine learning and the promotion of open science and open data.

A change coming to GHRSSST this summer is that the GHRSSST Project Office, funded by the European Union's Copernicus programme, will be transitioning to the Danish Meteorological Institute in July 2021.

I hope you all have an enjoyable and productive meeting, and hope to see you all in person next year.

Have a great week!



## **Table of contents**

### **Welcome**

## **Science Session 1 - Challenging Regions: The Coastal Margin and The Arctic**

### **Oral presentations**

Introducing the ISRO-CNES TRISHNA mission for high resolution SST observations in coastal ocean and continental waters

SST at 70-m scale from ecostress on the space station: application to complex coasts and intertidal flats

Development of consistent surface temperature retrieval algorithms for the sea surface, marginal ice zone and sea ice in the Polar regions

Status and plans for the sea-ice concentration data records from the EUMETSAT OSI SAF and ESA CCI: possibilities for polar SST products

### **Poster presentations**

Ultra high-resolution SST from NASA ECOSTRESS resolves fine structure of upwelling zones

Validation of satellite sea surface temperatures and long-term trends in Korean coastal regions (1982–2018)

A CMEMS level 4 SST and IST climate data set for the Arctic

Using Saildrones to Validate Sea Surface Temperatures in the Arctic

## **Science Session 2 - Applying The Data: Spatio-temporal Variation, Extreme Events**

### **Oral presentations**

Detection and Characterisation of Marine Heat Waves in the Mediterranean Sea in the past 40 years

Deep Learning of Sea Surface Temperature Patterns to Identify Ocean Extremes

Instrument Noise, Retrieval Issues or Geophysical Signal?

Studying the thermal skin layer using thermofluorescent dyes

### **Poster presentations**

The NOAA STAR SOCD OceanView (OV): An application for integrated visualization of satellite, in situ, and model data & ocean events – the v1.0 release

The intermittency of Sea Surface Temperature: a global perspective

Is there a need for yet another model to account for SST diurnal variability?

Observations of Infrared SST Autonomous Radiometer (ISAR) Skin Temperatures in the Seas around Korean Peninsula, Indian Ocean, and Northwest Pacific

Revealing Fundamental SST Patterns with Deep Learning

## **Science Session 3 - Calibration, Validation and Product Assessment**

### **Oral presentations**

Uncertainty validation of shipborne radiometers

A completeness and complementarity analysis of the data sources in iQuam

Saharan dust effects on North Atlantic sea surface skin temperatures

Use of ESA CCI SST analysis to validate sampling and measurement error models for SST from ships

### **Poster presentations**

Evaluation of AIRS and CrIS SST measurements relative to three globally gridded SST products between 2013 and 2019

Assessment and intercomparison of NOAA Daily Optimum Interpolation Sea Surface Temperature (DOISST), version 2.1

Using SAILDRONE Campaigns to assess the accuracy of SST gradients in Level 2 SST datasets

EUMETSAT SLSTR SST multi-mission matchup database: ongoing work, TRUSTED MDB and evolutions

Validation of SGLI SST

## **Science Session 4 - Algorithms**

### **Oral presentations**

Optimal Estimation of SST from INSAT-3D/3DR Imagers

A New Operational Mediterranean Diurnal Optimally Interpolated SST Product within the Copernicus Marine Service

Bias-aware optimal estimation for sea surface temperatures from historic AVHRRs

Developments towards a 40-year climate data record from the ESA Climate Change Initiative

### **Poster presentations**

Open source algorithms for AMSR3

Historical and Near-real Time SST retrievals from Metop AVHRR FRAC with ACSPO 1

USE of ERA-5 Sea Surface Temperature Fields as prior in Optimal Estimation retrieval of SST from MODIS

Towards Improved ACSPO Clear-Sky Mask for SST from Geostationary Satellites

Bayesian Cloud Detection Scheme improvements for the SLSTR instrument

## **Science Session 5 - Computing and Products**

### **Oral presentations**

Science Storms the Cloud

Analysis Ready Data applications for GHRSSST and related data

PODAAC milestone: GHRSSST data migrating to AWS Cloud

The Sea Surface Temperature analysis in the NCEP GFS and the future NCEP UFS

First Evaluation of the Diurnal Cycle in the ACSPO Global Super-Collated SST from Low Earth Orbiting Satellites (L3S-LEO)

### **Poster presentations**

Towards ACSPO Super-Collated Gridded SST Product from Multiple Geostationary Satellites (L3S-GEO)

Use of ESA SST CCI data in HadISST2

Himawari-8 and Multi-sensor sea surface temperature products and their applications

Recent Updates Of CMC SST Analysis

Copernicus Sentinel-3 SLSTR Sea (and sea-Ice) Surface Temperature: product status, evolutions and projects

Updates of AMSR3 on GOSAT-GW and its Ocean Products

Presenting a new high-resolution Climate Data Record product

S5-P8-ID-007 - Filtering cold outliers in NOAA AVHRR SST for ACSPO GAC RAN2

## **Agency news**

## **GHRSSST connections with CEOS SST-VC**

## **GHRSSST Priorities**

## **Task Team Reporting**

Climate Data Assessment Framework

GHRSSST MDB

Feature Resolution

Shipborne Radiometry

Cloud masking

SSES and L4  
High Latitude SST

Climatology and L4 Intercomparison

Coral Heat Stress User SST Requirements

HRSST for Satellite SST

Regional and Global Task Sharing

### **Closing Session**

### **APPENDICES**

Agenda

List of participants

Group photo

Science team members 2021-22

Credits pictures

## SCIENCE SESSION 1

# CHALLENGING REGIONS: THE COASTAL MARGIN AND THE ARCTIC



## S1 – SESSION REPORT

**Chair: Andy Harris<sup>(1)</sup>, Rapporteur: Steinar Eastwood<sup>(2)</sup>**

(1) NOAA-CISESS, University of Maryland, College Park, MD, USA, Email: [andy.harris@noaa.gov](mailto:andy.harris@noaa.gov)

(2) Norwegian Meteorological Institute, Oslo, Norway, Email: [steinare@met.no](mailto:steinare@met.no)

## HIGHLIGHTS

- New ISRO/CNES TRISHNA mission for coastal/continental waters
- New Sea Ice Concentration (SIC) data records from EUMETSAT OSI-SAF and ESA CCI
- 70m SST retrievals from ECOSTRESS onboard the ISS

## INTRODUCTION

The first science session was dedicated to challenging regions of the world for SST retrieval and analysis, with particular focus on coastal regions and the Arctic. Coasts are challenging due to close proximity to land, turbidity, tidal motion / mixing and high gradients. All of these effects make for highly variable observing conditions that are often outside of those encountered in the open ocean. Another difficulty is the relative lack of in situ data for both algorithm training and validation purposes. Many of these issues are also present in Arctic waters, along with conditions of perpetual night during winter, and perpetual daylight during summer. The growth and retreat of sea ice presents further challenges. Firstly, the ice edge is seldom “clean”, and yet knowledge of temperatures in the marginal ice zone is highly desired in order to predict growth/decay of sea ice. Furthermore, the inability to observe the temperature directly requires a proxy estimate of ocean temperature, which is often parameterized in terms of salinity and ice concentration. Finally, retrieval conditions in the Arctic in particular are usually an extrapolation beyond those of normal the typical ocean-atmosphere.

The session consisted of 4 pre-recorded oral presentations, along with 4 presentations in poster format. All presentations were available for viewing throughout the week of the meeting, and discussions were facilitated via Moodle forums.

## RESOURCES

- View presentations (recordings): <https://training.eumetsat.int/mod/url/view.php?id=14059>
- Discussion forum for recordings: <https://training.eumetsat.int/mod/forum/view.php?id=14060>
- Download the slides: <https://training.eumetsat.int/mod/folder/view.php?id=14061>
- Posters padlet: <https://padlet.com/TrainingEUMETSAT/e4plfma88e4a1t>

## **ORAL PRESENTATIONS**

**Jacob Høyer\*, Gorm Dybkjær, Anne o'Carroll, Wiebke Kolbe, Pia Nielsen-Englyst - development of consistent surface temperature retrieval algorithms for the sea surface, marginal ice zone and sea ice in the polar regions**

The presentation argued the importance of having consistent sst/ist products in the polar regions. Recent developments in this field were shown, including a l2 ist prototype for sentinel 3 slstr data, and a gap-free arctic level 4 sst/ist reanalysis. The presentation also illustrated the difficulties in getting good reference measurements of ist. Regarding the l2 slstr ist product, results from 2 different algorithms (simple split-window and dual-view single-channel) were presented, with validation results being inconclusive (the dual-view performed better over sea-ice, but the split-window showed more promise around the margins of the greenland ice sheet). The biggest challenge, however, remains the automated cloud screening process, which is significantly more challenging over ice than open water. A l4 sst/ist analysis spanning 1982-2019 has been generated from a combination of cci/c3s, aasti sst/ist cdr v2, and operational datasets. The temperature anomalies above 60n from this "interim" dataset show a striking temporal trend (figure 1), and a more thorough reprocessing with cdr-quality inputs should be even more compelling.

The discussion touched upon several issues with ist products. It was agreed that a combined sst/ist product is useful, although perhaps outside of the current GHRSSST remit. Users also would like it for the antarctic. Ist varies more than sst, both spatially and temporally, and this was discussed in terms of validation. Again, availability of ist validation data was discussed and if validation can be done in the antarctic as well. Validation data also influences the selection of algorithm formalism, since there is not sufficient good validation data available for good comparison. It should also be possible to encode ist products as close as possible to the gds standard, which will be further iterated on.

**Emmanuelle Autret\* - introducing the isro-cnes trishna mission for high resolution sst observations in coastal ocean and continental waters**

Details of the joint CNES-ISRO TRISHNA mission were presented. It can be considered a precursor to the ESA LSTM (currently planned for 2028 launch). The instrument will provide 60m resolution SST observations in coastal and continental waters, as well as other parameters, from 2024. The possibilities and scientific challenges that such fine resolution will provide were presented, in addition to the other parameters. The relatively wide swath (1030 km) for such a high-resolution sensor provides quite a high revisit frequency (Figure 2). For illustrations of the capabilities and applications of a ~similar sensor already in orbit, see the presentation by David Wethey on the ISS ECOSTRESS instrument.

The discussion was about technical issues such as the noise level and accuracy of this exciting new mission. It should be noted that, due to the relatively narrow width of the TIR spectral channels, all 4 may be used for SST retrieval. There was also discussion on how far from the coast the high resolution data will be available. The instrument will operate in high resolution mode typically 100km from the coast, but the details on this are still TBD. As an example, the Great Barrier Reef is up to 160km from the coast.

**Thomas Lavergne\*, Atle Sørensen, Jacob Høyer, Pia Nielsen-Englyst, Gorm Dybkjær, Rasmus Tonboe and Steinar Eastwood - Status and Plans for the Sea-Ice Concentration Data Records from the EUMETSAT OSI SAF and ESA CCI: Possibilities For Polar SST Products**

The sea ice concentration data records from EUMETSAT OSI SAF and ESA CCI were presented. The focus was on how to achieve the best consistency between sea ice and SST when using sea ice products to filter out sea ice in SST retrieval. The four primary characteristics of the sea ice products that are important to get the best consistency were presented, namely spatial resolution, accuracy at open water concentration range, open water filters (a.k.a. weather filters) and land spill-over effects. In addition, the summary performance characteristics of a wide variety of SIC algorithms were shown. The use of SST as a flag/predictor for screening of sea ice in the open ocean (3 Celsius) was demonstrated, raising the prospect of an interesting interdependence, since SIC is used as a flag for SST processing. Another revealing plot showed the stability of various SIC products at low ice concentration across the timeline of sensors (SMMR, SSMI, SSMI/S, see Figure 3).

During the discussion the issue of filtering in the sea ice concentration products, both in climate data records and near real time products was elaborated. Some products are filtered differently and the users would like to know these details. Also the issue of physical concentration is restricted to the range 0-100%, while some expert users use the available uncut values from the retrieval algorithm to get the uncertainties correct.

**David S Wetthey\*, Nicolás F Weidberg, Sarah A Woodin - SST at 70-m scale from ECOSTRESS on the Space Station: Application to Complex Coasts and Intertidal Flats**

The available 70m resolution SST data from the ECOSTRESS instrument onboard the International Space Station was presented, with focus on the application in areas with complex coasts and intertidal flats. The capability of the Ecostress instrument in comparison with MODIS and VIIRS in coastal areas was shown (see Figure 4), and how this makes it possible to do detailed monitoring of ECOSTRESS on, for example, shellfish beds. Examples of how detailed changes in tidal regions can be monitored were shown. Validation results and calibration issues was presented, including a ~1 K cold bias in the SSTs and the effects of residual cloud (and land) contamination.

The discussion showed a large interest for these data. The issue on how the algorithms were set up for varying surfaces were discussed, and how the validation was done. Then potential for using the high resolution ECOSTRESS data together with the "standard" 1 km data was also discussed. The bias in the validation results gave a detailed discussion on the calibration of the instrument. Good suggestions for possible cause of the problem were presented and elaborated. The author noted that the retrieved emissivity in the NASA product appeared to be erroneous (too low). It was pointed out that this in itself cannot be the cause of the cold bias in retrieved SST, since that would require emissivity to be too high. This confirms the likelihood of calibration as the primary cause, and GHRSSST ST calibration experts have offered their assistance. The utility of SST validation to confirm instrument calibration and characterization is important because it can feed into other products (e.g. land surface temperature) that are much harder to validate.

## **POSTER PRESENTATIONS**

**Nicolás F Weidberg, Sarah A Woodin, SST at 70-m scale from ECOSTRESS on the Space Station: Application to Complex Coasts and Intertidal Flats**

This poster gave more examples of the fine structures that can be observed with the ECOSTRESS ultra high-resolution SST product, in comparison with VIIRS (Figure 5). There were also further illustrations of the underestimation of SST in the ECOSTRESS product, with a bias of ~1C.

Much of the discussion was on validation of such fine scale products, with the possibility of using Saildrone or shipborne observations that typically sample each minute. There were also questions about availability of the ECOSTRESS product, which is not yet publicly available.

**Pia Englyst, Jacob L. Høyer, Wiebke M. Kolbe, Gorm Dybkjær, Thomas Lavergne, A CMEMS level 4 SST and IST climate data set for the Arctic**

This poster presented details on the level 4 SST and IST climate data record for the Arctic from CMEMS. Input data, how consistency and filtering (see Figure 6) is done, and how the product validates were all described.

The discussion revealed interest for a similar product in the Antarctic, which is yet not planned. There was also discussion on how the IST values could be used/assimilated in NWP coupled models.

**Kyung-Ae Park and Eun-Young Lee, Validation of satellite sea surface temperatures and long-term trends in Korean coastal regions**

This poster presented work done on validating the OISST record in the coastal regions around the Korean Peninsula, where there is a network of both moored buoys and regular oceanic transects. The data set was also compare long-term trends from OISST and in situ, as well as intrinsic accuracy of OISST.

RMS values of OISST against moored buoys varied between 0.75 K and 2 K, with biases ranging from -0.5 K to +1.3 K (Figure 7). Comparisons against ship transects showed similar patterns. Distinct regimes in differences in temporal warming trends between in situ and OISST were also observed, with the East/Japan Sea showing a positive trend w.r.t. proximity to the coast, while the Yellow Sea displayed the opposite trend.

**Jorge Vazquez, Mike Chin, Ed Armstrong and Chelle Gentemann, Using Saildrones to Validate Sea Surface Temperatures in the Arctic**

This poster presented from a NASA Saildrone cruise (that deployed in the Arctic in 2019, with a focus on using these data to validate eight GHRSSST L4 SST products (GMPE, DOISST, MUR, REMSS, OSTIA, DMI, CMC, NAVO-K10). Taylor diagrams (see Figure 8) compared the eight analyses vs SBE37 and Wing temperatures showed reasonable correlations (around ~0.95 for most analyses vs the Sea Bird), with slightly less variability than the Saildrone, which occasionally displayed substantial variability on the short time/length scales. Salinity changes due to the Yukon River discharge are observed in both the Saildrone CTD data and corresponding SMAP product.

The discussion was on the details in the comparisons; why some data was missing (possibly land or ice contamination) and on interpretation of the spectral plots.

Figures and Tables

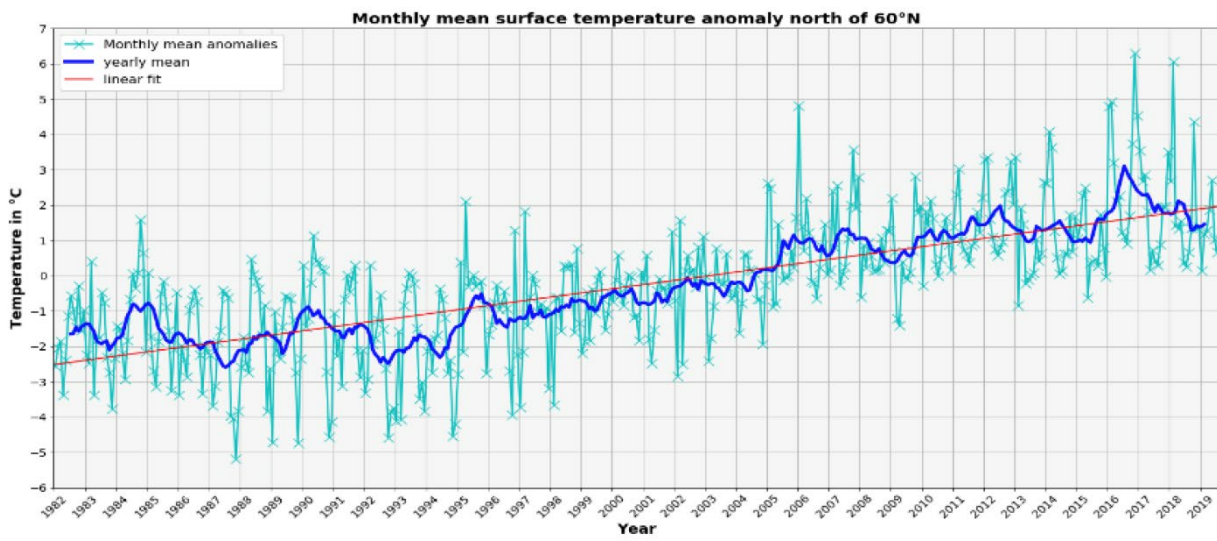


Figure 1: Temperature anomalies above 60°N from the new L4 combined SST/IST analysis (1982-2019)

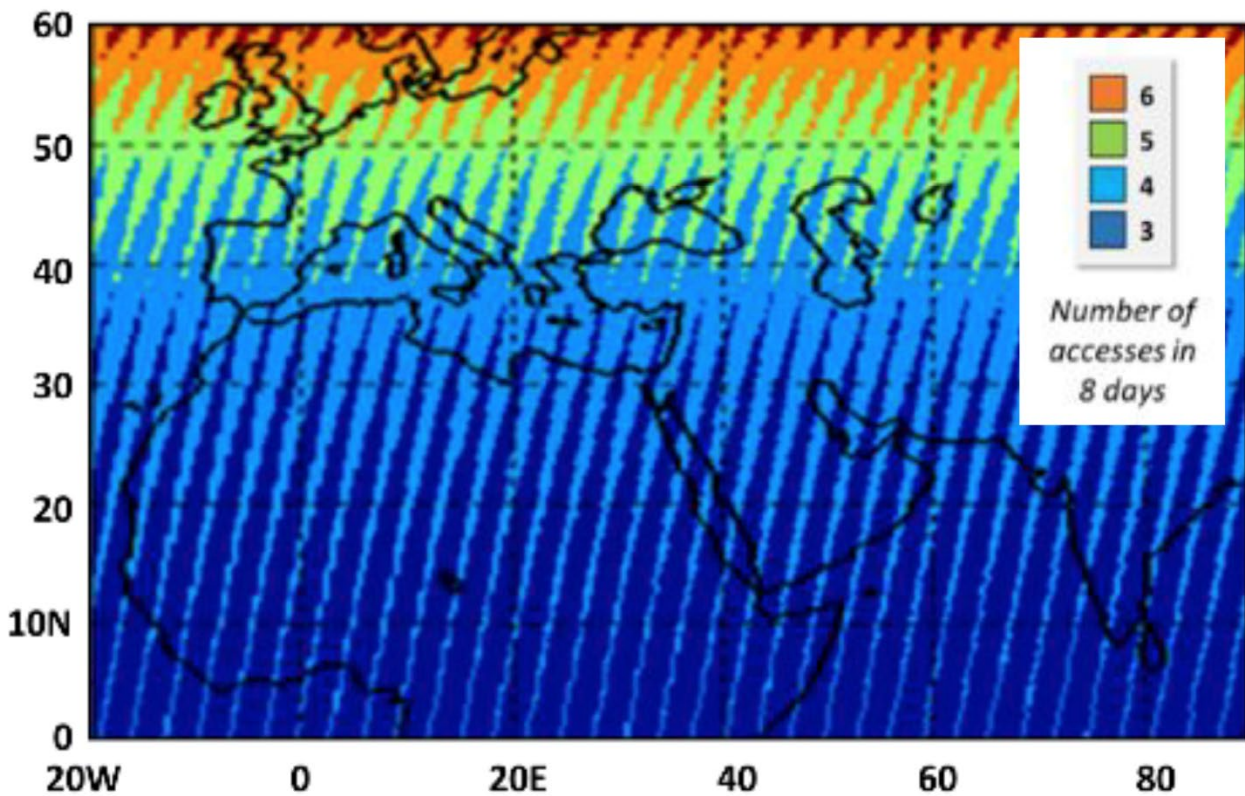


Figure 2: TRISHNA revisit frequency

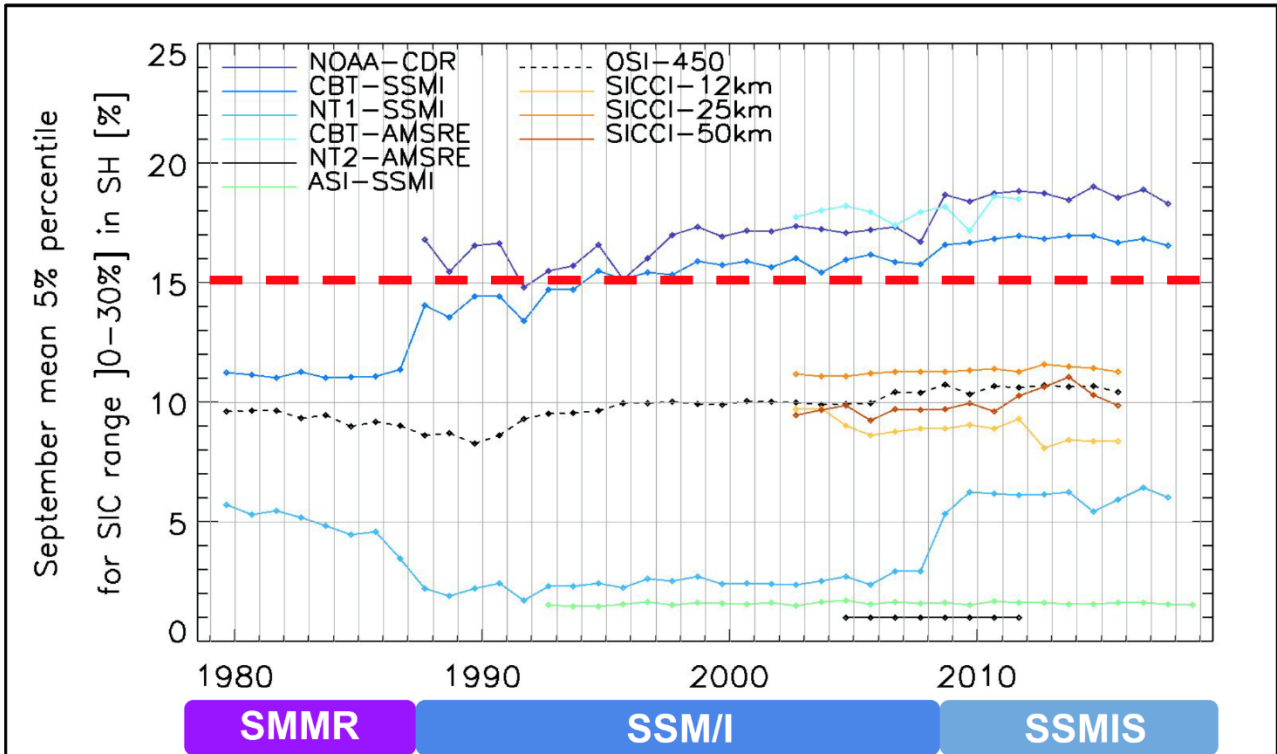
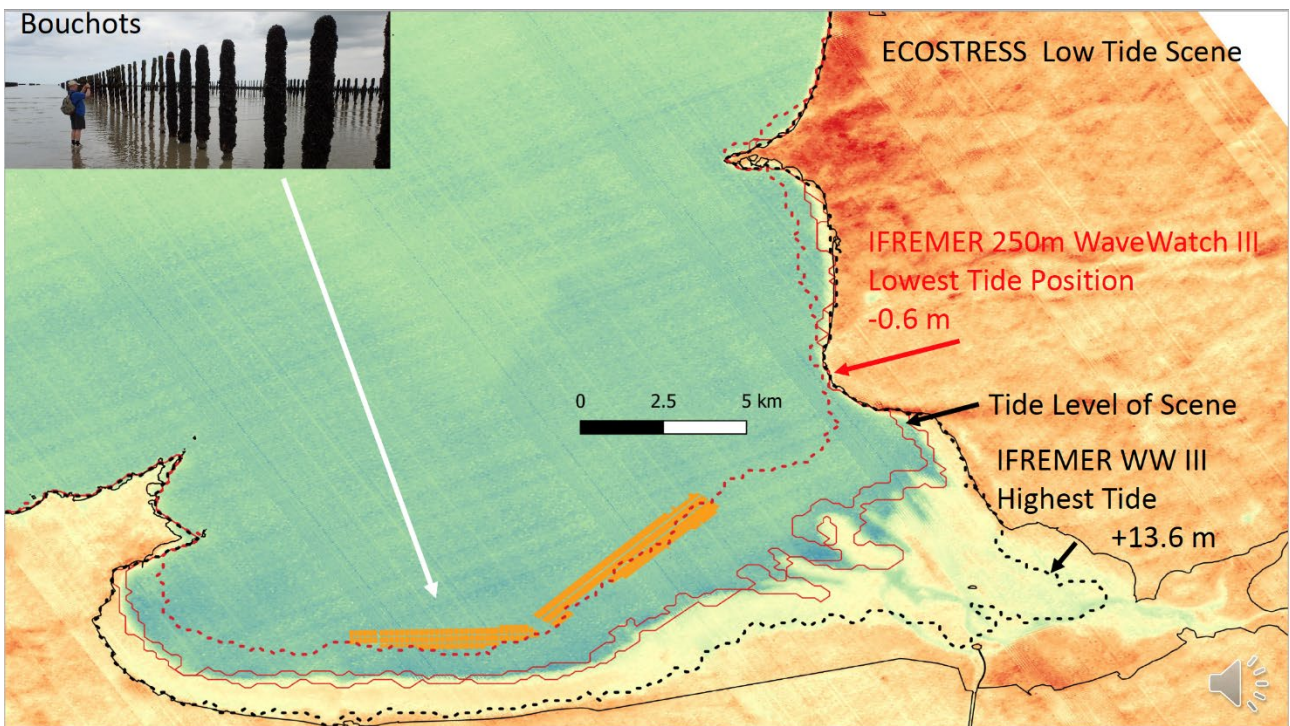


Figure 3: SIC low concentration product consistency across various PMR missions



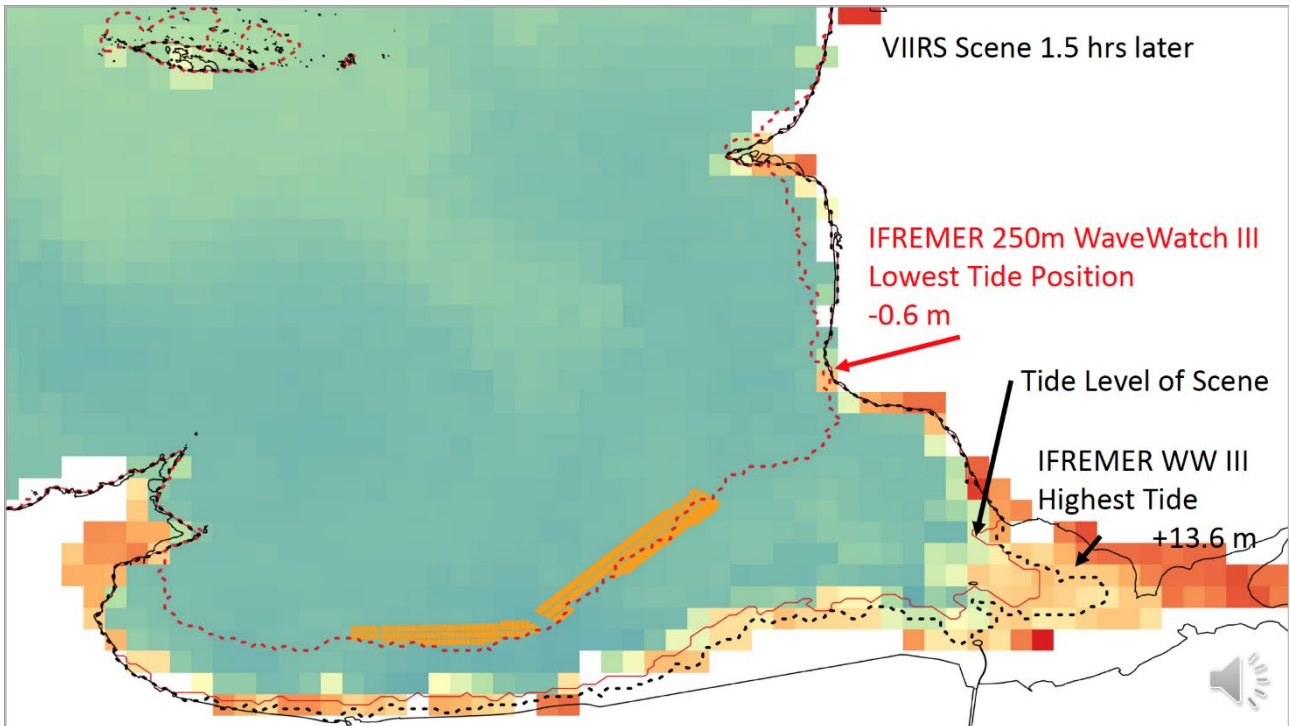


Figure 4: Mont Saint Michel Bay and mussel beds from ECOSTRESS (top) and VIIRS (bottom)

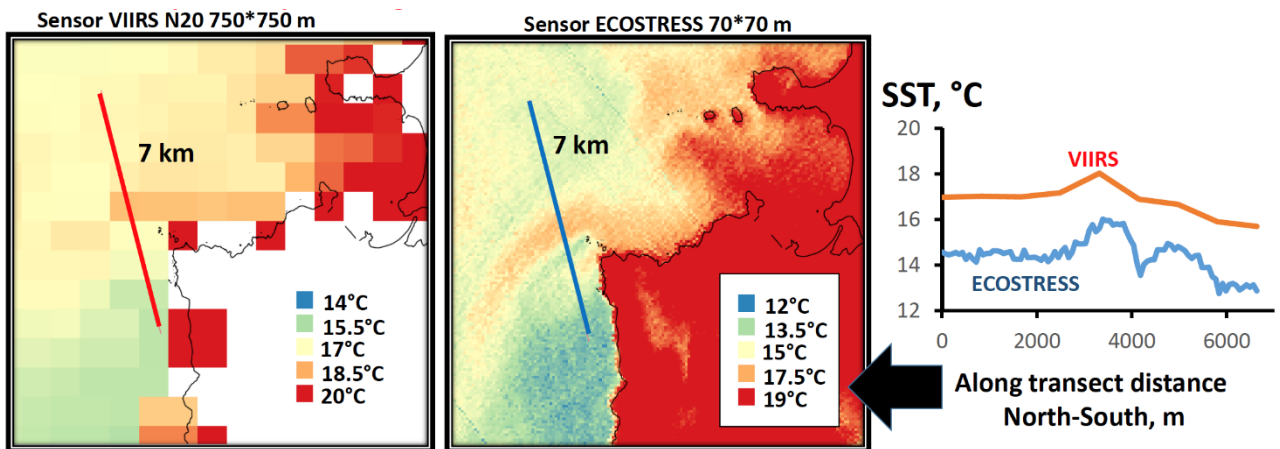
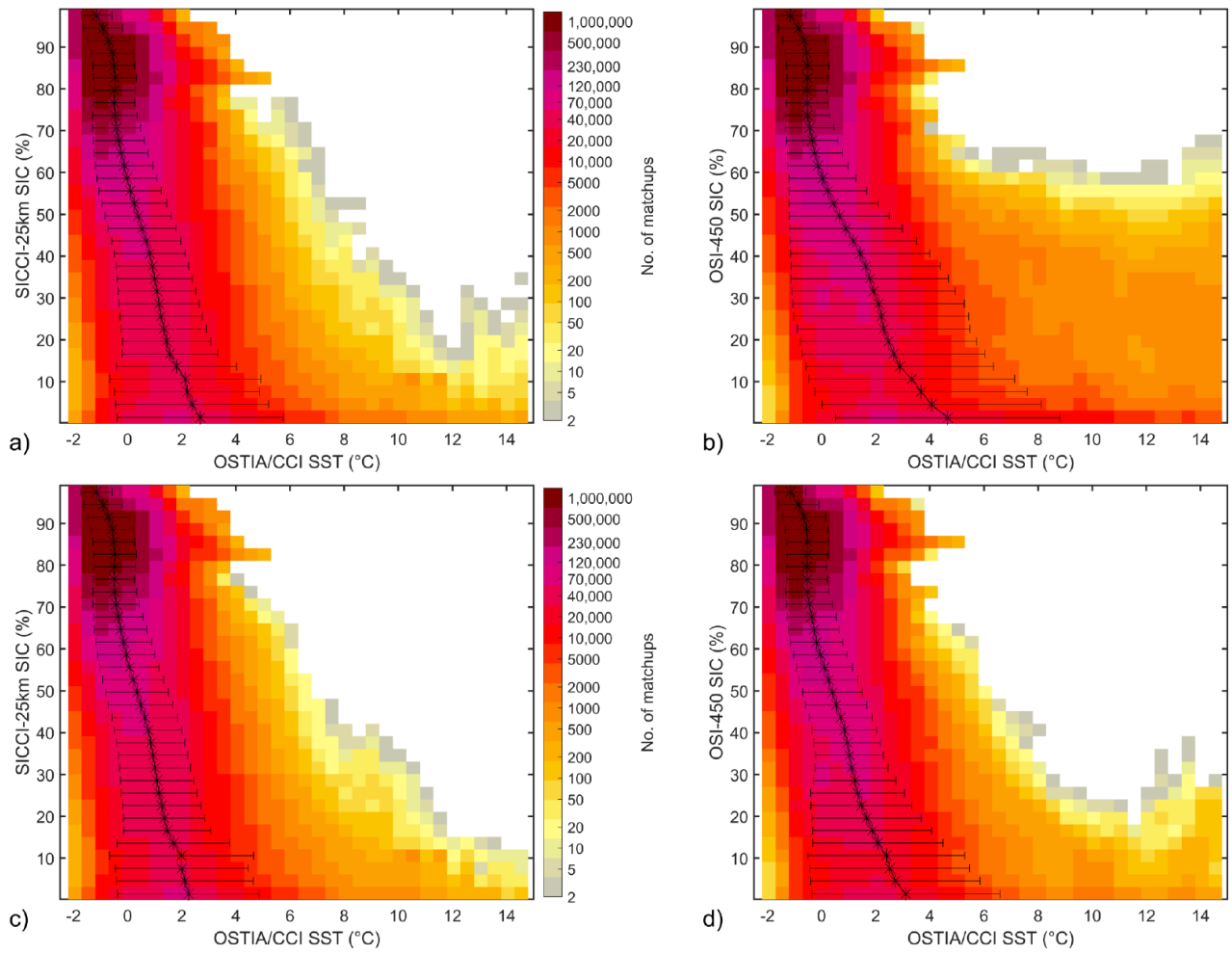


Figure 5: VIIRS and ECOSTRESS comparison for NW Spain: Upwelling shadow front (07/24/20). N.B. the temperature range of the colour scale is different for the images from each sensor. Also, note lower temperatures in ECOSTRESS data for N/S transect.



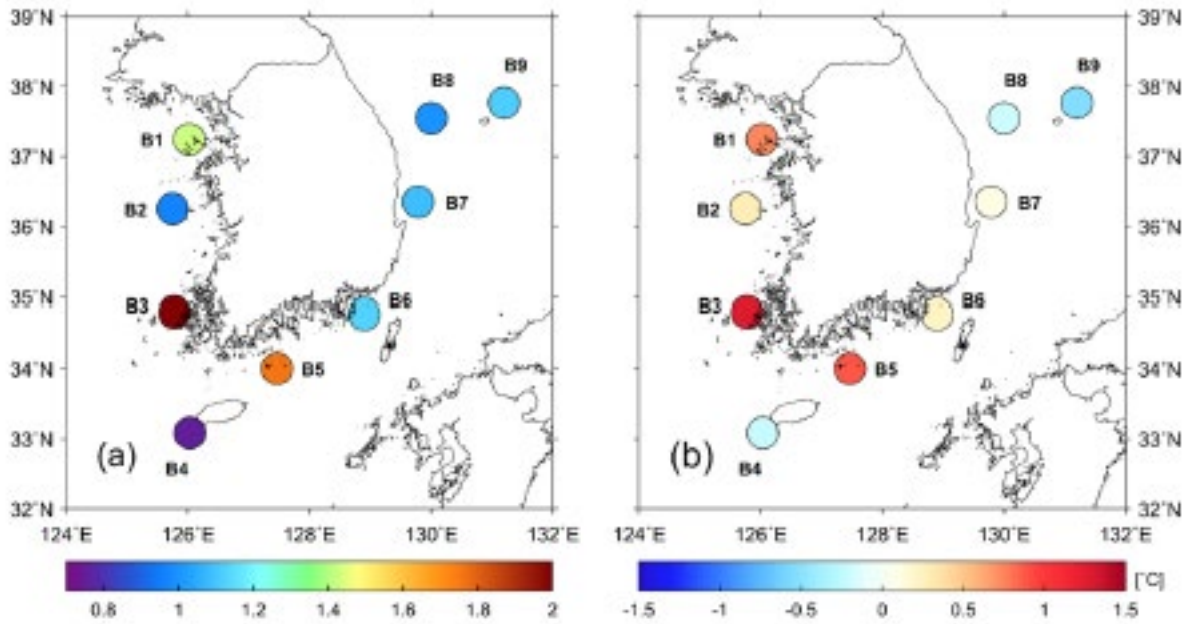


Figure 7: Comparison between satellite SST and in-situ KMA buoy SST for each buoy station of KMA, where the color represents (a) RMSE and (b) bias error.

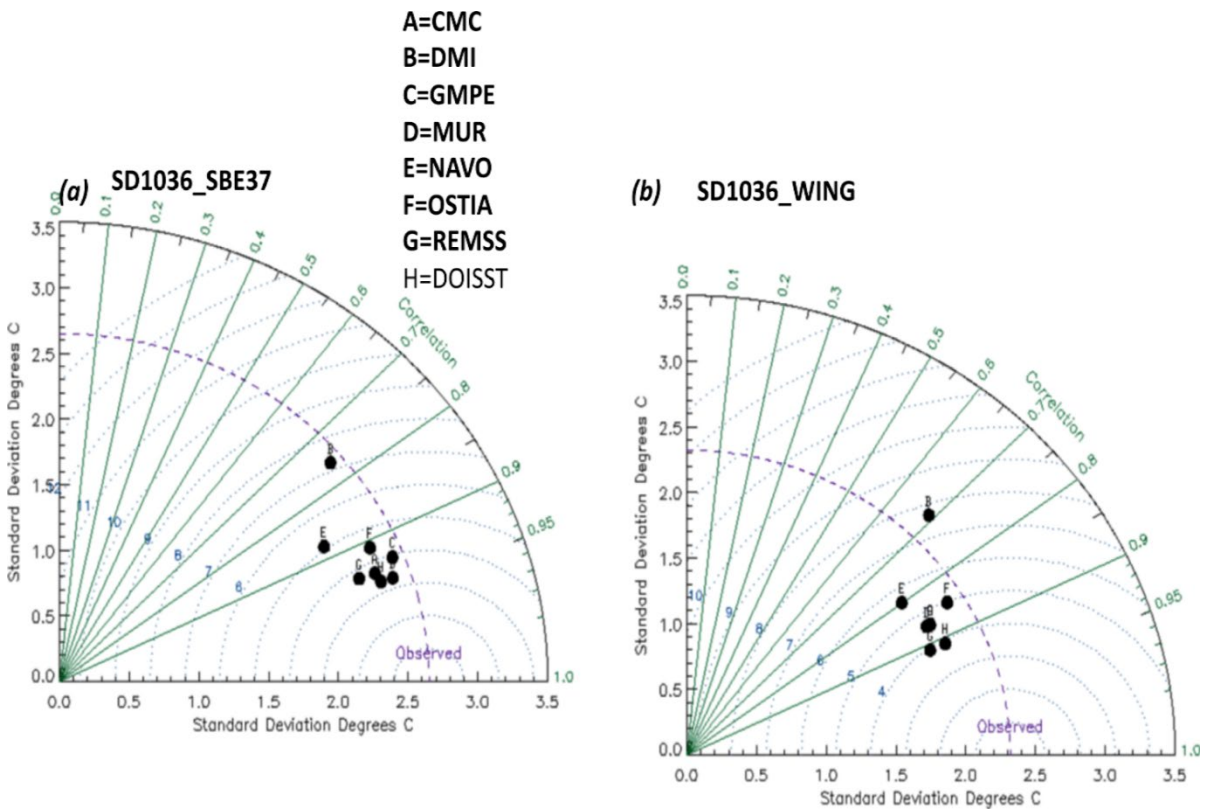


Figure 8: Taylor Diagrams for the SBE CTD and Wingfor Saldrone SD1036 deployment and the 8GHRSSST Level 4 products

## **S1 - ORAL PRESENTATIONS - ABSTRACTS**

## **S1-1: INTRODUCING THE ISRO-CNES TRISHNA MISSION FOR HIGH RESOLUTION SST OBSERVATIONS IN COASTAL OCEAN AND CONTINENTAL WATERS**

**Autret E.<sup>(1)</sup>, Saux-Picart S.<sup>(2)</sup>, Dadou I.<sup>(3)</sup>, Laignel B.<sup>(4)</sup>, Jardani A.<sup>(4)</sup>, Van Beek P.<sup>(3)</sup>, Flipo N.<sup>(5)</sup>, Rejiba F.<sup>(3)</sup>, Léger E.<sup>(6)</sup>, Tormos T.<sup>(7)</sup>, Lifferman A.<sup>(8)</sup>, Roujean J. L.<sup>(9)</sup>, Bhattacharya B.<sup>(10)</sup>, Gamet P.<sup>(8)</sup>, Maisongrande P.<sup>(8)</sup>**

(1) Ifremer, Univ. Brest, CNRS, IRD, Laboratoire d'Océanographie Physique et Spatiale (LOPS), IUEM, Brest, France,

(2) CNRM UMR3589, Météo-France – CNRS, Centre d'Etudes en Météorologie Satellitaire, France,

(3) LEGOS UMR 5566 Toulouse, France,

(4) UMR 6143 Morphodynamique Continentale et Côtière (M2C), Univ. Rouen Normandie,

(5) MINES ParisTech, PSL Université, Systèmes Hydrologiques et Réservoirs, Centre de Géosciences, Paris,

(6) Géosciences Univ. Paris Saclay, Orsay, France,

(7) Office Français pour la biodiversité, ECLA, Paris, France,

(8) CNES, Toulouse, France,

(9) CESBIO, France,

(10) ISRO/SAC, India

The TRISHNA mission (Thermal infraRed Imaging Satellite for High-resolution Natural resource Assessment) is a cooperation between the French (CNES) and Indian (ISRO) space agencies. It will measure the optical and thermal spectra emitted and reflected by the Earth from a low-altitude Sun synchronous orbit, over a swath with a width of 1026 km. It is intended to measure approximately twice a week the thermal infrared signal of the surface-atmosphere system at 57 m resolution for the continents and the coastal ocean, and a resolution of 1000 meters over deep ocean. The primary scientific objectives of the mission will be to provide high-quality imagery of vegetation, snow, ice and sea surface temperature and albedo. In coastal areas, the deep interactions between the ocean, the atmosphere and the land generate a strong variability in the surface temperature at very fine scales. It is therefore interesting to measure the temperature of the water at the surface with high spatial and temporal precision, as this information can have several uses. Thermal imaging with high spatial resolution and frequent observation, including night-time acquisitions will bring key information on sea surface temperatures, sub-mesoscale activity in coastal areas and in the high seas, continental waters (lakes and rivers) as well as oil spills, thermal pollutants, effluents and wastewater discharges.

## **S1-2: SST AT 70-M SCALE FROM ECOSTRESS ON THE SPACE STATION: APPLICATION TO COMPLEX COASTS AND INTERTIDAL FLATS**

**Wethey, David S.<sup>(1)</sup>, Weidberg, Nicolás F.<sup>(1,2)</sup>, Woodin, Sarah A.<sup>(3)</sup>**

(1) Dept Biological Sciences, Univ South Carolina, Columbia, SC, USA, Email: [wethey@biol.sc.edu](mailto:wethey@biol.sc.edu)

(2) Dept Ecología e Biología Animal, Universidade de Vigo, Vigo, Spain, Email: [j.weidberg@hotmail.com](mailto:j.weidberg@hotmail.com)

(3) Dept Biological Sciences, Univ South Carolina, Columbia, SC, USA, Email: [woodin@biol.sc.edu](mailto:woodin@biol.sc.edu)

### **Introduction**

The ECOSTRESS instrument on the International Space Station (ISS) has 3 spectral infrared bands centred on 8.78  $\mu\text{m}$ , 10.49  $\mu\text{m}$ , and 12.09  $\mu\text{m}$ . It acquires a cross-track swath approximately 400 km wide. The instrument has 2 black bodies at 20°C and 46°C which are used to calibrate the sensor radiances on every rotation of the two-sided scan mirror. Because of the inclination of the ISS orbit, it captures scenes between 51°N and 51°S, revisit intervals are subdaily to 5 day, and overpass times vary throughout the day.

ECOSTRESS surface temperature (Hook & Hulley 2019) is retrieved with a Temperature Emissivity Separation (TES) algorithm (Hook et al. 2020). We carried out an in-flight validation of ECOSTRESS surface temperatures over the ocean with quality controlled data from the NOAA in-situ SST Quality Monitor (iQuam, Xu & Ignatov 2013), and with collocated GHRSSST Level-2 SST from VIIRS on NOAA-20 and instruments on geostationary satellites (ABI on GOES-16 and 17, AH1 on Himawari-8, SEVIRI on MSG-1 and MSG-4).

The 70-m pixel scale of ECOSTRESS has the potential to resolve both surface temperature of aeri ally exposed intertidal surfaces as well as SST in adjacent submerged areas. We examined small scale spatial and tidal variation in surface temperature on intertidal flats with 3-10 m tidal ranges to determine the utility of the data in this dynamic region where land and tidal contamination of larger scale pixels is a serious problem.

### **Methods**

#### **Matchups**

Triple collocations (e.g. Xu & Ignatov 2016) paired single ECOSTRESS pixels to NOAA iQuam observations and to single Level-2 GHRSSST SST clear sky pixels from geostationary satellites. The ECOSTRESS-iQuam matchups were within 30 min and 100 m and the ECOSTRESS-geostationary matchups within 30 min and 1.5 km. All triple clear sky collocations over the period 2018-12-01 to 2021-02-28 were used.

For whole-scene matchups, we used ECOSTRESS observations centred on Level-2 GHRSSST VIIRS SSTsubskin observations collected within 90 minutes of the VIIRS scene.

#### **ECOSTRESS Bias Analysis**

ECOSTRESS SST Bias was calculated as ECOSTRESS LST – Reference SST. Bias was calculated relative to iQuam and geostationary triple collocations, and relative to whole-scene collocations with VIIRS on NOAA-20.

ECOSTRESS IR channel brightness temperatures were calculated from L1B calibrated channel radiances (Hook et al. 2019) using the instrument brightness temperature lookup tables (Krehbiel 2020). IR channel brightness temperatures from the geostationary satellites were obtained from the L2 GHRSSST data files for GOES-16, GOES-17 (ABI sensor) and Himawari-8 (AH1 sensor).

Radiative transfer modelling of channel brightness temperatures was carried out with RTTOV 12.3 (Hocking et al. 2019), using the iQuam observation as the surface temperature, and using ECMWF ERA-5 hourly 0.25° reanalysis data for vertical profiles of temperature and specific humidity and surface temperature, specific humidity and wind speed, all bilinearly interpolated in space to the iQuam coordinates, and linearly interpolated in time to the ECOSTRESS scene time. The K (Jacobian) model was used to calculate atmospheric absorption and at-sensor brightness temperatures, in conjunction with RTTOV coefficient files for ECOSTRESS and the geostationary satellite instruments.

Observation-Model brightness temperature double differences (Liang & Ignatov 2011) were calculated by comparing ECOSTRESS Observation-Model bias to Geostationary ABI/AHI Observation-Model bias.

### Spatial variation in SST in coastal regions

The spatial distribution of surface temperature (LST and SST) on tidal flats was compared to the position of the water line in Mont Saint Michel Bay, France (tidal range 10 m). Water line position in Mont Saint Michel Bay was retrieved from the MARC 200 m Wave Watch III model (IFREMER 2020).

## Results

### Bias analysis

The mean ECOSTRESS bias relative to VIIRS was  $-1.02$  K (SD 0.67). The mean ECOSTRESS bias relative to iQuam was  $-1.04$ °K (SD 2.34) during the day and  $-1.08$  (SD 2.75) at night (Figure 1).

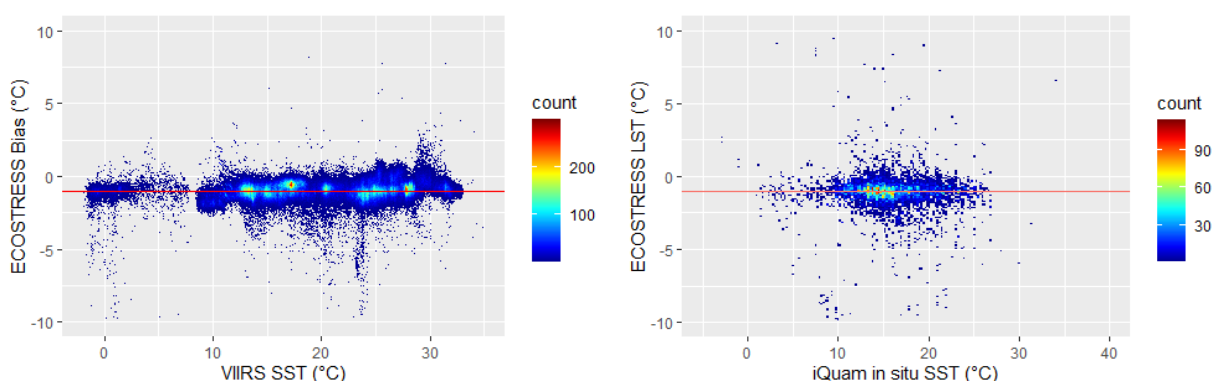


Figure 1. Left Panel: ECOSTRESS bias plotted against VIIRS SST. Right panel: ECOSTRESS bias plotted against iQuam SST. Colors are numbers of observations, scale on right. Horizontal red line is through mean bias.

Double differences of Observation-RTTOV radiance transfer model brightness temperatures indicate that the ECOSTRESS instrument is as temporally stable as the ABI sensors on geostationary satellites, but that the ECOSTRESS brightness temperatures are lower than the ABI brightness temperatures relative to RTTOV (Figure 2).

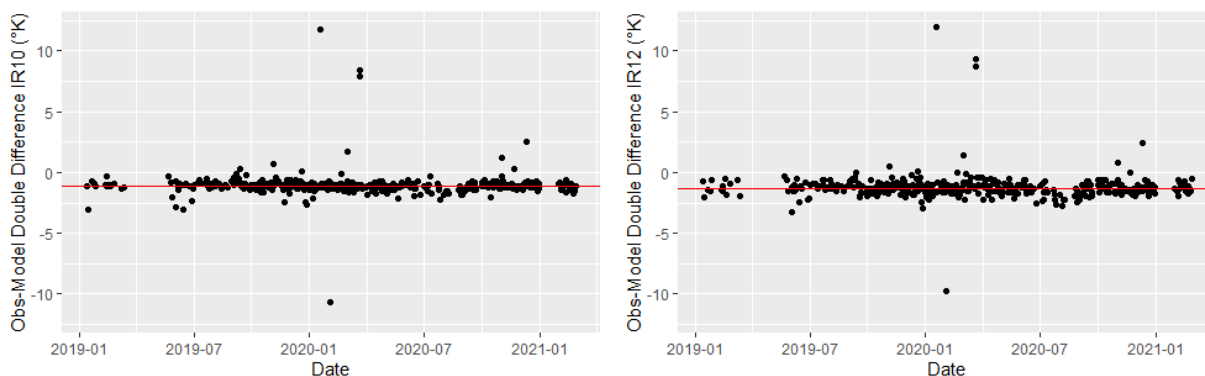


Figure 2: Double difference of Observation-Model bias, comparing ECOSTRESS to ABI sensors from Jan 2019 through Feb 2021. Left panel: ECOSTRESS  $10.49$   $\mu$ m BT versus ABI  $10.33$   $\mu$ m BT (mean =  $-1.077$ °K). Right panel: ECOSTRESS  $12.09$   $\mu$ m versus ABI  $12.26$   $\mu$ m BT (mean =  $-1.340$ °K). Horizontal red lines through means.

There was no evidence of increasing bias at temperatures below that of the cold black body on ECOSTRESS (20°C). Most SSTs in the iQuam dataset are below 20°C (Fig 1), and the linear calibration of the sensor radiances relative to the black bodies could lead to errors in this range.

### Spatial variation in SST in coastal regions

Sharp temperature discontinuities on intertidal surfaces in ECOSTRESS surface temperature images have the potential for resolving the position of the tide line. The temperature discontinuity maps very close to the predicted tide position on the flats at Mont Saint Michel Bay at tide stages from low water on spring low tides (0.31 m) to high water on spring high tides (11.26 m) (Figure 3).

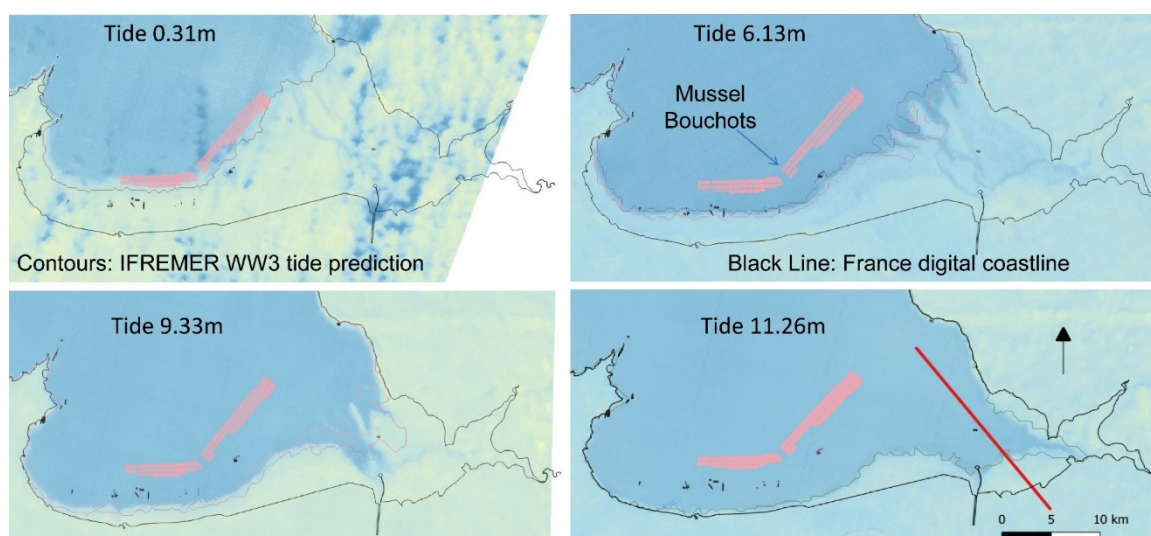


Figure 3: ECOSTRESS images of Mont Saint Michel Bay, France at different stages of the tide. Contour lines indicate the predicted tide position (IFREMER 2020), black line is France digital coastline, tide levels indicated.

Because ECOSTRESS surface temperatures include both water and land, the instrument can resolve thermal gradients during low tide. The higher spatial resolution of ECOSTRESS results in far less land contamination than VIIRS in regions with intertidal flats and complex coastlines (Figure 4). In the ECOSTRESS image, the temperature gradient from the high to low tide marks is 8°C (Figure 4), a gradient not resolved at all in the simultaneous VIIRS image.

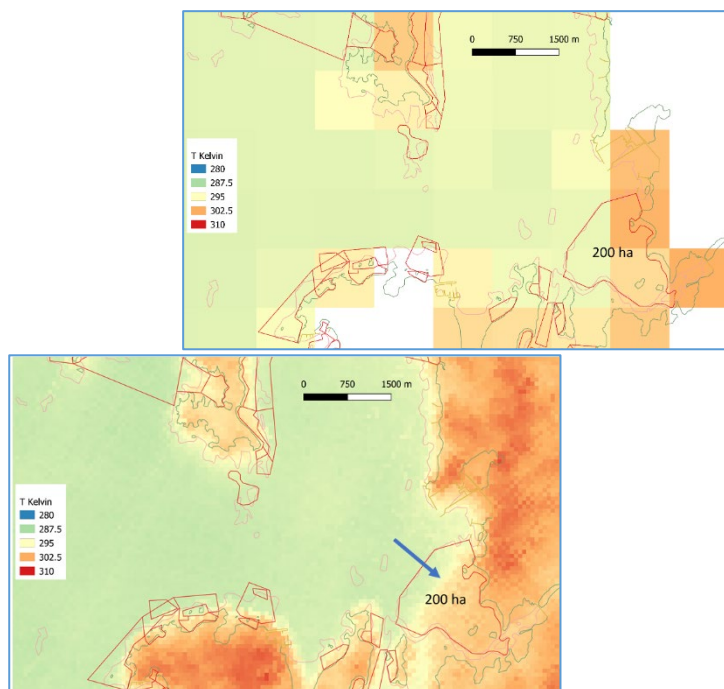


Figure 4: Low tide temperature, Cambados, Galicia, Spain. Images were acquired 9 min apart, 2 hours after low tide of 0.49 m. Left image: VIIRS SST, Right image: ECOSTRESS surface temperature. Tide level (1.25 m) is at sharp temperature discontinuity in right image (arrow). Green lines: high tide mark, Red polygons: shellfish beds.

## Conclusions

The ECOSTRESS SST pixel scale (70 m) is 10× greater than VIIRS (750 m), meaning that the instrument can resolve much finer thermal structure than other sensors used for SST.

The L2 surface temperature product has a 1°K cold bias relative to VIIRS observations and to in situ observations (Figure 1), and the brightness temperatures have a similar cold bias relative to RTTOV radiance transfer simulations and to geostationary satellite sensors (Figure 2). The instrument is temporally stable (Figure 2). The origin of the bias remains unclear. The ECOSTRESS surface emissivities calculated by the TES algorithm in the iQuam matchup dataset are too low relative to measured ASTER spectral library emissivities for seawater (mean  $\epsilon_{8.78\mu} = 0.9667$ ,  $sd=0.0091$  vs ASTER  $\epsilon_{8.78\mu} = 0.9842$ ; mean  $\epsilon_{10.49\mu} = 0.9808$ ,  $sd=0.0042$  vs ASTER  $\epsilon_{10.49\mu} = 0.9898$ ; mean  $\epsilon_{12.09\mu} = 0.9666$ ,  $sd= 0.0100$  vs ASTER  $\epsilon_{12.09\mu} =0.9852$ ). Low emissivities should cause a hot bias, but the lower than expected brightness temperatures (Figure 2) may be balancing the effect of low TES emissivity, leading to an overall cold bias. Regression algorithms for SST would not have this problem.

The revisit interval (sub-daily to 5 days) can resolve patterns relative to tides (Figures 3, 4). Bias correction of ECOSTRESS surface temperatures yields an ultra-high resolution product with broad applications in biological and physical oceanography, especially in the coastal zone where land contamination of SST is a serious problem. It can resolve SST gradients around complex headlands, fjords and islands, and can resolve intertidal gradients in temperature at the spatial scale of sessile organism populations and aquaculture operations (Figure 4).

## Acknowledgements

Supported by NASA 80NSSC20K0074. We thank Jon Mittaz, Helen Beggs, Praj Dash, and Andy Harris for helpful discussions.

## References

- Hocking, J., P. Rayer, D. Rundle, R. Saunders, M. Matricardi, A. Greer, P. Brunel, J. Vidot. RTTOV v12 Users Guide, Eumetsat Numerical Weather Prediction SAF, NWPSAF-MO-UD-037, 2019.
- Hook, S., M. Smyth, T. Logan, W. Johnson, ECOSTRESS At-sensor Calibrated Radiance Daily L1B Global 70m V001 [Data set], NASA EOSDIS Land Processes DAAC 2019. <https://doi.org/10.5067/ECOSTRESS/ECO1BRAD.001>
- Hook, S. J., K. Cawse-Nicholson, J. Barsi, R. Radocinski, G. C. Hulley, W. R. Johnson, G. Rivera, B. Markham, IEEE Trans. Geosci. Remote Sens. **58**, 1294-1302, 2020.
- Hook, S. J., G. C. Hulley, ECOSTRESS Land Surface Temperature and Emissivity Daily L2 Global 70m V001 [Data set], NASA EOSDIS Land Processes DAAC, 2019. <https://doi.org/10.5067/ECOSTRESS/ECO2LSTE.001>
- IFREMER, MARC Wave Watch III Model [Data set], IFREMER Laboratory for Ocean Physics and Satellite Remote Sensing, 2020. [http://tds1.ifremer.fr/thredds/MARC-MANCHE-WW3\\_COTENTIN200M-FOR/MARC-MANCHE-WW3\\_COTENTIN200M-FOR.html](http://tds1.ifremer.fr/thredds/MARC-MANCHE-WW3_COTENTIN200M-FOR/MARC-MANCHE-WW3_COTENTIN200M-FOR.html)
- Krehbiel, C., EcostressBrightnessTemperatureV01.h5 [Data set]. NASA EOSDIS Land Processes DAAC, 2019, [https://git.earthdata.nasa.gov/projects/LPDUR/repos/ecostress\\_swath2grid/browse/](https://git.earthdata.nasa.gov/projects/LPDUR/repos/ecostress_swath2grid/browse/)
- Liang X., A. Ignatov, Monitoring of IR clear-sky radiance over oceans for SST (MICROS), J Atmos. Ocean. Tech. **31**, 1228-1242, 2011.
- Xu, F., A. Ignatov, In situ SST Quality Monitor (iQuam), J Atmos. Ocean. Tech. **31**, 164-180, 2013.
- Xu, F., A. Ignatov. Error characterization in iQuam SSTs using triple collocations with satellite measurements. Geophys. Res. Lett., **43**, 10826-10834, 2016.

## S1-3: DEVELOPMENT OF CONSISTENT SURFACE TEMPERATURE RETRIEVAL ALGORITHMS FOR SEA SURFACE, MARGINAL ICE ZONE AND SEA ICE IN THE POLAR REGIONS

**Jacob L. Høyer<sup>(1)</sup>, Gorm Dybkjær, <sup>(1)</sup> Anne O'Carroll <sup>(2)</sup> Wiebke Kolbe<sup>(1)</sup> and Pia Nielsen-Englyst<sup>(1)</sup>**

(1) Danish Meteorological Institute, Lyngbyvej 100, DK-2100 Ø, Denmark, Email: jlh@dmi.dk

(2) EUMETSAT, Eumetsat Allee 1, D-64295 Darmstadt, Germany

### Introduction

The Earth's surface temperature is a key variable to observe to determine the global energy balance and the heat fluxes between surface and atmosphere. Where Sea Surface Temperature (SST) satellite retrievals are relatively mature, less focus has been on the development of sea Ice Surface Temperature (IST) products and the consistency with the SST algorithms in the Marginal Ice Zone (MIZ). SST and IST products are produced daily within the OSI-SAF and a prototype SST/IST algorithm for SLSTR instrument on Sentinel 3 has been developed within a recent Copernicus and EUMETSAT project.

In this paper, the EUMETSAT SLSTR SST/IST prototype processor is presented together with validation results demonstrating the performance of the retrieval. In addition a new gap-free reprocessed SST/IST product from the Copernicus Marine System (CMEMS) will be presented. This product is the first of its kind and allows for the first time to perform an assessment of the Arctic Ocean (sea and ice) surface temperature developments since 1982.

### L2 IST prototype for Sentinel 3 SLSTR

A prototype L2 IST processor was developed as part of a EUMETSAT and Copernicus project, where DMI was lead and Met.no, Ifremer and Univ. Leicester were partners.

The following reports are available, describing the outcome of the project (see also: <https://www.eumetsat.int/S3-SLSTR-SIST>):

- Requirement Baseline Document (RB)
- Product Validation Plan (PVP)
- Input Output Data Definition Document (IODD)
- Product Validation and Evolution Report (PVR)
- ATBD
- Product Validation and Evolution Report (PVR)

Based upon criteria, such as precision, stability and accuracy, two algorithms were selected out of 15 tested algorithms:

**IST Algorithm2** – a traditional split window based on nadir view only

$$= a_0 + a_1 T_{b_{11nadir}} + a_2 T_{b_{12nadir}} + a_3 \left( (T_{b_{11nadir}} - T_{b_{12nadir}}) \left( \frac{1}{\cos \theta} - 1 \right) \right)$$

**IST Algorithm12** – a dual view algorithm

$$= a_0 + a_1 T_{b_{11nadir}} + a_2 T_{b_{11oblique}}$$

These two algorithms were combined in the marginal ice zone with the SST retrievals to make a consistent surface temperature product from the open ocean towards 100% sea ice concentration

**Marginal Ice Zone Temperature,**

$$= 0.5(T_{b_{11nadir}} - 268.95) * SST - 0.5 * (T_{b_{11nadir}} - 270.95) * IST$$

Where the SST is the WST product from the SLSTR SST product portfolio. All the algorithm coefficients are calculated with regression analysis using Radiation Transfer Model simulations (RTTOV), with incidence angle dependent emissivity.

Validation from Greenland against Promice IST observations observations showed a standard deviation of 1.1 K and bias of -2.2 K for the IST 2 algorithm and standard deviation of 1.8 K and bias of -2.9K for the IST12 algorithm.

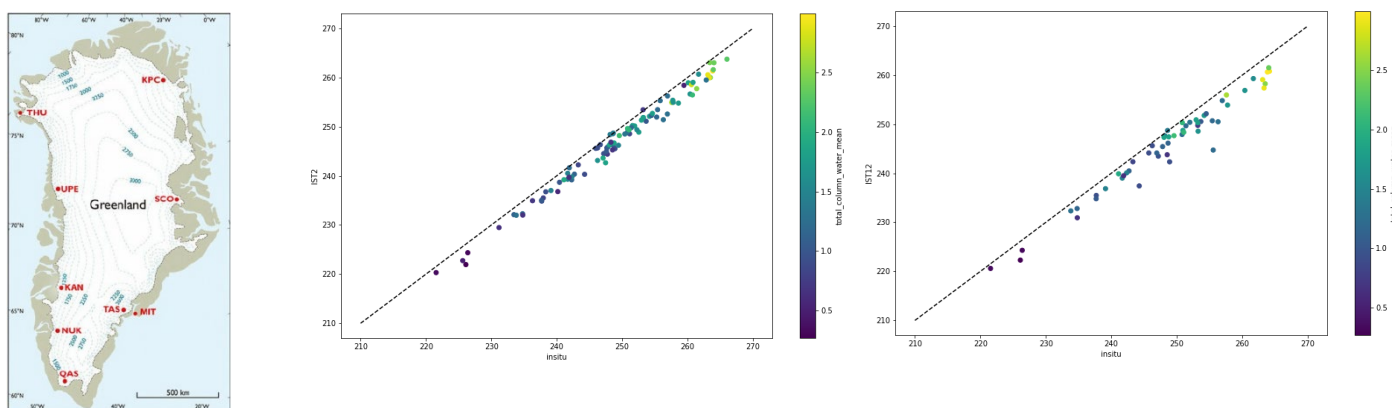


Figure 1: Position of the Promice stations (right) and best all day performance against PROMICE Upper stations and EAST GRIP SLSTR IST2 (middle) and IST12 (right). March 2017.

## L4 SST/IST reanalysis

Level 2 satellite IST observations have been used to generate a gap free level 4 product within the CMEMS Sea ice Thematic assembly Centre. The characteristics of the product is listed below:

- New SST and IST L4 reanalysis within CMEMS (1982-Sep 2019)
- The product is based upon input satellite data from

ESA SST CCI + C3S products

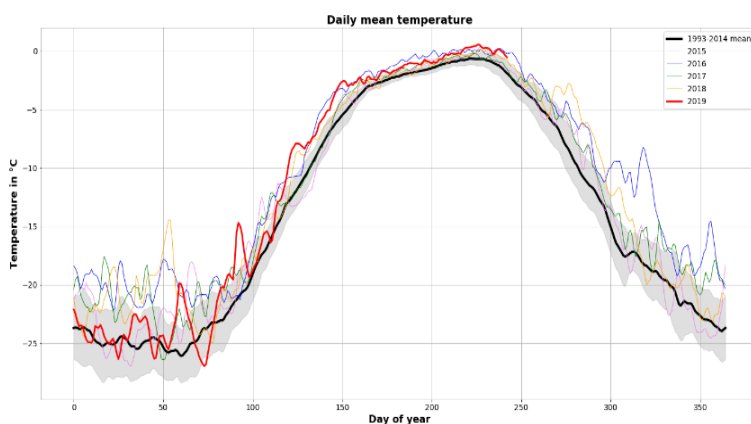
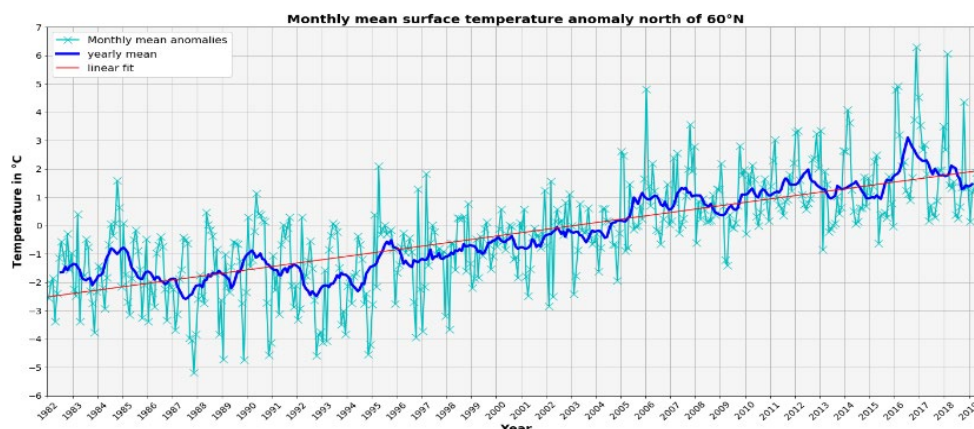
AASTI SST/IST CDR version 2 (CLARA L1)

Operational SST/IST products after 2015, where no iCDR is available

The reprocessed product is available for download at [www.marine.copernicus.eu](http://www.marine.copernicus.eu)

With user id: SEAICE\_ARC\_PHY\_CLIMATE\_L4\_MY\_011\_016

The product can be used to assess the Arctic Ocean surface temperature for both ocean and sea ice. A few examples on the type of monitoring and climate indicators are given in the figures below:



## Conclusion

There is a need to have a for consistent SST and IST products to model and monitor the Arctic Ocean, where the observed climate changes are largest.

Recently, several new SST and IST products have become available from DMI. One product is the Sentinel 3, SLSTR Level 2 prototype processor, which has been developed in a project for EUMESAT and Copernicus. It is expected that the processor will be implemented for operational production in late 2021 or early 2022.

A gap-free level 4 arctic SST and IST product has been produced within the Copernicus CMEMS Sea Ice thematic Assembly centre. The product covers from 1982 to present and provides the ability for the first time to assess the total Arctic surface (ocean and sea ice) temperature changes in the Arctic. The product will thus be used to assess the climatic changes and monitor the present conditions within the climatic context.

#### **S1-4: STATUS AND PLANS FOR THE SEA-ICE CONCENTRATION DATA RECORDS FROM THE EUMETSAT OSI SAF AND ESA CCI: POSSIBILITIES FOR POLAR SST PRODUCTS**

**Thomas Lavergne**<sup>(1)</sup>, **Atle Sørensen**<sup>(1)</sup>, **Jacob Høyer**<sup>(2)</sup>, **Pia Nielsen-Englyst**<sup>(2)</sup>, **Gorm Dybkjær**<sup>(2)</sup>, **Rasmus Tonboe**<sup>(2)</sup> and **Steinar Eastwood**<sup>(1)</sup>

(1) Norwegian Meteorological Institute, Email: [thomas.lavergne@met.no](mailto:thomas.lavergne@met.no)

(2) Danish Meteorological Institute

Satellite-based Sea Surface Temperature (SST) products that cover the polar oceans rely on accurate sea-ice cover information. Such information can be used e.g. for masking pixels at Level1&2, for preparing Level3&4 SST analyses, and for controlling the transition between SST and Ice Surface Temperature (IST). For climate-quality SST data, it is a key requirement that the sea-ice information does not introduce trends or jumps in the data record.

In this contribution, we present the status and plans for sea-ice concentration climate data records from the EUMETSAT Ocean and Sea Ice Satellite Application Facility (OSI SAF) and from the ESA Climate Change Initiative (CCI). We show how these two European initiatives have coordinated to prepare climate-quality sea-ice cover information from the suite of passive microwave satellite missions, to achieve maximum temporal coverage, and to improve the spatial resolution and fidelity along the sea-ice edge. We describe the algorithm steps that are most relevant for the SST/IST community when using such sea-ice information in their climate products. We illustrate our presentation with examples from the Copernicus Climate Change Service (C3S) Arctic Regional ReAnalysis (CARRA), and from the Copernicus Marine Environment Monitoring Service (CMEMS) service.

We finally invite the SST/IST community to a dialogue about their needs and requirements for such sea-ice concentration products.

## **S1 - POSTER PRESENTATIONS – ABSTRACTS**

## **S1-P1: ULTRA HIGH-RESOLUTION SST FROM NASA ECOSTRESS RESOLVES FINE STRUCTURE OF UPWELLING ZONES**

**Weidberg, Nicolás<sup>(1,2)</sup>, Woodin, Sarah A.<sup>(1)</sup>, Wethey, David S.<sup>(1)</sup>**

(1) Department of Biological Sciences, University of South Carolina, Columbia SC, USA

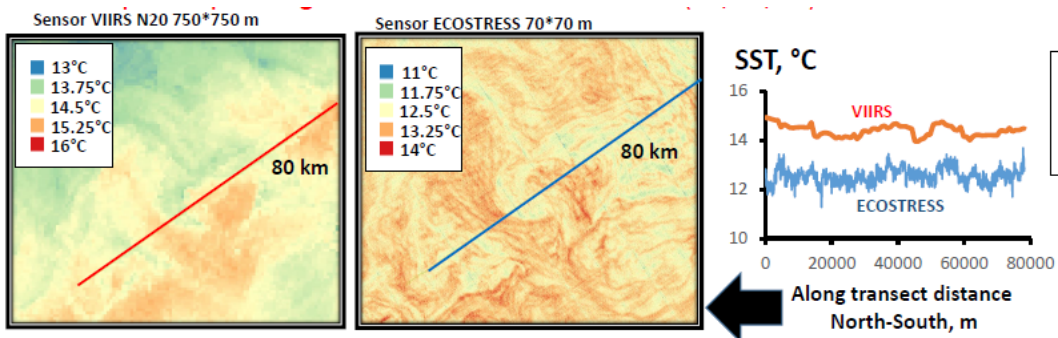
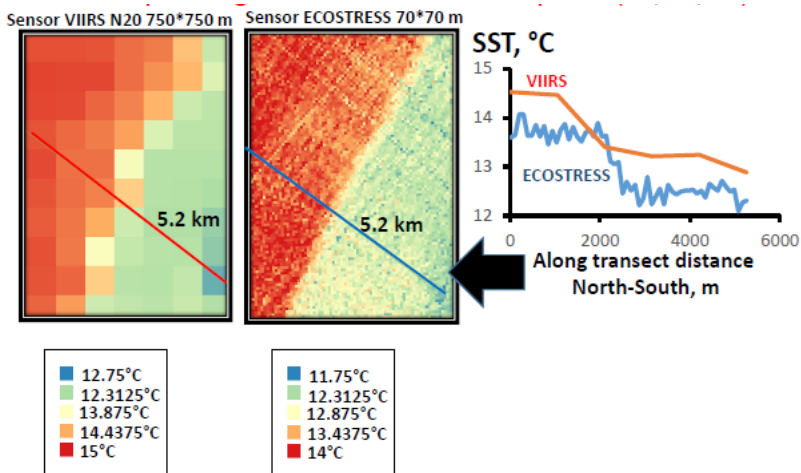
(2) Departamento de Ecoloxía e Bioloxía Animal, Universidade de Vigo, Vigo, Spain

To resolve fine scale environmental forces relevant for marine ecosystem function, new satellite derived products are required, especially along the coasts of the world. In this context, the Ecosystem Spaceborne Thermal Radiometer Experiment on Space Station (ECOSTRESS) provides sea surface temperature imagery with an unprecedented 70×70m pixel size. To assess its performance, we compared processed ECOSTRESS images on the coastal upwelling systems of Western Iberia, Chile, South Africa and California with quasi-simultaneous (less than 90 minutes apart) NOAA-20 VIIRS images with a pixel size of 750×750 m. ECOSTRESS successfully quantifies sub-pixel scale physical structures like upwelling shadows, fronts and filaments that are not properly resolved with NOAA-20 VIIRS. Moreover, it also provides a much more detailed characterization of thermal gradients across fronts. The novel imagery from ECOSTRESS provides an important complement to the operational GHRSSST L2 suite of products for the study of fine-scale ocean dynamics.

Especially interesting are the improvements in spatial resolution across a very conspicuous upwelling front in Chile when using ECOSTRESS. It seems that VIIRS cannot resolve well enough the exact location and sharpness of this structure. Also some intriguing features appear off NW Spain within gyres and upwelling filaments that look like internal waves. However, they are not always parallel to the shelf-break. These very fine structures cannot be observed with VIIRS imagery.

During the meeting we had the opportunity to discuss our results with the GHRSSST community. Specifically, we have now joined the Task 3 Meeting Group (Feature inter-comparison of SST analyses) thanks to the support of Helen Beggs, Jorge Vazquez, Prasanjit Dash and Chunxue Yang. With their help and advice, we should be able to expand our matchup comparisons to other datasets, like Saildrone data (<https://podaac.jpl.nasa.gov/Saildrone>) and the IMOS ship SST data (<https://imos.org.au/facilities/srs/sstproducts/sstdata0>). In addition, we also discussed potential non linear biases in ECOSTRESS brightness temperatures with Jon Mittaz. As far as we know, we have currently detected a uniform bias of -1°C across the SST worldwide range from 0 to 35°C. However, thanks to the work of Jon, we are now aware that such bias can increase at lower temperatures. We will continue to check the ECOSTRESS dataset in search of these non-linear characteristics.

### FIGURES AND TABLES



## **S1-P2: VALIDATION OF SATELLITE SEA SURFACE TEMPERATURES AND LONG-TERM TRENDS IN KOREAN COASTAL REGIONS (1982-2018)**

**Kyung-Ae Park** <sup>(1)</sup> and **Eun-Young Lee** <sup>(2)</sup>

<sup>(1)</sup> Department of Earth Science Education / Research Institute of Oceanography, Seoul National University, Korea, Email: kapark@snu.ac.kr

<sup>(2)</sup> Department of Earth Science Education, Seoul National University, Korea

Validation of daily Optimum Interpolation Sea Surface Temperature (OISST) data from 1982 to 2018 was performed by comparison with quality-controlled in situ water temperature data from Korea Meteorological Administration moored buoys and Korea Oceanographic Data Center observations in the coastal regions around the Korean Peninsula. In contrast to the relatively high accuracy of the SSTs in the open ocean, the SSTs of the coastal regions exhibited large root-mean-square errors (RMSE) ranging from 0.75 °C to 1.99 °C and a bias ranging from -0.51 °C to 1.27 °C, which tended to be amplified towards the coastal lines. The coastal SSTs in the Yellow Sea presented much higher RMSE and bias due to the appearance of cold water on the surface induced by vigorous tidal mixing over shallow bathymetry. The long-term trends of OISSTs were also compared with those of in situ water temperatures over decades. Although the trends of OISSTs deviated from those of in situ temperatures in coastal regions, the spatial patterns of the OISST trends revealed a similar structure to those of in situ temperature trends. The trends of SSTs using satellite data explained about 99% of the trends in in situ temperatures in offshore regions (>25 km from the shoreline). This study discusses the limitations and potential of global SSTs as well as long-term SST trends, especially in Korean coastal regions, considering diverse applications of satellite SSTs and increasing vulnerability to climate change.

## S1-P3: A CMEMS LEVEL 4 SST AND IST CLIMATE DATA SET FOR THE ARCTIC

**Pia Nielsen-Englyst**<sup>(1,2)</sup>, **Jacob L. Høyer**<sup>(2)</sup>, **Wiebke M. Kolbe**<sup>(2)</sup>, **Gorm Dybkjær**<sup>(2)</sup>, and **Thomas Lavergne**<sup>(3)</sup>

(1) DTU-Space, Technical University of Denmark, DK-2800 Lyngby, Denmark, Email: [pne@dmi.dk](mailto:pne@dmi.dk)

(2) Danish Meteorological Institute, Lyngbyvej 100, DK-2100 Copenhagen Ø, Denmark, Email: [jlh@dmi.dk](mailto:jlh@dmi.dk), [wk@dmi.dk](mailto:wk@dmi.dk), [gd@dmi.dk](mailto:gd@dmi.dk)

(3) Norwegian Meteorological Institute, Email: [thomasl@met.no](mailto:thomasl@met.no)

### Introduction

Climate change is most pronounced in the Arctic, and therefore, it is crucial to accurately estimate sea surface temperatures (SST) and sea ice surface temperatures (IST) in this region. We present the first Arctic (>58°N) gap-free climate data set covering the surface temperatures of the ocean, sea ice and the marginal ice zone (MIZ) from 1982-2019. The underlying algorithm combines multi-satellite observations and performs a statistical optimal interpolation (OI) to obtain daily gap-free fields at a spatial resolution of 0.05°. Each region (sea ice, open ocean and MIZ) has its own characteristics and thus, it is very important with an accurate sea ice concentration (SIC) field to identify the regions. A combination of several SIC products and additional filtering have been used to produce an improved SIC product. Drifting buoys, moored buoys and ships have been used to derive consistent validation statistics of the surface temperatures over the ocean and sea ice. The combination of sea and sea ice surface temperature provides a consistent climate indicator, which is crucial for studying climate change and trends in the Arctic.

### Input SST/IST data

The SST CCI version 2.1 are used for the period January 1982 to December 31st, 2019, and they are obtained through the ESA CCI project (Merchant et al., 2019). The SST CCI data include observations from the ATSR 1 instrument on board the ERS-1 satellite, ATSR 2 on board the ERS-2 satellite, and the AATSR on board ENVISAT and AVHRR on board the NOAA satellites.

SST observations are used from the Copernicus Climate Change Service (C3S) for 2016-2019. Level 2 data are obtained through personal communication (Owen Embury, 2018) and corresponds to the L3U data products available from <https://cds.climate.copernicus.eu/> except for the higher spatial resolution. The C3S data include observations from the SLSTR A/B instruments on board the Sentinel 3 satellites and the AVHRRs on board the NOAA and Metop satellites.

The main source of SST/IST observations is the Arctic and Antarctic ice Surface Temperatures from thermal Infrared (AASTI) satellite data set (Dybkjær et al., 2014). This data covers the period Jan 1982 to Dec, 2014. From 2015 the operational OSI-SAF Metop AVHRR SST/IST product has been used (Dybkjær et al., 2012). These data sets are consistent as the type of algorithms used to retrieve the SST and IST are similar.

### Sea ice concentration data

The SIC data are obtained from the EUMETSAT OSISAF Global SIC CDR product, OSI-450 (1979-2015) and the ESA CCI SICCI-25km product (2002-2017). A special rerun of the SICCI-25km processing has been performed to provide consistent SICCI-25km up to 2019. Both products have coastal challenges and for that reason we use a SIC product from the SMHI (1982-2011) and the CMEMS 1 km SIC fields (2012-present) for the Baltic Region (Høyer and Karagali, 2016).

### Pre-processing of OI Sea Ice Concentration field

The SICCI-25km and OSI-450 SIC fields have been interpolated onto the L4 0.05° regular latitude longitude grid. The SICCI-25km product is used whenever it is available and the OSI-450 product otherwise. For days with missing SIC data the field closest in time is used. The SIC field has been extrapolated along the coasts to cover the fjords. Low SIC (<15%) is defined as no ice. Land-spillover effects are more pronounced for OSI-450 than SICCI-25km (Lavergne et al., 2019). To improve OSI-450 and to increase the consistency of the full SIC record, two filters were used. Both filters use a 15x15 filter around each L4 grid cell. The first filter (F1) removes sea ice from the center grid if the group of grids contains at least one land and one ocean grid

cell. The second filter (F2) removes sea ice from the center grid cell if any of the grids within the group of grids is land and the SST (from OSTIA/CCI) of the center grid cell exceeds the temperature threshold,  $T_0$ .  $T_0$  varies linearly over time from  $\sim 1^\circ\text{C}$  to  $2.5^\circ\text{C}$  for the period 1982-2019, based on the observed SST trend. Figure 1 shows the distribution of SICs as a function of SST in July 2016 for OSI-450 and SICCI-25km with and without the filters. Before filtering, OSI-450 has many cases of sea ice with SIC up to 60% in warm (6-15°C) waters which are not seen in SICCI-25km. After filtering, the distribution of OSI-450 looks more like SICCI-25km.

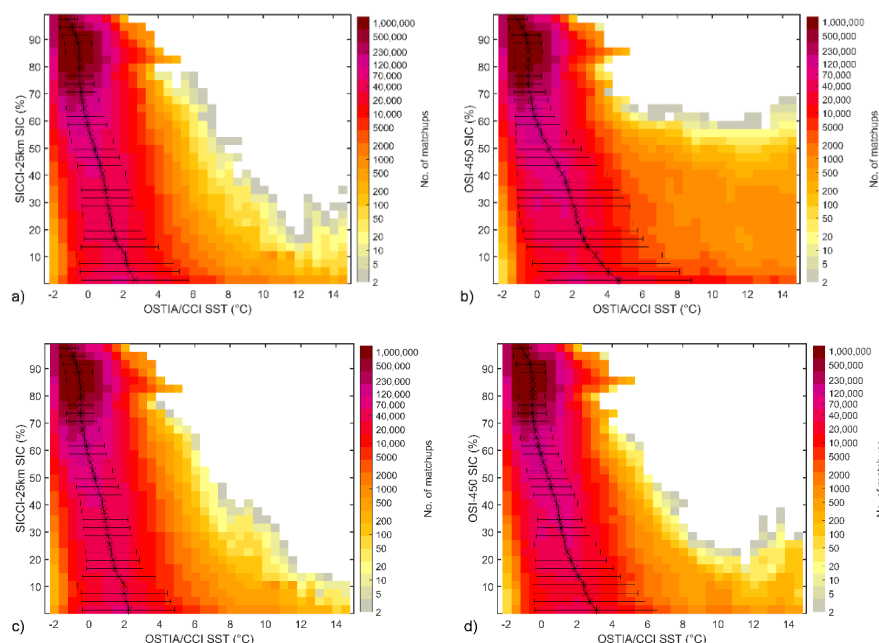


Figure 1: ESACCI/OSTIA SST versus SIC from OSI-450 (right) and SICCI-25km (left) during July 2016 without filtering (top) and with both filter applied (bottom). The average distribution is shown as asterisks with related error-bars showing the standard deviations considering bins with more than 30 members.

## DMIOI L4 Processing System

The full DMIOI L4 processing system is illustrated in Figure 2. All satellite data available within 12 h from the analysis are considered. Various quality checks and processing steps are performed to generate separate L3 products. The bias correction corrects the AASTI SST and METOP AVHRR SST data against the available SST CCI and C3S SST observations. The temporal window for the comparison is 7 days and the bias fields are smoothed over 500 km (Høyer et al., 2014). An additional bias static correction is performed based on the SST validation against independent drifting buoys. The OI method is used to construct the merged and gap free SST/IST analysis (Høyer and She, 2007; Høyer et al., 2014). It works with anomalies from a guess field. Here, the previous analysis field has been used as the guess field. The OI method will for each grid point find the solution that has the lowest errors, given statistical input, such as a guess error variance, error covariance functions and uncertainties on the individual observations. Due to the different physical conditions for ocean and sea ice surface temperature variability, separate statistics have been derived for the ocean, sea ice and the MIZ. The OI SIC field is used to construct the full SST/IST/MIZT field in this way:

- SST: SIC < 15%: SST statistical parameters are used
- IST: SIC > 70%: IST Statistical parameters are used
- MIZT: SIC > 15 < 70%: Linear weighting of the SST and IST parameters are used, based on the SIC

The SST guess variance and error covariance are very similar to those in Høyer and She (2007) and Høyer et al. (2014). The guess IST variability was derived using 1 year of Metop AVHRR L3 aggregated observations. The guess field and the error covariance used in the MIZ is a weighted linear combination of

the open water and the ice values where the SIC was used as the weighting factor. Spatially dependent error covariance functions have been fitted in latitude/longitude directions based on a year of analysis of L3 SST and IST observations. The observation error covariance is assumed to be a diagonal matrix (i.e. observation errors are uncorrelated with each other). The diagonals are specified using the error obtained from validation against in situ observations and the reduced error estimate from the noise weighting procedure. The error covariance functions, the first guess fields and the satellite observations are combined in the OI algorithm which inverts the covariance matrix and determines the optimal weights for the observations for each grid point. Each analysis value is accompanied by an uncertainty estimate which is also a result of the OI algorithm

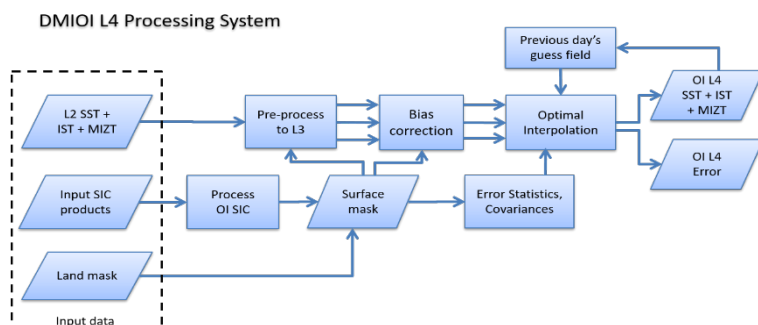


Figure 2: Schematic diagram of the DMIOI L4 processing system.

## Results

### Validation

For SST validation, observations from drifting buoys, moored buoys and ships are obtained from the HADIOD database (Atkinson, et al., 2014). Table 1 shows the statistics. The larger stds for ships are likely explained by larger uncertainties related to SST observations from ships compared to those from traditional buoys. The drifting buoy SSTs were used for a static mean bias correction of the L4 SST analysis, while the moored buoy and ship observations represent an independent estimate of the performance. For IST validation, we use 2 m air temperature (T2m) measurements from ECMWF (Sep 15th, 1993- Jan 1st, 2015) and CRREL (Apr 14th, 2001- Sep 4th, 2017) drifting buoys. The physical difference between Tskin and T2m may introduce a temperature difference (up to several degrees; Nielsen-Englyst et al., 2019), which inflates the biases in the comparison. IST has also been validated against surface temperatures from Icebridge flights (IAKST1B, 2012-2014; Bennett and Studinger, 2012). Figure 3 shows an example of one Icebridge flight.

Type	Parameter	Mean	Std	RMS	Nobs
Drifting buoys	SST (°C)	0.03	0.66	0.66	2497478
Moored buoys	SST (°C)	0.08	0.62	0.63	71792
Ship	SST (°C)	0.11	1.13	1.14	2154399
Drifting buoys ECMWF – Tair	IST (°C)	-3.73	3.44	5.08	56136
Drifting buoys CRREL – Tair	IST (°C)	-3.40	3.40	4.80	22952
Icebridge (SIC>=15%)	IST (°C)	0.67	3.57	3.63	96863

Table 1: Validation statics for SST and IST with all differences calculated as satellite – in situ.

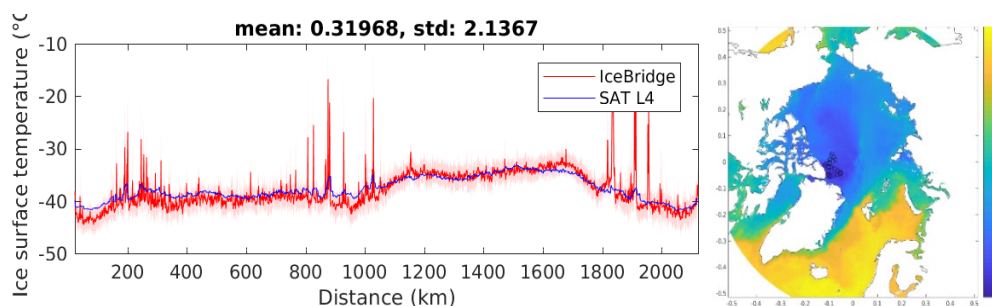


Figure 3: Example of L4 IST comparison with observations from one Icebridge flight over the Arctic sea ice.

## Climate indicators

The Arctic SST/IST reanalysis can be used to assess the changes and trends of the combined sea and ice surface temperatures in the Arctic. The overall trend from 1982 to 2019 is shown in Figure 4, and on average the temperature has risen with +0.12 degrees per year, which is more than 4 degrees over the 38 years.

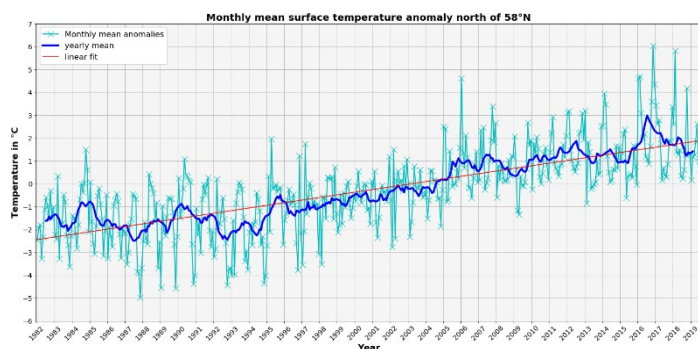


Figure 4: The light blue curve shows the monthly temperature anomaly for the Arctic, 1982-2019. The anomaly is calculated as the difference between the monthly mean temperature and the monthly climatology for 1993-2014.

## Conclusion and outlook

The first Arctic gap-free climate data set covering the surface temperatures of the ocean, sea ice and the MIZ since 1982 has been constructed (CMEMS product ID: SEAICE\_ARC\_PHY\_CLIMATE\_L4\_MY\_011\_016). The combined SST/IST/MIZT data enables monitoring of daily surface temperatures and climate trends. Future work will include a comparison of the SST-only trend with existing SST products as well as a more extensive validation over sea ice e.g. using more recent Icebridge flights.

## References

- Bennett, R. and Studinger, Michael: IceBridge KT19 IR Surface Temperature, Version 1, <https://doi.org/10.5067/I883KXU7ZO8O>, 2012.
- Dybkjær, G., Tonboe, R., and Høyer, J. L.: Arctic surface temperatures from Metop AVHRR compared to in situ ocean and land data, 8, 959–970, <https://doi.org/10.5194/os-8-959-2012>, 2012.
- Dybkjær, G., Høyer, J. L., Tonboe, R., and Olsen, S. M.: Report on the documentation and description of the new Arctic Ocean dataset combining SST and IST., NACLIM Deliverable D32.28, 2014.
- Høyer, J. L. and Karagali, I.: Sea Surface Temperature Climate Data Record for the North Sea and Baltic Sea, 29, 2529–2541, <https://doi.org/10.1175/JCLI-D-15-0663.1>, 2016.
- Høyer, J. L. and She, J.: Optimal interpolation of sea surface temperature for the North Sea and Baltic Sea, *Journal of Marine Systems*, 65, 176–189, <https://doi.org/10.1016/j.jmarsys.2005.03.008>, 2007.
- Høyer, J. L., Le Borgne, P., and Eastwood, S.: A bias correction method for Arctic satellite sea surface temperature observations, 146, 201–213, <https://doi.org/10.1016/j.rse.2013.04.020>, 2014.

Lavergne, T., Sørensen, A. M., Kern, S., Tonboe, R., Notz, D., Aaboe, S., Bell, L., Dybkjær, G., Eastwood, S., Gabarro, C., Heygster, G., Killie, M. A., Brandt Kreiner, M., Lavelle, J., Saldo, R., Sandven, S., and Pedersen, L. T.: Version 2 of the EUMETSAT OSI SAF and ESA CCI sea-ice concentration climate data records, 13, 49–78, <https://doi.org/10.5194/tc-13-49-2019>, 2019.

Nielsen-Englyst, P., Høyer, J. L., Madsen, K. S., Tonboe, R., Dybkjær, G., and Alerskans, E.: In situ observed relationships between snow and ice surface skin temperatures and 2 m air temperatures in the Arctic, 13, 1005–1024, <https://doi.org/10.5194/tc-13-1005-2019>, 2019.

## S1-P4: USING SAILDRONES TO VALIDATE SEA SURFACE TEMPERATURES IN THE ARCTIC

**Jorge Vazquez-Cuervo<sup>(1)</sup>, Toshio M. Chin<sup>(1)</sup>, Edward Armstrong<sup>(1)</sup>, Chelle Gentemann<sup>(2)</sup>**

(1) Jet Propulsion Laboratory/California Institute of Technology, Pasadena, California, United States, [jorge.vazquez@jpl.nasa.gov](mailto:jorge.vazquez@jpl.nasa.gov), [toshio.mi.chin@jpl.nasa.gov](mailto:toshio.mi.chin@jpl.nasa.gov), [edward.m.armstrong@jpl.nasa.gov](mailto:edward.m.armstrong@jpl.nasa.gov)

(2) Farallon Institute, California, United States, Email: [cgentemann@faralloninstitute.org](mailto:cgentemann@faralloninstitute.org)

### Introduction

The Arctic is one of the most challenging areas for validating remote sensing data. It is also one of the most critical areas for understanding climate change. Accurate measurements of Sea surface Temperature (SST) as an Essential Climate Variable (ECV) are critical for monitoring and forecasting changes in the Arctic.

During 2019 two NASA deployments of the Saildrone uncrewed vehicle occurred off the Alaskan Coast in the Bering Strait. Both deployments left Dutch Harbour on approximately May 13, 2019. Four different onboard instruments were used to measure SST, including two CTDs and two radiometers. Comparisons were made with eight GHRSSST Level 4 products, including the Operational Sea Surface Temperature and Sea Ice Analysis (OSTIA), Canadian Meteorological Center (CMC), Danish Meteorological Institute (DMI), NASA's Multi-Scale Ultra High Resolution (MUR), Naval Oceanographic Center (NAVO), Remote Sensing Systems (REMSS), the GHRSSST Median Product Ensemble (GMPE), and the NOAA National Centers for Environmental Information (NCEI) Daily Optimum Interpolation SST (DOISST). Statistics were compared between the 4 Saildrone SSTs and each product. Overall Root Mean Square Differences (RMSD) varied between 0.7 to approximately 1.0 degrees Celsius with REMSS SSTs showing biases close to zero. Overall correlations were approximately 0.90, indicative of **excellent agreement between the GHRSSST Level 4 products and the four Saildrone sensors.**

### Abstract

Eight GHRSSST Level 4 products were co-located with two NASA MISST deployment SD1036 and SD1037. Co-locations were based on using a nearest neighbour between the L4 product and the Saildrone deployment. Due to the higher resolution of Saildrone compared to the satellite pixels, multiple Saildrone measurements occurred within the satellite pixel. The multiple co-locations of Saildrone SST were averaged to produce the co-located value identified with that satellite pixel. The number of co-locations thus varies with the spatial gridding/resolution of the GHRSSST L4 product. Statistics calculated included:

- 1) Mean difference between the GHRSSST L4 product and Saildrone SST.
- 2) Root Mean Squared Difference between the GHRSSST L4 product and Saildrone SST.
- 3) Correlation between the GHRSSST L4 product and Saildrone SST.
- 4) Signal to Noise ratio between the GHRSSST L4 product and Saildrone SST.
- 5) Wavenumber spectra for the GHRSSST L4 products and Saildrone SST. Slopes were derived for each of the wavenumber spectra.
- 6) For the sake of brevity in the poster, only results for the SBE CTD are shown for the time series plots and the bar graph.

Figure 1 shows the SST along the Saildrone SD1036 deployment from the SBE CTD, along the mean SST derived from the DOISST average over the period of time of the Saildrone deployment. For the sake of comparison, sea surface salinity from the SMAP is also shown. Clearly visible is the low salinity/warmer waters associated with the Yukon River Discharge and the warmer SST associated with the Saildrone SD1036 as it crossed the Yukon River Delta.

Figure 2 shows the time series plots for the co-located time series of the GHRSSST L4 products for the Saildrone SBE1036 and SBE1037 deployments. Clearly noticeable are the warmer temperatures at

approximately day 150 of 2019 associated with the crossing of the Yukon Delta. All the GHRSSST L4 products reproduce the warming but with different magnitudes.

Figure 3 shows the bar plots for the SD1036 deployments for the comparisons with the SBE CTD. Overall the REMSS product had the smallest bias close to zero. The REMSS bias close to zero could be due to the processing of the REMSS product which applies a diurnal correction. Negative biases indicate that the Sailer SST is cooler than the corresponding GHRSSST product. Correlations, overall were between 0.8 and 0.9. Highest correlations were seen in the DOISST and the REMSS products. High correlations in the MUR data are encouraging indicating the higher resolution of the MUR product is not significantly increasing the noise. This is confirmed by the high signal to noise ratio which is equivalent to the REMSS and the DOISST products. RMSD are in general between 0.5 and 1.0 degrees Celsius. Considering these comparisons are being done in the Arctic, the results are encouraging as RMSD are not significantly higher than observed in other parts of the oceans or previous studies.

Figure 4 shows the spectral plots for the SD1036 deployment for all four SST sensors on Sailer. Overall all the spectral slopes approximate the -2.0 associated with mesoscale and submesoscale variability. The power spectral density is likely reflective of the different feature resolutions of the data sets. OSTIA, with a 5km gridding, has the closest magnitude in power spectral density to the Sailer SST. Also important to point is the DOISST, with a gridding resolution of approximately 25km, shows a change in spectral slope at approximately 50 to 100km. This would reflect a smoother feature resolution than the higher resolution products. The DMI product also has a change in the slope and additionally is associated with a reduced power spectral density.

Figure 5 shows example Taylor Diagrams for the different products Taylor diagrams have proved to be effective plots for comparing multiple data sets against a reference data set. Results are shown for both the SBE CTD and the WING radiometer for SD1036. Overall all the data sets show good agreement, with the DMI SSTs along the Sailer track having the STD associated with the Sailer SST.

## Figures and Tables

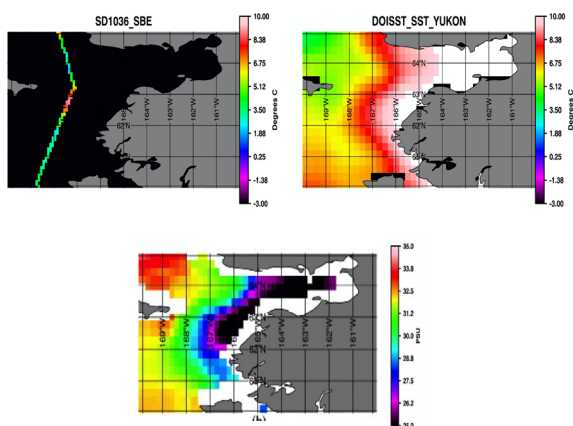


Figure 1: shows frontal structures associated with SST from DOISST and SMAP SSS off the Alaskan Coast. Also shown are SSTs from the SBE CTD onboard Sailer.

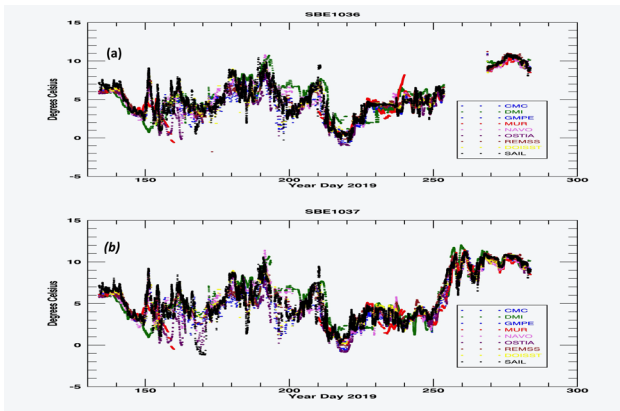


Figure 2: Shows time series for the 8 GHRSSST L4 products and Sairdron SBE CTD for SD1036 and SD1037

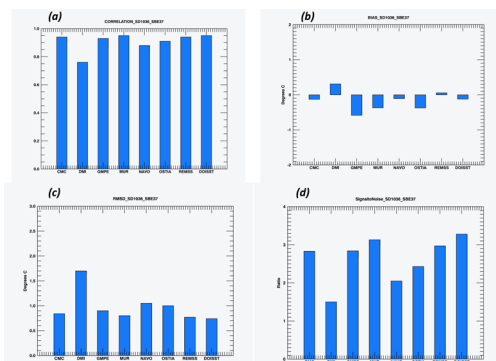


Figure 3: shows bar graphs summarizing statistics for the 8 GHRSSST L4 products versus SST derived from the SBE CTD onboard Sairdron

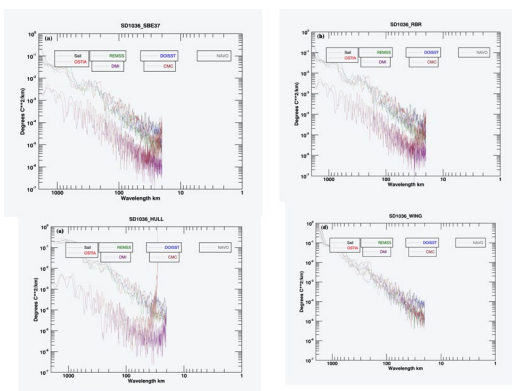


Figure 4: Shows spectral plots of wavenumber for the 8 GHRSSST L4 products and the 4 Sairdron SD1036 SST sensors, SBE, RBR, HULL, and Wing.

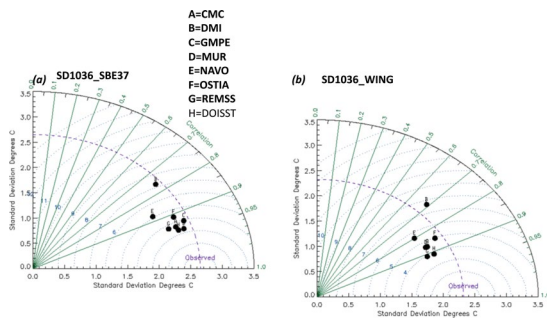


Figure 5: Taylor Diagrams for the SBE CTD and Wing for Saildrone SD1036 deployment and the 8 GHRSSST Level 4 products.

## Conclusions

Direct statistical comparison with SSTs from Saildrone lead to encouraging results for applications of satellite derived SSTs in the Arctic. Warm SSTs are associated with low salinity most likely due to river discharges from the Yukon Delta. Overall results appear to indicate the REMSS product, which applies a diurnal model, shows excellent agreement with the Saildrone SST. Correlations for all products between 0.8 and 0.9 are reflective are promising for future applications.

## **SCIENCE SESSION 2**

# **APPLYING THE DATA: SPATIO-TEMPORAL VARIATION, EXTREME EVENTS**



## S2 - SESSION REPORT

**Chair: Gary Wick<sup>(1)</sup>, Rapporteur: Christo Whittle<sup>(2)</sup>**

(1) NOAA OAR, Boulder, CO, Email: [gary.a.wick@noaa.gov](mailto:gary.a.wick@noaa.gov)

(2) CSIR, Cape Town, South Africa, Email: [CWhittle@csir.co.za](mailto:CWhittle@csir.co.za)

### HIGHLIGHTS

- Use of SST CDR to detect marine heat waves in the Mediterranean Sea
- New techniques to detect SST spatial features using deep learning methods
- New techniques to detect gradients in the thermal skin layer using thermo-fluorescent dyes

### INTRODUCTION

The session consisted of pre-recorded oral presentations, along with presentations in poster format. All presentations were available for viewing throughout the week of the meeting, and discussions were facilitated via Moodle forums.

### RESOURCES

- View presentations (recordings): <https://training.eumetsat.int/mod/book/view.php?id=14071&chapterid=626>
- Discussion forum for recordings: <https://training.eumetsat.int/mod/forum/view.php?id=14069>
- Download the slides: <https://training.eumetsat.int/mod/folder/view.php?id=14070>
- Posters padlet: <https://padlet.com/TrainingEUMETSAT/2dlttnpeni8e9mzed>

**ORAL PRESENTATIONS**

Francesca E Leonelli, Detection and Characterisation of Marine Heat Waves in the Mediterranean Sea in the past 40 years

The presentation examines the extent to which SST trends influence marine heat waves in the Mediterranean Sea over the past 40 years. Events were detected and characterized using both detrended and original SST inputs. The results suggested that regions with SST trends can experience biases in detected marine heat waves and use of detrended data was recommended.

Discussion: G. Liu asked why the number of marine heat waves increased at the start of the record with the detrended data when one might expect that detrending might reduce events toward the end of the record but have less impact at the start of the record. Leonelli responded that using the detrended data tends to level out the number of events across the record implying that there could be more events at the beginning of the record. C. Merchant asked if the size of the extremes relative to the detrended data showed any change in the Med. Leonelli responded that the initial results do not appear to show an increase in the size of events but suggested that a more focused analysis could show more. M. Worsfold asked what the climatology period was for the analysis to which the response was that it was the entire coverage period of the data – 1982-2019. S. Sun asked why use of the detrended data resulted in increased duration of detected events as well as increased frequency. Leonelli replied that following the question she rechecked her code and found an error in which the average statistics for the original data were not reported correctly. The revised average properties for the original detection are  $2.343 \pm 0.003$  °C (intensity),  $1.917 \pm 0.001$  events/year (frequency) and  $11.84 \pm 0.01$  days (duration), which agree more closely with the results for the detrended data. J. Vazquez asked if there were any plans to apply the methodology to other regions or with more recent data. Leonelli responded that more analyses would be interesting, but there were no specific plans for application to other regions. F. Pastor asked if marine heat waves were more prominent in any particular season. Leonelli replied that marine heat waves can occur in any season but they had not performed any dedicated seasonal analysis.

J. Xavier Prochaska, Deep Learning of Sea Surface Temperature Patterns to Identify Ocean Extremes

The presentation describes application of a new deep learning technique to MODIS data to identify the most out-of-distribution spatial patterns in SST. The outlier patterns exhibited large DT patterns and showed strong correspondence to western boundary current regions.

Discussion: G. Wick found the presentation very interesting and asked if there were any inherent limits on the size of the cutout that could be analysed. Since the technique just identifies whatever pattern is most anomalous, targeting specific regions might enable highlighting other types of patterns. Responses from P. Cornillon and Prochaska suggested that there were no inherent limits on the size and that smaller regions could be examined. Some of the ideas to explore different types of features are explored in more detail in the poster later in this session.

Peter Cornillon, Instrument Noise, Retrieval Issues or Geophysical Signal?

The presentation examined internal variability in individual “cut-outs” of MODIS data. One of the principal results was a finding that variability within these cutouts exhibited a near-linear increase with mean SST. There was also an anomalous grouping of points with low variability at higher mean SST that largely clustered around both sides of Northern Africa. It was not expected to be related to instrument noise and the presentation questioned the cause.

Discussion: Several of the results had also been presented as part of the feature-fidelity task team presentation on day 1 and elicited many comments suggesting possible reasons for the observed dependence. In this session C. Merchant commented that the Monday discussion suggested that an SST dependence of noise could be expected for many sorts of SST retrievals. In moist regions, algorithms can up the gain, which increases noise. He also noted that the low-noise region was too similar to desert dust patterns to be a coincidence and asked what exactly was the underlying retrieval algorithm used. P. Cornillon responded that the algorithm was described at <https://oceancolor.gsfc.nasa.gov/atbd/sst/>, and

agreed that further exploration of propagation of BT noise through the retrieval algorithm would be very interesting.

Peter Minnett, Studying the thermal skin layer using thermofluorescent dyes

The presentation explored use of a new technique to explore whether temperature gradients in the thermal skin layer could possibly be detected using thermofluorescent dyes that respond to temperature in different ways. While current hyperspectral radiometers have not been able to confidently resolve temperature gradients, these new techniques exhibit potential to reveal new information in a laboratory environment.

Discussion: C. Merchant asked about the current inability to resolve the gradients with hyperspectral radiometers, questioning if the limit was something fundamental related to the available spectral information. P. Minnett replied that the likely reason was noise in the M-AERI measurements and provided several references to the algorithms used in attempts to derive the temperature profile. He ultimately concluded that the approach is not feasible with current instruments, hence the need for a new approach. E. Armstrong questioned if the technique could eventually be moved out of the laboratory into the real world. Minnett responded yes, but commented that there is much more work to be done in the lab. G. Wick followed up with a question as to whether they felt that they could get at some of their underlying questions about the impact of longwave radiation in a lab environment. Minnett responded that he was confident they could learn a lot from the lab environment.

**POSTER PRESENTATIONS**

Prasanjit Dash, The NOAA STAR SOCD OceanView (OV): An application for integrated visualization of satellite, in situ, and model data & ocean events – the v1.0 release –

The poster provided an overview of the capabilities, benefits, and data sets included in the new Ocean View web-based viewer at NOAA STAR.

Discussion: H. Beggs asked when OV might include marine heat waves and which SST products would be used to derive those events. Dash responded that there are plans to add data on marine heat waves. G. Wick asked about the process to add products in the future and whether some formal NOAA review process was anticipated. Dash responded that the tool is more like a division resource and, as such, they have good flexibility in setting priorities for new products.

Jordi Isern-Fontanet, The intermittency of Sea Surface Temperature: a global perspective

The poster described the approach and sample results from an examination of intermittency in SST as observed in the LLC 4320 experiment.

Discussion: J. Vazquez found it fascinating that the approach could be applied to such high-resolution data and asked if the approach is applicable globally. There was no response.

Ioanna Karagali, Is there a need for yet another model to account for SST diurnal variability?

The poster presents modelled results of diurnal warming from the General Ocean Turbulence Model and the HIROMB-BOOS model (HBM) compared with observations from SEVIRI. The results showed generally good ability to reproduce the shape of the diurnal cycle though peak amplitudes were, perhaps, underestimated.

Discussion: G. Wick asked if the configurations she was using in GOTM were similar to what she had used in the past and if any new updates to GOTM have had any impact on the work. Karagali replied that new releases are easy to download and implement and she had implemented all of her old add-ons for consistency with past work. X. Li asked about the top layer thickness of HBM to which Karagali replied it was 2 m. S. Pimentel asked if she had any sense of how to improve the amplitude of the diurnal peak in GOTM – perhaps through the forcing or the solar absorption scheme. Karagali replied that solar absorption may indeed play an influence, but that the depth resolution in GOTM may also play an important role. She hopes to resume the activity in the near future.

Kyung-ae Park, Observations of Infrared SST Autonomous Radiometer (ISAR) Skin Temperatures in the Seas around Korean Peninsula, Indian Ocean, and Northwest Pacific

The poster presented preliminary results from multiple deployments of the ISAR around the Korean peninsula in recent years.

Discussion: G. Wick acknowledged a nice poster and asked if she had done the comparisons of diurnal warming against Himawari-8 shown for one cruise for the other cruises as well. He also asked about the source of Himawari data. Park responded that the data had been downloaded from the JAXA ftp site and said that they had not yet done the comparison for the NW Pacific cruise of interest. Y. Kurihara questioned a possible discrepancy between the bias noted between ISAR and H8 in the figure and caption but there was no response in the forum.

J. Xavier Prochaska, Revealing Fundamental SST Patterns with Deep Learning

Following on from the recorded presentation, this poster described more about the methodology for applying deep learning to reveal fundamental SST patterns and showed a result where different groupings of the patterns could be searched out from a representation of the model parameter space.

Discussion: G. Wick expressed that he liked the illustration of how different pattern clusters could be viewed in different ways and acknowledged that he should have looked at the poster before his questions on the recorded presentation. Prochaska expressed thanks and noted that they would be happy to explore the patterns in more detail.

## **S2 - ORAL PRESENTATIONS - ABSTRACTS**

## S2-1: DETECTION AND CHARACTERISATION OF MARINE HEAT WAVES IN THE MEDITERRANEAN SEA IN THE PAST 40 YEARS

**Francesca Elisa Leonelli**<sup>(1)(3)</sup>, **Andrea Pisano**<sup>(1)</sup>, **Salvatore Marullo**<sup>(2)</sup>, **Jacopo Chiggiato**<sup>(1)</sup>, **Chunxue Yang**<sup>(1)</sup>, **Rosalia Santoleri**<sup>(1)</sup>

(1) Consiglio Nazionale delle Ricerche, Istituto di Scienze Marine (CNR-ISMAR), via Fosso del Cavaliere 100 Rome (Italy); Email: [francesca.leonelli@artov.ismar.cnr.it](mailto:francesca.leonelli@artov.ismar.cnr.it); [andrea.pisano@artov.ismar.cnr.it](mailto:andrea.pisano@artov.ismar.cnr.it); [jacopo.chiggiato@ismar.cnr.it](mailto:jacopo.chiggiato@ismar.cnr.it); [chunxue.yang@artov.ismar.cnr.it](mailto:chunxue.yang@artov.ismar.cnr.it); [rosalia.santoleri@artov.ismar.cnr.it](mailto:rosalia.santoleri@artov.ismar.cnr.it)

(2) Agenzia Nazionale per le Nuove Tecnologie, l'Energia e lo Sviluppo Economico Sostenibile (ENEA), via Enrico Fermi 45, Frascati (Italy); Email: [salvatore.marullo@enea.it](mailto:salvatore.marullo@enea.it);

(3) Dipartimento di Matematica, Sapienza Università di Roma, Piazzale Aldo Moro 5, Rome (Italy)

## S2-2: DEEP LEARNING OF SEA SURFACE TEMPERATURE PATTERNS TO IDENTIFY OCEAN EXTREMES

**J. Xavier Prochaska**<sup>(1)</sup>, **Peter Cornillon**<sup>(2)</sup>, and **David Reiman**<sup>(1)</sup>

(1) University of California, Santa Cruz

(2) University of Rhode Island

We report on an out of distribution analysis of ~12,000,000 semi-independent 128x128 pixel<sup>2</sup> SST regions from all night-time granules in the MODIS R2019 L2 public dataset to discover the most complex or extreme phenomena at the ocean surface. Our algorithm (ULMO) is a probabilistic autoencoder, which combines two deep learning modules: (1) an autoencoder, trained on ~150,000 random regions from 2010, to represent any input region with a 512-dimensional latent vector akin to a (non-linear) EOF analysis; and (2) a normalizing flow, which maps the autoencoder's latent space distribution onto an isotropic Gaussian manifold. From the latter, we calculate a log-likelihood (LL) value for each region and define outliers to be those in the lowest 0.1% of the distribution. These exhibit large gradients and patterns characteristic of a highly dynamic ocean surface, and many are located within larger complexes whose unique dynamics warrant future analysis. Without guidance, ULMO consistently locates the outliers where the major western boundary currents separate from the continental margin. We will detail the analysis with emphasis on SST pre-processing and will highlight future directions.

## S2-3: INSTRUMENT NOISE, RETRIEVAL ISSUES OR GEOPHYSICAL SIGNAL

**Peter Cornillon**<sup>(1)</sup>, **Jörn Callies**<sup>(2)</sup>, **Xavier Prochaska**<sup>(3)</sup>

(1) University of Rhode Island, Narragansett, RI, USA, Email: [pcornillon@uri.edu](mailto:pcornillon@uri.edu)

(2) California Institute of Technology, Pasadena, CA, USA, Email: [jcallies@caltech.edu](mailto:jcallies@caltech.edu)

(3) University of California, Santa Cruz, CA, USA, Email: [xavier@ucolick.org](mailto:xavier@ucolick.org)

## S2-4: STUDYING THE THERMAL SKIN LAYER USING THERMOFLUORESCENT DYES

**Peter Minnett**<sup>(1)</sup>, **Françisco Raymo**<sup>(2)</sup>

(1) Rosenstiel School of Marine and Atmospheric Science University of Miami, Miami, FL, USA  
Email: [pminnett@rsmas.miami.edu](mailto:pminnett@rsmas.miami.edu)

(2) Laboratory for Molecular Photonics, Department of Chemistry University of Miami, Miami, FL, USA,  
Email: [fraymo@miami.edu](mailto:fraymo@miami.edu)

## **S2 - POSTER PRESENTATIONS – ABSTRACTS**

## **S2-P1: THE NOAA STAR SOCD OCEANVIEW (OV): AN APPLICATION FOR INTEGRATED VISUALIZATION OF SATELLITE, IN SITU, AND MODEL DATA & OCEAN EVENTS – THE DEBUT RELEASE**

**Prasanjit Dash<sup>(1)</sup>, Paul DiGiacomo<sup>(2)</sup>**

(1) NOAA NESDIS STAR SOCD; CSU CIRA, USA, Email: [prasanjit.dash@noaa.gov](mailto:prasanjit.dash@noaa.gov)

(2) NOAA NESDIS STAR SOCD; USA, Email: [paul.digiacomo@noaa.gov](mailto:paul.digiacomo@noaa.gov)

### **ABSTRACT**

The NOAA STAR SOCD OceanView (OV) is a web-based visualization application delivering an integrated display of remote sensing, in situ, and model output data over oceans, coastal waterways, and inland bodies of water. The recent release (v1.0 on 19 May 2021; v1.1 on 19 Jun 2021) is the culmination of nearly two years of work, from vision to design and implementation. OceanView's release follows a rigorous development and beta testing period beginning this past winter, and the debut verbal presentation and live demo were made at an AGU workshop in May 2021 (see reference).

OV's objective is to assist the satellite remote sensing community, oceanographers, researchers, ocean enthusiasts, students, and the general public in understanding these diverse water bodies in space and over time, both from a synoptic and an event-scale perspective. The OV incorporates data and products primarily from NOAA and some non-NOAA partner sources, spanning satellites, airborne and field platforms, and environmental modeling output.

OceanView will contribute to global earth observing activities, including the Committee on Earth Observation Satellites (CEOS) Coastal Observations, Applications, Services and Tools (COAST) Ad Hoc Team, as well as the Group on Earth Observations (GEO) Blue Planet and AquaWatch initiatives. These efforts are directed to the UN Decade of Ocean Science for Sustainable Development. The OV also contributes to the GHRSSST task team on climatology and L4 intercomparison.

### **INTRODUCTION**

Several agencies worldwide generate a large amount of remotely sensed and modeled products along with a sizeable amount of in situ measurements invaluable for the satellite oceanography community. These data assist in characterizing the state of the ocean and the overlying atmosphere, e.g., Sea Surface Temperature (SST), Ocean Color (OC), Sea Surface Height (SSH), Sea Surface Salinity (SSS), Sea Surface Wind (SSW), Geostrophic Surface Currents, True Color images, and various model data, e.g., Global Forecast Model (GFS) 10m wind speed. These datasets help us to incrementally improve upon our past understanding of the ocean and provide situational awareness. However, an integrated visualization of these images from an oceanographer's perspective is still non-trivial, although such efforts are rapidly evolving and gaining popularity. Along this line of evolution, the OceanView (OV) is a recently launched web-based geospatial viewer and event tracker developed at the Satellite Oceanography and Climate Division (SOCD) of NOAA STAR. Its objective is to assist ocean-enthusiasts and satellite data users in viewing the ocean's state and associated events using products primarily from NOAA STAR SOCD and other NOAA line offices and a few datasets from NASA WorldView. The OV is accessible from <https://www.star.nesdis.noaa.gov/socd/ov/>. The OV version 1.1 has several satellite/model products ingested in it: twelve SST, six chlorophyll-a, six sea wind, one sea surface height anomaly, one true-color image, two atmospheric information, i.e., rain rate and aerosol, three derived information, i.e., geostrophic currents, SAR hurricane windspeed images, and polar flight navigation, GFS model wind, NCEI IBTrACS storm track, NOAA oil spill location and information, and an experimental Level-4 thermal front. Other information to be included in the next version is marine heatwaves, polar flight images, HABs, ship tracks, and more. Besides serving the satellite remote sensing community and ocean enthusiasts, the OV will also contribute to other space-based earth science efforts (GEO Blue Planet Initiative, AquaWatch).

### **FIGURES AND TABLES**

Figure 1 is a snapshot of the web-based viewer accessible from <https://www.star.nesdis.noaa.gov/socd/ov/>.

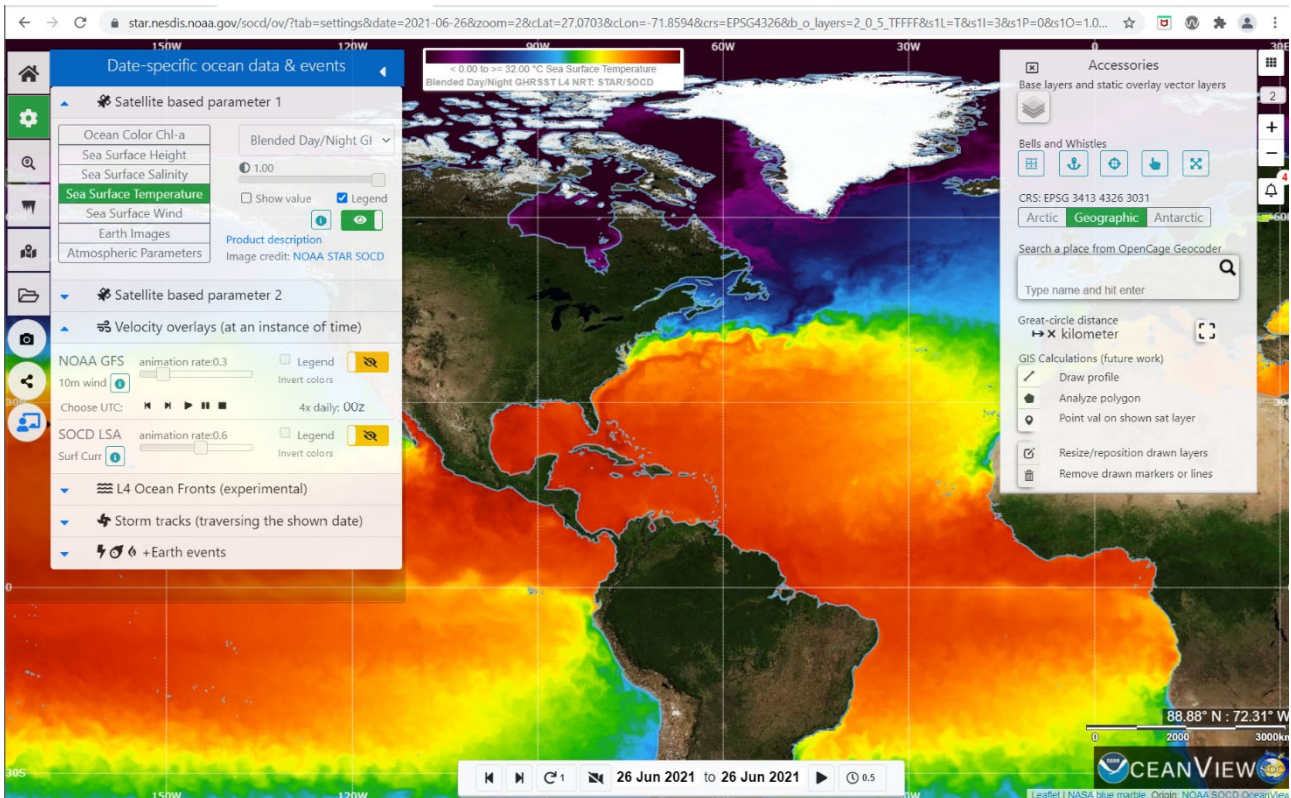


Figure 1: The NOAA STAR SOCD OceanView. The image is of SOCD blended level-4 SST.

Table 1 summarizes the features and applications (existing or future) available in OceanView.

Map controls & interactions	Scientific	Technology	Related efforts
zoom, pan, resize, multiple layers raster (on top or side-by-side) opacity, show value, legend vector vector animation multiple CRS export screen display display local file (desktop app) permalink, social media share customizable entry points semantic search (future)	various ocean, cryosphere, and selected atmosphere parameters deep-dive fronts (profiler) deep-dive polar flight path navigation (profile) track/search natural events track artificial objects visualize surface current motion visualize satellite/model/in situ (future)	opensource tools/formats OGC WMTS (JPL MRF) Python, JAVA, C, GDAL Leaflet, JS, jQuery client-side processing architecture original front-end design UX/UI has a high focus. graphical tour	support AquaWatch/GeoBl uePlanet customized application for CEOS COAST AdHoc project support polar Panarctic missions (near future)

Table 1: Current capabilities and future potential in OceanView (OV).

**OUTCOME**

The OceanView will continue to support the intercomparison task team on cross-consistency checks of various level-4 SST-based thermal fronts. Currently, only one L4 product has been tested, and we are exploring expanding it to other level-4 products contingent upon our available resources. Also of interest is to use multiple information for interpreting the cross-comparison results, such as sea surface height anomaly (SSHA) and geostrophic currents, in discussion with the community. We invite those interested in

contributing ideas in this direction. In addition, as identified through multiple side discussions, we are also exploring the possibility of including high-resolution products useful specifically for coastal applications, which comprises both spaceborne and airborne images.

## **OUTLOOK**

The OceanView (OV) framework development will continue in different phases with future planned enhancements that will incorporate additional data sources, features, and technologies. The identified other data sources include Operation Icebridge Digital Mapping System (DMS) polar images, Marine Heatwave products, NOAA Real-Time Ocean Forecast Systems surface parameters, NSIDC pan-Arctic, and pan-Antarctic Sea Ice Concentration (SIC), and additional data products.

## **REFERENCES**

Dash, P. and P. DiGiacomo, The NOAA STAR SOCD OceanView (OV): An Upcoming Web Application for Integrated Visualization of Satellite, In Situ, and Model Data & Ocean Events, American Geophysical Union (AGU) Workshop on 'Bringing Land, Ocean, Atmosphere and Ionosphere Data to the Community for Hazard Alerts'. **24-28** May 2021 (<https://agu.confex.com/agu/21workshop2/meetingapp.cgi/Paper/789611>).

## **ACKNOWLEDGMENTS**

Marouan Bouali developed the level-4 thermal front generation algorithm, and we are collaborating on improving it and extending it to biological fronts. Thanks to NASA GSFC (Ryan Boller), NASA JPL (Joe Roberts) for critical technological discussions and insight of NASA WorldView, and the use of some GIBS tiles. The use of various data produced by NOAA STAR SOCD science teams and publicly distributed either via the Coastwatch program or publicly accessible online media is acknowledged. Also, thanks to the colleagues for beta testing feedback: NASA JPL (Vardis Tsontos, Jorge Vazquez, Thomas Huang, Ed Armstrong); NOAA STAR (Casey Shoup, Lori Brown, Joe Sapp, John Knaff, Sathyadev Ramachandran, Tyler Ruff, Andy Harris).

## **S2-P2: The intermittency of Sea Surface Temperature: a global perspective**

**Jordi Isern-Fontanet(1) (2), Antonio Turiel(1) (2) , Cristina González-Haro(1) (2)**

<sup>(1)</sup> Institut de Ciències del Mar (CSIC), Barcelona, EU

<sup>(2)</sup> Barcelona Expert Centre in Remote Sensing, Barcelona, EU

The observed patterns in Sea Surface Temperature (SST) are a manifestation of the direct cascade of potential energy from large scales towards small scales. The hallmark of such a turbulent cascade is the intermittency of SST. Recently, we have proposed a new approach to investigate and quantify it. The proposed approach, which has its roots in the Multifractal Theory of Turbulence, has allowed to develop new metrics to characterize the variability of SST and has underlined the importance of the strongest fronts to reproduce the statistical properties of SST variability.

Preliminary results has shown that, the investigation of intermittency using real SST observations presents two difficulties that need to be understood: the noise present in observations and the masking of strong fronts by cloud detection algorithms. A key step necessary to address these problems is the characterization of intermittency and SST variability at a global scale. To this end we have analyzed the SST issued from realistic numerical simulations of the global ocean. These simulations have spatial resolutions close to SST observations (~ 2 km) and temporal samplings of the order of 1 hour. The firsts results of this analysis will be presented and discussed and compared with some real observations.

## S2-P3: IS THERE A NEED FOR YET ANOTHER MODEL TO ACCOUNT FOR SST DIURNAL VARIABILITY?

Ioanna Karagali<sup>(1),(2)</sup>, Jacob Høyer<sup>(2)</sup>, Jun She<sup>(2)</sup>, Jens Murawski<sup>(2)</sup>

(1) Technical University of Denmark - DTU Wind Energy, Frederiksborgvej 399, Roskilde, Denmark, Email: [ika@dmi.dk](mailto:ika@dmi.dk)

(2) Danish Meteorological Institute - DMI, Lyngbyvej 100, Copenhagen, Denmark, Emails: [jlh@dmi.dk](mailto:jlh@dmi.dk), [js@dmi.dk](mailto:js@dmi.dk), [jmu@dmi.dk](mailto:jmu@dmi.dk)

### INTRODUCTION

Exchange of heat, gas and momentum between the ocean and atmosphere depends on the near-surface oceanic and lower atmospheric layers and their properties. Sea Surface Temperature (SST) is an essential climate variable that due to its contribution to air-sea interaction mechanisms. SST's day-time variability is triggered by moderately low winds and solar heating has long been of interest for the GHRSSST community and beyond. Diurnal warming events have been observed in the Mediterranean Sea (Merchant et al. 2008), the Gulf of California (Ward, 2006), the Atlantic Ocean (Karagali and Høyer, 2014), the Baltic Sea (Karagali et al. 2012) and the Arctic (Eastwood et al., 2011) using combinations of in situ and satellite observations. Some components of diurnal variability and cool skin effects (Fairall et al, 1996) have been reproduced (Fallmann et al., 2017) by forced ocean and coupled ocean-atmosphere models, the vertical grid resolution of such systems is of meter-scale and overall, no consensus on the numerical representation of diurnal SST variability has been reached. This can result in erroneous heat budget estimates (Ward, 2006) and inconsistent merging of SSTs from different satellite sensors with a direct impact on efforts to create climate records (Donlon et al., 2007). Furthermore, a misrepresentation in the diurnal variability of upper ocean temperature can result in errors when modelling harmful algal blooms, which are promoted by high SST values (Kahru et al., 1993).

A wide suite of numerical approximations to reproduce and resolve diurnal SST variability have been developed, ranging from statistical relations based on local measurements (e.g. Filipiak et al., 2012) to turbulence closure models (e.g. Kantha and Clayson, 1994), with mixed results in reproducing the amplitude, frequency and shape of the diurnal cycle. Within the latter concept, the present study, supported by the Copernicus Marine Service (CMEMS) Service Evolution through the project "Improved Diurnal Variability Forecast Of Ocean Surface Temperature through Community Model development (DIVOST-COM)", focused on applying the existing one-dimensional General Ocean Turbulence Model (GOTM, Buchard et al., 1999) for large scale simulations in the Baltic Sea, using initial conditions for the state of the ocean and atmosphere from the CMEMS Baltic Modelling & Forecasting Centre (MFC) 3D physical-biological HIROMB-BOOS Model (HBM) and the HARMONIE atmospheric component, respectively. The aim was to assess how and if GOTM and the operational HBM system reproduced diurnal variability compared to hourly infrared SST retrievals from SEVIRI. Furthermore, utilising GOTM's high vertical resolution capabilities, to assess the depth range for which the CMEMS SST TAC Level 4 North/Baltic Sea analysis product can be considered representative. To achieve this, GOTM simulations were compared to HBM outputs and the CMEMS SST TAC Level 4 North/Baltic Sea analysis for night-time conditions and to SEVIRI SST during day-time. Data and methods used for the simulations and comparisons are described in Section 2, main findings are presented in Section 3, discussions and conclusions follow in sections 4 and 5.

### DATA AND METHODS

#### Model description

The General Ocean Turbulence model solves the one-dimensional equations for the transport of heat, momentum, and salt allowing for different options for the description of turbulence quantities (Buchard et al. 1999); version 5.4 was used, available from GitHub (<https://github.com/gotm-model/>). The first-order K- $\epsilon$  turbulence scheme from Burchard and Baumert (1995) was used in agreement with Pimentel et al., (2008). Surface heat and momentum fluxes were calculated from surface meteorological variables using the bulk algorithm of Fairall et al. (1996) including skin and warm layer adjustments. For the attenuation of light in the water column, a new parameterization was added (e.g. Karagali et al., 2017); a 9-band model with attenuation lengths and proportional coefficients from Paulson and Simpson (1981). Large scale simulations

over the Baltic Sea domain were performed for the period June-August 2018, with a finely resolved vertical grid consisting of 34 layers for the upper 25 m of the water column. Of these, 25 layers were placed within the top 5 meters with layer thickness ranging from 0.05 m to 1 m.

#### Forcing fields

Hourly values of the u- and v- wind components, pressure, air temperature, humidity, rain and shortwave radiation at the surface were obtained from HARMONIE (Yang et al., 2017); a non- hydrostatic, mesoscale forecast system jointly developed by the international HIRLAM (High Resolution Limited Area Model) consortium in collaboration with Meteo France and the ALADIN consortium. Hourly data for the 3D parameters of interest, i.e. ocean temperature and salinity profiles, were obtained from the CMEMS operational physical product for the Baltic Sea (BALTIC\_SEA\_ANALYSIS\_FORECAST\_PHY\_003\_006) (CMEMS, 2018), based on simulations with the HBM ocean model HIROMB-BOOS-Model (Aas et al, 2013).

#### Validation data

Hourly sub-skin SST (Donlon et al., 2007) from the Spinning Enhanced Visible/Infrared Imager (SEVIRI) on the geostationary Meteosat Second Generation (MSG), gridded at a 0.058 regular grid, was obtained from the Ocean & Sea Ice Satellite Application Facility (O&SI SAF, 2013) through IFREMER/CERSAT for 2013. Only SEVIRI retrievals with a quality flag of 3 and higher (maximum 5) are used, to exclude ambiguous retrievals. For direct comparisons between GOTM 2D simulations, HBM and SEVIRI, the model grids are re-sampled to match the SEVIRI grid, which is coarser than the simulations; approximately 5.5 by 3.5 km for the domain of interest. The SST TAC provides a state-of-the art Level 4 (L4) SST product for the North and Baltic Seas, primarily based on L2P SST satellite data from different producers (NASA, NOAA, IFREMER and EUMETSAT OSI-SAF) in GHRSSST compliant format. The L2P data currently used in DMI OI include infra-red data from the AVHRR instruments on board NOAA and MetOp-A satellites, SEVIRI on board the MSG satellite, VIIRS on board Suomi NPP and SLSTR data from Sentinel 3 A and B (CMEMS, 2019). To avoid contamination from observations affected by diurnal warming, only observations between 19.00 in the evening and 8.00 in the morning local time are used. When comparisons between GOTM 2D, HBM and L4SST are considered, the latter is re-gridded to match the HBM and GOTM 2D grid.

### COMPARISONS OF SST SIMULATIONS WITH L4SST AND SEVIRI

The L4SST is representative of night-time, well mixed conditions assumed to be free of diurnal variability and is used to assess the performance of HBM and GOTM at various depths; in addition, this is expected to provide insight on the depth range for which the L4SST is most representative. For each grid point of their common grid, HBM and GOTM simulations for 00-04 am were averaged into single values and the differences  $HBM_d - L4SST$  and  $GOTM_d - L4SST$ , were estimated for the period June-August 2018, where the subscript "d" indicates the depth. GOTM depth layers have a finer vertical resolution, two approaches were used for the comparison, GOTM Int was integrated to the HBM vertical grid, while comparisons were also performed using the individual GOTM depth level closer to the one from HBM. Table 1a shows the mean, median and standard deviation values for the comparisons at four selected depths of the HBM grid and the associated GOTM integrated and closest grid level. For the depth of zero meters, metrics are lowest for HBM-L4SST compared to GOTM (both integrated and single layer), yet the differences are in the order of 0.03-0.05°C. For depths of 5m and down to 15m, integrated GOTM temperatures at those depths show better metrics against L4SST compared to HBM and the single-layer GOTM method and differences can be up to 0.5°C. Table 1b shows GOTM-L4SST metrics for various GOTM depths, at a high vertical resolution not available by the operational HBM simulations. The depth for which metrics for the  $GOTM_d - L4SST$  are minimised, ranges between 0.5m and 0.9m. To assess the capability of HBM and GOTM in capturing diurnal warming, day-time comparisons were limited to the interval 06:00-18:00 when SEVIRI SST retrievals of quality 3 or higher were available and the SEVIRI "dt\_analysis" parameter was at least 1°C in at least one grid point of the domain. Table 1c shows the mean, median and standard deviation between HBM, GOTM and SEVIRI for various depths; all metrics are lowest for the GOTM simulations representative of the top model layer.

Metric	Depth (m)	HBM-L4SST	GOTM (LE8) Int-L4SST	GOTM (LE8)- L4SST	Depth (m)	Mean (°C)	Median (°C)	Std. (°C)	Metric	Depth (m)	HBM-SEVIRI	GOTM-SEVIRI LE8-vs.4
Mean (°C)	0	<b>-0.29</b>	-0.35	-0.34	0.0025	-0.35	-0.11	1.44	Mean (°C)	0	-1.17	<b>-0.93</b>
	5	-0.48	<b>-0.43</b>	-0.48	0.45	<b>-0.34</b>	<b>-0.09</b>	<b>1.45</b>		0.5	—	-1.18
	10	-1.71	<b>-1.33</b>	-1.94	0.90	-0.34	-0.09	1.46		1.0	—	-1.32
	15	-3.93	<b>-3.43</b>	-3.96	1.50	-0.36	-0.10	1.47		1.5	—	-1.43
	5	-0.07	-0.10	-0.09	3.00	-0.41	-0.12	1.54		5	-1.62	-1.79
Median (°C)	0	-0.15	<b>-0.13</b>	-0.16	4.67	-0.48	-0.16	1.59	Median (°C)	0	-0.86	<b>-0.72</b>
	5	-0.82	<b>-0.71</b>	-1.12	5.80	-0.67	-0.3	1.69	0.5	—	-0.91	
	10	-3.12	<b>-2.67</b>	-3.12	10.60	-1.94	-1.12	2.7	1.0	—	-1.02	
	15	1.41	1.46	1.45					1.5	—	-1.12	
	5	1.63	<b>1.57</b>	1.59					5	-1.27	-1.46	
Std (°C)	0	2.69	<b>2.18</b>	2.70					Std (°C)	0	1.40	<b>1.31</b>
	5	3.86	<b>3.46</b>	3.82					0.5	—	1.36	
									1.0	—	1.41	
									1.5	—	1.44	
									5	1.52	1.52	

Table 1: Comparison of HBM, GOTM, L4SST and SEVIRI. Left: Night-time comparisons using HBM reference depth, middle: GOTM-L4SST at various GOTM depths, right: day-time HBM, GOTM and SEVIRI.

### DIURNAL VARIABILITY ESTIMATES

Diurnal signals were computed from night-time foundation temperatures; the latter were computed by averaging SST for 00-04 am of each day at each grid point, separately for SEVIRI, HBM and GOTM. The top layer for each model was used, i.e. 2 m for HBM and 2.5 mm for GOTM. To estimate the hourly “temperature anomaly”, the foundation temperature was subtracted from the hourly temperature; positive anomalies indicate warming. The maximum temperature anomaly for each grid point and day was recorded while the mean of the temperature anomaly and its standard deviation were computed only for positive anomalies. A statistical analysis of diurnal warming for temperature above 18°C, considered indicative of conditions favourable for cyanobacteria blooms in the Baltic Sea, was also performed. Figure 1 shows an example of the mean diurnal variability for June 01 2018 as estimated from GOTM (left), SEVIRI (middle) and HBM (right). GOTM reproduces the patterns and amplitude of mean diurnal variability found in the SEVIRI observations, e.g. 1.5°C-2°C amplitude on the eastern part of the basin as well as between the Gotland island and east coast of Sweden; yet such patterns are mostly absent in the HBM simulations (right).

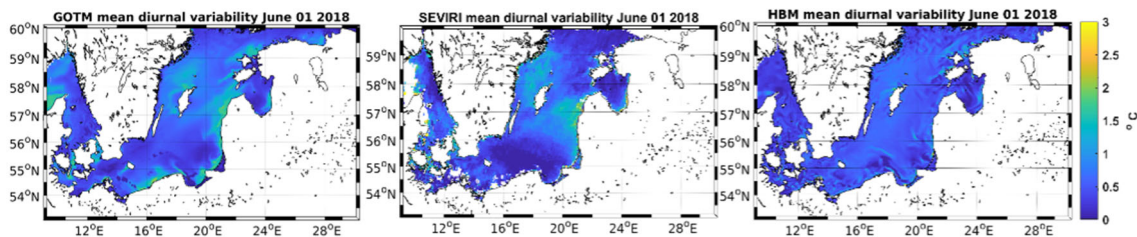


Figure 1: Example of mean diurnal warming on June 1st 2018 from GOTM, SEVIRI, HBM.

Based on the mean diurnal variability during the period June to August 2018 the mean diurnal cycle was estimated as the mean hourly value over the given period and for all grid points in the domain that indicated a positive anomaly from the night-time foundation value. Figure 2a) shows a pronounced mean diurnal cycle from SEVIRI (blue), reaching up to 1.4°C warming at 14:00. GOTM (red) reproduces well the shape of the diurnal cycle, albeit with a 1-hour delay in the initiation of the morning warming phase and its peak, which also has a significantly reduced amplitude reaching at 0.7°C, i.e. half of the SEVIRI value. HBM (yellow) misses the shape of the diurnal cycle, as observed by SEVIRI, with a very slow increase during day-time, peaking at approximately 17:00-18:00, only reaching 0.55 °C and an almost non-existent cooling phase. Figure 2b) shows histograms, normalised over the total number of cases in each dataset, of coincident temperature anomalies above 1°C when the temperature is 18°C and higher, indicating that SEVIRI and GOTM have very similar distributions especially for warming above 1.6°C while HBM reproduces most warming between 1°C and 1.4°C.

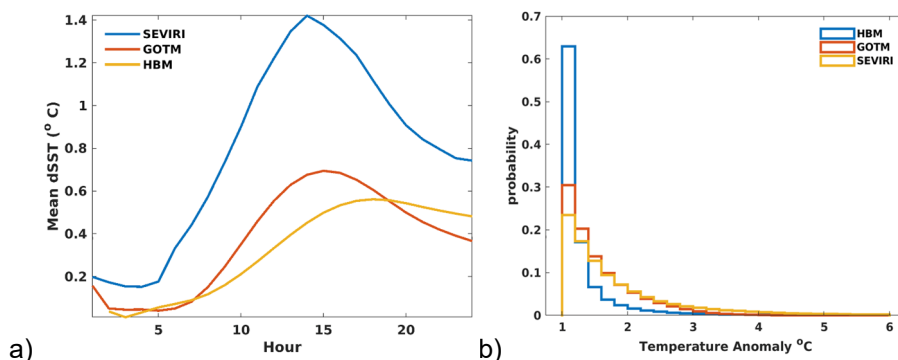


Figure 2: Example of mean diurnal warming on June 1st 2018 from GOTM, SEVIRI, HBM.

## CONCLUSIONS

GOTM and HBM simulations showed overall good comparison when averaged night-time temperatures were compared to the North Sea/Baltic Sea dedicated L4 SST product. GOTM's finer vertical resolution allowed for identification of a representative depth for the L4SST, manifested as the depth for which metrics were lowest, between 0.5 m and 1 m. Day-time comparisons against SEVIRI SST retrievals indicated that GOTM simulations showed lower mean and median biases and standard deviation values, compared to HBM. GOTM was able to better resolve the spatial patterns of mean diurnal warming, as observed from SEVIRI, and overall provide a better representation of the diurnal cycle albeit to a lesser amplitude than the observed one. For spatial patterns to be accurately resolved, forcing fields play an important role especially when the spatial patterns and timing of favourable conditions coincide. SEVIRI observations showed large potential warming during day-time even when SST was above 18°C, which is considered proxy condition to enhance algal blooms. This warming was poorly resolved by HBM in terms of frequency and amplitude, while GOTM was able to approximate the conditions described by the observations. Such findings support GOTM as a candidate model to simulate daily diurnal variability estimates.

## REFERENCES

- Aas, E., Højerslev, N.K., Høkedal, J., and K. Sørensen, Optical water types of the Nordic Seas and adjacent areas, *Oceanologia* **55**, 2013.
- Burchard, H. and H. Baumert, On the performance of a mixed-layer model based on the  $k-\epsilon$  turbulence closure, *J. Geophys. Res.* **100**, 1995.
- Burchard, H., Bolding, K., and M. Villarreal, GOTM - A general ocean turbulence model. Theory, applications and test cases, Technical Report EUR **18745** EN, European Commission, 1999.
- CMEMS Product User Manual for Baltic Sea Physical Analysis and Forecasting Product, Copernicus Marine Service **2** edition, 2018.
- CMEMS Product User Manual for Baltic Sea SST 4 Products, Copernicus Marine Service **2.7** edition, 2019.
- Donlon, C., Rayner, N., Robinson, I., Poulter, D.J.S., Casey, K.S., Vazquez-Cuervo, J., Armstrong, E., et al., The Global Ocean Data Assimilation Experiment High-resolution Sea Surface Temperature Pilot Project, *B. Am. Meteorol. Soc.* **88**, 1197-1213, 2007.
- Eastwood, S., Borgne, P.L., Péré, S., and D. Poulter, Diurnal variability in sea surface temperature in the Arctic, *Remote Sens. Environ.* **115**, 2594-2602, 2011.
- Fairall, C.W., Bradley, E.F., Godfrey, J.S., Wick, G.A., Edson, J.B., and G.S. Young, Cool-skin and warm-layer effects on sea surface temperature, *J. Geophys. Res. Oceans* **101**, 1295-1308, 1996.
- Fallmann, J., Lewis, H., Castillo, J.M., Arnold, A., and S. Ramsdale, Impact of sea surface temperature on stratiform cloud formation over the North Sea, *Geophys. Res. Lett.* **44**, 2017.
- Filipiak, M. J., Merchant, C.J., Kettle, H., and P.L. Borgne, An empirical model for the statistics of sea surface diurnal warming. *Ocean Sci.* **8**, 197-209, 2012.
- Kahru, M., Leppanen, J.-M., and O. Rud, Cyanobacterial blooms cause heating of the sea surface, *Mar. Ecol. Prog. Ser.* **101**, 1-7, 1993.

- Kantha, L.H., and C.A. Clayson, An improved mixed layer model for geophysical applications, *J. Geophys. Res.* **99**, 25235-25266, 1994.
- Karagali, I., Høyer, J., and C. Hasager, SST diurnal variability in the North Sea and the Baltic Sea, *Remote Sens. Environ.* **121**, 2012.
- Karagali, I. and J. Høyer, Characterisation and quantification of regional diurnal SST cycles from SEVIRI, *Ocean Sci.* **10**, 2014.
- Karagali, I., Høyer, J., and C. Donlon, Using a 1-D model to reproduce the diurnal variability of SST, *J. Geophys. Res. Oceans* **122**, 2017.
- Merchant, C.J., Filippiak, M. J., Borgne, P.L., Roquet, H., Autret, E., Piollé, J.-F., and S. Lavender, Diurnal warm-layer events in the Western Mediterranean and European shelf seas, *Geophys. Res. Lett.* **35**, L04601, 2008.
- OSISAF, Geostationary Sea Surface Temperature (Products OSI 206, 207) Product User Manual, Ocean Sea Ice Satellite Application Facility, EUMETSAT, 1.3 edition, 2013.
- Paulson, C.A. and J.J. Simpson, The temperature difference across the cool skin of the ocean, *J. Geophys. Res.* **86**, 1981.
- Pimentel, S., Haines, K., and N.K. Nichols, Modeling the diurnal variability of sea surface temperatures, *J. Geophys. Res.* **113**, C11004, 2008.
- Ward, B., Near-surface ocean temperature, *J. Geophys. Res.* **111**, C02004, 2006.
- Yang, X., Andersen, B.S., Dahlbom, M., Hansen Sass, B., Zhuang, S., Amstrup, B., Petersen, C., et al., NEA - the operational implementation of HARMONIE 40h1.1 at DMI, Technical Report **8**, ALADIN-HIRLAM Newsletter, 2017.

## **S2-P4: Observations of Infrared SST Autonomous Radiometer (ISAR) Skin Temperatures in the Seas around Korean Peninsula, Indian Ocean, and Northwest Pacific**

**Kyung-Ae Park** <sup>(1)</sup>, **Hee-Young Kim** <sup>(2)</sup>, and **Hye-Jin Woo** <sup>(2)</sup>

(1) Department of Earth Science Education / Research Institute of Oceanography, Seoul National University, Korea. Email: kapark@snu.ac.kr

(2) Department of Earth Science Education, Seoul National University, Korea

This study presents preliminary results on Infrared SST Autonomous Radiometer (ISAR) measurements in the seas around Korean Peninsula in recent years. ISAR observations have been also conducted in the Indian Ocean (19 March - 14 April, 2019) and the Northwest Pacific (13–26 May, 2020) using R/V ISABU in 2019 and 2020. An additional cruise for ISAR measurements has been conducted in the eastern region off the Korean Peninsula from 21 April to 6 May 2020. For understanding characteristics of skin-bulk temperature differences, the temperature differences between ISAR measurements and shipborne thermosalinograph data were analyzed. Atmospheric and oceanic variables such as air temperature, sea surface wind, currents were also measured during the cruises for the study area. The temperature differences between ISAR skin temperatures and the thermosalinograph presented well-known features of the previous literature. The observation data revealed diurnal variations of the skin-bulk temperatures, which showed a good agreement with the previous studies. In the study region, diurnal variations of the differences, cool-skin effect, daytime warm biases, and wind effects were well presented. The temperature differences showed a large range from  $-2$  K to 5 K at low winds ( $<3$  m/s) at 12-15h, while a small range from  $-1$  K to 1 K at high winds of 12-15 m/s. Compared with the previous studies, the present measurements indicated relatively large amplitudes of the positive differences amounting to 5 K in daytime and to  $-2.2$  K in night. More cruise observations need to be performed for further understanding skin-bulk temperature differences.

## **S2-P5: REVEALING FUNDAMENTAL SST PATTERNS WITH DEEP LEARNING**

**J. Xavier Prochaska<sup>(1)</sup> and Peter Cornillon<sup>(2)</sup>**

(1) University of California, Santa Cruz;

(2) University of Rhode Island

We have developed an Artificial Intelligence model termed a probabilistic autoencoder (PAE) to analyze ~12,000,000 128x128 pixel<sup>2</sup> regions extracted from the MODIS AQUA Level 2 SST dataset. These were restricted to nighttime and to areas with less than 5% cloud coverage. While our initial study focused on the most extreme SST patterns (i.e., outliers; Prochaska, Cornillon, Reiman 2021), the PAE latent vectors (akin to EOF coefficients) enable global analyses of the full SST distribution. Here, we will examine the fundamental SST patterns of the ocean and explore their spatial and temporal distribution to assess the underlying ocean dynamics. We will also briefly describe development of the PAE model and our plans to share the analysis products with the community for new investigations.

## **SCIENCE SESSION 3**

### **CALIBRATION, VALIDATION AND PRODUCT ASSESSMENT**

### S3 - Session Report

**Chair: Sandra Castro<sup>(1)</sup>, Rapporteur: Yukio Kurihara<sup>(2)</sup>**

(1) University of Colorado, Boulder, USA, Email: [sandrac@colorado.edu](mailto:sandrac@colorado.edu)

(2) JAXA EORC, Japan, Email: [ykuri.kiyo@gmail.com](mailto:ykuri.kiyo@gmail.com)

## HIGHLIGHTS

- Saharan dust events can decrease surface shortwave radiation (~190 W/m<sup>2</sup>) and increase surface long-wave radiation (~14 W/m<sup>2</sup>). Corresponding SST<sub>skin</sub> changes suggest dust-induced cooling effects as large as -0.24 K during daytime and a warming effect of up to 0.06 K during daytime and nighttime respectively
- Level 2 SST are in very good agreement with in situ Saildrone measurements, yet derived gradients are not, likely due to sensor noise

## INTRODUCTION

The session consisted of pre-recorded oral presentations, along with presentations in poster format. All presentations were available for viewing throughout the week of the meeting, and discussions were facilitated via Moodle forums.

## RESOURCES

- View presentations (recordings): <https://training.eumetsat.int/mod/book/view.php?id=14071&chapterid=630>
- Discussion forum for recordings: <https://training.eumetsat.int/mod/forum/view.php?id=14076>
- Download the slides: <https://training.eumetsat.int/mod/folder/view.php?id=14077>
- Posters padlet: <https://padlet.com/TrainingEUMETSAT/klmswuubrmqci0pg>

## **ORAL PRESENTATIONS**

**Werenfrid Wimmer, Uncertainty validation of shipborne radiometers**

Discussion: Werenfrid Wimmer presented validation results for the Infrared Sea Surface Temperature Autonomous Radiometers (ISAR), based on an uncertainty model of shipborne radiometers, evaluated against inter-comparisons with other ISAR and SiSTeR radiometers. Results indicate an overestimation of the ISAR uncertainty. Sandra Castro, Jon Mittaz, and Wimmer discussed possible causes of the overestimation in the ISAR uncertainty, such as systematic errors in ISAR-to-ISAR comparisons (Sandra) and the impact of correlated errors (Jon). Wimmer explained that maybe not all components of the uncertainty are being captured in the current model.

**Haifeng Zhang, A completeness and complementarity analysis of the data sources in iQuam**

Discussion: Haifeng presented analyses on the completeness and complementarity of the data sources ingested by iQuam and summarized results for each platform (drifting and moored buoys, ships, and Argo floats). Helen Beggs, Haifeng, and Sasha Ignatov discussed the comparison of in situ data against CMC L4 to assess the relative quality of the different types of in situ sensors. Igor Tomazic, Haifeng, and Sasha discussed data consistency between different data sources. The reply from Haifeng is that the number of matchups differ among data sets due to differences in initial QC methods and resolutions.

**Bingkun Luo, Saharan dust effects on North Atlantic sea surface skin temperatures**

Discussion: Luo presented impacts of the Saharan dust on the skin temperatures based on in situ data (M-AERI and radiosonde datasets) and radiative transfer simulations using RRTMG (Rapid Radiative Transfer Model for General Circulation Models Applications). Gary Wick and Luo discussed the effect of dust on the air temperatures. The reply from Luo is that the effect of the dust is mainly on the shortwave radiation and the effect on the turbulent fluxes is not significant.

## **POSTER PRESENTATIONS**

**Jorge Vazquez, Evaluation of AIRS and CrIS SST measurements relative to three globally gridded SST products between 2013 and 2019.**

Discussion: Jorge discussed validation result of SSTs from AIRS on EOS Aqua and CrIS on SNPP. The results were obtained from comparisons against the RTG, CMC, and OSTIA L4 SST analyses. Sandra Castro asked a question about the reason for the seasonal variation in the standard deviations of the difference of AIRS against CMC and OSTIA at high latitudes; there was no response.

**Boyin Huang, Assessment and intercomparison of NOAA Daily Optimum Interpolation Sea Surface Temperature (DOISST) version 2.1.**

Discussion: Boyin presented validation results of the NOAA DOISST version 2.1, and other seven L4 SST products, against buoy and Argo data. Helen suggested the results should be published, and Boyin replied that he submitted a paper and it is under review at the time of the discussion. Helen and Boyin discussed whether the observed bias was introduced by the bias correction of satellite-based SSTs (using SSES) and about future plans for validating DOISST using Argo data.

**Marouan Bouali, Using Saildrone campaigns to assess the accuracy of SST gradients in Level 2 SST datasets**

Discussion: Marouan presented validation results of SST gradients in Terra/Aqua MODIS and SNPP VIIRS L2 SST datasets obtained from comparisons against Saildrone data. Helen and Marouan discussed validation of SST gradients using the 70m-resolution ECOSTRESS products and its effectiveness. Marouan showed interest in the NASA ECOSTRESS high-resolution data. Prasanjit and Marouan discussed the importance of the day/night comparisons and the observation requirements for the comparison. Yukio and Marouan discussed possible causes for the low gradient correlation and the benefits of correlation analysis over a particular range of gradients.

**Igor Tomazic, EUMETSAT SLSTR SST multi-mission matchup database: ongoing work, TRUSTED MDB and evolutions**

Discussion: The poster introduces the SLSTR SST Multi-mission Matchup Database (MMDB). Collocations against the MMDB confirm that SLSTR SST satisfies the accuracy requirements.

**Yukio Kurihara, Validation SGLI SST**

Discussion: Helen and Yukio discussed inter-comparison of SGLI and VIIRS. The reply from Yukio was that it is difficult because the difference in the orbits between SGLI and VIIRS. Prasanjit and Yukio discussed why the statistics of the V3 appear slightly degraded from the V2. Yukio replied that the statistics are reasonable when the wind speed (WS) is higher than 6 m/s and that the result for WS > 6 m/s suggests that the statistics for V3 are, in fact, more realistic than the V2 ones. Prasanjit showed interest in SGLI V3 test data.

## **S3 - ORAL PRESENTATIONS - ABSTRACTS**

### S3-1: UNCERTAINTY VALIDATION OF SHIPBORNE RADIOMETERS

**Werenfrid Wimmer<sup>(1)</sup>**

(1) University of Southampton, European Way, Southampton, SO14 3ZH, UK  
Email: [w.wimmer@soton.ac.uk](mailto:w.wimmer@soton.ac.uk)(2)

#### INTRODUCTION

With a number of satellite sensors providing high quality sea surface temperature (SST) products, the need for validation data of a similar quantity is increasing. This is especially true for the Copernicus Sentinel-3 Sea and Land Surface Temperature Radiometer (SLSTR). In order to address the need for such reference data sources ESA is building on almost 15 years of continuous Fiducial Reference Measurements (FRM) from UK-funded shipborne radiometers by establishing a service to provide historic and ongoing FRM measurements to the wider SST community through an International SST FRM Radiometer Network (ships4sst).

One of the key components of FRM are the uncertainty models and per measurement uncertainty. These uncertainty models have only been validated in the laboratory during inter-comparison and their theoretical basis has been verified. However field comparison of two or more shipborne radiometers have been limited, mainly due to cost, and as a result no at sea comparison of the uncertainty models has been conducted to date. This paper will first show the data from side by side of shipborne radiometers comparison in 2015, 2018, 2019 and 2020 and second the validity of the uncertainty models in the at sea conditions. Furthermore the possible improvements to the shipborne radiometer models will be shown on the example of the Infrared Sea-surface temperature Autonomous Radiometer (ISAR) uncertainty model.

#### UNCERTAINTY MODELS

Uncertainty models can be fairly simple, especially in linear uncertainty propagation model, as they only require adding the quadrature, as how in equation 1:

$$\sigma = \sqrt{\sigma_1^2 + \sigma_2^2 + \dots + \sigma_n^2} \quad (\text{Eq. 1})$$

For more complex instrumentation the simple adding of adding the uncertainty in quadrature is not sufficient and the measurement equation and all its components has to be considered (GUM, 1995). For ISAR the uncertainty model was derived by analyzing the measurement equation, shown in equation 2 and all its components. A simplified schematics of the uncertainty components of ISAR are shown in figure 1.

$$\text{SST} = \frac{R2T*(R_{\text{sea}} - (1-\epsilon)R_{\text{sky}})}{\epsilon} \quad (\text{Eq. 2})$$

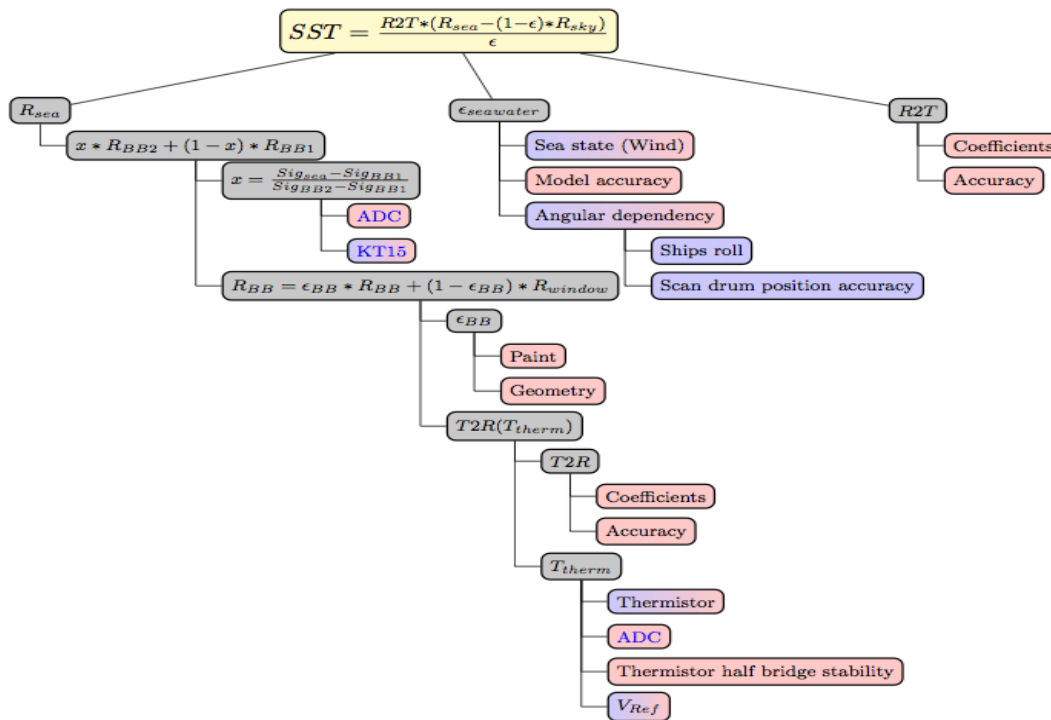


Figure 1: The ISAR uncertainty model flow chart, boxes shaded in red are type B uncertainties and boxes 1. shade in blue are type A uncertainties.

2.

For a full description of the ISAR uncertainty model see Wimmer and Robinson (2016).

**DATA**

The data for the uncertainty validation was collected on four different ship measurement campaigns as shown in table 1. All campaigns used ISAR 03 which has been also used on all inter-comparison campaigns including the FRM4STS project. There is a slight bias towards comparing ISAR data with ISAR data in the calibration data, this is not deliberate but was due to instrument availability and cost implications.

The data was produced in ships4sst netcdf L2R files and went through the standard shipborne radiometer quality control process. Data acquired at ships speed lower than 2kts was excluded.

Table 1: Uncertainty validation measurement campaigns.

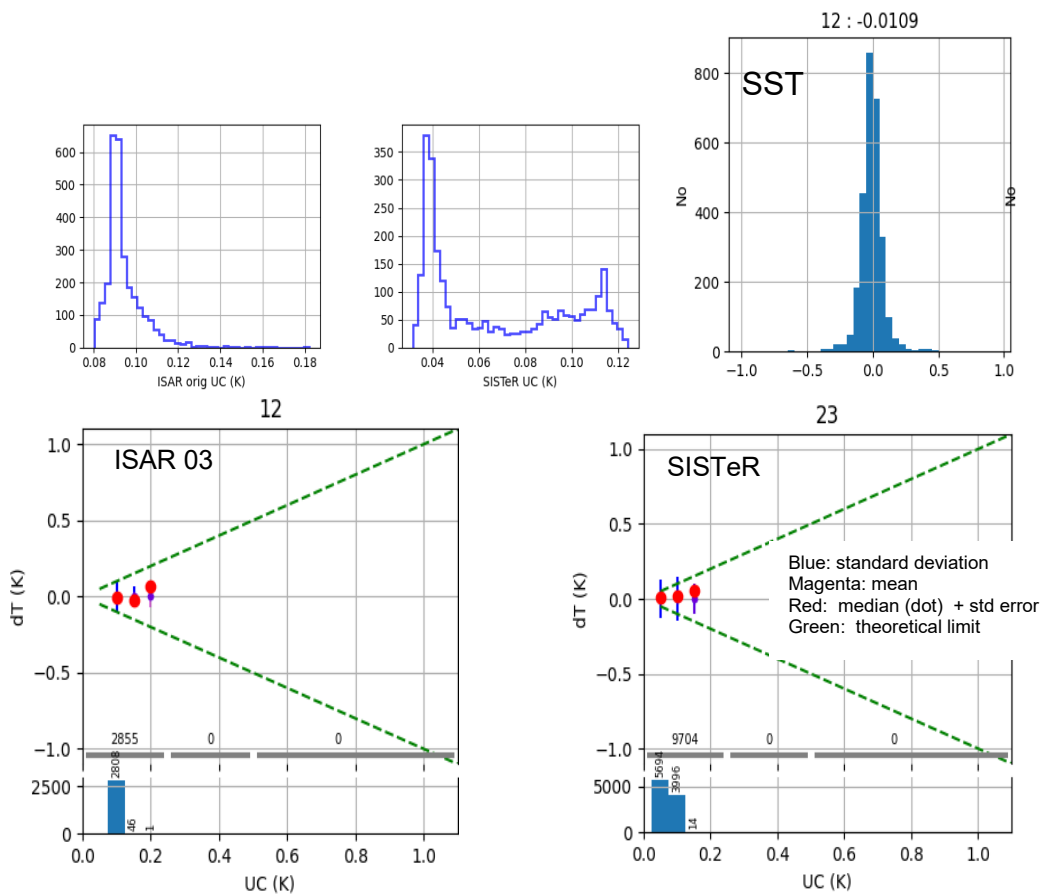
Date	Ship	Radiometer 1	Radiometer 2
18.10. – 05.11. 2015	M/V Queen Mary 2	ISAR 03	SISTeR A
24.09. – 29.10. 2018	RRS James Clark Ross	ISAR 03	ISAR 12
12.10. - 22.11. 2019	RRS Discovery	ISAR 03	ISAR 07
01.09. – 23.09. 2020	M/V Friedrichshafen	ISAR 03	KIT KT15

**UNCERTAINTY VALIDATION**

The uncertainty validation is split into the four different measurement campaigns as different instruments and oceanographic areas are covered by each of those four campaigns.

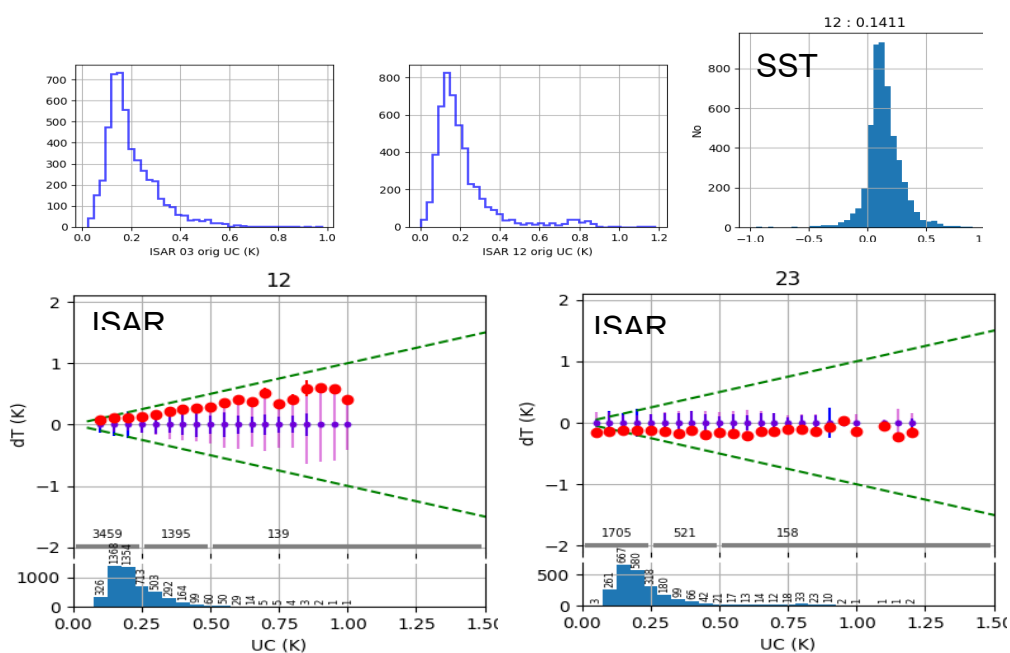
**ISAR-SISTeR – Queen Mary 2**

Figure 2: ISAR - SISTeR uncertainty validation, the top two left hand panels show the histogram of the ISAR (left) and SISTeR (right) per SST uncertainty. The right hand top panel shows a histogram of the SST difference between SISTeR and ISAR with a mean difference of -0.011 K. The bottom two panels show the SST difference as a function of the radiometer uncertainty, for ISAR on the left and for SISTeR on the right. Blue lines show the standard deviation in each uncertainty bin, Magenta lines show the mean in each uncertainty bin, Red dots show the median and the error bar shows the standard error around the median, and finally the green dashes show the theoretical limit the uncertainty should follow. At the bottom of both bottom panels there are histograms showing the number of data points in each uncertainty bin and a grouping of data points below 0.25K, 0.5K and above 0.5K in gray.



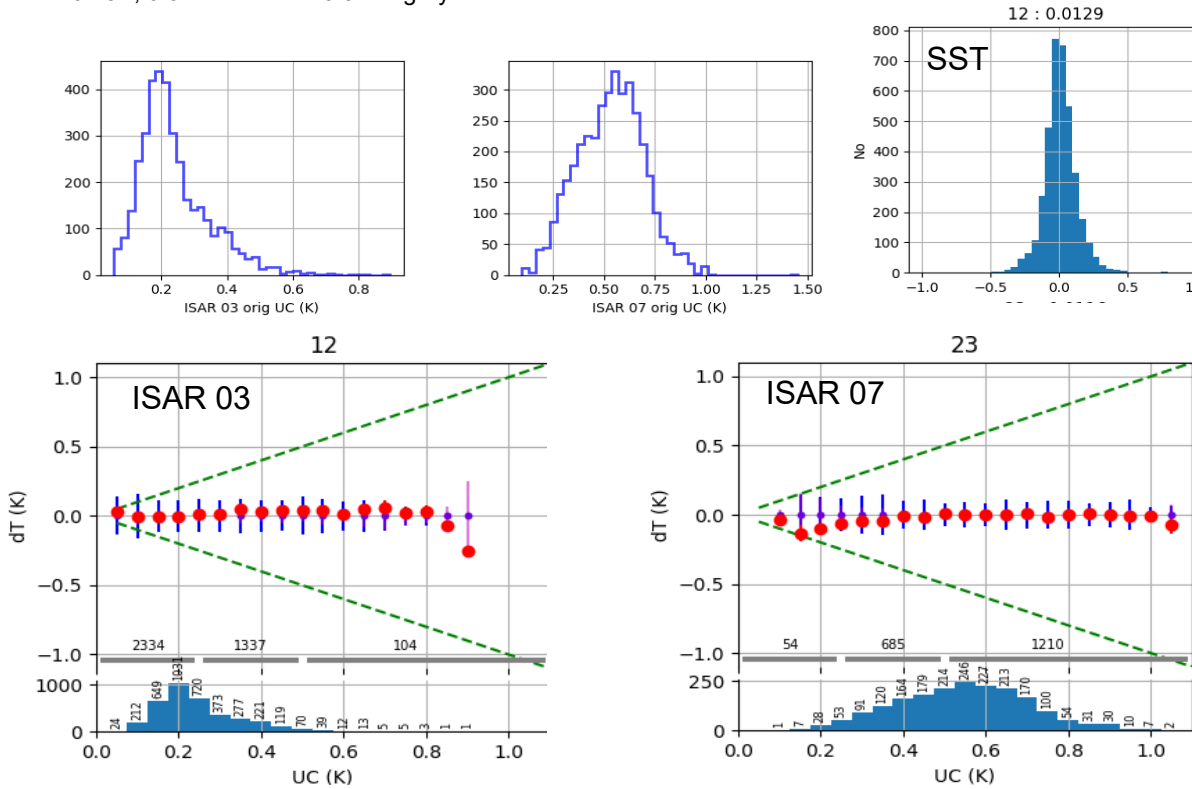
### ISAR - ISAR – James Clark Ross

Figure 3: ISAR 03– ISAR 12 uncertainty validation, the top two left hand panels show the histogram of the ISAR 03 (left) and ISAR 12 (right) per SST uncertainty. The right hand top panel shows a histogram of the SST difference between ISAR 12 and ISAR 03 with a mean difference of 0.14 K . The bottom two panels show the SST difference as a function of the radiometer uncertainty, for ISAR 03 on the left and for ISAR 12 on the right. Blue lines show the standard deviation in each uncertainty bin, Magenta lines show the mean in each uncertainty bin, Red dots show the median and the error bar shows the standard error around the median, and finally the green dashes show the theoretical limit the uncertainty should follow. At the bottom of both bottom panels there are histograms showing the number of data points in each uncertainty bin and a grouping of data points below 0.25K, 0.5K and above 0.5K in gray.



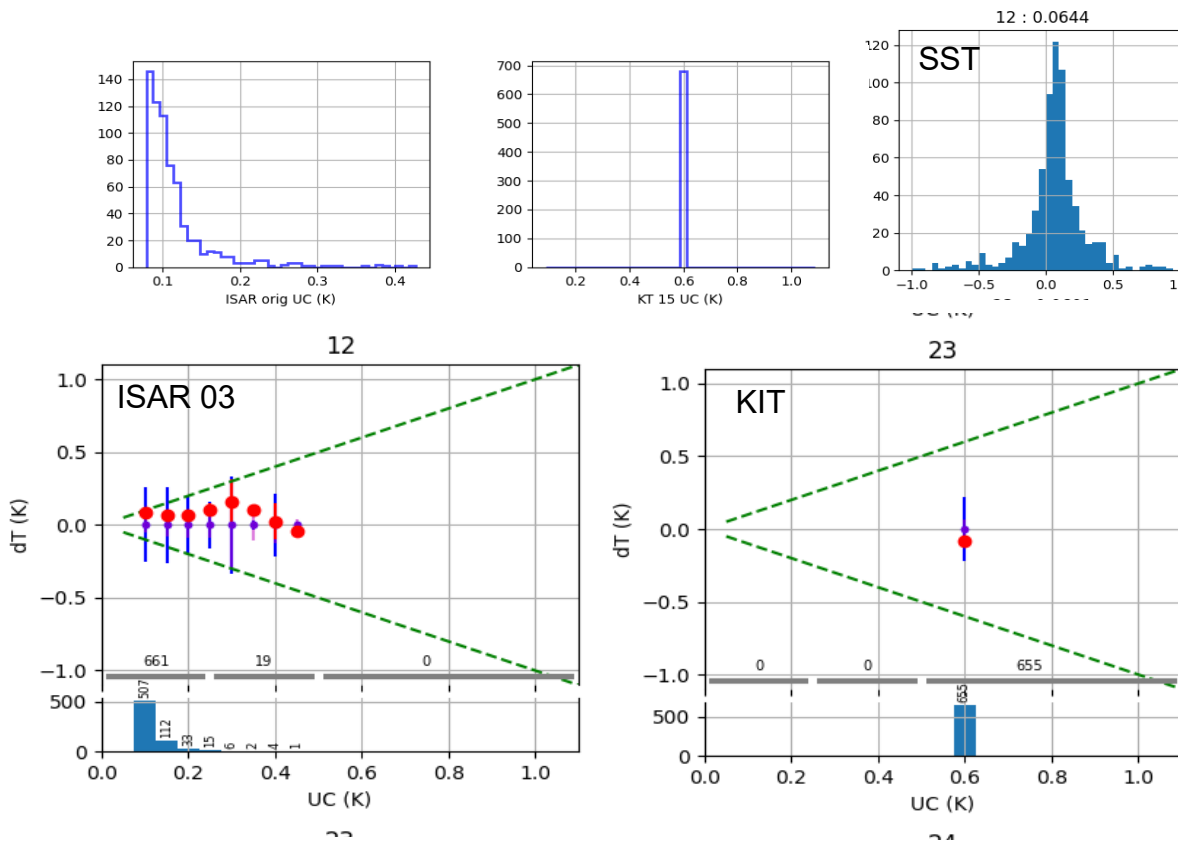
### ISAR – ISAR – Discovery

Figure 4: ISAR 03– ISAR 07 uncertainty validation, the top two left hand panels show the histogram of the ISAR 03 (left) and ISAR 07 (right) per SST uncertainty. The right hand top panel shows a histogram of the SST difference between ISAR 07 and ISAR 03 with a mean difference of 0.013 K. The bottom two panels show the SST difference as a function of the radiometer uncertainty, for ISAR 03 on the left and for ISAR 07 on the right. Blue lines show the standard deviation in each uncertainty bin, Magenta lines show the mean in each uncertainty bin, Red dots show the median and the error bar shows the standard error around the median, and finally the green dashes show the theoretical limit the uncertainty should follow. At the bottom of both bottom panels there are histograms showing the number of data points in each uncertainty bin and a grouping of data points below 0.25K, 0.5K and above 0.5K in gray.



**ISAR – KIT – Friedrichshafen**

Figure 5: ISAR 03–KIT uncertainty validation, the top two left hand panels show the histogram of the ISAR 03 (left) and KIT (right) per SST uncertainty. The right hand top panel shows a histogram of the SST difference between ISAR 07 and KIT with a mean difference of 0.064 K . The bottom two panels show the SST difference as a function of the radiometer uncertainty, for ISAR 03 on the left and for KIT on the right. Blue lines show the standard deviation in each uncertainty bin, Magenta lines show the mean in each uncertainty bin, Red dots show the median and the error bar shows the standard error around the median, and finally the green dashes show the theoretical limit the uncertainty should follow. At the bottom of both bottom panels there are histograms showing the number of data points in each uncertainty bin and a grouping of data points below 0.25K, 0.5K and above 0.5K in gray.



**UPDATED ISAR UNCERTAINTY MODEL**

The result of the uncertainty validation showed that in general the ISAR uncertainty model produces uncertainties which are too large, which is mainly due to the roll dependence of the emissivity model and unresolved covariance matrix dependencies in the measurement equation.

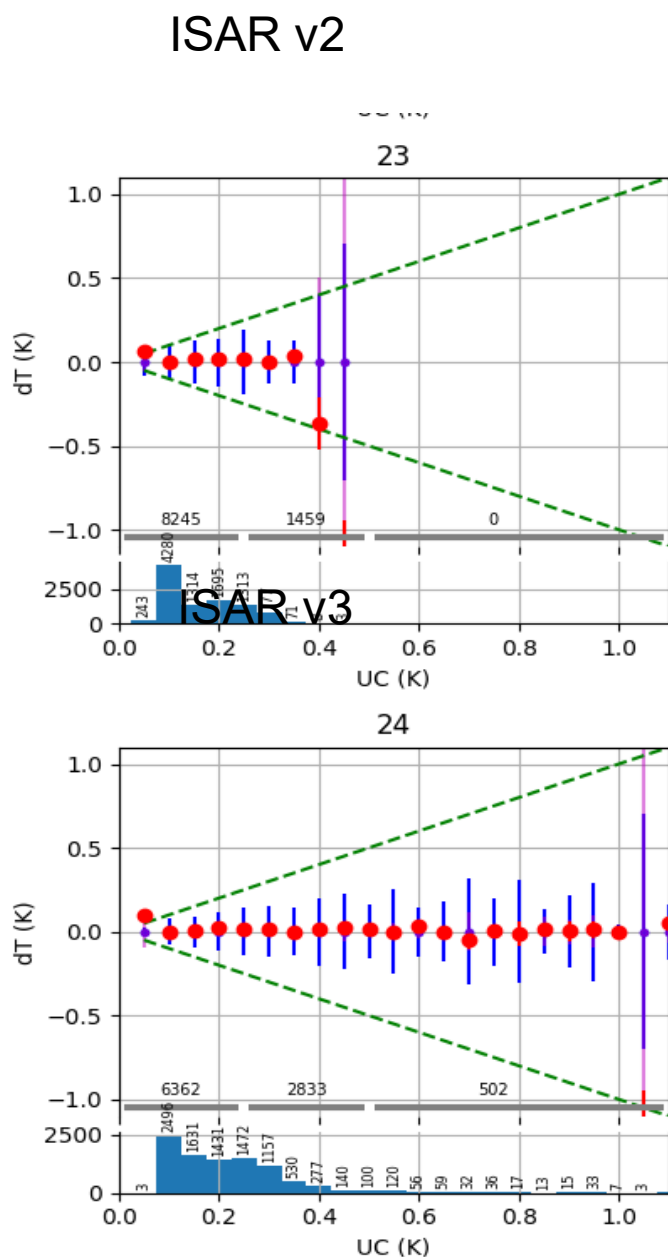
While the roll dependence was reduced by Hanning filtering the roll measurements of ISAR, resolving cross correlation dependencies requires a lot more work and has not been included in the new uncertainty model. The following changes have been made for the ISAR uncertainty model V2:

- Roll is Hanning filtered, length is 11 values
- Sky, sea signal over 5 SST samples
- Centre Weighted average - 1, 4, 4, 1
- Variance of the signal gets added to the sea and sky signal uncertainty before internal calibration

And V3 adds an extra uncertainty variable as and geophysical indicator of variability in the SST to the data to aid identification of environments which will produce higher SST mismatches. The indicators used is the standard deviation over the weighted SST from 5 SST samples.

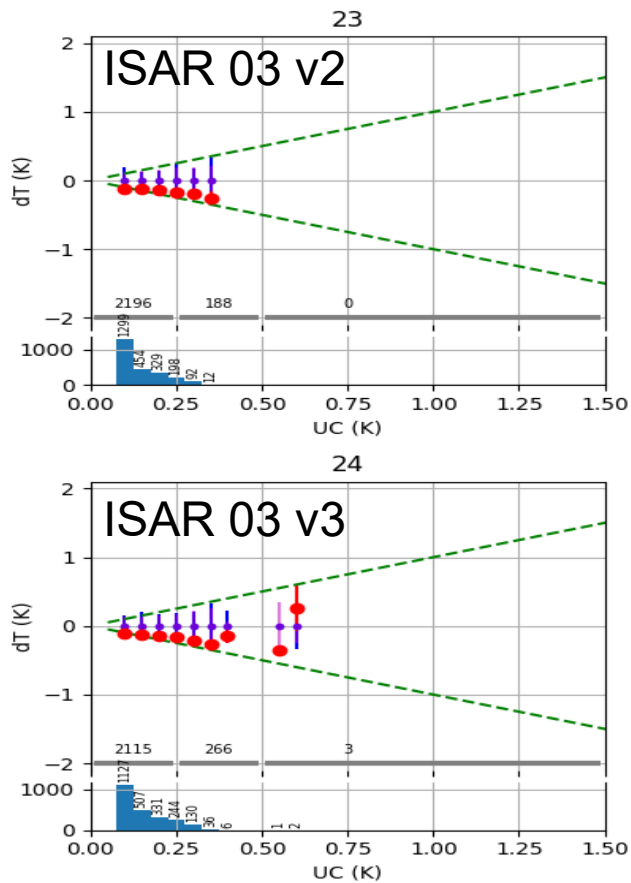
**ISAR-SISTeR – Queen Mary 2**

Figure 6: ISAR - SISTeR uncertainty comparison, new ISAR uncertainty model V2 (top) and V3 (bottom). The plot colours are the same as in section 4.



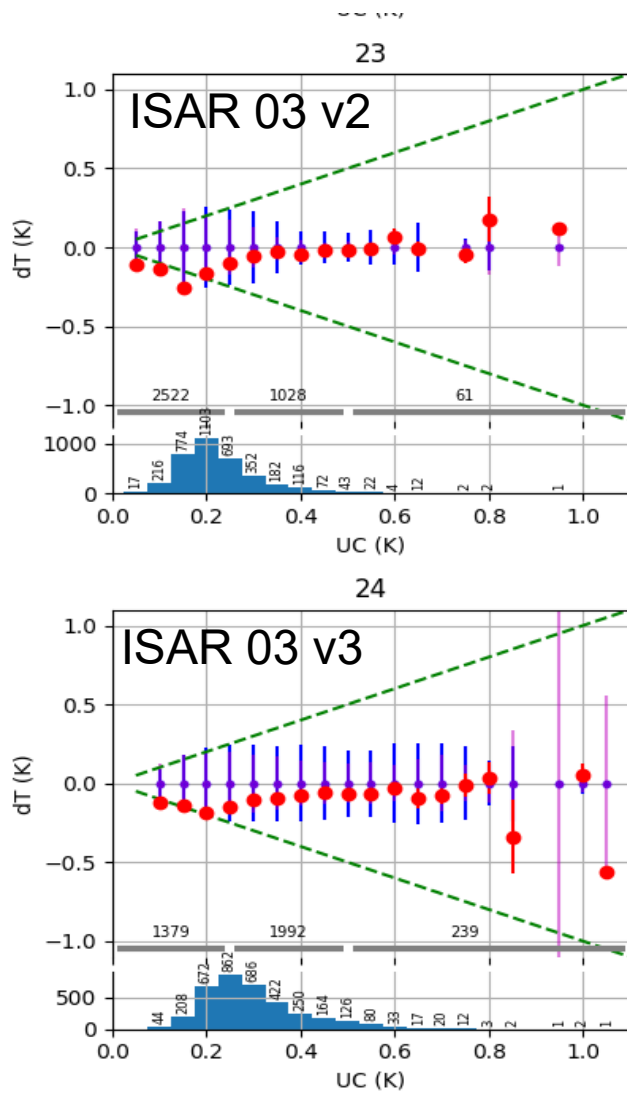
**ISAR - ISAR – James Clark Ross**

Figure 7: ISAR 03 - ISAR12 uncertainty comparison, new ISAR uncertainty model V2 (top) and V3 (bottom). The plot colours are the same as in section 4.



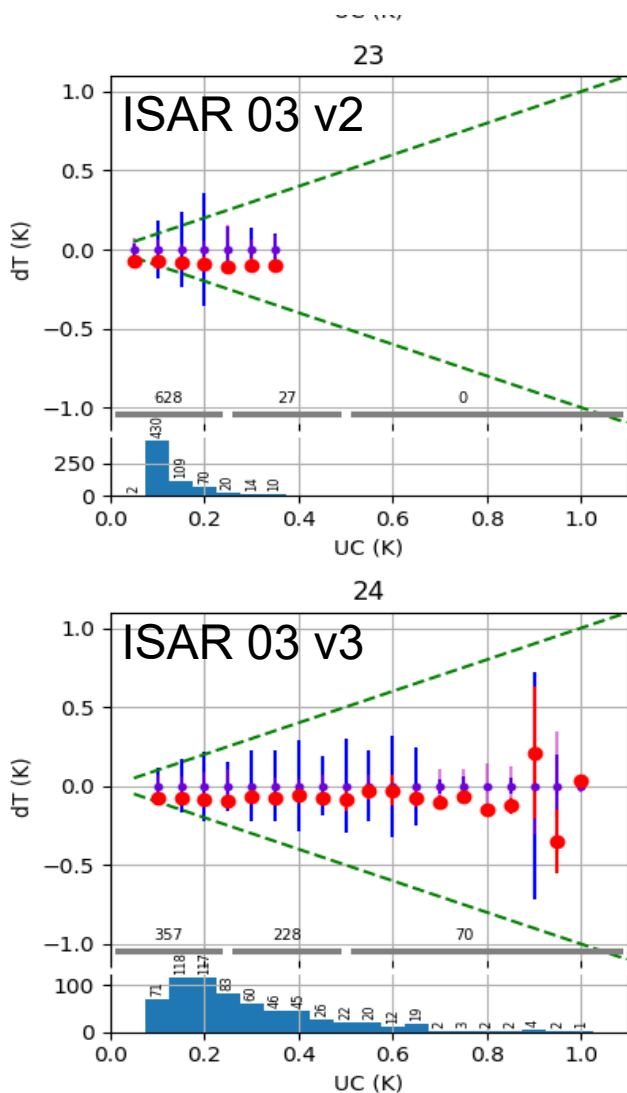
**ISAR – ISAR – Discovery**

Figure 8: ISAR 03 – ISAR 07 uncertainty comparison, new ISAR uncertainty model V2 (top) and V3 (bottom). The plot colours are the same as in section 4.



**ISAR – KIT – Friedrichshafen**

Figure 9: ISAR 03 – KIT uncertainty comparison, new ISAR uncertainty model V2 (top) and V3 (bottom). The plot colours are the same as in section 4.



**CONCLUSION**

Field inter-comparisons are essential for ensuring the validity of uncertainty estimates. However because of the time and effort it takes to conduct field inter-comparisons there have not been many carried out for shipborne radiometers. The paper showed four such inter-comparisons in a range of conditions, but also showed that there are very few data points for high uncertainties making larger uncertainties very difficult to verify. Over 70 percent of the data showed uncertainties below 0.25 K and over 95% of the data showed uncertainties lower than 0.5K (not k=2 here).

The inter-comparisons showed that, in general, the ISAR uncertainties (Wimmer and Robinson, 2016) are too large. This is mainly due to the roll dependence of the sea water emissivity model used in the uncertainty estimation. The other issue is that while the measurement equation was used to derive the

uncertainty model the covariance matrix does have some unresolved issues which would need a great deal of work and funding to be resolved.

An updated version of the ISAR uncertainty model was presented, which resolves most of the issues, however does not explain all the issues shown in the uncertainty validation. The remaining issues are non trivial to solve and are:

- Type B uncertainties which are not perfect, as we rely on literature to estimate them
- Covariance issues of the measurement equation
- Real physical differences not measured → this is a more a match-up uncertainty than part of the instrument uncertainty

## REFERENCES

BIPM, IEC, IFCC, ISO, IUPAC, IUPAP, OIML. Guide to the Expression of Uncertainty in Measurement. International Organization for Standardization, Geneva. ISBN 92-67-10188-9, First Edition 1993, corrected and reprinted 1995. (BSI Equivalent: BSI PD 6461: 1995, Vocabulary of Metrology, Part 3. Guide to the Expression of Uncertainty in Measurement. British Standards Institution, London.)

Wimmer, Werenfrid and Robinson, Ian S. (2016). The ISAR Instrument Uncertainty Model. Journal of Atmospheric and Oceanic Technology, 33 (11), 2415-2433. ([doi:10.1175/JTECH-D-16-0096.1](https://doi.org/10.1175/JTECH-D-16-0096.1)).

## S3-2: A COMPLETENESS AND COMPLEMENTARITY ANALYSIS OF THE DATA SOURCES IN IQUAM

**Haifeng Zhang<sup>(1)</sup>, Alexander Ignatov<sup>(2)</sup>, Dean Hinshaw<sup>(3)</sup>**

(1) STAR, NOAA Center for Weather and Climate Prediction (NCWCP), College Park, Maryland, USA & Cooperative Institute for Research in the Atmosphere (CIRA), Colorado State University, Fort Collins, Colorado, USA. Email: [haifeng.zhang@noaa.gov](mailto:haifeng.zhang@noaa.gov)

(2) STAR, NOAA Center for Weather and Climate Prediction (NCWCP), College Park, Maryland, USA. Email: [alex.ignatov@noaa.gov](mailto:alex.ignatov@noaa.gov)

(3) STAR, NOAA Center for Weather and Climate Prediction (NCWCP), College Park, Maryland, USA & Global Science and Technology, Inc., College Park, Maryland, USA. Email: [dean.hinshaw@noaa.gov](mailto:dean.hinshaw@noaa.gov)

### INTRODUCTION

In situ sea surface temperature (SST) measurements play a critical role in the calibration and validation (Cal/Val) of satellite SST retrievals (e.g., Saunders, 1967; Donlon et al., 2002; O'Carroll et al., 2008). To facilitate this task, the in situ SST Quality Monitor (iQuam) system was developed at the National Oceanic and Atmospheric Administration (NOAA) in 2009. The iQuam strives to provide the most authoritative Cal/Val standard for the satellite SST community, which is both maximally complete and uniformly quality controlled using a flexible, community consensus QC algorithm (Xu and Ignatov, 2014; Zhang et al., 2021).

In the current iQuam version 2.10, in situ SST from the following platforms are reported: drifting buoys (including heritage and high-resolution, HR, drifters; Le Menn et al., 2019; Poli et al., 2019), ships (including vessels of opportunity, VOS, research vessels, R/V, commercial ships, and the Integrated Marine Observing System, IMOS, ships; Beggs et al., 2012), coastal and tropical moorings, Argo floats and Coral Reef Watch (CRW) buoys. Redundancy is one of the key iQuam principles. Whenever possible, SST data are collected from more than one data source, to provide back-up (in case of occasional outages in individual feeds) and to take advantage of their complementarity, hence ensuring a more complete coverage. For example, drifting buoys in iQuam come from three sources: (1) the International Comprehensive Ocean-Atmosphere Data Set (ICOADS); (2) the Fleet Numerical Meteorology and Oceanography Center (FNMOC); and (3) the Global Telecommunications System (GTS) stream from the NOAA National Centers for Environmental Prediction (NCEP). The three datasets differ, due to different data inputs and processing, and their holdings are not identical. The relative completeness and complementarity of different data sets are often unknown and are the focus of this study. The analyses have been performed for four platform types that are critical for the Cal/Val of satellite retrievals: drifting and moored buoys, ships, and Argo floats.

### DATA SETS

Data sources explored in this study include: (1) ICOADS R3.0.1, (2) FNMOC, (3) Atlantic Oceanographic and Meteorological Laboratory (AOML) drifting buoys, (4) Copernicus Marine Environment Monitoring Service (CMEMS) in situ products, and (5) Argo products. Note that AOML and CMEMS data are not yet ingested into iQuam and are currently under consideration, hence their inclusion in these analyses. Two full years of data from all described datasets (Jan 2016-Dec 2017) are consistently analyzed.

All the analyses are stratified by four in situ platform types: drifting buoys, ships, moorings (including tropical and coastal moorings) and Argo floats.

### RESULTS

#### DRIFTING BUOYS

The summary of the number of UIDs (unique IDs) in each data set is shown in Table 1. Combining all four data sets, we find a total of  $N_{\text{tot}}=4,020$  UIDs, which is considered as 100% in this analysis. The UID numbers found in CMEMS ( $N=3,776$ ) and FNMOC ( $N=3,798$ ) are close yet not identical, accounting for 93.9% and 94.5% of  $N_{\text{tot}}$ , respectively. Fewer UIDs ( $N=3,294$ ) are observed in the AOML dataset (81.9% of  $N_{\text{tot}}$ ). The reason why AOML has ~500 fewer UIDs than CMEMS or FNMOC, is due to processing only SVP drifters.

Data Set	UIDs	Nobs
ICOADS	1,974 (49.1%)	17,002,663
AOML	3,294 (81.9%)	26,194,669
CMEMS	3,776 (93.9%)	26,309,702
FNMOG	3,798 (94.5%)	26,536,008
	Total: 4,020 (100%)	

Table 1. The number of observations (Nobs) and unique IDs (UIDs) in four data sets. The total is the sum of all UIDs observed in all sources and set as 100%.

In contrast, there are only N=1,974 (~49.1%) UIDs included in the ICOADS R3.0.1. Recall that R3.0.1 does not include the 7-digit ID buoys (in 'BUFR' format rather than 5-digit 'TAC') deployed after November 2016. Pending release of ICOADS 3.0.2, the R3.0.1 release is not included in the analyses in this section.

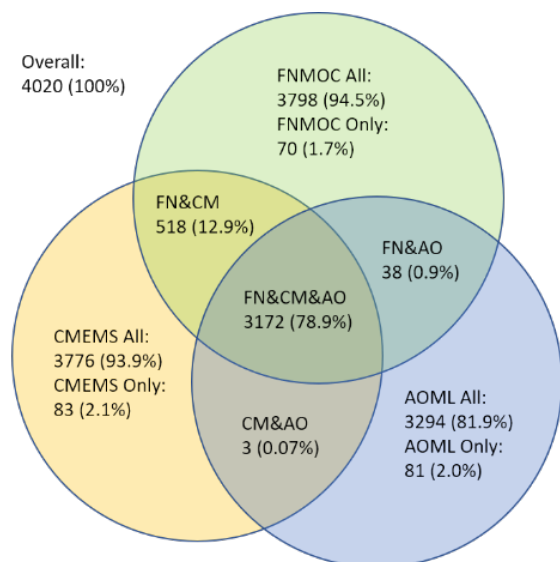


Fig. 1. Distribution of UIDs across the three data sets: CMEMS, AOML, and FNMOG.

### SHIPS

Since CMEMS does not yet include ship SSTs from GTS, only two data sources are used in this section: FNMOG and ICOADS. ICOADS and FNMOG have close amounts of ship UIDs, accounting for 88.0% and 84.0% of  $N_{tot}$ , respectively. In terms of Nobs, FNMOG has a noticeably larger number than that of ICOADS.

Data Sets	UIDs	Nobs
ICOADS	4,442 (88.0%)	4,824,113
FNMOG	4,236 (84.0%)	6,403,646
	Total: 5,046 (100%)	

Table 2. The number of ship UIDs and Nobs in ICOADS and FNMOG. The total is the sum of all UIDs observed in both sources and set as 100%.

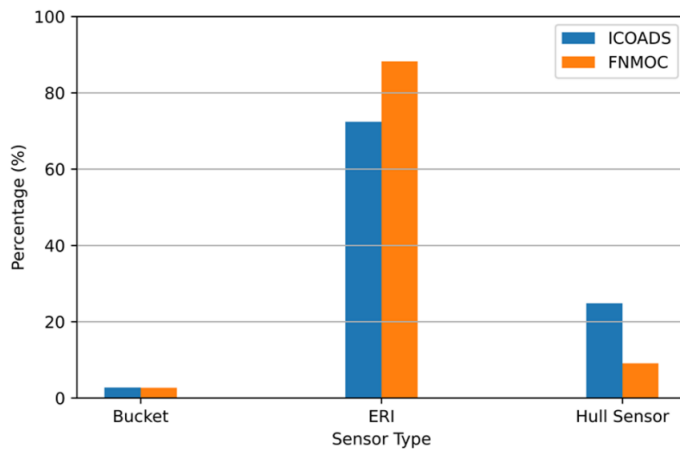


Fig. 2. The normalized distribution of the SST measurements obtained from different ship sensor types, i.e., bucket, Engine Room Intake (ERI), and hull-contact sensors, for ICOADS (blue) and FNMOC (orange).

### MOORINGS

This section focuses on three data sets: ICOADS, CMEMS, and FNMOC.

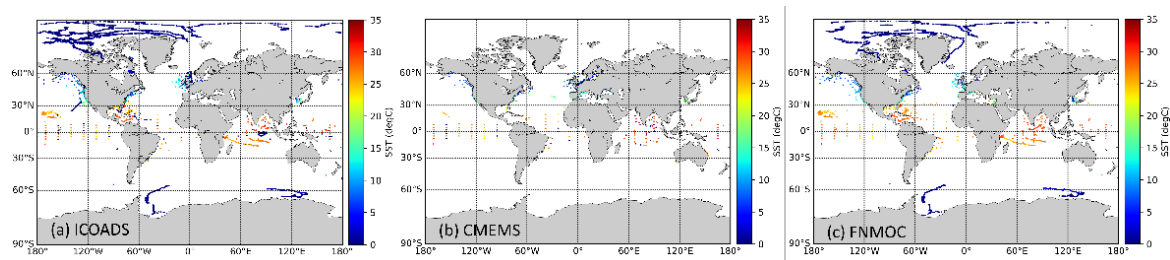


Fig. 3. Spatial distributions of all moorings (coastal + tropical) from: (a) ICOADS, (b) CMEMS, and (c) FNMOC. The color bar represents SST.

Apparently, some 'moorings' are moving (in ICOADS and FNMOC datasets; no 'moving' moorings found in CMEMS). In iQuam, these are identified and re-classified into other platform types (e.g., drifters or ships).

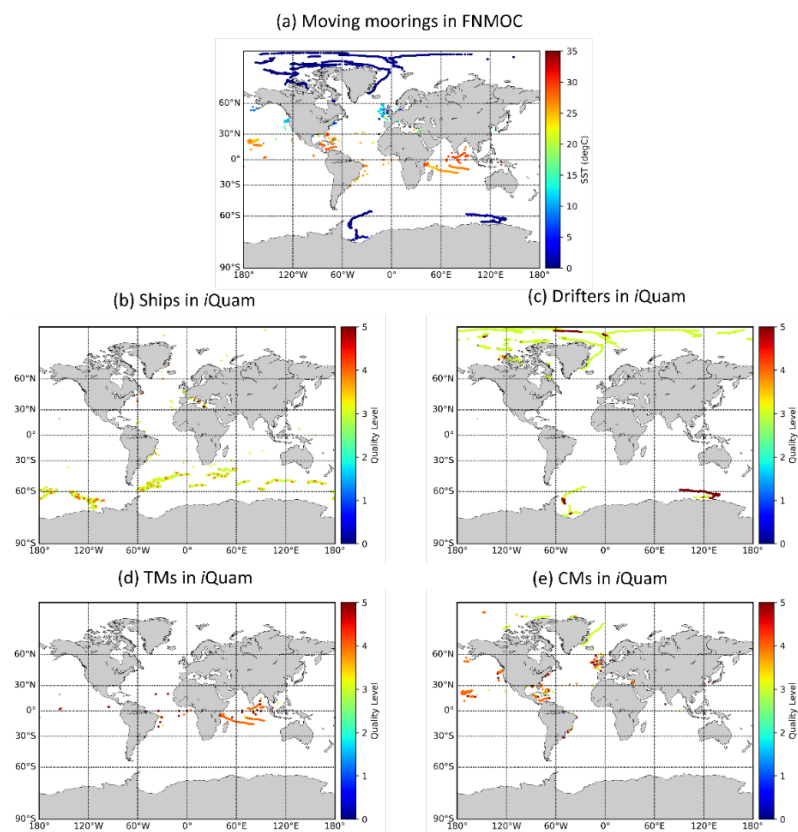


Fig. 4. (a) The ‘moving moorings’ in FNMOC. The color bar indicates SST. These platforms have been reclassified in iQuam as (b) ship, (c) drifting buoys, (d) tropical moorings, and (e) coastal moorings. Note the color bars in panels b-e represent the quality level values in iQuam.

### ARGO FLOATS

Data sources included in this section are from two Argo GDACs (i.e. IFREMER and USGODAE) and CMEMS.

Data Set	UIDs	Nobs
IFREMER	5,173 (100%)	1,320,299
USGODAE	5,173 (100%)	1,320,782
CMEMS	5,138 (99.3%)	4,828,651
	Total 5,173 (100%)	

Table 3. The number of observations and UIDs of Argo floats in three data sets.

Reasons for much larger Nobs in CMEMS are likely due to including measurements from primary and near-surface (< 5 dbar) SST reports. For primary measurements, all three data sources have similar Nobs (Table 3 and Fig. 5b). However, CMEMS has more measurements across the whole pressure range (0-10 dbar) due to the near-surface reports, especially within the 0-1 dbar bin (Fig. 5a).

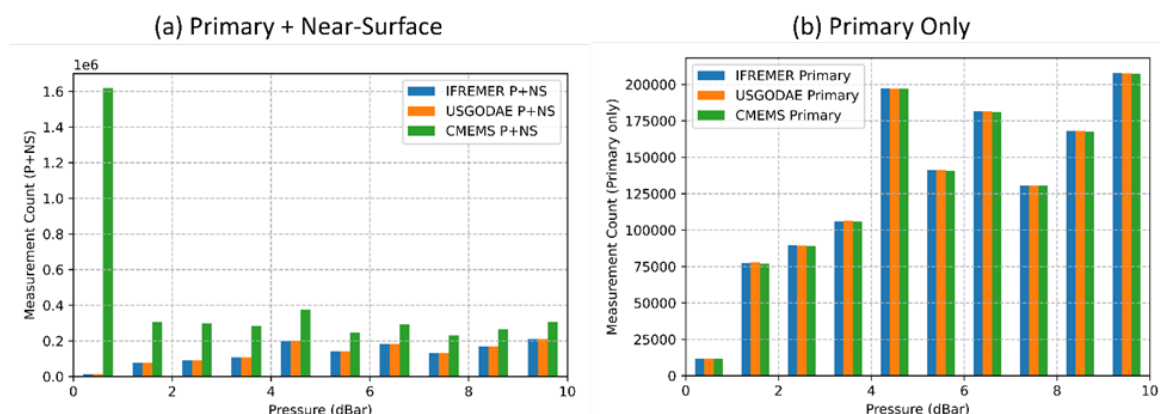


Fig. 5. Distribution of Nobs from all three data sets against pressure: (a) all primary and near-surface scheme measurements are included; and (b) only primary measurements are included.

## CONCLUSIONS

The NOAA in situ SST Quality Monitor (iQuam) aims to collect and distribute, after uniform quality control, a maximally complete set of SSTs obtained from all available in situ platforms. For each in situ data type, iQuam strives to ingest data from several independent sources, to ensure most complete coverage, even at the cost of some redundancy in data feeds. The relative completeness of various data sources and their consistency and mutual complementarity are often unknown, and are the focus of this study. For four platform types customarily employed in satellite Cal/Val (drifting and moored buoys, ships, and Argo floats), five widely known data sets are analyzed, produced by the (1) ICOADS, (2) FNMOC, (3) AOML, (4) CMEMS, and (5) Argo project. Each data set comprises SSTs from one or more platform types. It is found that drifting buoys are more fully represented in FNMOC and CMEMS. Tropical moorings are well represented in ICOADS, FNMOC, and CMEMS. Ships are reported in FNMOC and ICOADS, which are best used in conjunction with each other. Some CMEMS mooring reports are sampled every 10 minutes, compared to 1 hour sampling in the other datasets. While the two Argo official distributors provide nearly identical data sets, CMEMS shows some differences which are currently being explored.

## REFERENCES:

- Beggs, H.M., Verein, R., Paltoglou, G., Kippo, H., Underwood, M., 2012. Enhancing ship of opportunity sea surface temperature observations in the Australian region. *J. Oper. Oceanogr.* 5, 59–73. <https://doi.org/10.1080/1755876X.2012.11020132>.
- Donlon, C.J., Minnett, P.J., Gentemann, C., Nightingale, T.J., Barton, I.J., Ward, B., Murray, M.J., 2002. Toward improved validation of satellite sea surface skin temperature measurements for climate research. *J. Clim.* 15, 353–369. [https://doi.org/10.1175/1520-0442\(2002\)015<0353:TIVOSS>2.0.CO;2](https://doi.org/10.1175/1520-0442(2002)015<0353:TIVOSS>2.0.CO;2).
- Le Menn, M., Poli, P., David, A., Sagot, J., Lucas, M., O'Carroll, A., Belbeoch, M., Herklotz, K., 2019. Development of Surface Drifting Buoys for Fiducial Reference Measurements of Sea-Surface Temperature. *Front. Mar. Sci.* 6, 578, <https://doi.org/10.3389/fmars.2019.00578>.
- O'Carroll, A.G., Eyre, J.R., Saunders, R.W., 2008. Three-Way Error Analysis between AATSR, AMSR-E, and In situ Sea Surface Temperature Observations. *J. Atmos. Ocean. Technol.* 25, 1197–1207, <https://doi.org/10.1175/2007JTECHO542.1>.
- Poli, P., Lucas, M., O'Carroll, A., Le Menn, M., David, A., Corlett, G.K., Blouch, P., Meldrum, D., Merchant, C.J., Belbeoch, M., Herklotz, K., 2019. The Copernicus Surface Velocity Platform drifter with Barometer and Reference Sensor for Temperature (SVP-BRST): genesis, design, and initial results. *Ocean Sci.* 15, 199–214, <https://doi.org/10.5194/os-15-199-2019>.
- Saunders, P., 1967. Aerial Measurements of Sea Surface Temperature in the Infrared. *J. Geophys. Res.* 72, 16, 4109–4117.

Xu, F., Ignatov, A., 2014. In situ SST Quality Monitor (iQuam). *J. Atmos. Ocean. Technol.* 31, 164–180, <https://doi.org/10.1175/JTECH-D-13-00121.1>.

Zhang, H., Ignatov, A., Hinshaw, D., 2021. Evaluation of the in situ Sea Surface Temperature Quality Control in the NOAA in situ SST Quality Monitor (iQuam) System. *J. Atmos. Ocean. Technol.*, in press.

### S3-3: SAHARAN DUST EFFECTS ON NORTH ATLANTIC SEA SURFACE SKIN TEMPERATURES

**Bingkun Luo<sup>[1]</sup>, Peter J. Minnett<sup>[1]</sup>, Paquita Zuidema<sup>[1]</sup>, Nicholas R. Nalli<sup>[2]</sup>, Santha Akella<sup>[3]</sup>**

[1] Rosenstiel School of Marine and Atmospheric Science, University of Miami, Miami, FL 33149

[2] IMSG, Inc. at National Oceanic and Atmospheric Administration (NOAA) NESDIS/STAR, College Park, MD 20740

[3] NASA Goddard Space Flight Center, Global Modeling and Assimilation Office (GMAO), Greenbelt, MD 20771

#### INTRODUCTION

Saharan dust outbreaks frequently propagate westward over the Atlantic Ocean; accurate quantification of the dust aerosol radiative effects on the surface radiative fluxes (SRF) is fundamental to understanding the sea surface radiation budget. By exploiting large sets of measurements from many ship campaigns in conjunction with reanalysis products, this study characterizes the sensitivity of the SRF and skin Sea-Surface Temperature (SST<sub>skin</sub>) to the Saharan dust aerosols using models of the atmospheric radiative transfer, diurnal heating in the ocean, and thermal skin effect. Saharan dust outbreaks can decrease the surface shortwave radiation up to 190 W/m<sup>2</sup>, and an analysis of the corresponding SST<sub>skin</sub> changes suggests dust-induced cooling effects as large as -0.24 K during daytime and a warming effect of up to 0.06 K during nighttime respectively. Greater physical insight into the radiative transfer through an aerosol-burdened atmosphere and the response thermal response will substantially improve the predictive capabilities of weather and climate studies on a regional basis.

#### EXTENDED ABSTRACT

Accurate independent shipboard measurements in the tropical Atlantic Ocean area provide an independent representation of the atmosphere and ocean that can be used to investigate the influence of the dust aerosols on SST<sub>skin</sub> variability. The NASA MERRA-2 reanalysis fields augment the radiosonde data to characterize the vertical dust aerosol profiles at the times and places where radiosondes were launched, and to provide inputs for radiative transfer calculations. This study includes the RRTMG-simulated surface shortwave and net longwave downwelling radiative changes due to dust and calculates the corresponding thermal skin layer temperature changes.

#### FIGURES

In situ measured data from research ships collected during a series of AEROSE campaigns (Morris et al. 2006; Nalli et al. 2011) onboard the NOAA Ship Ronald H. Brown and the R/V Alliance and remotely derived datasets are used to assess the Saharan dust effects on SST<sub>skin</sub>. AEROSE was a sequence of Atlantic field campaigns from 2004 to the present, aiming to take accurate oceanic and atmospheric measurements of the tropical Atlantic Ocean under Saharan dust outbreaks; Figure 1 shows the AEROSE ship tracks of each year, where the colors indicate day of the year. Table 1 summarizes the cruise starting and ending dates as well as the number of radiosondes deployed in each of the AEROSE cruises that were used in this study. A total of 751 radiosonde profiles over a span of 231 days were used. The measurements made during these campaigns provided data that were required as inputs for radiative transfer models and models of the thermal skin and diurnal heating.

One of the key instruments is the Marine-Atmospheric Emitted Radiance Interferometer (M-AERI), which is a Fourier-transform infrared spectro-radiometer which measures spectra in the wavenumber range of 500-3000 cm<sup>-1</sup> (3.3 -20 μm) (Minnett et al. 2001). An M-AERI was mounted on the ships for each AEROSE cruise. Highly accurate SST<sub>skin</sub> can be retrieved from M-AERI measurements. An error budget of the SST<sub>skin</sub> derived from the M-AERI measurements gives a root mean square accuracy of about 40 mK. The M-AERI infrared spectra can also be used to retrieve the lower troposphere temperature and humidity profiles from the measurements of CO<sub>2</sub> emission spectra (Szczo drak et al. 2007).

During the AEROSE cruises, two to four radiosondes were deployed each day to measure the vertical air temperature and water vapor profiles. Figure 1, rows 1-2, show the relative humidity and rows 3-4 show the air temperature along each of the AEROSE tracks. These intensive observations provide us with the

opportunity to quantify dust aerosol radiative forcing on the SRF and SSTskin; the dense network of observations will benefit the radiative transfer model simulations.

This study uses data from the NASA MERRA-2 (Gelaro et al. 2017), which contains geolocated dust aerosol mixing ratio at 72 standard pressure levels with one or three hours temporal resolution which is extraordinarily useful for this study; aerosols in MERRA-2 are constrained via data assimilation, see Randles et al. (2017) and Buchard et al. (2017) for further details.. Figure 1 (rows 5-6) shows the MERRA-2 dust mass mixing ratio at the radiosonde deployment location along with each AEROSE track; clearly, as intended, AEROSE campaigns have encountered significant Saharan dust outflows.

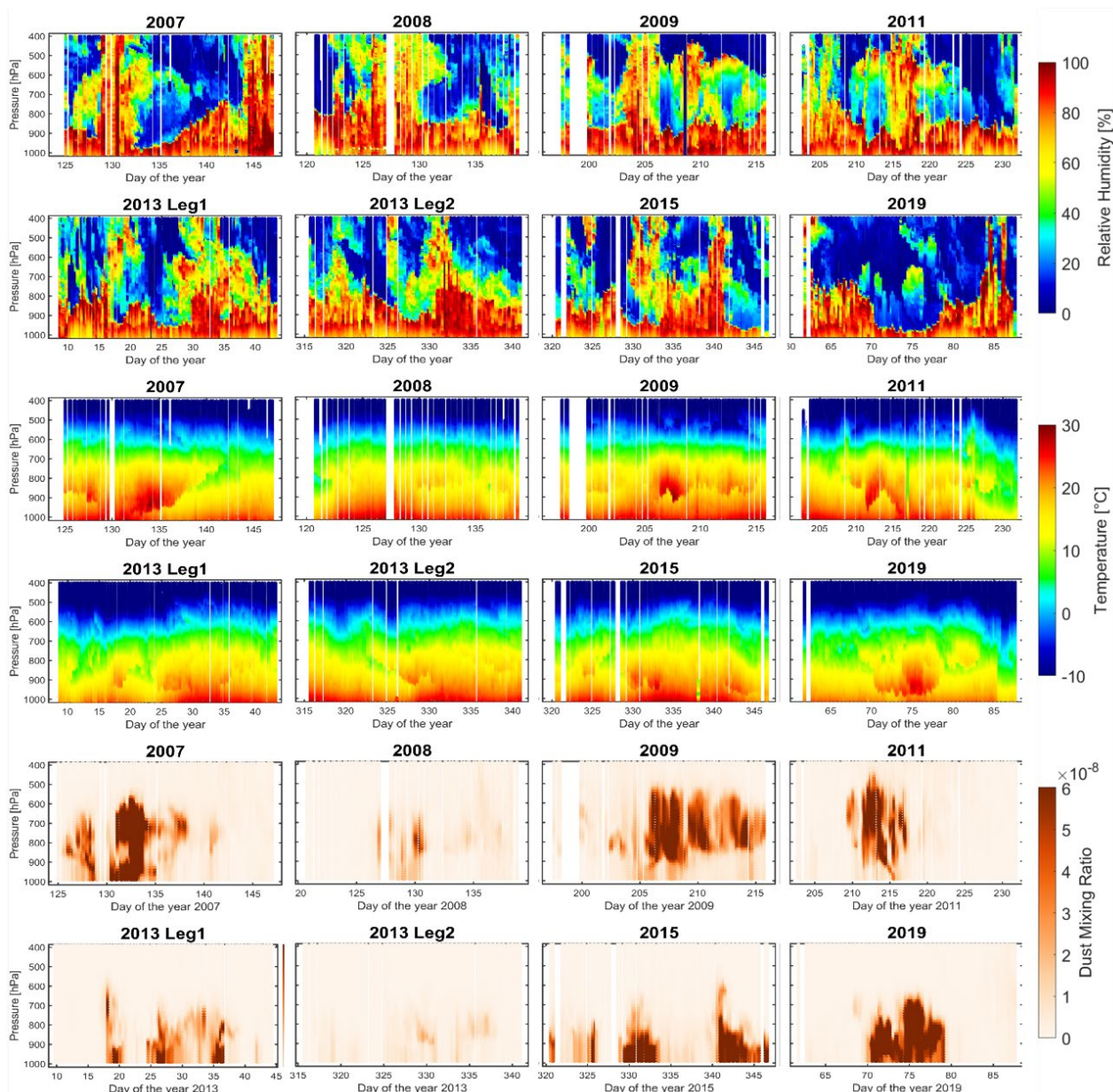


Figure 1. Rows 1-2: Relative humidity measured by radiosondes launched from the ships, the dust introduced dry layers are visible on some days. Rows 3-4: Air temperatures measured by radiosondes (Luo et al. 2020). Rows 5-6: MERRA-2 dust mixing ratio at radiosonde deployment location and times along each AEROSE track, the shading indicates the dust mixing ratio as shown on the right.

RRTMG (Iacono et al. 2008) was developed by Atmospheric and Environmental Research, Inc. and uses a correlated-k method to improve the computational efficiency of radiative transfer calculations by dividing the longwave spectrum into 16 and shortwave spectrum into 14 continuous bands. The atmospheric relative humidity and air temperatures are from the radiosondes, the SST<sub>skin</sub> and near surface air temperatures are those from M-AERI, the dust aerosol inputs are taken from the MERRA-2. The surface shortwave and longwave radiation are the outputs from RRTMG.

There are many diurnal heating and cooling models with varying complexity and dependences on forcing parameters. Some models are driven by surface fluxes, such as those used in ERA-5 (Akella et al. 2017; ECMWF 2016), and some others use ship measurements (Gentemann et al. 2009; Minnett et al. 2011). The SST<sub>ind</sub> for this study is taken from the ship-based thermosalinographs. The SST<sub>skin</sub> variations can be expressed by the cool skin layer and the warm layer schemes (Akella et al. 2017; ECMWF 2016; Takaya et al. 2010; Zeng and Beljaars 2005). The net solar radiation at the surface  $SW_{net}$  and the net longwave radiation  $LW_{net}$  at the surface are taken from the RRTMG simulation outputs with and without aerosols (Section 3.1); so the SST<sub>skin</sub> response to the dust can be expressed as the difference between the SST<sub>skin</sub> schemes with and without aerosols.

Figure 2 shows the time series of the SST<sub>skin</sub> changes due to dust aerosol (top), and the distributions of the SST<sub>skin</sub> change at the times and places of radiosonde launches (bottom). Clearly, the significant SST<sub>skin</sub> changes are within the dust outflow region; overall, the dust aerosols introduce cooling anomalies to SST<sub>skin</sub>. When the wind speed is low, the absorbed solar radiation leads to a stable stratification in the upper ocean that results in an increase in temperature located near the ocean surface, establishing a diurnal warming layer. The diurnal warming temperature increase can be several K, and it has been captured in field measurements (Donlon et al. 2002; Minnett et al. 2011) and in satellite data. However, the dust aerosols reduce the downward shortwave radiation, reducing the SST<sub>skin</sub> by as much as -0.24 K. The overall cooling magnitudes are consistent with those of previous studies (Foltz and McPhaden 2008).

Since the SST is nearly everywhere higher than the air temperature, the upward longwave radiation is greater than downward. With the dust-introduced increased net longwave radiation, the surface net heat flux  $Q_c$  will decrease, so the temperature drop across the thermal skin layer will be reduced; thus the dust aerosol longwave radiation can introduce a warm SST<sub>skin</sub> anomaly during the nighttime. However, the nighttime warming anomalies have only been calculated for low wind speeds; the averaged magnitudes of warming anomalies are usually < 0.03 K.

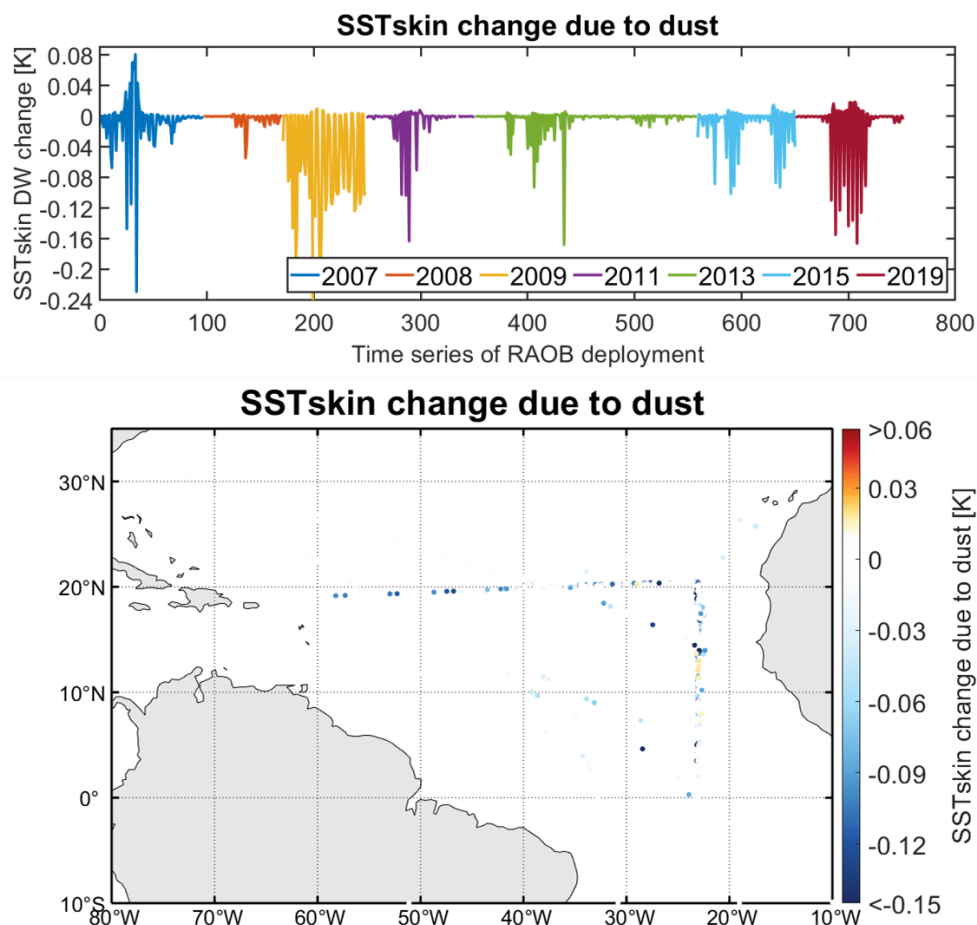


Figure 2. Top: Time series of the SST<sub>skin</sub> changes due to dust. The x-axis is the radiosonde deployment number, and the y-axis shows the simulated SST<sub>skin</sub> changes, which are calculated as the difference between the SST<sub>skin</sub> with and without dust. The unit is K. The colors indicate the deployment year. Bottom: Geographic distributions of the calculated SST<sub>skin</sub> changes due to dust. The colors indicate the SST<sub>skin</sub> change due to dust, as shown on the right with the unit of K. Note there are many points which have almost zero SST<sub>skin</sub> change.

## CONCLUSION

As our ship-based sampling covered weak to strong dust outbreaks, the dust aerosol effects on SST<sub>skin</sub> also vary temporally and spatially. Based on the RRTMG model calculations under various dust distributions, we estimate the dust can introduce a reduction of up to 190 W/m<sup>2</sup> in surface shortwave radiation at around 13:30 local time and an increase of 14 W/m<sup>2</sup> surface longwave radiation. As the SST variability is mainly responsive to wind-induced turbulent latent and sensible heat loss at the surface (Foltz and McPhaden 2008), we have simulated the SST<sub>skin</sub> variations with models of the thermal skin layer for wind speeds < 4 m/s. The dust aerosols can introduce warming and cooling anomalies to SST<sub>skin</sub> during daytime, depending on the solar zenith angle, dust layer concentration, temperature and altitude; the reduction in surface shortwave radiation can decrease the SST<sub>skin</sub> by as much as -0.24 K. The anomalous increase in the surface longwave radiation is associated with an increase in SST<sub>skin</sub> of up to 0.06 K, which is identifiable at daytime and nighttime.

This research was funded by NASA Physical Oceanography program (Grant # NNX14AK18G), and Future Investigators in NASA Earth and Space Science and Technology (FINESST) Program (Grant # 80NSSC19K1326).

**REFERENCES**

- Akella, S., Todling, R., & Suarez, M. (2017). Assimilation for skin SST in the NASA GEOS atmospheric data assimilation system. *Quarterly Journal of the Royal Meteorological Society*, 143, 1032-1046. 10.1002/qj.2988
- Buchard, V., Randles, C.A., da Silva, A.M., Darmenov, A., Colarco, P.R., Govindaraju, R., Ferrare, R., Hair, J., Beyersdorf, A.J., Ziemba, L.D., & Yu, H. (2017). The MERRA-2 aerosol reanalysis, 1980 onward. part II: evaluation and case studies. *Journal of Climate*, 30, 6851-6872. 10.1175/jcli-d-16-0613.1
- Donlon, C.J., Minnett, P.J., Gentemann, C., Nightingale, T.J., Barton, I.J., Ward, B., & Murray, J. (2002). Toward improved validation of satellite sea surface skin temperature measurements for climate research. *Journal of Climate*, 15, 353-369.
- ECMWF (2016). Part IV: Physical Processes. IFS Documentation CY43R1: ECMWF <https://www.ecmwf.int/en/elibrary/17117-ifs-documentation-cy43r1-part-iv-physical-processes>
- Foltz, G.R., & McPhaden, M.J. (2008). Impact of Saharan dust on tropical north Atlantic SST. *Journal of Climate*, 21, 5048-5060. 10.1175/2008jcli2232.1
- Gelaro, R., McCarty, W., Suárez, M.J., Todling, R., Molod, A., Takacs, L., Randles, C.A., Darmenov, A., Bosilovich, M.G., Reichle, R., Wargan, K., Coy, L., Cullather, R., Draper, C., Akella, S., Buchard, V., Conaty, A., Silva, A.M.d., Gu, W., Kim, G.-K., Koster, R., Lucchesi, R., Merkova, D., Nielsen, J.E., Partyka, G., Pawson, S., Putman, W., Rienecker, M., Schubert, S.D., Sienkiewicz, M., & Zhao, B. (2017). The Modern-Era Retrospective Analysis for Research and Applications, Version 2 (MERRA-2). *Journal of Climate*, 30, 5419-5454. 10.1175/jcli-d-16-0758.1
- Gentemann, C.L., Minnett, P.J., & Ward, B. (2009). Profiles of Ocean Surface Heating (POSH): a new model of upper ocean diurnal thermal variability. *Journal of Geophysical Research*, 114, C07017. 10.1029/2008JC004825
- Iacono, M.J., Delamere, J.S., Mlawer, E.J., Shephard, M.W., Clough, S.A., & Collins, W.D. (2008). Radiative forcing by long-lived greenhouse gases: Calculations with the AER radiative transfer models. *Journal of Geophysical Research: Atmospheres*, 11310.1029/2008jd009944
- Luo, B., Minnett, P.J., Szczodrak, M., Nalli, N.R., & Morris, V.R. (2020). Accuracy assessment of MERRA-2 and ERA-Interim sea-surface temperature, air temperature and humidity profiles over the Atlantic Ocean using AEROSE measurements. *Journal of Climate*, 33, 6889–6909. 10.1175/JCLI-D-19-0955.1
- Minnett, P.J., Knuteson, R.O., Best, F.A., Osborne, B.J., Hanafin, J.A., & Brown, O.B. (2001). The Marine-Atmospheric Emitted Radiance Interferometer (M-AERI), a high-accuracy, sea-going infrared spectroradiometer. *Journal of Atmospheric and Oceanic Technology*, 18, 994-1013. [https://doi.org/10.1175/1520-0426\(2001\)018%3C0994:TMAERI%3E2.0.CO;2](https://doi.org/10.1175/1520-0426(2001)018%3C0994:TMAERI%3E2.0.CO;2)
- Minnett, P.J., Smith, M., & Ward, B. (2011). Measurements of the oceanic thermal skin effect. *Deep Sea Research Part II: Topical Studies in Oceanography*, 58, 861-868. 10.1016/j.dsr2.2010.10.024
- Morris, V., Clemente-Colón, P., Nalli, N.R., E. Joseph, R. A. Armstrong, Y. Detrés, M. D. Goldberg, Minnett, P.J., & Lumpkin, R. (2006). Measuring trans-atlantic aerosol transport from africa. *EOS, Transactions of the American Geophysical Union*, 87, 565,571. <https://doi.org/10.1029/2006EO500001>
- Nalli, N.R., Joseph, E., Morris, V.R., Barnett, C.D., Wolf, W.W., Wolfe, D., Minnett, P.J., Szczodrak, M., Izaguirre, M.A., Lumpkin, R., Xie, H., Smirnov, A., King, T.S., & Wei, J. (2011). Multiyear observations of the tropical Atlantic atmosphere: multidisciplinary applications of the NOAA aerosols and ocean science expeditions. *Bulletin of the American Meteorological Society*, 92, 765-789. 10.1175/2011BAMS2997.1
- Randles, C.A., Da Silva, A.M., Buchard, V., Colarco, P.R., Darmenov, A., Govindaraju, R., Smirnov, A., Holben, B., Ferrare, R., Hair, J., Shinozuka, Y., & Flynn, C.J. (2017). The MERRA-2 Aerosol Reanalysis, 1980 - onward, Part I: System Description and Data Assimilation Evaluation. *J Clim*, 30, 6823-6850. 10.1175/JCLI-D-16-0609.1

Szczodrak, M., Minnett, P.J., Nalli, N.R., & Feltz, W.F. (2007). Profiling the Lower Troposphere Over the Ocean With Infrared Hyperspectral Measurements of the Marine-Atmosphere Emitted Radiance Interferometer. *Journal of Oceanic and Atmospheric Technology*, 24, 390-402.

Takaya, Y., Bidlot, J.-R., Beljaars, A.C.M., & Janssen, P.A.E.M. (2010). Refinements to a prognostic scheme of skin sea surface temperature. *Journal of Geophysical Research: Oceans*, 11510.1029/2009JC005985

Zeng, X., & Beljaars, A. (2005). A prognostic scheme of sea surface skin temperature for modeling and data assimilation. *Geophysical Research Letters*, 32, L14605. doi:10.1029/2005GL023030

**S' - POSTER PRESENTATIONS – ABSTRACTS**

### S3-P1: EVALUATION OF AIRS AND CRLS SST MEASUREMENTS RELATIVE TO THREE GLOBALLY GRIDDED SST PRODUCTS BETWEEN 2013 AND 2019

**Jorge Vazquez-Cuervo<sup>(1)</sup>, H. H. Aumann<sup>(1)</sup>, E. M. Manning<sup>(1)</sup>, H. R. Wilson<sup>(1)</sup>**

(1) Jet Propulsion Laboratory/California Institute of Technology, Email: [Jorge.Vazquez@jpl.nasa.gov](mailto:Jorge.Vazquez@jpl.nasa.gov)

(1) Email: [hartmut.h.aumann@jpl.nasa.gov](mailto:hartmut.h.aumann@jpl.nasa.gov), [evan.m.manning@jpl.nasa.gov](mailto:evan.m.manning@jpl.nasa.gov), [robert.c.wilson@jpl.nasa.gov](mailto:robert.c.wilson@jpl.nasa.gov)

#### INTRODUCTION

Globally gridded sea surface temperatures (SSTs) provide key data for the long-term monitoring of the stability of satellite data. Despite apparent limitations, accurate hyperspectral data can provide useful independent information to critique the stability of global SST products on the annual-to-decadal time scale. We compared data from AIRS on EOS Aqua and CrIS on SNPP to the SST products from NOAA/NESDIS (RTG), the Canadian Meteorological Centre (CMC) and the UK Met Office (OSTIA). For the 2013 through 2019 period, the overall standard deviation of the difference between AIRS and the RTG was 0.55K, with an increasing trend over time. In contrast, the standard deviation of the difference between the AIRS, the CMC and the OSTIA dropped steadily to below 0.4 K, a level previously seen only in SST products relative to independent buoy data. Unexplained biases between the observed and the gridded SSTs at the 100 mK level are consistent with already existing estimates of the AIRS and CrIS absolute calibration accuracy. However, the AIRS and CrIS observations both show artifacts in all three SST products, increasing with distance from the equator, with the CMC artifacts being the smallest. Even with the CMC a trend of 4 mK per year relative to AIRS and CrIS was observed between 2013-2019 for the 30S-30N oceans. Investigation of the underlying causes of the observed discrepancies requires further work. Comparisons between the AIRS and the CtlS and the gridded GHRSSST L4 provide an independent assessment of the products.

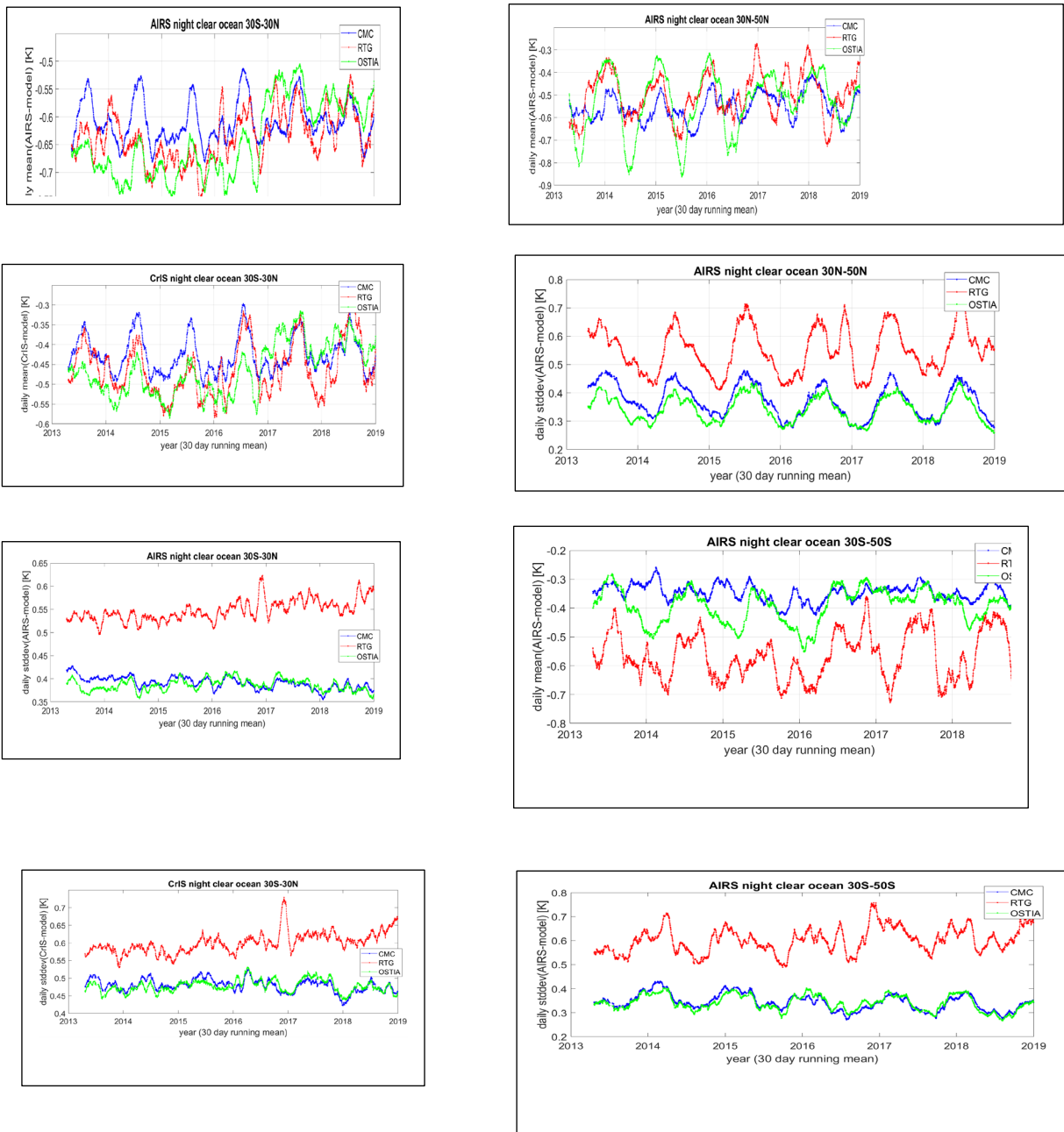
Direct comparisons were made between sea surface temperatures (SSTs) derived from the Atmospheric Infrared Sounder (AIRS), Cross Track Infrared Sound (CtlS), and NOAA's RTG SST, the Canadian Meteorological Center (CMC) SST, and the UK Met Office's Operational Sea Surface Temperature and Sea Ice Analysis (OSTIA). Mean differences and standard deviations were examined in different zonal latitudinal bands. Overall, trends in the differences were derived and compared. See Tables.

#### RESULTS

Figures show results for the time series of the mean and standard deviations for the different zonal latitudinal bands. Largest standard deviations (root mean square differences) were seen in comparisons with the RTG product in the band between 30S to 30N. Tables show the derived trends of the differences between the different products for 2013-2019.

Globally gridded sea surface temperatures (SSTs) provide key data for the long-term monitoring of the stability of satellite data. Despite apparent limitations a simple SST product derived from accurate hyperspectral data can provide useful independent information to critique the stability of global SST products on the annual-to-decadal scale. We compared the mean, standard deviation, and trend of daily Sea Surface Temperatures (SST) derived from clear sky AIRS and CrIS radiances relative to daily matchups with gridded SST products for the 2013 and 2019 period. Between 2013 and 2019 the mean standard deviation of the difference between AIRS and the RTG was 0.55K and increased steadily. During the same time the standard deviation of the difference between AIRS and the CMC and the OSTIA dropped steadily to below 0.4 K, a level previously only seen in gridded SST products relative to the independent buoy data. Unexplained biases between the observed and all three gridded SSTs at the 100 mK level are reasonably consistent with already existing estimates of the AIRS and CrIS absolute calibration accuracy. AIRS and CrIS observations both show artifacts in the time series of bias and standard deviation relative to all three gridded SST products, increasing with distance from the equator, the CMC artifacts being the smallest. With the CMC, they create a 4 mK/yr trend artifact in the 2013-2019 time series for data within 30 degrees of the equator. In a twenty year data set, as is expected from AIRS, CMC artifacts will contribute only 1 mK/yr to the AIRS trend. Investigation of the underlying causes of the observed discrepancies requires further work.

FIGURES AND TABLES



Figures: Time series of mean and STDs of (SST-AIRS/CrIS) for different zonal bands

AIRS-CMC	Day trend [mK/yr]	Day bias [K]	Day count	Night trend [mK/yr]	Night bias [K]	Night count	Day-night bias [K]
30-50N	+8.4 ± 1.6	-0.28	2154	+10.5 ± 1.5	-0.66	1848	0.38
0-30N	+6.9 ± 1.1	-0.25	6935	+6.3 ± 0.7	-0.71	4623	0.46
30S-0	+1.5 ± 0.9	-0.23	8187	+0.6 ± 0.8	-0.67	4177	0.44
50S-30S	-4.6 ± 1.2	-0.13	2773	-3.2 ± 0.9	-0.47	1892	0.34

CrIS-CMC	Day trend [mK/yr]	Day bias [K]	Day count	Night trend [mK/yr]
30-50N	+7.5 ± 1.7	+0.04	1771	+7.1 ± 2.0
0-30N	+4.2 ± 1.5	-0.03	6153	+3.6 ± 1.4
30S-0	+1.0 ± 1.2	-0.08	7274	+0.3 ± 1.3
50S-30S	-5.1 ± 1.3	0.21	2200	-2.2 ± 1.4

AIRS-CrIS	Day trend [mK/yr]	Day bias [K]	Day count	Night trend [mK/yr]
30-50N	+0.9 ± 1.2	-0.27	1771	+3.1 ± 1.4
0-30N	+3.0 ± 0.9	-0.17	6153	+2.3 ± 1.1
30S-0	+0.7 ± 0.7	-0.13	7274	-0.0 ± 1.0
50S-30S	+0.4 ± 0.9	-0.28	2200	-1.4 ± 1.0
30S-30N	+1.8 ± 1.4	-0.15	13429	+1.4 ± 0.6

Tables showing statistics for trends in differences between SST and AIRS/CrIS

## CONCLUSION

In a twenty year data set, as is expected from AIRS, CMC artifacts will contribute only 1 mK/yr to the AIRS trend. Investigation of the underlying causes of the observed discrepancies requires further work.

### **S3-P2: ASSESSMENT AND INTERCOMPARISON OF NOAA DAILY OPTIMUM INTERPOLATION SEA SURFACE TEMPERATURE (DOISST), VERSION 2.1**

**Boyin Huang<sup>(1)</sup>, Chunying Liu<sup>(1), (2)</sup>, Eric Freeman<sup>(1), (2)</sup>, Garrett Graham<sup>(3)</sup>, Tom Smith<sup>(4)</sup>, Huai-Min Zhang<sup>(1)</sup>.**

- (1) NOAA NCEI,
- (2) Riverside Technology inc.,
- (3) North Carolina Institute for Climate Studies,
- (4) NOAA Center for Satellite Applications and Research.

#### **SHORT ABSTRACT**

NOAA DOISST has recently updated to v2.1 starting from January 2016. Its accuracy may impact the climate assessment, monitoring and prediction, and environment-related applications. Its performance, together with those of seven other well-known SST products, is assessed by comparing against buoy and Argo observations in the global oceans on daily  $0.25^{\circ} \times 0.25^{\circ}$  resolution from January 2016 to June 2020. These seven SST products are NASA MUR25, GHRSSST GMPE, BoM GAMSSA, UKMO OSTIA, NOAA GPB, ESA CCI, and CMC.

Our assessments indicate that biases and RMSDs in reference to all buoys and Argo floats are lower in DOISST, GMPE and MUR25 than other products. The bias and RMSD in DOISST in reference to the independent 10% of buoy SSTs remain low as those in reference to full buoy SSTs. The bias in DOISST in reference to the independent 10% of Argo SSTs also remain low as that in reference to full Argo SSTs. The RMSD in DOISST becomes higher in reference to the 10% of Argo SSTs than in reference to full Argo SSTs. Both biases and RMSDs in reference to the independent 10% of Argo observations are low in GMPE and CMC. The biases are similar in GAMSSA, OSTIA, GPB, CCI, and CMC whether they are compared against all buoy or independent Argo observations, while the RMSDs become slightly smaller. These features suggest that ingesting the Argo observations, rather than reserving purely for independent validation, is beneficial in providing expanded global and regional spatial coverage for effective bias correction of satellite data. Overall, DOISST, GMPE, and MUR25 performs better.

More details can be found in: Huang, B., C. Liu, E. Freeman, G. Graham, T. Smith, and H.-M. Zhang, 2021: Assessment and Intercomparison of NOAA Daily Optimum Interpolation Sea Surface Temperature (DOISST) version 2.1. *J. Climate*, DOI: 10.1175/JCLI-D-21-0001.1.

### S3-P3: USING SAILDRONE CAMPAIGNS TO ACCESS ACCURACY OF SST GRADIENTS IN LEVEL 2 SST DATASETS

**Marouan Bouali<sup>(1)</sup>, and Jorge Vazquez<sup>(2)</sup>**

(1) Institute of Oceanography of the University of São Paulo, Brazil, Email: [marouan.bouali@usp.br](mailto:marouan.bouali@usp.br)

(2) NASA/Jet Propulsion Laboratory/Caltech

#### INTRODUCTION

Sea Surface Temperature (SST) gradients and fronts provide pivotal information on the physical state of the ocean, its biological composition, its interaction with the atmosphere and have therefore become an important variable for the study of long term changes in ocean dynamics.

Because standard in situ observations derived from drifting/moored buoys and Argo floats are only representatives of one specific geographical point, they cannot be used to measure spatial gradients of ocean parameters (i.e., two-dimensional vectors). In this study, we exploit the high temporal sampling of the unmanned surface vehicle (USV) Saildrone (i.e., one measurement per minute) and compare the magnitude of SST gradients derived from satellite-based Level 2 products with those captured by Saildrone.

#### DATA

##### SATELLITE DATA:

Three different satellite-based SST datasets were used to evaluate the accuracy of SST gradients. These correspond to Terra and Aqua MODIS Level 2 SST and SNPP VIIRS Level 2 SST. All these datasets are produced by NASA's Ocean Biology Processing Group (OBPG) and have been downloaded from the Physical Oceanography Distributed Active Archive Center (PODAAC: <https://podaac.jpl.nasa.gov/>).

##### SAILDRONE DATA:

In 2019, a Saildrone mission (ATL2MED) was set to depart from the western Atlantic Ocean near Cabo Verde and headed to the Mediterranean Sea (see Figure 1). The location of this mission is particularly interesting for the analysis of satellite SST gradients given the relatively low cloud coverage. The campaign which took place between October 18, 2019 and July 17, 2020, included two separate Saildrones (i.e. SD1030 and SD1053) and covered the region between Latitudes 13.91 and 45.7 and Longitudes -25.96 and 18.95.

#### METHODOLOGY

All Level 2 SST datasets have been reprojected into a lat/lon grid with 0.05° resolution using bilinear interpolation. To evaluate the impact of the quality flag (QF) on the accuracy of SST gradients, two SST fields were tested, one with QF=5 (best quality) and one with QF=4,5 (best quality + good/acceptable). Given that the sampling frequency of Saildrone is significantly higher than the temporal scale of ocean submesoscale processes, gradients in the spatial domain can be estimated from successive measurements.

Denoting  $ds$  the spatial resolution of the grid, for each grid point  $(i,j)$ , all Saildrone measurements acquired between latitudes  $i-ds$  and  $i+ds$  and longitudes  $j-ds$  and  $j+ds$  are averaged. Then, at each grid location  $(i,j)$ , we compute the average time of Saildrone measurements which can be sorted to derive a collocated time series of SST observations from satellite Level 2 and Saildrone. The magnitude of SST gradients can then be approximated using forward finite differences of successive measurements, i.e.:

$$\nabla \text{SST} = \frac{\text{SST}(t+1) - \text{SST}(t)}{d_t^{t+1}}$$

Where  $d_t^{t+1}$  is the distance between collocated observations obtained at times  $t+1$  and  $t$ .

## RESULTS

We illustrate in Figure 1 the matchup time series obtained for both SST and SST gradients from SNPP VIIRS and the Sairdrone SD 1030 campaign. Biases, Root Mean Square Error (RMSE) and correlation for SST and SST gradients for all three sensors and Sairdrone campaigns SD1030/1053 are reported in Table 1.

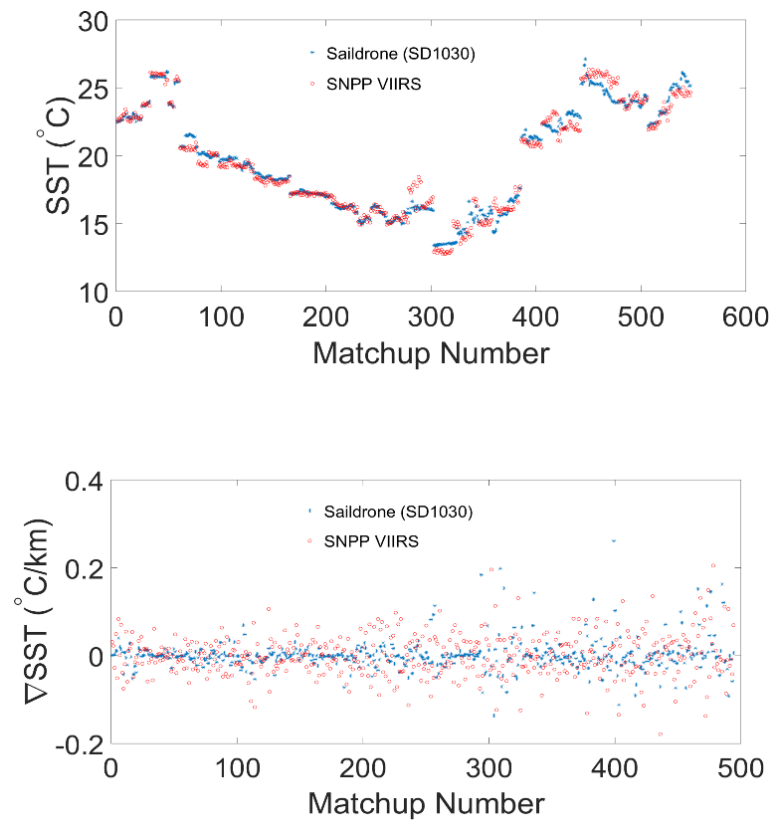


Figure. 1: Validation statistics of SST and SST gradients for Terra/Aqua MODIS and SNPP VIIRS using Sairdrone campaigns SD130 and SD1053, Atlantic to Mediterranean mission from Oct 18, 2019 to July 17, 2020

SD1030								SD1053							
	Quality Level	Bias		RMSE		Correlation			Quality Level	Bias		RMSE		Correlation	
		SST	$\nabla$ SST	SST	$\nabla$ SST	SST	$\nabla$ SST			SST	$\nabla$ SST	SST	$\nabla$ SST		
Terra MODIS	QF=5	-0.107	--	0.660	0.069	0.986	0.144	Terra MODIS	QF=5	-0.037	--	0.696	0.072	0.983	0.006
	QF=4+5	0.057	--	0.676	0.074	0.980	0.148		QF=4+5	0.053	--	0.664	0.077	0.981	0.011
Aqua MODIS	QF=5	-0.019	--	0.485	0.055	0.976	0.079	Aqua MODIS	QF=5	-0.042	--	0.484	0.055	0.978	0.175
	QF=4+5	-0.117	--	0.622	0.061	0.967	0.024		QF=4+5	-0.108	--	0.540	0.056	0.975	0.162
SNPP VIIRS	QF=5	0.036	--	0.651	0.057	0.985	0.084	SNPP VIIRS	QF=5	0.094	--	0.719	0.056	0.979	0.185
	QF=4+5	-0.039	--	0.670	0.061	0.983	0.084		QF=4+5	0.058	--	0.773	0.060	0.975	0.185

Table. 1: Bias, Root Mean Square Error and correlation of SST and SST gradients for Terra/Aqua MODIS and SNPP VIIRS using data from Saildrone SD1030 and SD1053

### CONCLUSION AND FUTURE WORK

Unlike other in situ platforms, Saildrone provides a unique opportunity to evaluate the accuracy of satellite-based ocean parameters but also their corresponding gradients.

Results based on the Atlantic to Mediterranean campaign using Terra/Aqua MODIS and SNPP VIIRS show that while satellite estimates of Level 2 SST are in very good agreement with Saildrone measurements, derived gradients are not.

This is likely due to sensor noise (Gaussian + striping) that significantly affects pixel-to-pixels variations and leads to observed gradient magnitudes higher than true SST gradients.

Future work will use other Saildrone campaigns to investigate the accuracy of SST gradients over other regions with additional satellite sensors (N20 VIIRS, S3A/S3B SLSTR).

## S3-P4: EUMETSAT SLSTR SST MULTI-MISSION MATCHUP DATABASE: ONGOING WORK, TRUSTED MDB AND EVOLUTIONS

Igor Tomazic<sup>(1)</sup>, Anne O'Carroll<sup>(2)</sup>, Gary Corlett<sup>(3)</sup>, Jean-Francois Piollé<sup>(4)</sup>

- (1) EUMETSAT, Darmstadt, Germany, Email: igor.tomazic@eumetsat.int
- (2) EUMETSAT, Darmstadt, Germany, Email: anne.ocarroll@eumetsat.int
- (3) EUMETSAT, Darmstadt, Germany, Email: gary.corlett@eumetsat.int
- (4) IFREMER, Plouzane, France, Email: jean-francois.piolle@ifremer.fr

### INTRODUCTION

Sea surface temperature (SST) is an essential variable for operational forecasting and global climate monitoring, and is one of the main products provided by the Copernicus Sentinel-3 Sea and Land Surface Temperature Radiometer (SLSTR) instruments (<https://www.eumetsat.int/slstr>). As such, there are stringent requirements on SLSTR SST product performance: Its absolute accuracy should be better than 0.3 K and its temporal stability better than 0.1 K/decade.

Comparison against in situ reference measurements using the EUMETSAT SST multi-mission matchup database (MMDB) is performed to confirm these requirements are met. This paper provides details on the status of the SLSTR SST MDB, information about reprocessing of radiometer matches, the addition of the TRUSTED dataset, and how to access the MMDB along with expected evolutions.

### SST MULTI-MISSION MATCHUP DATABASE (MMDB)

The SST MMDB is generated using the felyx application customized and configured for processing at EUMETSAT, from which we then analyse differences between the satellite and in situ SST measurements. EUMETSAT is currently generating SST MMDBs from several instrument (SLSTR-A/B, AVHRR-B, IASI-B, VIIRS-NPP), using several in situ measurement types: drifters, Argo, moorings and ship-borne radiometers. We now include in situ measurements from drifters built and deployed through the EUMETSAT/Copernicus TRUSTED project (<https://www.eumetsat.int/TRUSTED>) and are in the process of adding Sairdrone measurements (see Figure 10).

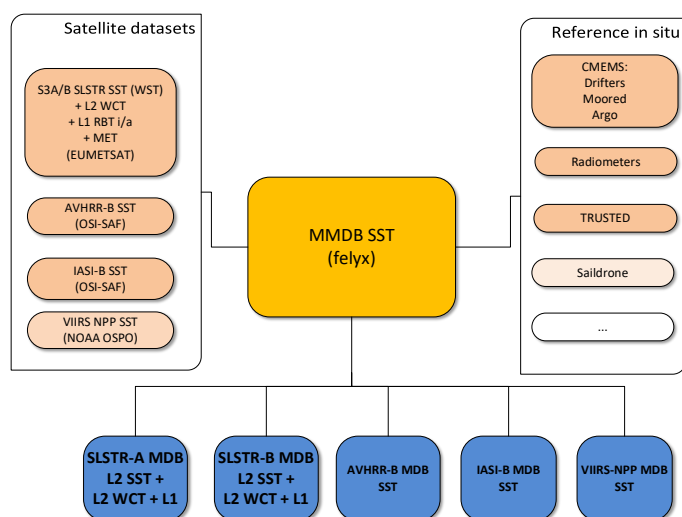


Figure 10. Schematic diagram of all produced SST MMDBs

### SLSTR SST MDB

The SLSTR SST MDB contains variables from SLSTR Level-1 (L1) RBT and Level-2 (L2) SST products (user WST and internal WCT), as well as the main variables from the in situ datasets; the MDBs for AVHRR-

B SST, IASI-B SST and VIIRS-NPP SST contain L2 variables only along with the in situ data. The matchup generation procedure is dependent on the in situ and satellite data. Table 1 summarizes the main criteria and timeliness.

Satellite data	In situ data	Temporal	Spatial	Window size	Timeliness
SLSTR: SST, L1 1 km	Drifters	±2h	5 km	21x21	NRT ( 7 days delay)
AVHRR: SST	Argo	±12h	5 km	21x21	NRT ( 7 days delay)
VIIRS: SST	Moored buoys	±2h	5 km	21x21	NRT ( 7 days delay)
	Radiometers	±2h	5 km	401x401	Offline

Table 2. Primary SST MMDB temporal and spatial matchup criteria and extracted window size for each in situ type and satellite data types and the production timeliness.

The SLSTR SST MDB output consists of one core and four auxiliary NetCDF files (Figure 11). The core file contains all variables from the SST (WST/L2P) products, and the four auxiliary datasets contains: 1) SST and corresponding annotation datasets based on different algorithms from internal WCT product (WCT), 2) meteorological variables (MET), 3) selected L1 1 km variables (RBT-i) and 4) selected L1 500 km (a stripe) variables (RBT-a). The MMDB is produced on daily basis at 7 days delayed to allow collection of all in situ measurements (drifters, Argo, moored). The drifter dataset is split in 6-hourly files (4 per day) to reduce the file volume, while other dataset types (Argo, moored, radiometer) contain one file per day (covering 24 h). The radiometer matches are processed in an offline mode and will be described in following section.

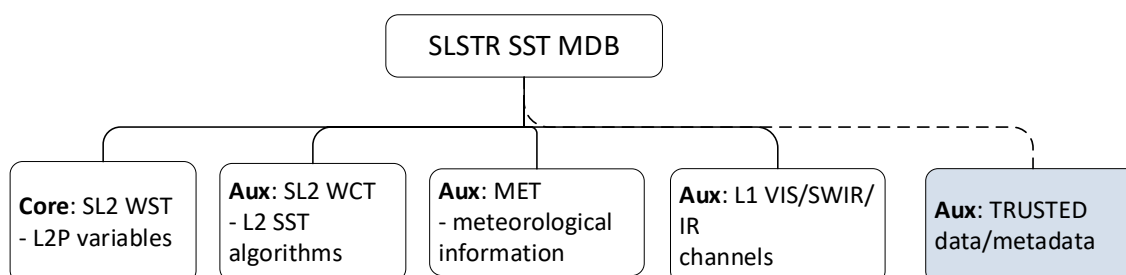


Figure 11. Schematic diagram of SLSTR SST MDB subsets (1 core and 4 auxiliary subsets)

### RADIOMETER MDB

Shipborne radiometer in situ data are collected from the ISFRN (the International Sea surface temperature Fiducial reference measurements Radiometer Network) project (<https://www.ships4sst.org/>). Processing is performed in a non-regular offline mode to allow collection of quality-controlled radiometer measurements from different teams across the world.

The latest radiometer reprocessing covered 2019 (Figure 12) and currently only the core dataset is available (additional AUX WCT and MET fields will be completed by the end of this year). It is expected that updates will be done on an approximate 6-monthly timescale (for newly available quality controlled dataset and for core, WST and MET auxiliary dataset). A full radiometer reprocessing will follow reprocessing of SLSTR L1/L2 SST data (including tandem phase) and will include complete MDB with core and all aux datasets (variables from both L1 and L2 SST products).

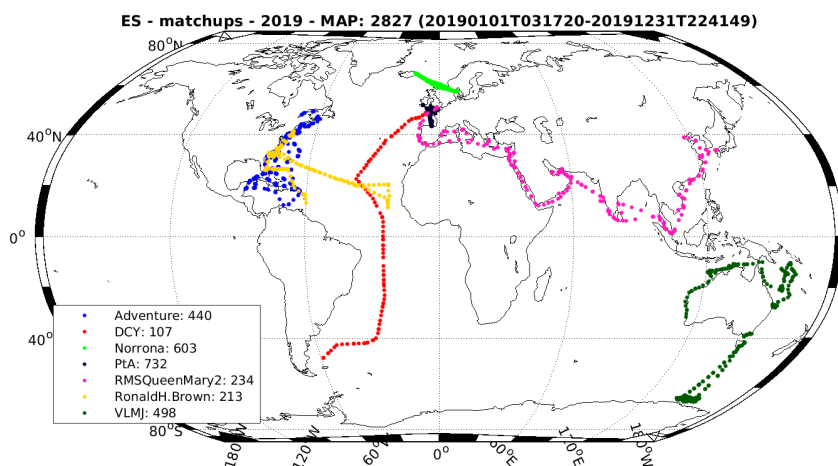


Figure 12. 2019 radiometer matchup locations aggregated by ship name.

### TRUSTED MDB

Measurements from the TRUSTED project (Towards fiducial Reference measurements of Sea-Surface Temperature by European Drifters, <https://www.eumetsat.int/TRUSTED>, Figure 13) are now included in the SLSTR SST MMDB. The matchups include the two SSTs as well as measurement from other sensors, and high-frequency (1 Hz) SSTs where available. All data and metadata from the raw measurement files provided by CLS are propagated to the matchup dataset to ensure full traceability if needed for further analysis.

Additional diagnostics are prepared for inspecting and investigating all drifters and key parameters and are available via the URL <https://s3calval.eumetsatint/ma/sst/trusted>.

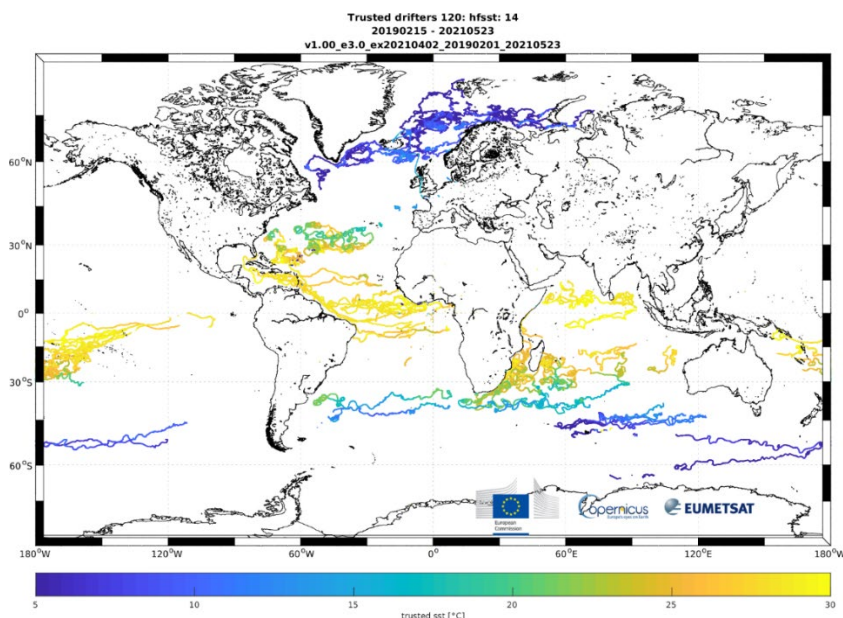


Figure 13. Sea surface temperature from TRUSTED drifters from beginning of the project.

### **SST MMDB ACCESS AND FUTURE EVOLUTIONS**

Access to the SLSTR SST MDB, including the TRUSTED data, is available to all Sentinel-3 Validation Team (S3VT) members through sftp access (<sftp://s3calval.eumetsat.int>). Participation to the S3VT can be considered through the submission of a proposal at <http://s3vt.org>. Evolutions of the SLSTR SST MMDB are planned as part of the Copernicus Sea and Sea-ice Surface Temperature Product Improvement and Cal/Val Tool Development project (Sci4MaST). The next full reprocessing of the SLSTR SST MMDB is expected following the release of the Day-2 SST processor, while shorter reprocessing is planned to cover SLSTR-A/B tandem phase and early SLSTR-A commissioning phase.

### S3-P5: VALIDATION OF SGLI SST

**Yukio Kurihara, Kazunori Ogata, Hiroshi Murakami**

Japan Aerospace Exploration Agency (JAXA) Earth Observation Research Center (EORC),  
Email: [kurihara.yukio@jaxa.jp](mailto:kurihara.yukio@jaxa.jp)

#### INTRODUCTION

The Second-generation GLObal Imager (SGLI) is an optical sensor onboard the GCOM-C satellite, launched from the Tanegashima Space Center of the Japan Aerospace Exploration Agency (JAXA) in December 2017. JAXA provides the SGLI SST product at the JAXA G-Portal and the JAXA GHRSSST server. The SGLI SST product is planned to be updated from version 2 (V2) to 3 (V3) by the end of 2021. Some issues with SGLI V2 SST will be corrected in V3. Preliminary retrieved V3 SST was validated by comparison with in-situ buoy data, and the validation results were compared with those of V2.

#### SGLI SST

SGLI SST is determined using GCOM-C/SGLI split-window data. The SST method: the quasi-physical method<sup>[1]</sup>, originally developed for the Himawari-8 SST, was applied to the split-window data of SGLI. The spatial resolution is 250 m in the inland and inshore seas and 1 km in the open ocean. SGLI SST covers the world's oceans in 2–3 days. The accuracy of the SGLI SST is monitored at the GCOM-C Calibration and Validation Monitor Web in near real time. The bias and RMSE of SGLI SST from January to March 2021 are -0.150 and 0.401, derived by comparison with buoy data. There are some issues with SGLI SST V2. One of which is cloud masking. The clear percentage of the highest quality level SST is only around 10%, and SSTs are often lost around SST fronts. Another issue is high SST biases, where WV is high. High WV may cause the resulting SSTs to be underestimated.

#### HIGHLIGHTS OF V3

There are three highlights with the version change from V2 to V3.

- A new filtering technique will be introduced for the destriping of SST (Figure 1). This is to improve SSTs determination and cloud masking. Stripe noise in determined SSTs is generated by that in the brightness temperature difference (BTD) of the split-window data. Stripe noise in BTD sometimes results in unrealistic SST values. Moreover, stripe noise conspicuous in the SST gradient field degrades cloud masking. The introduced filter is expected to reduce stripe and random noise in BTD data, resulting in SST determination and cloud masking improvement.

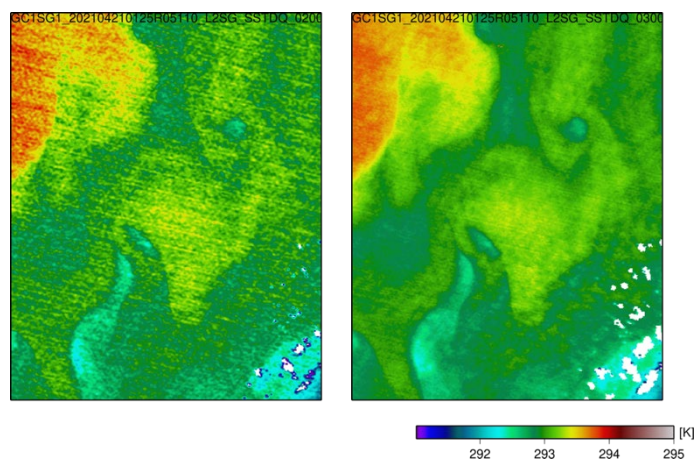
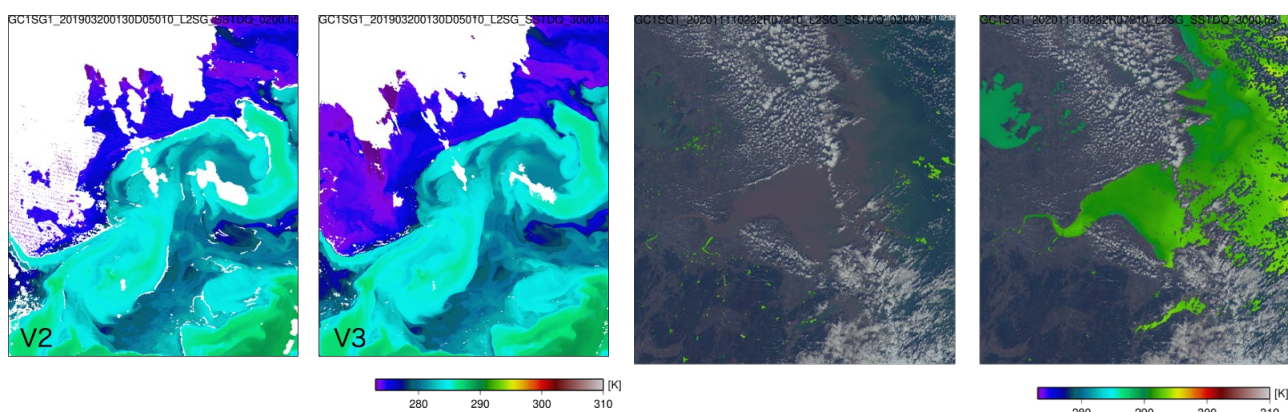


Figure 1: Stripe noise in retrieved SST. Stripe noise is seen in V2 (left) but not in V3 (right).

- The 1.6  $\mu\text{m}$  short-wavelength infrared (SWIR) data is used to improve cloud masking at SST fronts and turbid waters in the daytime (Figures 2 and 3). V2 uses visible data for cloud masking in the daytime. However, visible data are strongly affected by turbid water and bright sea floors under the shallow water, making it difficult to detect clouds near the coast. Meanwhile, SWIR data is not affected by suspended matters and seafloor types. Because of this, cloud masking is improved near the coast by using SWIR.
- SST method is improved by introducing climatology for the atmospheric optical thickness at the split window. This compensates for the insensitivity of split-window data to atmospheric  $\text{WV}^{[1]}$ . The climatology was generated using NWP data and RTTOV 10.2. Some of the known issues with SGLI V2 SST will be updated in V3. Highlights of the update are as follows.



*Figure 2: SST fronts (East of Hokkaido, Japan). The SST is masked on some SST fronts in V2, but not in V3.*

*Figure 3: Turbid water (Hangzhou Bay, China). V2 cloud masking using visible channel data falsely detected turbid water as clouds, meanwhile V3 cloud masking using 1.6  $\mu\text{m}$  channel data correctly detected the turbid water as the sea surface.*

## VALIDATION

Preliminary retrieved SGLI V3 SSTs were validated by comparing them with the nearest moored or drifting buoy data within a 1 h / 1 km matchup window. Table 1 describes the quality levels of SGLI SST. Quality levels are determined based on the cloud probability and other parameters indicating clear/cloudy (e.g., NDWI).

Figures 4–8 show the results for the daytime SGLI SST. Except for QL3, there was no significant statistical difference between V3 and V2 (Fig. 4). The clear percentage is higher for V3 than for V2, especially for QL5. The high clear percentages are likely due to improved cloud masking, as there is no significant degradation in SD and bias. On the other hand, the QL3 threshold of V3 seems to need to be adjusted to improve the statistics. Meanwhile, there is no significant improvement in cloud masking at night because of limited information to detect clouds or clear sky. The box chart (Fig. 7) shows that bias (median) of V3 is flatter than V2 at SSTs from 297 K to 303 K and at each latitude. This is believed to have been brought about by the SST method using the climatic values of the atmosphere's optical depth. Figure 8 shows the difference between V3 and buoy data as the function of the surface wind speed (WS), and Table 2 shows statistics of the data where the surface wind speed is higher than 6 m/s. In the figure, high positive biases are found when the wind speed is low. The high biases suggest diurnal warming. The statistics show almost no bias in V3 SSTs. Although the total number of matchups is small, the figure and statistics suggest V3 SST has no significant bias.

QL	Description
3	Possibly cloudy (suitable for qualitative use)
4	Acceptable (suitable for quantitative use)
5	Good (suitable for quantitative use)

Table 1: Quality Level

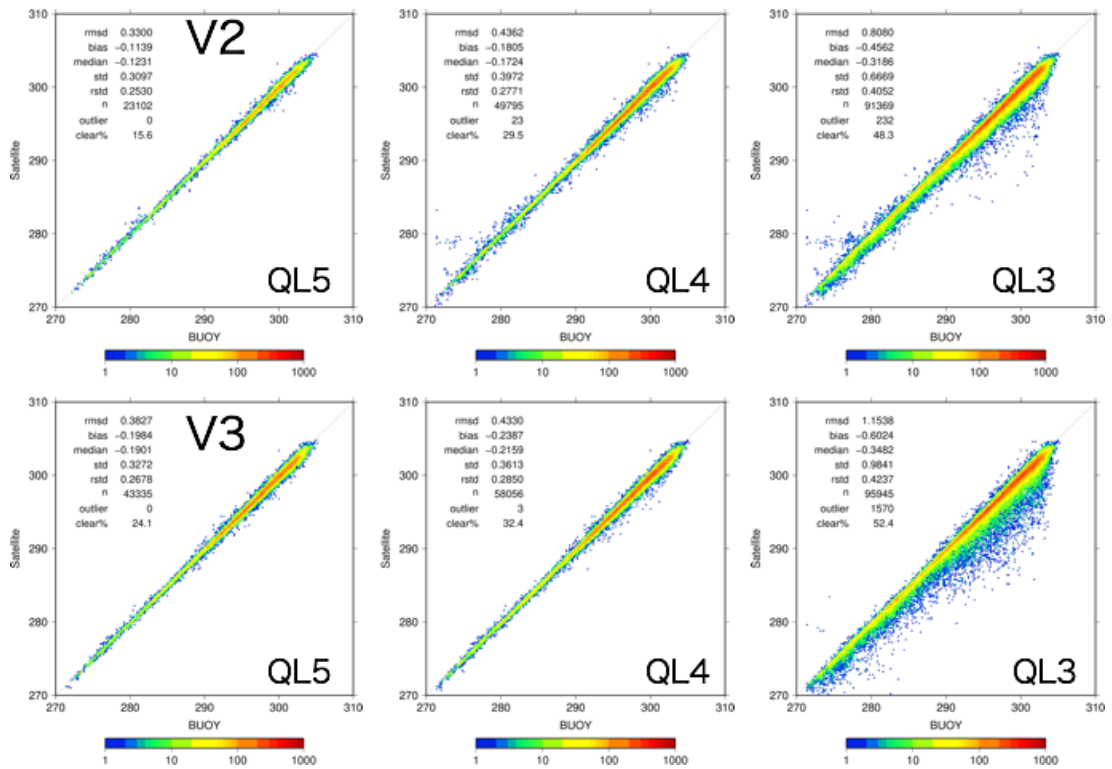


Figure 4: Daytime statistics (September 2019 to March 2020).

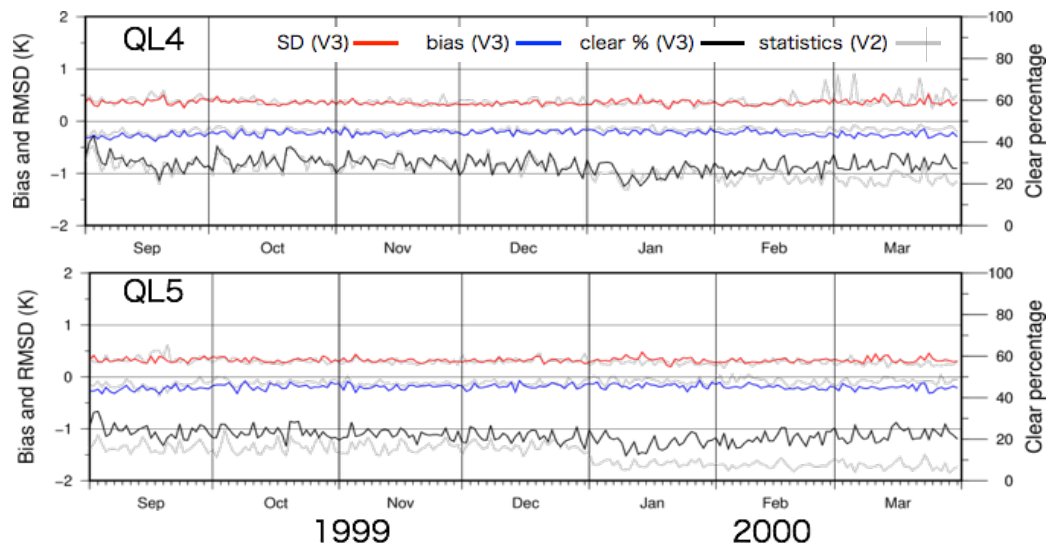


Figure 5: Daily Daytime statistics.

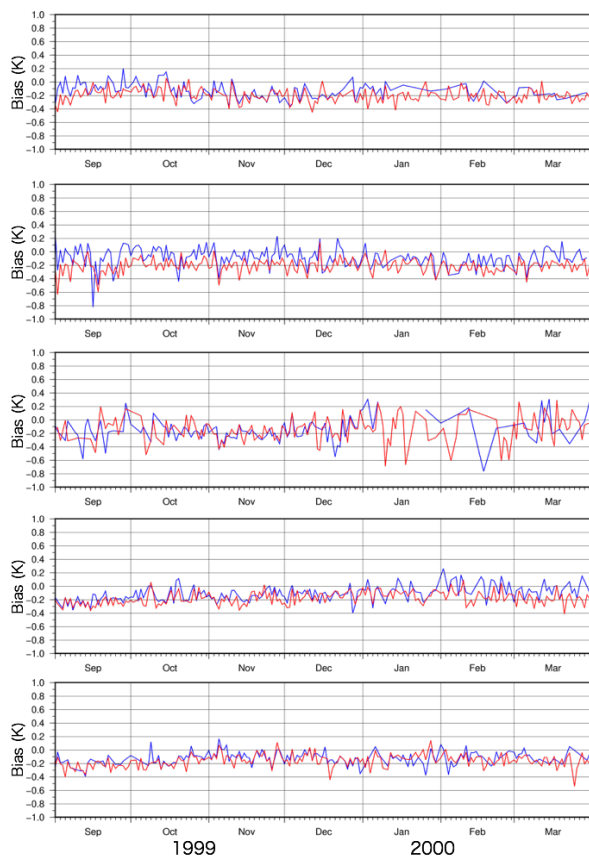


Figure 6: Daily daytime bias (median) in each latitude band. Biases were calculated for SGLI SST QL5. Red shows V3 and blue shows V2. Bias of V3 changes around  $-0.2$  K except for the equatorial zone.

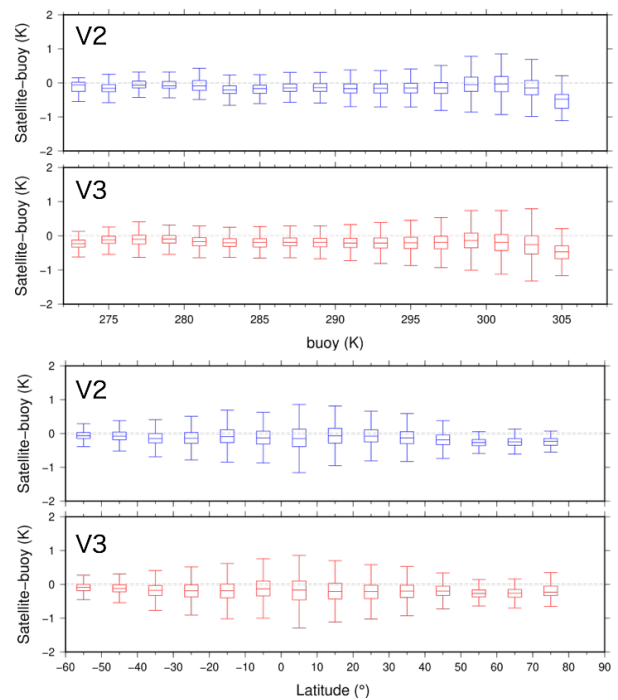
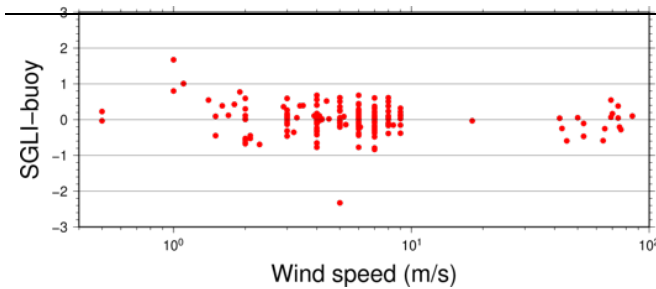


Figure 7: Box plots



Bias	Median	SD	RSD	N
-0.048	-0.030	0.30	0.26	71

Table 2: Statistics under high wind speed (> 6 m/s) conditions.

Figure 8: Differences as the function of the surface wind speed.

## CONCLUSION

The SGLI is an optical sensor onboard the GCOM-C satellite. The SGLI SST is retrieved from the split-window data from the SGLI. SGLI SST is provided as the SGLI SST product by JAXA. SGLI SSTs from 2018 to the latest are available at the JAXA G-Portal site (<https://www.gportal.jaxa.jp/gp/top.html>), and the JAXA GHRSSST server (<https://suzaku.eorc.jaxa.jp/GHRSSST/>), and the current version number of the product is version 2 (V2). SGLI SST accuracy is monitored at the GCOM-C Calibration and Validation Monitor Web in near-real-time ([https://suzaku.eorc.jaxa.jp/GCOM\\_C/Validation//index.html](https://suzaku.eorc.jaxa.jp/GCOM_C/Validation//index.html)).

JAXA plans to update the SGLI SST product from V2 to V3 by the end of 2021. Cloud masking and the SST method will be improved in V3. Preliminary retrieved SGLI V3 SSTs were validated by comparing them with buoy data. The validation results show improved cloud masking by introducing a destriping filter and using SWIR data. Meanwhile, the results show that V3 still needs adjustments to improve QL3 statistics. The latitudinal variation of biases has been reduced by using the atmospheric optical thickness climatology. The results also say that SGLI SST has nearly zero bias at wind speeds above 6 m/s, suggesting that other high SGLI SST biases are likely to have increased due to the differences in skin and bulk temperatures.

## ACKNOWLEDGMENTS

Buoy data were downloaded from the iQuam of NOAA. NWP data was generated by JMA.

## REFERENCES

- [1] Y. Kurihara, H. Murakami, K. Ogata, and M. Kachi, A quasi-physical sea surface temperature method for the split-window data from the Second-generation Global Imager (SGLI) onboard the Global Change Observation Mission-Climat (GCOM-C) satellite, *Remote Sensing of Environment*, vol. 257, p. 112347, 2021.

**SCIENCE SESSION 4**

**ALGORITHMS**



## **S4 - SESSION REPORT**

**Chair: Jacob L. Høyer<sup>(1)</sup>, Rapporteur: Simon Good<sup>(2)</sup>**

(1) Danish Meteorological Institute, Denmark. Email: [jlh@dmi.dk](mailto:jlh@dmi.dk)

(2) UK Met Office, England, Email: [simon.good@metoffice.gov.uk](mailto:simon.good@metoffice.gov.uk)

### **HIGHLIGHTS**

- New version of CCI SST CDR with extended temporal coverage spanning 40 years and including new sensors
- New diurnal SST product for the Mediterranean Sea using a combination of satellite SST and model data
- Improved cloud detection scheme for SLSTR

### **INTRODUCTION**

The document is a report from session 4 from the the GHRSSST XXII science team meeting, 2021. The session consisted of oral presentations and posters. A summary of each of the presentations and the online discussions is given in the following sections.

### **RESOURCES**

View presentations (recordings): <https://training.eumetsat.int/mod/book/view.php?id=14071&chapterid=629>

Discussion forum for recordings: <https://training.eumetsat.int/mod/forum/view.php?id=14082>

Download the slides: <https://training.eumetsat.int/mod/folder/view.php?id=14083>

Posters padlet: <https://training.eumetsat.int/mod/book/view.php?id=14071&chapterid=629>

**ORAL PRESENTATIONS**

Owen Embury - Developments towards a 40-year climate data record from the ESA Climate Change Initiative

Describes third version of the SST CCI climate data record. Compared to the previous versions, it is longer (40 years), has improved AVHRR SSTs, and now includes SLSTR and PMW data.

The instruments contributing to the CDR are the aerosol robust ATSR / SLSTR reference sensors, MetOp full resolution AVHRRs which are tuned to ATSR / SLSTR, NOAA AVHRRs which are tuned to in situ and AMSRE / AMSR2. There is improved coverage in the 1980s through the addition of data that couldn't be processed in CDR2.

The AVHRR retrievals now use bias aware optimal interpolation. An updated version of RTTOV is used which allows use of aerosol components from CAMS. The prior is now a bias corrected version of CDR2.1. There are reduced dust biases in CDR3 and improvements in coverage and length of data record from some of the AVHRR instruments. CDR3 includes NOAA-6, 8 and 10, which weren't processed in CDR2.

The PMW retrievals use statistical retrievals and RFI/QC filtering.

Discussion: It was asked whether there is sufficient in situ data to validate back to the 1980s. The response was that this is an issue, including in the 1990s. In addition to direct comparisons between in situ and the CCI data, there will be a comparison with HadSST. A second question asked whether upgrading from RTTOV 11 to 12 made a difference in aerosol free conditions. The answer was no, but that there are updated coefficients released with RTTOV 13 which does make a difference and these are compatible with RTTOV 12.

Chris Merchant - Bias-aware optimal estimation for sea surface temperatures from historic AVHRRs

Describes work done as part of the ESA CCI project. Optimal estimation (OE) to retrieve SST is only optimal if underlying assumptions are met. Bias aware OE helps to ensure the OE assumptions are met. OE is a well understood method and provides uncertainty and sensitivity information. However, it relies on zero-mean bias in the observations and prior. It also requires covariance matrices, but there is not a clear way to obtain these.

To obtain the covariance matrices, one option is a detailed uncertainty analysis but this has not been done for RTTOV. Instead, it is done using empirical methods using 'Desroziers' methods.

Bias aware OE gives estimates of bias in satellite BTs relative to simulations, bias in the total column water vapour from NWP and estimates of the error covariance matrices. These can be examined for dependencies such as TCWV, SST, dust, view zenith angle, latitude...

Bias corrections for BTs were found to be ~tenths of a K, which seems plausible. It was expected that the prior water vapour values would be wet because the retrievals are only done for clear sky conditions, but the NWP grid cells cover a larger area. This is consistent with what is found, with lowest biases occurring in dry conditions. The estimates of in situ uncertainty were found to have improved over time from ~0.325 in 1980 to ~0.15 from ~2000 onwards. These include point-to-pixel uncertainty. BT uncertainty relative to RTTOV were larger than just the instrument NEDT due to calibration and RTTOV errors. They were lower in the 11 micron channel, which may be because of the way the matchups were constructed (see below).

Results from NOAA6 SSTs look relatively unbiased but not of the quality obtained from later AVHRRs. NOAA19 was the 'best' AVHRR in CDR2 but showed strong seasonal dust biases which are largely removed in CDR3.

It was found that interactions with cloud detection needs careful handling. The local standard deviation of the 11 micron channel is used in cloud detection, which affects use of covariances in the bias-aware OE cloud detection.

In the future bias aware OE will be used in harmonising MetOp AVHRRs and MODIS to dual view references, to explore HIRS SST retrievals and for MW SSTs. Experiments have started to harmonise low Earth orbit and geostationary satellites.

Discussion: A question was asked about how the improvements in dust aerosol affected regions are made. The response was that this was mainly due to improvements in the forward modelling to include dust.

It was asked how the set of parameters used in the OE was formulated for each sensor and why is solar zenith angle used at all. Solar zenith angle is related to stray light and other AVHRR instrumental biases. The list of parameters was empirically chosen one by one by inspection in order to avoid overfitting.

Andrea Pisano - A New Operational Mediterranean Diurnal Optimally Interpolated SST Product within the Copernicus Marine Service

The Copernicus Marine Service (CMEMS) produces near real time and delayed mode single/multi-sensor L3C/L3S SST products and merged, gap-free products (L4). The products are being continually evolved. These include products for the Mediterranean Sea. In May 2021 a diurnal SST product was released. This contains hourly mean sub-skin SST centred at 00:00, 01:00, 02:00 etc. at 1/16 degree resolution. Analyses are produced once a day.

The algorithm combines satellite data with a first guess model analysis using optimal interpolation (OI). The satellite data are OSI SAF SEVIRI L3C. The model data are hourly sea water potential temperature at ~1m depth from the CMEMS Mediterranean Sea model. Drifting buoys were used for validation.

The accuracy of the results were assessed for 2019-2020 by comparing the output analyses and the model data to the drifting buoys. The mean differences between the analyses and drifters was 0.034K compared to -0.101K for the model. The RMS differences were 0.44 and 0.48K respectively. The analyses compare well to the diurnal cycle from the drifters, while the model underestimates the amplitude of the diurnal cycle.

Diurnal warming events were studied by defining them as the maximum SST minus the foundation SST. The Mediterranean Sea has diurnal warming amplitudes from ~0.7K to 1K, but on a daily basis can be > 5K, and these correspond to low wind speeds. This analysis also shows that the model underestimates the diurnal amplitude, probably due to the size of the model level.

Rishi K Gangwar - Optimal Estimation of SST from INSAT-3D/3DR Imagers

The INSAT-3D/3DR imagers were launched in July 2013 and September 2016. The imager channels 5 and 6 (corresponding to ~11 and 12 microns) were used to retrieve SSTs. The retrieval uses optimal estimation (OE) / 1DVAR. A cost function is minimised to obtain the retrieved SST. The first guess is from the Global Forecast System from NCEP. RTTOV 11.3 is used to simulate TOA brightness temperatures. The atmospheric state is modelled by atmospheric temperature and humidity at 25 levels and SST. A cloud masking scheme is applied (details provided in the presentation). Bias correction is applied to the satellite data to avoid erroneous, biased retrievals. A comparison of two different retrieval schemes has been done. Non-linear SST (NLSST) and 1DVAR is compared. In situ reference data were obtained from iQuam. The validation was not done during the monsoon period because of the persistent cloud coverage, so the validation covered Dec 2019 – May 2020. 1DVAR performs better than NLSST for both instruments. There was not much difference between robust and non-robust statistics indicating few outliers. 1DVAR also has smaller spatial variation in biases compared NLSST.

Discussion: How were the error covariances defined? They were defined as described in Remote Sens. 2020, 12(19), 3142; <https://doi.org/10.3390/rs12193142>. The method is to compare forecasts with analyses over a year. For example, for SST the error standard deviation was calculated as 0.51 K.

Is the atmospheric state modified in the retrieval? Yes, but SST is kept as the final retrieval.

There was a discussion related to the question: What is the sensitivity of the retrieval, as the strength of the SST gradients relative to NLSST retrievals might indicate a strong dependence on the prior? The response was this has been calculated but wasn't shown due to time constraints in the presentation. The prior does not contain gradients, indicating that the retrieval is not strongly dependent on it. The NLSST retrieval is directly related to the satellite data so will tend to produce stronger gradients. Also, on other days the OE retrieval had stronger gradients than NLSST. The questioner clarified that the gradients may still be being smoothed by the presence of the prior, even if they are present, and that the NLSST (and other split window retrievals) have an implicit prior and that two channels is not sufficient information to retrieve SST without additional constraints, making it challenging to meet emerging requirements from NWP. This was followed by a question asking what extra channels would help. ~8.7 microns is being tested with SEVIRI, although it behaves a bit like 11 microns in some atmospheric conditions and at some zenith angles. A study is needed

to assess what would be valuable for TIR SST retrievals. Investigating use of the ~3.9 micron channel during the day is another possibility, but the correction for reflection components would need to be addressed.

It was asked if there was a strong diurnal signal around midnight local time. The response was that yes, there is a calibration issue that causes this effect in INSAT imagers. A real time bias correction procedure is applied to correct this.

**POSTER PRESENTATIONS**

Chelle Gentemann: Open source algorithms for AMSR3: Accelerating and expanding AMSR3's scientific impact

The tools of science (i.e. computers, data and software) are rapidly evolving. How can the advances be leveraged within GHRSSST for algorithm development? Cloud computing allows open collaboration instead of individual groups working alone. The challenge is to coordinate within GHRSSST on developing standard open software for AMSR3 retrievals. This would reduce duplication of effort.

Claire Bulgin: Bayesian Cloud Detection Scheme Improvements for the SLSTR instrument

The Bayesian Cloud Detection Scheme (BCDS) is used to screen data before SST retrievals. This is particularly challenging in regions such as coasts. A pre-processor was added to the BCDS to optimise the way that visible imagery is used with IR. The visible pixels do not match the IR pixels and some are only available in certain strips. Instead of a simple regridding, the new pre-processor uses nearest neighbours. This better matches the visible data to the infrared pixel. 10 test scenes have been examined to find the optimum number of nearest neighbours to use.

Alex Semenov: Towards Improved ACSPO Clear-Sky Mask for SST from Geostationary Satellites

The ACSPO clear sky mask (ACSM) identifies valid SST pixels and screens out e.g. cloudy data. It is produced using several tests, in particular differences between retrieved SSTs and a reference (L4 CMC). The results for geostationary data are currently not as good as for low earth orbit. A set of 68 validation areas were used to assess performance of the mask. The current approach has false alarms in dynamic areas and cloud leakages. Improvements were made by applying current tests everywhere except the identified challenging areas. In those regions, other tests were tried and the best performers selected based on how much over-screening occurs, how many pixels the test is triggered on and whether it is providing unique information. Results from the new mask showed reduced false alarms and cloud leakages.

Discussion: Was screening of clouds where cloud top temperature is higher than SST considered? Future work on Himawari-8 will include improved warm cloud detection. A validation dataset will be needed for this.

Goshka Szcrodrak: Use of ERA-5 Sea Surface Temperature Fields as prior in Optimal Estimation retrieval of SST from MODIS

The ERA5 sea surface temperature (sst; this is the temperature at buoy level so 0.17K is subtracted to obtain skin temperature) and skin temperature (skt) have been tested as priors in the OE retrieval of SST from MODIS. When using 'sst', there is a bias in the daytime retrievals. It was found that this can be corrected for. The 'skt' retrievals were worse, even without the bias correction being applied to 'sst'. This was surprising as 'skt' includes the SST diurnal cycle.

Discussion: How was the Jacobian for the TCWV calculated? This was done by calculating the difference in radiances from two cases that are identical except for the TCWV and dividing by the change in TCWV.

Victor Pryamitsyn: Historical and Near-real Time SST retrievals from Metop AVHRR FRAC with ACSPO

Full resolution MetOp AVHRR datasets have been generated using ACSPO and are available from PO.DAAC. They contain subskin SSTs produced by global regression which are trained to in situ and are sensitive to skin SST, and a be-biased SST (which can be obtained by subtracting SSES bias) generated from piecewise regression, which is less sensitive to skin SST but more accurate relative to in situ. Validation statistics are stable over time and are easily better than NOAA specifications. Ongoing work aims to mitigate L1B calibration errors and to improve SST retrieval and training algorithms.

## **S4 - ORAL PRESENTATIONS - ABSTRACTS**

## S4-1: OPTIMAL ESTIMATION OF SST FROM INSAT-3DR IMAGERS

**Rishi Kumar Gangwar**<sup>(1)</sup>, **Pradeep Kumar Thapliyal**<sup>(2)</sup>

(1) Space Applications Centre (ISRO), Ahmedabad, Gujarat, India-380015, Email: [rgbly1986@sac.isro.gov.in](mailto:rgbly1986@sac.isro.gov.in)

(2) Space Applications Centre (ISRO), Ahmedabad, Gujarat, India-380015, Email: [pkthapliyal@sac.isro.gov.in](mailto:pkthapliyal@sac.isro.gov.in)

### ABSTRACT

The accurate estimation of sea surface temperature (SST) is very crucial for Earth's climate monitoring. The satellite-based measurements provide a unique opportunity to estimate the global SST at frequent intervals. In this regard, we have exploited optimal estimation (OE) or one-dimensional Variational (1DVAR) technique for developing a retrieval algorithm for SST from thermal infrared observations of Imagers flown on-board the Indian geostationary satellites INSAT-3D & 3DR. To evaluate the efficacy of the 1DVAR based retrieval algorithm, it has been applied on the six months of INSAT-3D/3DR observations to retrieve SST. Thereafter, the retrieved SST has been assessed against the in-situ measurements of SST. The quantitative measure of the retrieval errors in the SST was computed in terms of standard statistical parameters viz. bias and the standard deviation of the differences (SD), etc. The slightly negative bias of -0.20K with 0.6K SD were obtained in the retrieved SST when compared against the in-situ measurements. Moreover, the spatial gradients of the daily SST were also computed to observe the fine scale features of the ocean. The spatial gradients in the retrieved SST from INSAT-3D/3DR show the similar pattern as observed in the daily Multiscale Ultrahigh Resolution (MUR) level-4 analysis SST acquired from Group for High-Resolution Sea Surface Temperature (GHRSSST). The spatial gradients are the primary inputs for generating the thermal fronts in predicting the potential fishery zones (PFZ). This methodology of SST retrieval is now operational for INSAT-3D/3DR Imager at India Meteorological Department (IMD), New Delhi, India.

### INTRODUCTION

Sea surface temperature (sst) is an essential climate variable (ecv), which is very important for understanding the earth's climate variability (e.g., merchant et al., 2019). It is also a critical boundary condition in the numerical weather prediction (nwp) models, ocean and coupled models to predict the weather and ocean state (liang et al., 2017). This is mainly because sst as a parameter plays an important role in determining the exchange of heat, moisture, and momentum fluxes at the interface of the ocean and the atmosphere (bentamy et al., 2017). Furthermore, sst also provides an insight into various physical processes that are responsible for several oceanographic as well as meteorological phenomena, thereby directly affecting large and small-scale weather and climate patterns (o'carroll et al., 2019).

Although the in-situ measurements provide an accurate estimate of sst, they are sparse in spatial coverage due to the high cost involved to cover vast oceanic regions. Space-based instruments have made it possible to sample the sst over the global ocean from low earth orbiting (leo) satellites but less frequently, typically a few ascending and descending orbits over a particular location. To overcome this and obtain frequent observations over a fixed location the geostationary earth orbiting (geo) satellites are used, but these observations are mostly limited to the tropics and mid-latitudes. Currently, most of the ir sensors are flown on the leo satellite platforms that provide observations for sst estimation over a fixed location, typically twice a day. However, many applications, like identifying potential fishery zones, require the diurnal variations in the sst gradients that are not possible from leo platforms. Therefore, geostationary (geo) satellite observations are required for high temporal resolution sst estimates.

Currently, india has two geostationary satellites insat-3d and 3dr in the orbits, launched in 2013 and 2017, and located over 82°e and 74°e, respectively. These satellites have two identical instruments: (1) 6 channels imager and (2) 19 channels sounder. The imager provides observations in 6 channels: visible (0.52-0.72  $\mu\text{m}$ ), shortwave infrared (swir) 1.55-1.70  $\mu\text{m}$ , 3.80-4.00  $\mu\text{m}$  medium-wave infrared (mir), 6.50- 7.00  $\mu\text{m}$  (water vapour), thermal infrared (tir) 10.2-11.2  $\mu\text{m}$  (tir-1) and 11.5-12.5  $\mu\text{m}$  (tir-2)) bands. The spatial resolutions are 1km  $\times$  1km for visible and swir bands and 4km  $\times$  4km for one mir and both tir bands.

At present, sst is being produced operationally using the non-linear sst (nlsst) algorithm (walton et al., 1998) based on split-window observations from both the insat-3d/3dr imagers. Imager's channel number 5 (tir-1)

and 6 (tir-2) form the required split-window channels for sst estimation. The nlsst algorithm is a globally used algorithm for estimating the state-of-the-art sst products from satellite ir observations. However, it also suffers from some inherent limitations like regional biases, improper midnight calibration of satellite observations, predominantly for the observations from geo satellites that use a three-axis stabilization system. To address these limitations, algorithms based on 1-dimensional variational (1dvar) or optimal estimation (oe) have been developed in the recent past for estimating sst from various satellite-based ir observations (e.g., merchant et al., 2008, 2009, 2014). The 1dvar utilizes a forward model to simulate satellite observations using prior information of atmosphere and oceanic state, which leads to improvement in the accuracy of sst retrievals.

**Kindly note that the most of the study content is taken from our already published article Gangwar and Thapliyal 2020.**

## METHODOLOGY

As we know that the IR radiation cannot penetrate through the clouds, the information about the underlying surfaces cannot be obtained. Therefore, the cloudy pixels have to be masked prior to SST estimation from IR observations. Herein, we have used several threshold and spatial uniformity and homogeneity based tests to mask the cloudy pixels. Moreover, the satellite observations must be well calibrated and unbiased prior to their use in the retrieval algorithms (Merchant et al., 2008); otherwise, it will lead to erroneous and biased retrievals. Hence, the matching of the cumulative density function (CDF) has been utilized here for bias correction of the actual INSAT-3D/3DR observations. First, CDFs of both actual and simulated observations are computed. Then, the actual observations have been mapped according to the simulated CDF to get the corrected observations. After the cloud masking and bias correction of the INAST-3D/3DR observations, the 1DVAR-based technique has been utilized for SST estimation from these observations.

## 1DVAR ALGORITHM

The relationship between geophysical parameter and satellite measurements can be written in a generalized form as:

$$y = F(x) + e \quad (1)$$

where,  $y$  is the measurement vector (satellite observations),  $F(x)$  is the nonlinear forward model (radiative transfer (RT) model) which transforms  $x$ , the state vector containing the relevant geophysical parameters of the ocean and atmosphere, into measurement vector (Merchant et al., 2008).  $e$  is a residual uncertainty term containing uncertainties of measurement and the forward model.

The forward model, i.e., RT model synthesizes the top-of-atmosphere brightness temperatures that should be measured by the individual channels of a radiometer given priori knowledge of the relevant atmosphere state and surface condition ( $x$ ). A fast RT model RTTOV11.3 has been used as the forward model in this study.

Now, by inverting equation (1), we can retrieve the most likely geophysical parameters ( $x$ ) that can reproduce the top-of-the atmosphere brightness temperatures,  $y$ . In this paper, we have used an inverse approach (1DVAR or optimal estimation (OE)) developed by Rodgers (2000) for retrieving the  $x$  (e.g., SST).

Assuming the forward model is a general function of the state, the representative (measurement + model) error has a Gaussian distribution, and there is a prior estimate with a Gaussian uncertainty distribution, the maximum probable state  $x$  can be found by minimizing the cost function,  $J$ :

$$J(x) = (x - x_0)^T B^{-1} (x - x_0) + (y - y(x))^T R^{-1} (y - y(x)) \quad (2)$$

where,  $y$  is the observations with error covariance  $R$ ;  $x_0$  being the prior atmospheric state having error covariance  $B$  and  $y(x)$  is the observations simulated through forward model using atmospheric state  $x$ .

Rodgers (1976) gives the following iterative solution to the minimization of  $J(x)$ :

$$x_{n+1} = x_0 + B H_n^T (H_n B H_n^T + R)^{-1} [y - y(x_n) - H_n (x_0 - x_n)] \quad (3)$$

where,  $x_n$  is the  $n$ th estimate of atmospheric state,  $x_0$  being the background atmospheric state.  $y$  represents the actual brightness temperatures of concerned channels and  $y(x_n)$  are the simulated brightness temperatures corresponding to  $n$ th atmospheric state ( $x_n$ ).  $H_n$  is the sensitivity of the simulated observations with respect to state variables also known as Jacobian matrix.  $H_n$  consists of the partial derivatives of the brightness temperatures in a particular channel with respect to each parameter of the state vector ( $x_n$ ). Due to non-linearity, these partial derivatives need to be computed at each iteration (state).

The equation (3) implies that the sensitivity information ( $H_n$ ) together with the difference between the actual brightness temperatures,  $y$ , and the simulated brightness temperatures  $y(x_n)$  can be used to estimate the difference between the prior information about the state and the actual state, and thereby to estimate the actual state.

## RESULTS

To examine the efficacy of the developed algorithm, it has been applied on six months of INSAT-3D/3DR split-window observations to estimate the SST for December 2019 to May 2020 period. Thereafter, the retrieved SST was validated against the concurrent in-situ SST measurements for the entire six months. The in-situ SST data was acquired from the iQuam portal of the National Oceanic and Atmospheric Administration (NOAA). For the validation, a matchup dataset comprising the pairs of the retrieved and in-situ SST was prepared. To prepare the matchup dataset the spatial resolution of  $0.04^\circ$  and temporal window of  $\pm 15$  minutes was assumed. The error in the retrieved SST was quantified through standard statistical quality indicators viz. bias (Bias), median (Median), standard deviation of the difference between the retrieved and the reference SST (Std) and the median absolute deviation (MAD). Figures 1-2 are showing all four-quality indicators, viz., Bias, Std, Median and MAD computed on daily-scale for the six months, the collocation is done on instantaneous SST basis and not on the daily-averaged SST. For making MAD comparable to Std, we have multiplied MAD by a factor of 1.4826. The scale factor is computed with the assumption that the concerned data distribution is Gaussian.

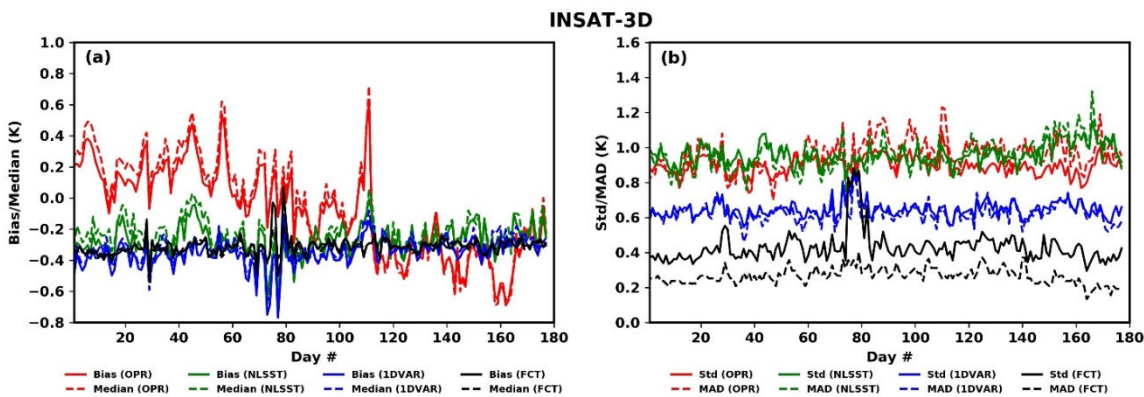


Figure 1: Validation statistics generated on a daily scale for retrieved SST from INSAT-3D observation against iQuam SST, (a) Bias/Median, and (b) Std/MAD

To monitor the improvement in the retrieved SST products using 1DVAR algorithm over the NLSST algorithm, the validation of the operational SST products (OPR) of INSAT-3D/3DR were also carried out with the same in-situ SST measurements. Moreover, the comparison of the first guess SST (FCT) is also shown in the respective figures. Another SST products denoted herein by NLSST were also compared with the same reference SST products to observe the impact of the real-time bias correction of the INSAT-3D/3DR observations. The retrieval algorithm is the same for both NLSST and OPR products, only difference is the inclusion of the real-time bias correction procedure in case of NLSST products.

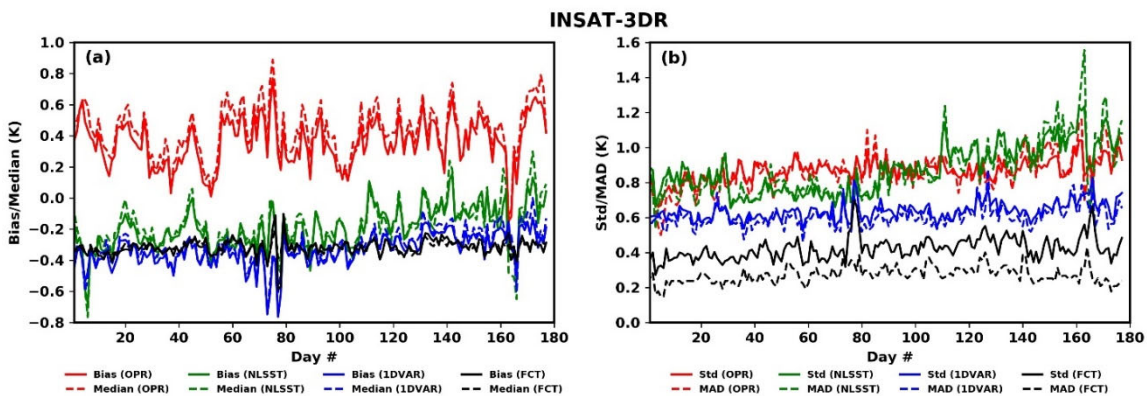


Figure 2: Validation statistics generated on a daily scale for retrieved SST from INSAT-3D observation against iQuam SST, (a) Bias/Median, and (b) Std/MAD

It can be observed in figure 1 that the Bias and Median do not show any significant difference so as Std and MAD. This implies the robustness of the matchup data. We can further observe that 1DVAR shows the higher accuracy (0.6K) than NLSST (0.9K). However, both algorithms are showing negative biases, i.e., underestimating SST values as compared to iQuam SST. Moreover, the performance of 1DVAR is more consistent than NLSST throughout the period, demonstrating superior efficacy of 1DVAR over NLSST. A point to be mentioned here is that for the overall period the biases in SST derived from NLSST (-0.27K in INSAT-3D and -0.18K in INSAT-3DR) are smaller compared to 1DVAR SST (-0.36K in INSAT-3D and -0.34K in INSAT-3DR). It may be noted that the NLSST and 1DVAR SST are skin SST without any correction for bulk-skin SST, whereas, the iQuam SST is representative of subsurface or bulk SST. Therefore, the bulk-skin SST correction of -0.2K needs to be applied on the retrieved skin SST (Donlon et al., 1999). This means that the effective biases in the retrieved SST should be around -0.07K (0.02K) in NLSST and -0.16K (-0.14) in the 1DVAR for INSAT-3D (INSAT-3DR). It may be further noted that the INSAT-3D/3DR Imager observations undergo large biases and uncertainties during the satellite eclipse period (peak mid-night sun/stray-light problem) as discussed in Shukla and Thapliyal (2020). This leads to the large bias/uncertainties in the operational SST (OPR) products presently available from INSAT-3D/3DR.

## CONCLUSION

In the present study, we have exploited the 1DVAR technique to retrieve the SST using thermal split-window infrared observations from INSAT-3D/3DR. Although the conventional regression based retrieval technique NLSST is already implemented from mid-June 2018 at MOSDAC/SAC and MMDRPS/IMD, it does not have mechanism to correct for diurnal and seasonal dependent biases. Therefore, herein it has been corrected using a real-time bias correction of satellite observations using model forecast fields as input in the RT model. Since both the algorithms, NLSST and 1DVAR, utilizes RT model for coefficient generation as well as forward/Jacobian computation, this procedure makes satellite observations consistent with the RT model. Both these algorithms are tested for six months of INSAT-3D & 3DR observations to retrieve SST in order to capture seasonal variability ranging from winter (cold SST) to summer (warm SST). The qualitative assessment of the retrieved SST is carried out by validating with the iQuam SST.

The 1DVAR based retrieval shows the similar accuracy with Std (Bias) of 0.63K (-0.36K) for both INSAT-3D & 3DR. Whereas, NLSST provides slightly lesser accurate SST with Std (bias) of 0.87K (-0.18K) for INSAT-3DR and 0.95K (-0.27K) for INSAT-3D, respectively. It may be noted that an additional cold bias of about -0.2K may also be because the satellite SST fields are skin-SST whereas; the iQuam is bulk or sub-skin SST. This brings bias value in both the 1DVAR and NLSST very close to zero. This implies a significant improvement in SST retrieval accuracy using 1DVAR algorithm over NLSST.

## REFERENCES

Bentamy, A.; Piollé, J.F.; Grouazel, A.; Danielson, R.; Gulev, S.; Paul, F.; Azelmat, H.; Mathieu, P.P.; von Schuckmann, K.; Sathyendranath, S.; et al. Review and assessment of latent and sensible heat flux

accuracy over the global oceans. *Remote Sens. Environ.* 2017, 201, 196–218, doi:10.1016/j.rse.2017.08.016.

Donlon, C.J.; Nightingale, T.J.; Sheasby, T.; Turner, J.; Robinson, I.S.; Emery, W.J. Implications of the oceanic thermal skin temperature Deviation at High Wind Speed. *Geophys. Res. Lett.* **1999**, 26, 2505.

Gangwar, R.K; Thapliyal, P.K. Variational Based Estimation of Sea Surface Temperature from Split-Window Observations of INSAT-3D/3DR Imager. *Remote Sensing*. 2020, 12(19), 3142.

Liang, X.; Yang, Q.; Nergler, L.; Losa, S.N.; Zhao, B.; Zheng, F.; Zhang, L.; Wu, L. Assimilating Copernicus SST Data into a Pan-Arctic Ice-Ocean Coupled Model with a Local SEIK Filter. *J. Atmos. Ocean. Technol.* 2017, 34, 1985–1999, doi:10.1175/JTECH-D-16-0166.1.

Merchant, C.J.; Embury, O.; Bulgin, C.E.; Block, T.; Corlett, G.K.; Fiedler, E.; Good, S.A.; Mittaz, J.; Rayner, N.A.; Berry, D.; et al. Satellite based time-series of sea-surface temperature since 1981 for climate applications. *Sci. Data* **2019**, 6, 223, 796 doi:10.1038/s41597-019-0236-x.

Merchant, C.J.; Le Borgne, P.; Marsouin, A.; Roquet, H. Optimal estimation of sea surface temperature from split-window observations. *Remote Sens. Environ.* 2008, 112, 2469–2484, doi:10.1016/j.rse.2007.11.011.

Merchant, C.J.; Le Borgne, P.; Roquet, H.; Marsouin, A. Sea surface temperature from a geostationary satellite by optimal estimation. *Remote Sens. Environ.* 2009, 113, 445–457.

Merchant, C.J.; Embury, O. Simulation and Inversion of Satellite Thermal Measurements. In *Experimental Methods in the Physical Sciences*; Elsevier: Amsterdam, The Netherlands, 2014; Volume 47, pp. 489–526, ISBN 978-0-12-417011-7.

O'Carroll, A.G.; Armstrong, E.M.; Beggs, H.M.; Bouali, M.; Casey, K.S.; Corlett, G.K.; Dash, P.; Donlon, C.J.; Gentemann, C.L.; Høyer, J.L.; et al. Observational Needs of Sea Surface Temperature. *Front. Mar. Sci.* 2019, 6, 420, doi:10.3389/fmars.2019.00420.

Rodgers, C.D. *Inverse Methods for Atmospheric Sounding—Theory and Practice*; Series on Atmospheric Oceanic and Planetary Physics; World Scientific Publishing Co. Pte. Ltd.: Singapore, 2000; Volume 2, ISBN 978-981-281-371-8.

Rodgers, C.D. Retrieval of atmospheric temperature and composition from remote measurements of thermal radiation. *R. Geophys. Space Phys.* 1976, 14, 609–624.

Walton, C.C.; Pichel, W.G.; Sapper, F.J.; May, D.A. The development and operational application of non-linear algorithms for the measurement of sea surface temperatures with NOAA polar orbiting environmental satellites. *J. Geophys. Res.* 1998, 103, 27999–28012.

## S4-2: A NEW OPERATIONAL MEDITERRANEAN DIURNAL OPTIMALLY INTERPOLATED SST PRODUCT WITHIN THE COPERNICUS MARINE SERVICE

**Andrea Pisano<sup>(1)</sup>, Salvatore Marullo<sup>(2)</sup>,  
Rosalia Santoleri<sup>(1)</sup>, Daniele Ciani<sup>(1)</sup>, Bruno Buongiorno Nardelli<sup>(3)</sup>**

(1) CNR-ISMAR, Via del Fosso del Cavaliere 100, 00133, Rome, Italy, Email: [andrea.pisano@cnr.it](mailto:andrea.pisano@cnr.it), [rosalia.santoleri@cnr.it](mailto:rosalia.santoleri@cnr.it), [daniele.ciani@cnr.it](mailto:daniele.ciani@cnr.it)

(2) ENEA, Via Enrico Fermi, 45, 00044 Frascati, Italy, Email: [salvatore.marullo@enea.it](mailto:salvatore.marullo@enea.it)

(3) CNR-ISMAR, Calata Porta di Massa, 80133 Napoli, Rome, Italy, Email: [bruno.buongiornonardelli@cnr.it](mailto:bruno.buongiornonardelli@cnr.it)

### INTRODUCTION

Within the Copernicus Marine Environment Monitoring Service (CMEMS, Le Traon et al., 2019), the Sea Surface Temperature Thematic Assembly Centre (SST-TAC) is in charge of the near real-time and reprocessed production of satellite-based SST products. The SST-TAC provides a variety of single and merged multi-sensor data (L3C/L3S) and gap-free (L4) SST data covering the global ocean and the European seas, characterized by different spatial and temporal resolutions in order to serve different user needs, and freely available at the [CMEMS](#) web catalogue.

For the Mediterranean Sea (MED), the SST-TAC provides daily mean (night-time) L3S and L4 foundation SST fields at high ( $1/16^\circ$ ) and ultra-high spatial resolution ( $1/100^\circ$ ) covering the period from 2008 to present (Buongiorno Nardelli et al., 2013). All these data are built by using L2P data derived from different infrared satellite sensors, which also include the new generation SLSTR sensor on board the ESA Sentinel-3A/3B satellites. A reprocessed Mediterranean SST dataset complements the near real time production, providing a stable, consistent, long-term (1982-present) time series of gap-free foundation SST fields (Pisano et al., 2016).

In May 2021, a new Mediterranean diurnal optimally interpolated SST (MED DOISST) product was released ([SST\\_MED\\_PHY\\_SUBSKIN\\_L4\\_NRT\\_010\\_036](#)). This product provides hourly mean L4 maps of subskin SST at  $1/16^\circ$  grid resolution covering the period from 1<sup>st</sup> January 2019 up to near real time. The MED DOISST operational chain is run daily and provides 24 hourly mean data of the previous day.

### MATERIAL AND METHODS

The MED DOISST product is built by combining satellite data as the input diurnal signal source and model analyses as first-guess using optimal interpolation (OI), following Marullo et al. 2014. The resulting SST anomaly field (satellite-model) is free, or nearly free, of any diurnal cycle, thus allowing to interpolate SST anomalies using satellite data acquired at different times of the day and then produce hourly gap-free SST fields.

The satellite data used here are hourly Level-3 collated (L3C) data acquired by SEVIRI and operationally produced by EUMETSAT at the OSI-SAF. These data provide sub-skin SST fields at about 5km grid resolution. Input model SST is derived from the CMEMS Mediterranean Sea Physical Analysis and Forecasting Product (CMEMS Product ID: MEDSEA\_ANALYSIS\_FORECAST\_PHY\_006\_013). This product contains 3D, 24 hourly mean fields of potential temperature at about 4km horizontal resolution. For our purposes, only surface (1.0182 meter) seawater potential temperature is considered and used as first-guess.

The diurnal operational chain has been implemented by adapting the consolidated MED SST processing chain for the near real time production (Buongiorno Nardelli et al., 2013). This operational chain is organized in four main modules (see also the product user manual, [PUM](#)), that perform the following steps: (1) download satellite and model data, (2) regridding to the Mediterranean diurnal product grid and quality control check (applied to SEVIRI data retaining only the best quality SSTs), (3) optimal interpolation and (4) upload to the CMEMS dissemination unit is performed.

Finally, surface drifting buoys have been used for the validation. Drifters' data are provided by the CMEMS INS-TAC. The information about the quality of these data has been used to exclude suspect measurements, keeping only the best quality data.

## RESULTS

The accuracy of the diurnal product has been assessed through a comprehensive validation by direct comparison of diurnal SSTs against surface drifting buoy measurements. More in detail, the validation is based on the compilation of a matchup database between satellite and drifter data covering the period 2019-2020. From the differences (SST minus and drifter) over the matchup points, the mean bias and root-mean-square-difference (RMSD) have been provided. The same statistics have been provided for the model, with the aim to also compare diurnal and model SSTs.

First, the spatial distribution of the matchup points (Figure 1) shows a homogeneous coverage over the entire domain, although an uneven in situ data coverage characterizes the North Adriatic and North Aegean Seas.

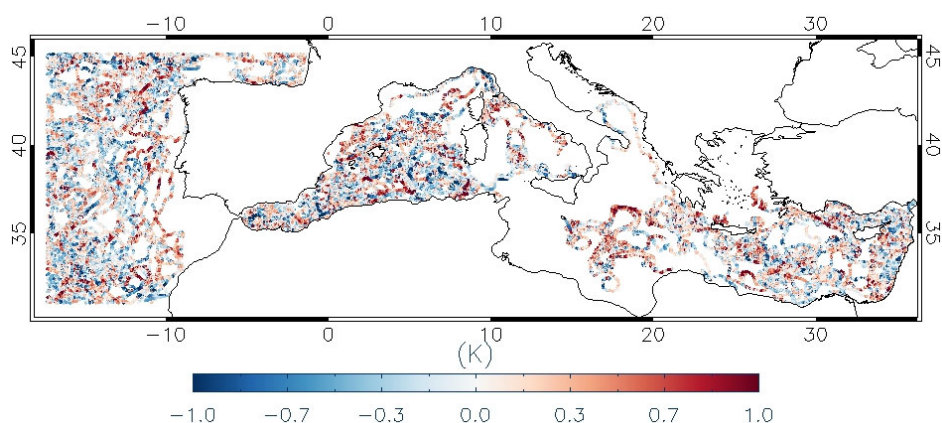


Figure 1. Spatial distribution of the matchup points along with their punctual bias (i.e., SST minus drifter data, K) over the CMEMS Mediterranean domain from 01/01/2019 to 12/31/2020.

When compared to in situ drifter data, the MED DOISST product shows a good accuracy in terms of both mean bias ( $\sim 0.054\text{K}$ ) and RMSD ( $\sim 0.53\text{K}$ ), being able to well reproduce the diurnal cycle (Figure 2). During the central warming hours, this dataset performs better than model data, which tend to depart from in situ data and slightly underestimate the diurnal cycle amplitude (Figure 2).

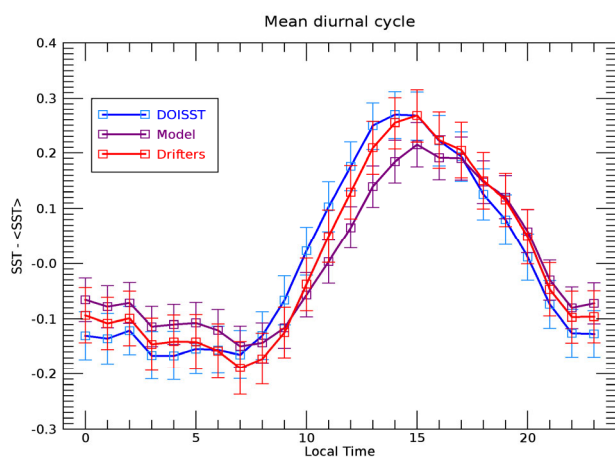


Figure 2. Mean diurnal cycle computed for MED DOISST (blue line), model (purple line) and drifters' data (red line) anomalies over the matchups for the period 2019-2020. Anomalies are computed by subtracting from each SST time series their average ( $\langle \text{SST} \rangle$ ) in order to remove eventual biases and better evidence the diurnal cycle amplitude.

The subskin temperature is the temperature at the base of the thermal skin layer (see also the [GHRSSST](#) SST definitions) and it is equivalent to the foundation SST at night, but during daytime it can be significantly

different under favourable (clear sky and low wind) diurnal warming (DW) conditions. Diurnal warming is very intense and frequent in the Mediterranean Sea, and the maximum amplitude can reach peaks greater than 5K (Minnett et al. 2019). The DW amplitude, which is the highest daily amplitude, is estimated (at a given location and over a day) as the maximum among the differences between SSTs and the corresponding foundation SST (Minnett et al. 2019). Applying this criterion to the MED DOISST product, we computed the spatial map of the mean DW amplitude during 2019 (Figure 3-left).

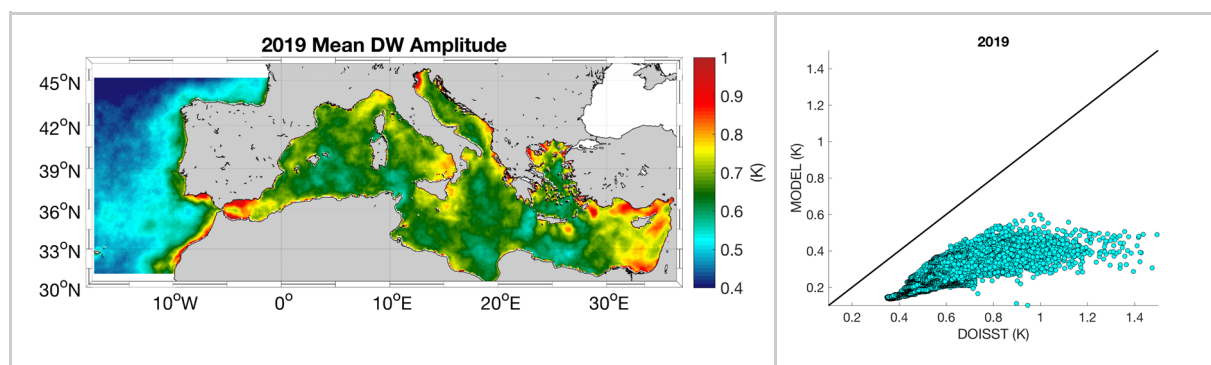


Figure 3. (Left) Mean diurnal warming amplitude estimated from the MED DOISST product over 2019. (Right) Scatter plot of diurnal warming amplitudes estimated from MED DOISST product and model data during 2019.

On a yearly average, the whole Mediterranean Sea is characterized by DW amplitudes from about 0.5 to 1 K. Furthermore, when DW amplitude is estimated by model data, it is well evident (**Figure 3-right**) how the model underestimates these amplitudes from about 0.2 to 0.5 K. This is likely due to the different depth provided by the model (about 1 meter).

## CONCLUSIONS

The recently released Mediterranean SST diurnal product within the Copernicus Marine Service shows a good accuracy in terms of both mean bias and error. It is also able to well reproduce the diurnal cycle, including diurnal warming events. This product performs better than the CMEMS model data during the central warming hours. Future work will investigate DW events on a daily basis, where such events can reach amplitudes > 5K.

This product can improve assimilation in NWF systems, heat budget estimates, and temperature extremes monitoring.

This product is freely available at <https://marine.copernicus.eu/> with its PUM and QUID.

## REFERENCES

- Buonignore Nardelli, B., Tronconi, C., Pisano, A., Santoleri, R. (2013). High and Ultra-High resolution processing of satellite Sea Surface Temperature data over Southern European Seas in the framework of MyOcean project. *Remote Sensing of Environment*, 129, 1-16.
- Le Traon, P. Y., Reppucci, A., Alvarez Fanjul, E., Aouf, L., Behrens, A., Belmonte, M., & Zacharioudaki, A. (2019). From observation to information and users: the Copernicus Marine Service perspective. *Frontiers in Marine Science*, 6, 234.
- Marullo, S., Santoleri, R., Ciani, D., Le Borgne, P., Péré, S., Pinardi, N., ... Nardone, G. (2014). Combining model and geostationary satellite data to reconstruct hourly SST cnrfield over the Mediterranean Sea. *Remote sensing of environment*, 146, 11-23.
- Minnett, P. J., Alvera-Azcárate, A., Chin, T. M., Corlett, G. K., Gentemann, C. L., Karagali, I., ... & Vazquez-Cuervo, J. (2019). Half a century of satellite remote sensing of sea-surface temperature. *Remote Sensing of Environment*, 233, 111366.
- Pisano, A., Buonignore Nardelli, B., Tronconi, C., Santoleri, R. (2016). The new Mediterranean optimally interpolated pathfinder AVHRR SST Dataset (1982–2012). *Remote Sensing of Environment*, 176, 107-116.

### **S4-3: BIAS-AWARE OPTIMAL ESTIMATION FOR SEA SURFACE TEMPERATURES FROM HISTORIC AVHRRS**

**C J Merchant**<sup>(1,2)</sup> and **O Embury**<sup>(1,2)</sup>

University of Reading and National Centre for Earth Observation

#### **INTRODUCTION**

Bias aware optimal estimation (BAOE) is a technique to estimate bias adjustment and error covariance parameters that bring retrievals using classical optimal estimation closer to their theoretical performance (Merchant et al. 2020a; Merchant et al. 2020b). We have applied BAOE to Advanced Very High Resolution Radiometers (AVHRRs) from NOAA 6 to Metop B.

BAOE leads to estimates of the following quantities.

First, corrections for brightness temperature relative to radiative transfer are obtained, as piecewise linear functions of a variety of predictors. Preference is given to using predictors that have a geophysical interpretation: for example, errors in spectral response function in infrared channels may lead to the need to correct brightness temperatures as a function of atmospheric water vapour path; instrumental errors may track quantities such as the temperature of the internal calibration target, and this is also often used as a predictor.

Secondly, the error covariance of discrepancies between simulations and observations is obtained, which characterizes uncertainty from calibration, noise and radiative transfer simulation. This reveals inter-channel error correlations that are important for optimal retrieval.

Thirdly and fourthly, the bias and uncertainty in prior information are also estimated, of most relevance here being the relationship between water vapour in numerical weather prediction (NWP) fields compared to clear-sky fields of view: in general, clear-sky areas appear to be drier than the all-sky NWP, which makes sense.

Lastly, in situ data, adjusted to skin values, are used as an anchoring reference for the BAOE parameter estimation step, and their uncertainty is also estimated. This estimated includes effects from geophysical mismatch between satellite and in situ data types, as well as the in situ error distribution. Nonetheless, when using drifting buoy sea surface temperatures as a reference, there is a clear tendency for the estimated uncertainty in the in situ data to improve over several decades.

After the bias and covariance parameters are evaluated, they are used within the optimal estimation of sea surface temperature, and the error covariance information is also exploited within Bayesian cloud detection, along with bias correction.

These techniques are being applied for the v3 climate data record from the SST climate change initiative, and results suggest improved bias and stability properties, including when validated against data not included in the BAOE of parameters.

#### **EARLY RESULTS**

Figure 1 shows early results for the bias correction of brightness temperature observations for the AVHRRs. The bias correction is parameterised using up to five predictors, as indicated per NOAA mission number in the upper table of the figure. The mean biases (lower left panel) are seen to be of order -0.5 to +0.1 K, the 3.7  $\mu\text{m}$  channel usually being the least biased channel. The corrections vary in a piece-wise linear fashion with each predictor, and some are more variable across the predictor ranges than other, as shown in the lower right panel.

	6	7	8	9	10	11	12	14	15	16	17	18	19
BT 11	x	x	x	x	x	x	x	x	x	x	x	x	x
Element	x		x		x		x		x	x		x	x
Sat. Zen.		x		x		x		x			x		
Sol. Zen.							x	x	x		x	x	x
ICT	x	x	x	x	x		x	x	x	x	x*	x	x
TCWV	x			x			x			x			
Latitude			x		x	x							
Time		x		x	x	x		x	x	x		x	x

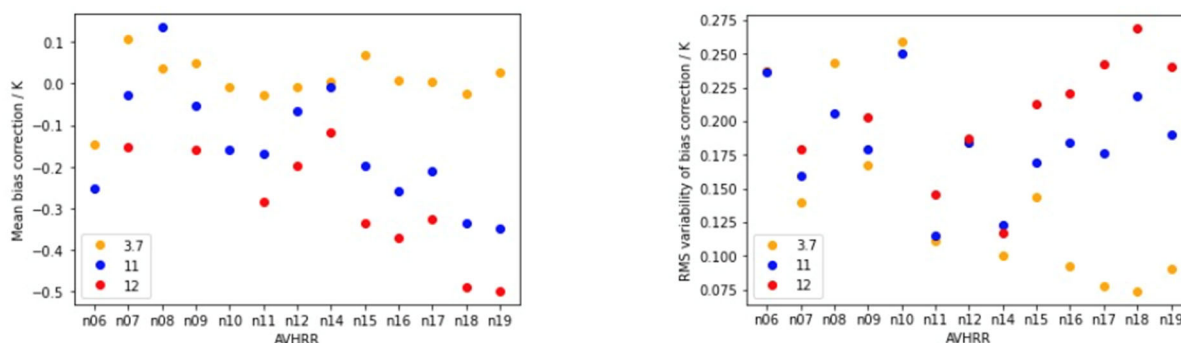


Figure 1. Summary of bias correction results for AVHRR BTs. See main text for details.

The prior bias in water vapour is estimated per AVHRR. Although the NWP system from which the prior atmospheric state is derived may not be fully stable over time, essentially we expect the main effect (clear skies being drier than all sky cells in a model) to be similar for all AVHRRs. The results do indeed show some commonality of dependence of prior water vapour bias in the expected direction (Figure 2, left panel), although the spread between sensors may be a result of uncertainty in the BAOE process rather than real differences between mission periods.

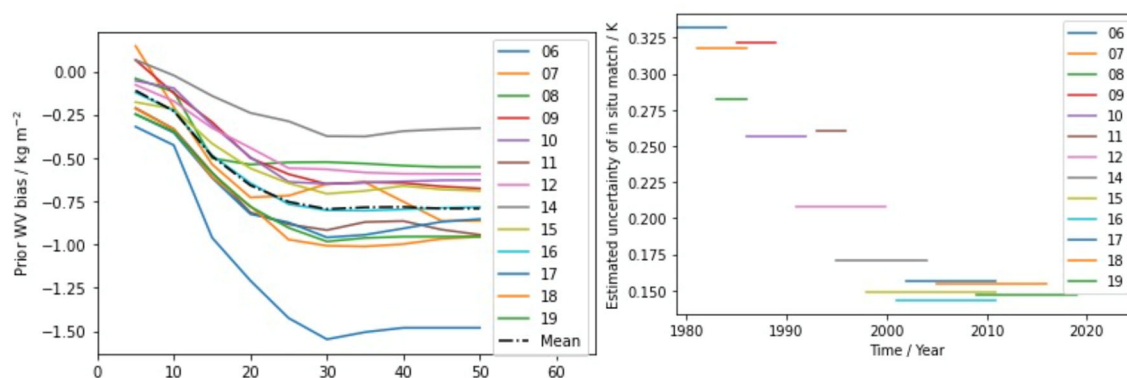


Figure 2. Left: estimates of dependence of prior water vapour bias on the prior water vapour itself (in kg/m<sup>2</sup>). Right: estimates of the uncertainty of the in situ SST measurements, including the geophysical difference between a point, bulk measurement and areal skin measurement.

Confidence in the BAOE results and their realism is increased by the systematic trend in the BAOE-generated estimate of in situ measurement uncertainty. It is expected that drifting buoys have become lower uncertainty over time, and this study confirms this (Figure 2, right panel).

## **CONCLUSION**

Applying BAOE theory to the series of NOAA AVHRRs has enabled estimates of quantities of general interest to be estimated, include brightness temperature corrections per sensor, biases in NWP humidity relative to clear-sky areas used for SST retrieval and the time evolution of drifting buoy uncertainty. The dependencies of the results obtained make sense with what is independently known, building confidence that the system is fitting real physical and instrumental error effects.

## **REFERENCES**

Merchant, C.J., Block, T., Corlett, G.K., Embury, O., Mittaz, J.P.D., & Mollard, J.D.P. (2020a). Harmonization of Space-Borne Infra-Red Sensors Measuring Sea Surface Temperature. *Remote Sensing*, 12

Merchant, C.J., Saux-Picart, S., & Waller, J. (2020b). Bias correction and covariance parameters for optimal estimation by exploiting matched in-situ references. *Remote Sensing of Environment*, 237

## S4-4: DEVELOPMENTS TOWARDS A 40 YEAR CLIMATE DATA RECORD FROM THE ESA CLIMATE CHANGE INITIATIVE

**O Embury** <sup>(1)</sup>, **C J Merchant** <sup>(2)</sup> **S A Good** <sup>(3)</sup> **J L Høyer** <sup>(4)</sup>

(1) University of Reading, UK, Email: [o.embury@reading.ac.uk](mailto:o.embury@reading.ac.uk)

(2) University of Reading, UK, Email: [c.j.merchant@reading.ac.uk](mailto:c.j.merchant@reading.ac.uk)

(3) Met Office, UK, Email: [simon.good@metoffice.gov.uk](mailto:simon.good@metoffice.gov.uk)

(4) Danish Meteorological Institute, Denmark, Email: [jlh@dmi.dk](mailto:jlh@dmi.dk)

### INTRODUCTION

Long-term, stable observational records of sea surface temperature (SST) and other essential climate variables (ECVs) are needed to understand the state of the climate. The ESA Sea Surface Temperature Climate Change Initiative (SST-CCI) is now developing a third version of our Climate Data Record (CDR) which will cover a 40-year period using data from Advanced Very High Resolution Radiometer (AVHRR), Along Track Scanning Radiometer (ATSR), Sea and Land Surface Temperature Radiometer (SLSTR) instruments, Advanced Microwave Scanning Radiometer (AMSR)-E and AMSR2. This presentation will cover the major developments since version 2 of the CDR.

This will be the first version of the SST CCI CDR to make use of data from AVHRR/1 instruments carried on board NOAA-6, -8, and -10 platforms. This will increase the data coverage in the 1980s and allow the dataset to extend back to late 1979. The quality of the AVHRR retrievals has been improved by using a new bias aware optimal estimation (BAOE) technique (described fully in the presentation by Merchant) and updated radiative transfer modelling including tropospheric dust which significantly reduces the SST biases due to dust aerosols seen in previous CDRs. Developments affecting the recent half of the record includes work to include the passive microwave AMSRE and AMSR2 sensors into the main CDR, use of full resolution MetOp data and the dual-view SLSTR sensors. CDRv3 data coverage is illustrated in Figure 1.

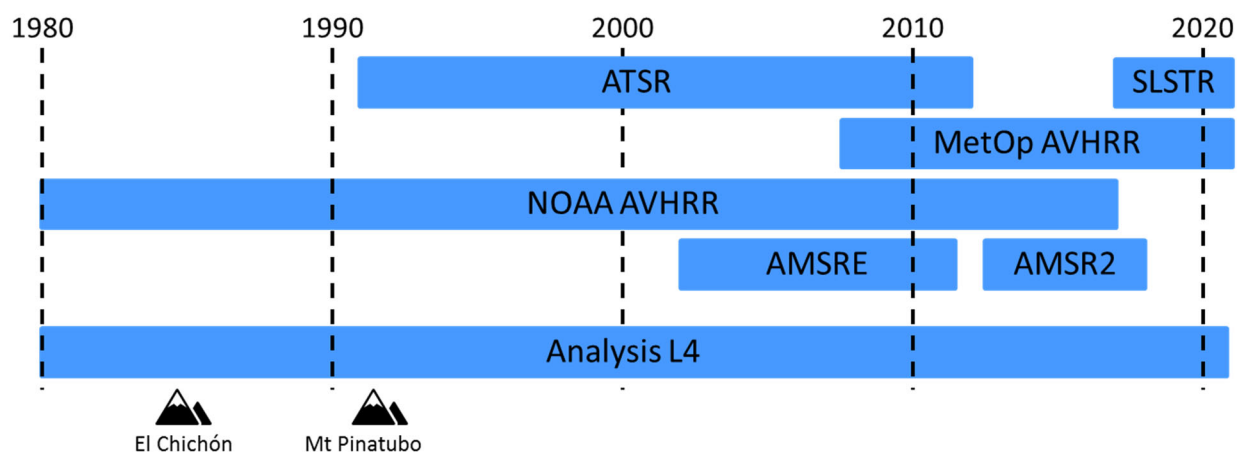


Figure 1: CDRv3 datasets and temporal coverage.

### SENSORS AND METHODS

The new version 3 SST-CCI CDR uses improved forward modelling capabilities compared to version 2. Firstly, the forward model used (RTTOV; Saunders et al. 2018) from version 11.3 to 12.3 which includes support for variable CO<sub>2</sub>, newer spectroscopy, and improved treatment of aerosol and scattering effects. Secondly, we now include dust in the tropospheric aerosol component of the forward modelling which significantly reduces biases in regions affected by desert dust such as the Atlantic Ocean and Arabian Sea. The aerosol prior is based on the CAMS aerosol climatology from Bozzo et al. 2020. Finally, the SST prior

used for the forward modelling is now taken from the previous version of the SST-CCI CDR (Merchant et al. 2019) with the desert-dust-bias correction of Merchant and Embury (2020).

The retrieval technique used for the AVHRR sensors is bias-aware optimal estimation as described in Merchant and Embury (2021) and Merchant et al. (2020). This uses data assimilation methods to estimate the biases in the a priori and forward model, and their respective estimate the error covariances. The BAOE retrieval for the NOAA AVHRRs is tuned to in situ data, while the MetOp AVHRRs are tuned to the dual-view reference sensors (ATSR, SLSTR). The typical improvement from CDR v2.1 to CDRv3.0 is shown in Figure 2 for NOAA-19 where the CDR has largely eliminated the regional dust-related biases.

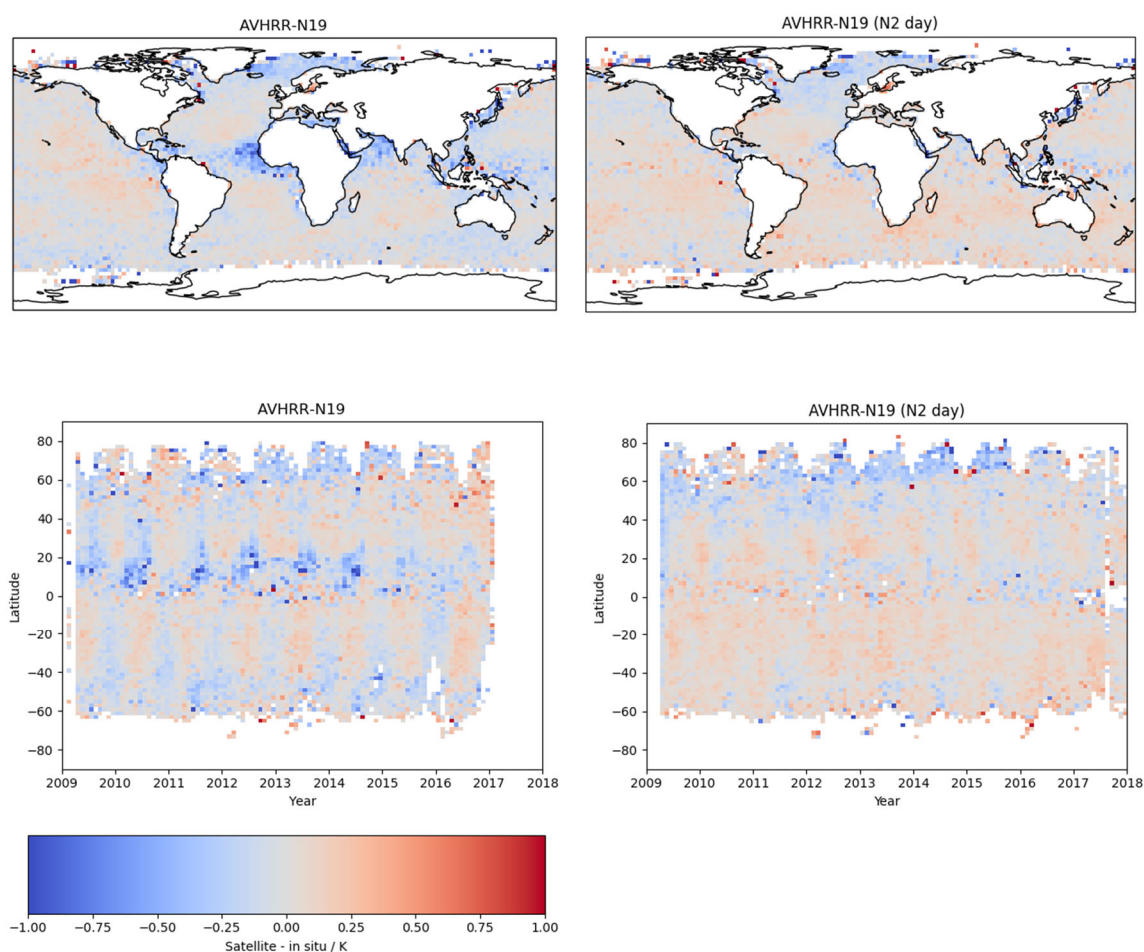


Figure 2: NOAA-19 daytime retrieval bias (satellite – in situ) for CDRv2.1 (left) and CDRv3.0 (right). In CDRv3 the new forward modelling and BAOE retrieval has significantly reduced regional dust biases and seasonal signal.

The new CDR v3 also includes data from the AVHRR/1 instruments carried on board the NOAA-6, -8, and -10 platforms. The AVHRR/1 instruments only have two infrared channels at 3.7 and 11  $\mu\text{m}$ . As such daytime retrievals rely on a single channel making them unsuitable for quantitative use and will be set to a maximum quality level of 2. However, the night-time retrievals using both channels provide a useful addition to the CDR coverage in the 1980s.

MetOp AVHRRs are now processed at full resolution (1 km) rather than the low resolution (GAC) format used in CDR v2. The full resolution products have 15 times as many pixels at L1/L2 resulting approximately double the number of observations at Level 3 (using a 0.05° grid) as shown in Figure 3

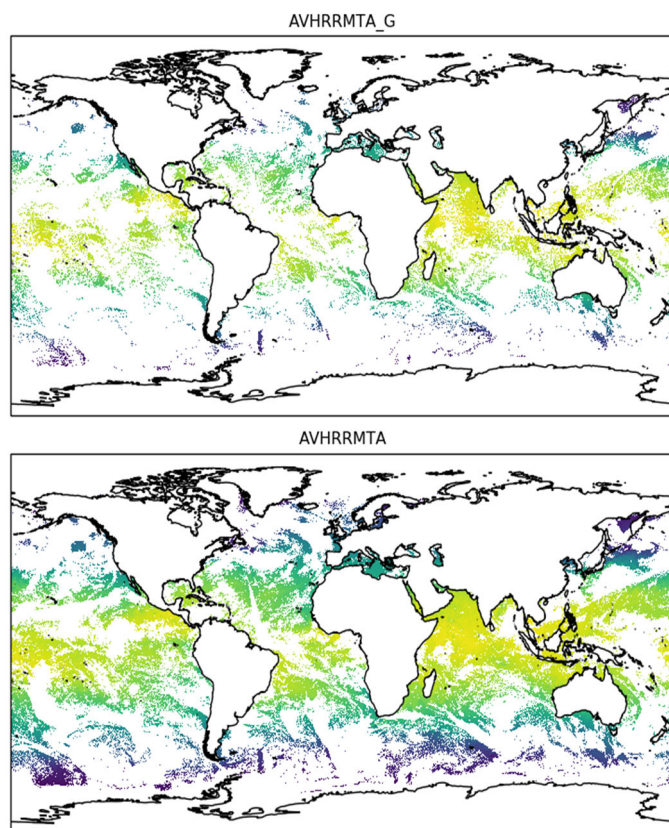


Figure 3: Typical daily L3C coverage from MetOp AVHRR (night-time). Top GAC resolution; Bottom: Full resolution.

In addition, CDRv3 will add SLSTR as another dual-view reference sensors, and include the passive microwave AMSRE and AMSR2 in the main CDR.

## CONCLUSION

The SST-CCI CDR v3 is due to be released in 2022. Compared to version 2 there is: a reduction in the dust-related biases affecting AVHRRs; improved coverage in the 1980s, update to full resolution MetOp AVHRR, and addition of SLSTR and passive microwave sensors to extend the dataset to just over 40 years.

## REFERENCES

- Bozzo, A., Benedetti, A., Flemming, J., Kipling, Z., and Rémy, S.: An aerosol climatology for global models based on the tropospheric aerosol scheme in the Integrated Forecasting System of ECMWF, *Geosci. Model Dev.*, **13**, 1007–1034, 2020, <https://doi.org/10.5194/gmd-13-1007-2020>
- Merchant, C. J., Embury, O., Bulgin, C. E., Block, T., Corlett, G. K., Fiedler, E., Good, S. A., Mittaz, J., Rayner, N. A., Berry, D., Eastwood, S., Taylor, M., Tsushima, Y., Waterfall, A., Wilson, R. and Donlon, C.: Satellite-based time-series of sea-surface temperature since 1981 for climate applications. *Scientific Data*, **6**, 223, 2019, <https://doi.org/10.1038/s41597-019-0236-x>
- Merchant, C. J. and Embury, O.: Adjusting for desert-dust-related biases in a climate data record of sea surface temperature. *Remote Sensing*, **12** (16). 2554, 2020, <https://doi.org/10.3390/rs12162554>
- Merchant, C., Saux-Picart, S. and Waller, J.: Bias correction and covariance parameters for optimal estimation by exploiting matched in-situ references. *Remote Sensing of Environment*, **237** (111590), 2020, <https://doi.org/10.1016/j.rse.2019.111590>
- Merchant, C. and Embury, O.: Bias-aware optimal estimation for sea surface temperature from historic AVHRRs, GHRSSST-XXII, 2021

Saunders, R., Hocking, J., Turner, E., Rayer, P., Rundle, D., Brunel, P., Vidot, J., Roquet, P., Matricardi, M., Geer, A., Bormann, N., and Lupu, C.: An update on the RTTOV fast radiative transfer model (currently at version 12), *Geosci. Model Dev.*, **11**, 2717-2737, 2018, <https://doi.org/10.5194/gmd-11-2717-2018>

## **S4 - POSTER PRESENTATIONS – ABSTRACTS**

#### **S4-P1: open source algorithms for AMSR3**

**Chelle Leigh Gentemann<sup>(1)</sup>**

(1) Farallon Institute, USA, Email: [cgentemann@faralloninstitute.org](mailto:cgentemann@faralloninstitute.org)

To date, algorithm development for pmw retrievals has been ‘siloeed’ – mostly restricted to a few select groups. This is partly due to the difficulty of moving research that involves working with the large orbital and ancillary datasets, and software developed for specific computational environments. Advances in cloud computing and open source software have created an ecosystem perfect for open collaboration and science through easily shared coding environments that can be deployed adjacent to cloud-stored datasets. Utilizing new shared tools that reduce redundant coding efforts has the potential to advance pmw algorithm development, opening it to collaborations with data scientists in addition to the remote-sensing specialists. These tools will be directly applicable to pmw sensors and will encourage open science as the new, more efficient, ‘norm’.

The creation of common tools for satellite data algorithm development reduces redundant code development within a science team, freeing time for algorithm refinement. While this type of ‘enterprise’ toolbox solutions have long been part of satellite science teams, they have suffered from difficulties related to deployments on different operating platforms and still require the downloading of large volumes of data to a local computer. By developing an entirely cloud-based algorithm development environment, any researcher can simply ‘fork’ a repository and build on existing software. This type of development has many advantages and builds a more inclusive scientific community where all scientists can contribute. This has been very effectively used by the Coupled Model Intercomparison Project-6 (CMIP6), High-Frequency (HF)-Radar and LandSat communities to drive new applications and data usage.

For previous PMW sensors, researchers described algorithms in peer-reviewed literature but algorithm software was generally not available or shared between colleagues, institutions, or agencies except as documented in algorithm theoretical basis documents (ATBDs). This resulted in substantial investments to develop software that had already been written by other groups. The most significant components of the SST and wind speed algorithm software are not normally the algorithm, but in the reading, filtering, and flagging of data. This project will provide a common suite of software, developed on GitHub, that will allow for international collaborations to occur more naturally, using a code base initially developed by this project, but ideally, eventually, with contributions from all members of the AMSR3 science team. This will substantially advance PMW SST and wind speed algorithms by freeing up research funding and efforts to develop innovative approaches.

If you are interested in collaborating on this, please contact [cgentemann@faralloninstitute.org](mailto:cgentemann@faralloninstitute.org).

## S4-P2: HISTORICAL AND NEAR-REAL TIME SST RETRIEVALS FROM METOP AVHRR FRAC WITH ACSPO 1

Victor Pryamitsyn<sup>(1)</sup>, Boris Petrenko<sup>(2)</sup>, Alexander Ignatov<sup>(3)</sup>, Olafur Jonasson<sup>(4)</sup>, Yury Kihai<sup>(5)</sup>

(1) NOAA/STAR and GST Inc, USA, Email: [victor.Pryamitsyn@noaa.gov](mailto:victor.Pryamitsyn@noaa.gov)

(2) NOAA/STAR and GST Inc, USA, Email: [Boris.Petrenko@noaa.gov](mailto:Boris.Petrenko@noaa.gov)

(3) NOAA/STAR, USA, Email: [alex.ignatov@noaa.gov](mailto:alex.ignatov@noaa.gov)

(4) NOAA/STAR and GST Inc, USA, Email: [Olafur.Jonasson@noaa.gov](mailto:Olafur.Jonasson@noaa.gov)

(5) NOAA/STAR and GST Inc, USA, Email: [Yury.Kihai@noaa.gov](mailto:Yury.Kihai@noaa.gov)

### Introduction

Three Metop First Generation satellites: Metop-A (2006-pr), -B (2012-pr) and -C (2018-pr) with the NOAA enterprise Advanced Clear Sky Processor for Ocean (ACSPO) SST system.

The dataset combines first historical reprocessing (or reanalysis, RAN1), starting from the beginning of each mission to present, with near-real time (NRT) processing.

The full Metop-FG SST records are archived at PO.DAAC [1,2].

This document describes the features of the ACSPO AVHRR FRAC dataset and evaluates its performance.

### The ACSPO Metop FRAC SST data set

The Metop-A/B/C FRAC datasets are produced as a part of a consistent line of ACSPO products, which includes SSTs from VIIRS, AVHRR (FRAC and GAC), MODIS, ABI, and AHI sensors.

The data files report two SST products:

Subskin SST, produced with global regression (GR), is highly sensitive to skin SST and unbiased with respect to in situ SST [3]

De-biased SST, produced with piecewise regression (PWR), is less sensitive to skin SST, but more precise with respect to in situ SST and serves as a proxy for 'depth' SST [4]. The PWR SST can be obtained from the ACSPO GDS2 files by subtracting the 'SSES\_bias' layer from the 'sea\_surface\_temperature' layer.

Both SSTs are calculated using two- and three-band regression equations for day and night, respectively, switched at solar zenith angle = 90°. The regression coefficients are trained against matchups with drifters and moored buoys from the iQuam system [5]. The specific shapes of regression equations and the training methodology are discussed in [6,7].

The clear-sky pixels are identified with the ACSPO Clear-Sky mask (ACSM) [8]

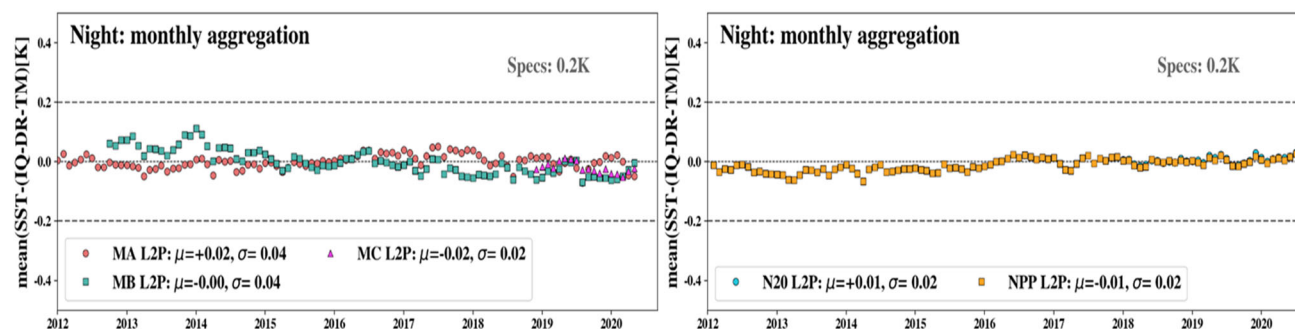


Figure 1: Time series of the monthly nighttime biases of De-biased – (D+TM) SST, for (left panel) AVHRR and (right panel) VIIRS, both produced with fixed regression coefficients

### The role of variable regression coefficients

Daily retraining of the regression coefficients helps mitigate the effects of AVHRR sensor and residual Metop orbits instabilities [9]. The coefficients are trained against matchups collected within the time windows of 91 day size for Subskin SST and 361 day for Depth (De-biased) SST. The offsets of regression equations are additionally corrected using shorter time windows of 31 day size. In RAN, all training windows are centered at the processed day. In NRT processing, the training windows end 4 -10 days before the processed day. The data, processed in the NRT mode, are reprocessed in the RAN mode with a ~2 months lag.

Figure 1 illustrates the need in variable regression coefficients for Metop AVHRRs by showing long-term trends of monthly nighttime biases in the Depth (De-biased) SSTs - (D+TM) for the Metop AVHRRs, computed with fixed regression coefficients. Larger variations in SST biases for Metop-A and -B suggest a more significant effect of long-term calibration trends on AVHRR SST. The use of variable regression coefficients reduces variations in the Metop SST biases as shown in the next section.

### Time series of ACSP0 Metop FRAC SST statistics

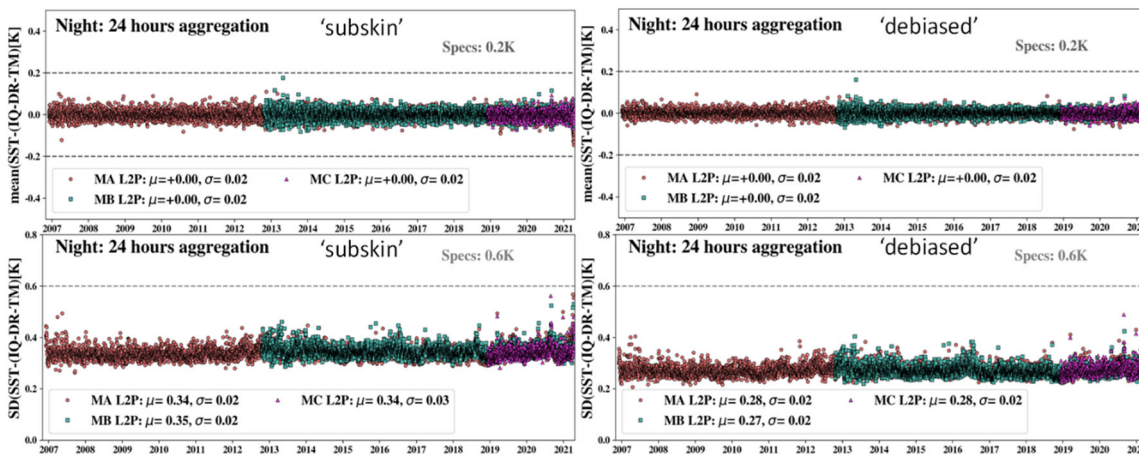


Figure 2: Time series of daily nighttime (top panels) biases and (bottom panels) SDs of Metop (Left panels) Subskin and (right panels) Depth (De-biased) SSTs with respect to (D+TM).

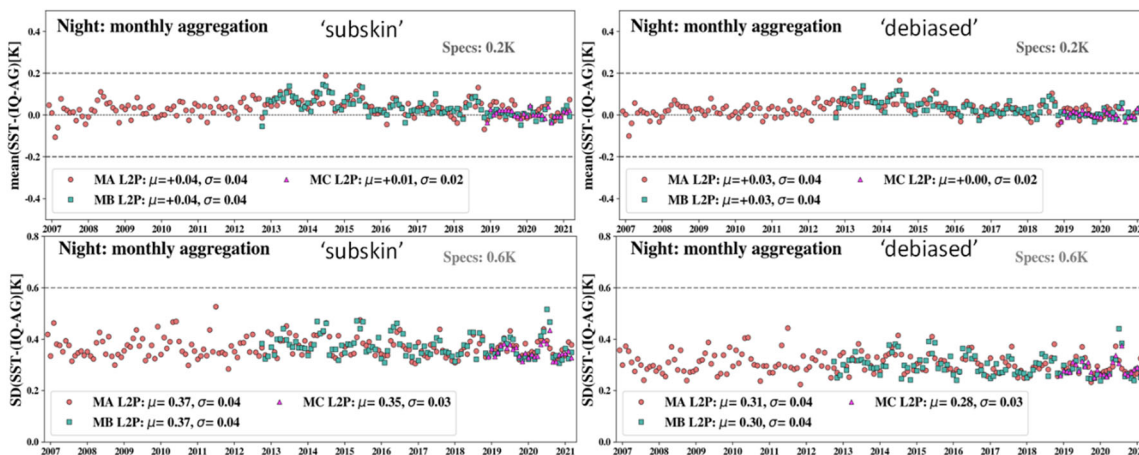


Figure 3: Time series of daily nighttime (top panels) biases and (bottom panels) SDs of Metop (left panels) Subskin and (right panels) Depth (De-biased) SSTs with respect to Argo floats.

Figure 2 shows full-mission time series of daily nighttime biases and SDs of Metop Subskin and De-biased SSTs - (D+TM). Figure 3 shows the time series of nighttime monthly statistics with respect to Argo floats (AF). Since the AFs are not used for training regression coefficients they represent an independent data set.

The statistics in Figures 2 and 3 are stable, consistent between the satellites and meet the NOAA specs (i.e., <0.2 K for biases and <0.6 K for SDs) with a wide margin. The De-biased SST is more consistent with (D+TM), with biases being grouped tighter around 0K and lower SDs than for Subskin SST. The biases with respect to AF are in general slightly positive, likely due to training against warmer (D+TM).

More detailed validation of the Metop FRAC SST, including its daytime statistics can be found at [10]. The daytime statistics are also stable, consistent between the satellites and meet the specs, although somewhat degrade compared with the nighttime, because of using for SST only two AVHRR bands.

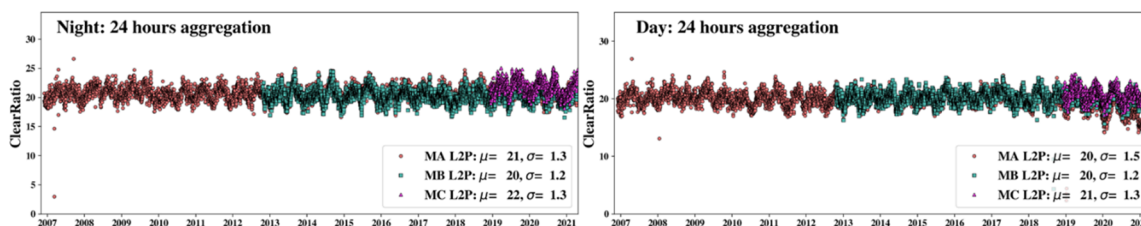


Figure 4: Time series of daily (left) nighttime and (right) daytime clear-sky fractions (in %).

Figure 4 shows the time series of clear-sky fractions (i.e., the percentages of clear-sky pixels, identified by the ACSM, in the total of ocean pixels). The daily clear-sky fractions are consistent across three platforms, at ~20-21% and show seasonality. The reduction in the daytime clear-sky fractions for Metop-A after 2019 is due to progressive deorbiting of Metop-A after Sep 2016.

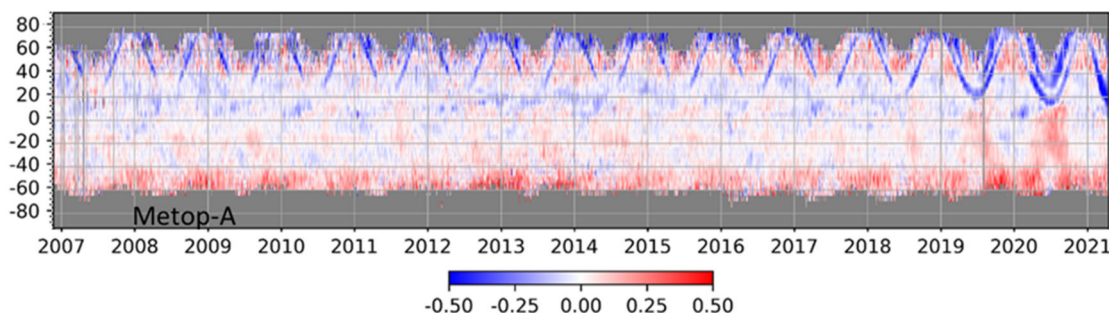


Figure 5: Hovmöller diagram of daily latitudinal biases of nighttime Metop-A Subskin – (D+TM) SST

### Future work

Figure 5 illustrates stable features of the latitudinal distributions of nighttime biases in Subskin SST - (D+TM), common for the Metop-A. The warm biases, reaching ~0.2-0.3 K, appear in high Southern latitudes during the SH summers and, almost synchronously, cold biases up to -0.2 K appear in the NH high latitudes. Also, the cold “arches” periodically appear in the Northern hemisphere due to calibration errors caused by Sun impingement on the AVHRR black body calibration target when the satellite orbit approaches the terminator from the dark side of the Earth. This effect has intensified in Metop-A SST since September 2019, when its orbit has stopped being controlled. Similar effects also take place in Metop-B and -C (not shown). Work is currently underway to mitigate these effects through the improved SST retrieval and training algorithms, and correcting the L1B calibration coefficients [11,12].

### Summary

The first full-mission SST dataset from Metop-FG AVHRR FRAC data has been created and archived with PO.DAAC. The plan is to also archive it with NOAA.NCEI.

The stability of the global validation statistics on time scales longer than 1 month, and their consistency between the Metop-A/B/C platforms, are ensured by daily recalculation of regression coefficients.

The ACSPO Subskin SST combines high precision and accuracy with respect to in situ SST with high sensitivity to skin SST (0.94-0.97 at night, 0.87-0.88 during the daytime). The SSES bias correction further improves fitting in situ SST.

The ongoing work on the next version of the Metop FRAC SST data set is aimed at mitigation of the AVHRR L1B calibration errors and improvements of SST retrieval and training algorithms.

#### References

GHRSSST NOAA/STAR Metop-A/B/C AVHRR FRAC ACSPO v2.80 1km L2P Datasets (GDS v2). 2021, <https://doi.org/10.5067/GHMTA-2PS28>; <https://doi.org/10.5067/GHMTB-2PS28>; <https://doi.org/10.5067/GHMTC-2PS28> ;

GHRSSST NOAA/STAR Metop-A/B/C AVHRR FRAC ACSPO v2.80 0.02° L3U Datasets (GDS v2). 2021, <https://doi.org/10.5067/GHMTA-3US28>; <https://doi.org/10.5067/GHMTB-3US28>; <https://doi.org/10.5067/GHMTC-3US28>

Petrenko, B.; Ignatov, A.; Kihai, Y.; Stroup, J.; Dash, P. JGR, 2014, 119, 4580-4599, <https://doi.org/10.1002/2013jd020637>

Petrenko, B.; Ignatov, A.; Kihai, Y.; Dash, P. JTECH , 2016, 33, 345-359, <https://doi.org/10.1175/Jtech-D-15-0166.1>

In situ SST Quality Monitor system (iQuam). Available online: <https://www.star.nesdis.noaa.gov/socd/sst/iquam/> (accessed on 2021-04-30).

Petrenko, B., Pryamitsyn, V., Ignatov, A., and Kihai, Y., Proc. SPIE 11420, Ocean Sensing and Monitoring XII, 1142004 (30 June 2020); doi: 10.1117/12.2558660

Pryamitsyn, V.; Petrenko, B.; Ignatov, A.; Jonasson, O.; Kihai, Y. Proc. SPIE, Ocean Sensing and Monitoring XIII 2021, 11752, <https://doi.org/10.1117/12.2585893>

Petrenko, B.; Ignatov, A.; Kihai, Y.; Heidinger, A. J Tech 2010, 27, 1609-1623, <https://doi.org/10.1175/2010jtecha1413.1>

Ignatov, A.; Zhou, X.J.; Petrenko, B.; Liang, X.M.; Kihai, Y.; Dash, P.; Stroup, J.; Sapper, J.; DiGiacomo, P. Remote Sens-Basel 2016, 8, <https://doi.org/10.3390/rs8040315>

SST Quality Monitor (SQUAM AVHRR FRAC). Available online: <https://www.star.nesdis.noaa.gov/socd/sst/squam/polar/avhrrfrac/> (accessed on 2021-04-30).

Petrenko, B.; Pryamitsyn, V.; Ignatov, A. Proc. SPIE, 2021, 11752, <https://doi.org/10.1117/12.2585908>

Petrenko, B.; Pryamitsyn, V.; Ignatov, A., Poster, the GHRSSST-XXII Online Science Team meeting, 7-11 June 2021.

**S4-P3: USE OF ERA-5 SEA SURFACE TEMPERATURE FIELDS AS PRIOR IN OPTIMAL ESTIMATION RETIREVAL OF SST FROM MODIS**

**Malgorzata Szczodrak<sup>(1)</sup>, Peter Minnett<sup>(2)</sup>**

(1) University of Miami, RSMAS, MIAMI, USA, Email: goshka@rsmas.miami.edu

(2) University of Miami, RSMAS, MIAMI, USA, Email: pminnett@rsmas.miami.edu

**Introduction**

The retrieval of sea surface temperature (SST) from satellite infrared radiometers through Optimal Estimation (OE; Rodgers, 2000) gained popularity in recent years with the promise of improving accuracy of the SST estimates over the traditional non-linear SST (NLSST; Walton et al. 1998, Kilpatrick et al. 2015) retrieval algorithms, and especially reducing the NLSST regional biases. The OE retrieval calculates a measurement-based correction to a prior ‘known’ SST which is typically taken from an NWP model. Here we consider two ERA5 SST fields, the ‘sst’ (sea surface temperature) and the ‘skt’ (skin temperature) as a prior for OE retrieval of SST from MODIS measurements. We compare the results with in-situ measurements from buoys and retrievals with the traditional NLSST.

**The OE retrieval approach**

OE retrieval method is based on the Bayesian concepts and can be summarized as follows:

- 1) we have some knowledge of the state before the measurement is made and the prior knowledge is expressed by a prior probability distribution function (pdf) of the state variables.
- 2) we have a forward model that maps the state variable into the measurement space.
- 3) we know the pdf of the measurement errors.
- 4) we can calculate posterior pdf by augmenting the prior pdf of the state vector with the measurement.

If the forward model is F, the prior state is xa and the measurements is y then for Gaussian pdfs the expected value of posterior pdf of state variables is given by:

$$x = x_a + (K^T S_\epsilon^{-1} K + S_a^{-1})^{-1} K^T S_\epsilon^{-1} (y - F(x_a)) \quad (1)$$

where K is a Jacobian of F and the covariance matrix of the posterior state is:

$$S^{-1} = K^T S_\epsilon^{-1} K + S_a^{-1} \quad (2)$$

with (3)

$$S_\epsilon = \begin{bmatrix} e_{31}^2 & 0 \\ 0 & e_{32}^2 \end{bmatrix} \quad \text{and} \quad S_a = \begin{bmatrix} e_{SST}^2 & 0 \\ 0 & e_{TCWV}^2 \end{bmatrix}$$

where ei is uncertainty of the prior state variables for Sa and measurement uncertainty in channels 31 and 32 of MODIS (0.05K) combined with an estimate of the forward model uncertainty (0.1K) for S $\epsilon$ . For retrievals discussed here eSST = 0.5 K, and eTCWV = 25%

## Satellite Data and the Prior knowledge

### MODIS Dataset

We applied the OE retrieval to a subset of MODIS Collection 6 (R2014) Match-Up Data Base (MUDB), for 2015 and 2016 from the North Atlantic Ocean and the Mediterranean Sea. The MUDB includes the 11 and 12  $\mu\text{m}$  radiance measurements (channels 31 and 32). The error specification is 0.05K, corresponding to a radiance of  $\sim 0.007 \text{ W/m}^2\text{-}\mu\text{m}\text{-sr}$ . Each MUDB record includes assessment of the confidence in the retrieved value expressed as the quality flag (qf). The bests match-ups have qf = 0 and the slightly worse qf = 1. Quality flags > 1 typically indicate contaminated pixels. Only qf = 0 data are used here.

### Prior knowledge

The MODIS NLSST algorithm (Kilpatrick et al., 2015) is based on the correction for the effect of the intervening atmosphere being different in two radiance measurements made at different infrared wavelengths; the difference in the measurements depending primarily on the water vapor distribution. Given we have only two measurements, we have to use a reduced state vector  $X = [\text{SST}, \text{TCWV}]$  where TCWV is the total column water vapor.

Prior knowledge is the SST and TCWV fields is taken from the European Centre for Medium-Range Weather Forecasts (ECMWF) ERA5 dataset (ref). We assume that the prior pdf of  $x$  is Gaussian with mean  $[\text{SST}_0, \text{TCWV}_0]$  given by ERA5, and some prior variance that we must specify. The ERA5 SST provides two SST products: 1) sea surface temperature 'sst' which corresponds to a subsurface temperature measured at a buoy level, and 2) skin temperature 'skt'. The 'sst' differs from the skin SST obtained by satellite measurements and the average offset has been estimated at -0.17 K (Donlon et al., 2002). This value is added to the ERA5 SST to estimate skin SST. The spatial resolution is  $0.4^\circ \times 0.4^\circ$  and the temporal resolution is 24 hours for the 'sst'. The 'skt' does not require this correction. It seems that the 'skt' would be a more appropriate as the prior SST for OE. It is provided 4 x daily which is another advantage over the 'sst'.

Additionally, for the forward radiative transfer modelling we use the ERA5 atmospheric profiles of temperature, water vapor, and ozone. The spatial resolution of these fields is  $0.4^\circ \times 0.4^\circ$  and the temporal resolution is 6 hours.

### Forward model

We use the Radiative Transfer for TOVS (RTTOV) v12.1 (Hocking et al., 2018). The ERA5 data are interpolated to the time and position of the match-up data point. Using RTTOV we simulate MODIS channel 31 and 32 radiances as well as the Jacobian matrix,  $K$ . The forward model is only an approximation and thus is an additional source of error.

## Results

The histograms of the difference between MODIS SST and in-situ measurements are shown in Figures 1 to 3. The in-situ measurements come from drifters, moored buoys and ship radiometers. The ship radiometers measure skin temperature, the drifter and buoy measurements were converted to skin temperature by adding the average value of the skin effect = -0.17 K.

Figure 1 shows MODIS SST – in situ temperatures for the OE retrievals with ERA5 'sst' as the prior SST for a) nighttime and b) daytime matchups. There is a marked bias in the daytime retrievals as compared with the nighttime. We interpret this as a poor representation of the daytime SST at the AQUA overpass time by the ERA5 daily average field resulting in a biased prior of the OE and thus a biased retrieval. Figure 2a shows ERA5 'sst' minus in situ for independent subset of daytime matchups with the mean value of -0.23 K whereas nighttime bias for an independent subset of nighttime matchups (not shown) is -0.03 K. If the daytime ERA5 'sst' is corrected for this bias, the statistics of the retrieved daytime SST are close to those of nighttime matchups as shown in Figure 2b.

Figure 3 shows MODIS SST – in situ temperatures for the OE retrievals with ERA5 ‘stk’ as the prior SST for a) nighttime and b) daytime matchups. Both nighttime and daytime statistics are markedly worse than the retrievals with ERA5 ‘sst’ as prior even without the corrections.

This is possibly surprising as the diurnal variability of the skin temperature should be better captured by the higher temporal resolution of the ‘stk’ field.

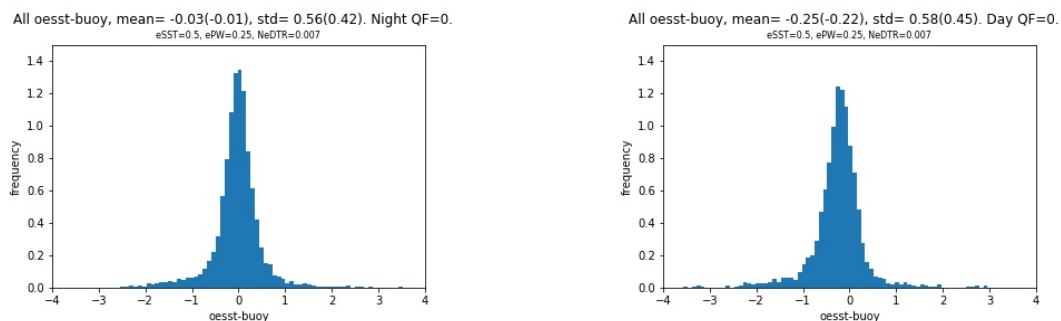


Figure 1. MODIS OE SST – in situ measurement for OE retrievals with ERA5 ‘sst’ as prior: left) nighttime and right) daytime matchups.

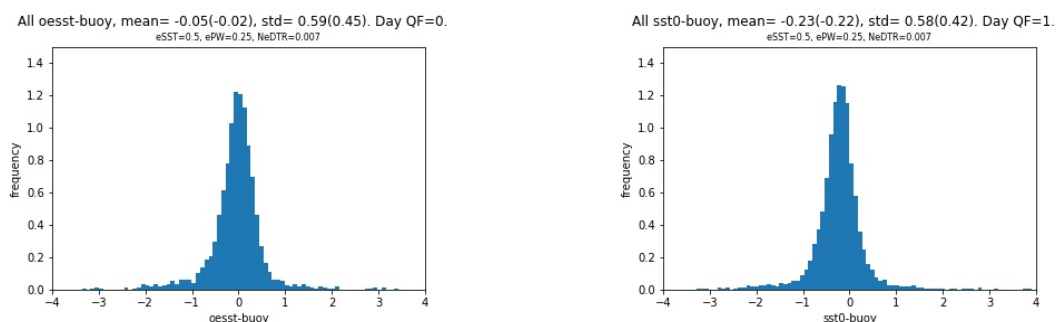


Figure 2. Left) ERA5 ‘sst’ – in-situ measurements for a subset of qf = 1 matchups and right) MODIS OE SST – in-situ measurements with ERA5 ‘sst’ prior corrected for the AQUA daytime bias.

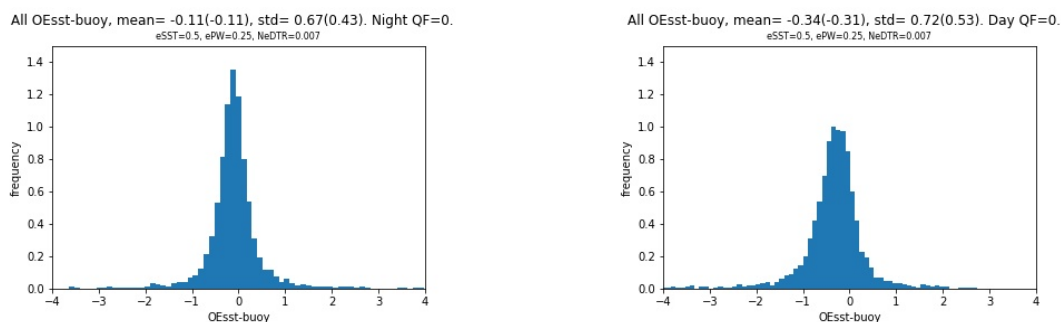


Figure 3. MODIS OE SST – in situ measurements for OE retrievals with ERA5 ‘stk’ as prior: left) nighttime and right) daytime matchups.

## Conclusion

ERA5 'sst' represents well the nighttime SST as measured by buoy and radiometers but this mean foundation temperature is not a good estimation of the daytime SST, at least at the time of the AQUA overpass when the ERA5 'sst' is ~0.23 K too cold compared to buoy measurements. This is not surprising as the ERA5 'sst' does not resolve the diurnal variability of SST.

ERA5 skin temperature 'stk' should in principle provide a better prior for OE as it does not require the skin effect correction and includes diurnal variability. However, despite the inclusion of the diurnal signal, the ERA5 'stk' seems to be a worse prior for OE than the 'sst' in terms of the OESST bias with respect to in situ measurements.

A simple diurnal bias correction can significantly improve the performance of OE with ERA5 'sst' for MODIS for daytime data.

## Acknowledgements

Funding from the NASA Physical Oceanography program is acknowledged.

## References

- Donlon, C. J., P. J. Minnett, C. Gentemann, T. J. Nightingale, I. J. Barton, B. Ward and J. Murray (2002). Toward improved validation of satellite sea surface skin temperature measurements for climate research. *Journal of Climate* 15: 353-369.
- Hocking, J., Rayer, P., Rundle, D., Saunders, R., Matricardi, M., Geer, A., Brunel, P., & Vidot, J. (2018). RTTOV v12 Users Guide, EUMETSAT Satellite Application Facility on Numerical Weather Prediction (NWP SAF), (142pp.): EUMETSAT. Available at [https://www.nwpsaf.eu/site/download/documentation/rtm/docs\\_rttov12/NWPSAF-MO-DS-029\\_Prod\\_Spec\\_RTTOV12.pdf](https://www.nwpsaf.eu/site/download/documentation/rtm/docs_rttov12/NWPSAF-MO-DS-029_Prod_Spec_RTTOV12.pdf).
- Kilpatrick, K.A., Podestá, G., Walsh, S., Williams, E., Halliwell, V., Szczodrak, M., Brown, O.B., Minnett, P.J., & Evans, R. (2015). A decade of sea surface temperature from MODIS. *Remote Sensing of Environment* 165, 27-41. <http://dx.doi.org/10.1016/j.rse.2015.04.023>.
- Rodgers, C.D. *Inverse Methods for Atmospheric Sounding: Theory and Practice* World Scientific Publishing, Singapore (2000) <https://doi.org/10.1142/3171>
- Walton, C.C., Pichel, W.G., Sapper, J.F., & May, D.A. (1998). The development and operational application of nonlinear algorithms for the measurement of sea surface temperatures with the NOAA polar-orbiting environmental satellites. *Journal of Geophysical Research* 103, 27,999-928,012.

#### **S4-P4: TOWARD IMPROVED ACSPO CLEAR-SKY MASK FOR SST FROM GEOSTATIONARY SATELLITES**

**Alexander Semenov<sup>(1,2)</sup>, Irina Gladkova<sup>(1,2,3)</sup>, Alexander Ignatov<sup>(1)</sup>, Olafur Jonasson<sup>(1,2)</sup> and Yury Kihai<sup>(1,2)</sup>**

(1) STAR, NOAA, NCWCP, 5830 University Research Ct, College Park, MD 20740, USA

(2) Global Science and Technology, Inc., 7855 Walker Drive, Greenbelt, MD 20770, USA

(3) City College Of New York, 160 Convent Ave., New York, NY, USA 10031

A crucial element of the NOAA Advanced Clear Sky Processor for Oceans (ACSPO) sea surface temperature (SST) system is identification of the clear-sky domain. One of the current priorities is advanced cloud detection by revisiting the existing set of cloud screening tests. Our goal is a comprehensive revision of the current status, and implementing computationally efficient and affordable algorithms for improved cloud detection, with a focus on challenging (dynamic, coastal, broken/multi-layer clouds etc.) scenes. New algorithms, including computationally intensive pattern recognition approaches, are tested on a diverse set of representative imageries/tiles (both where the current ACSPO Clear-Sky Mask, ACSM, performs well and where it produces false positive/negative detections). Our goal is robust clear-sky detection for SST, with minimized cloud leakages and false alarms. The initial priority is on the SST from the Advanced Baseline and Himawari Imagers (ABI/AHI) onboard NOAA GOES-16 and -17, and JMA Himawari-08 geostationary satellites, with a possible extension to data of Low Earth Observing (LEO) satellite sensors. We start with a comprehensive assessment of the current status of (ACSM), focusing on its current limitations. Using a representative set of ABI/AHI granules, we first evaluate possible algorithm improvement options. Next step will be implementation in ACSPO and comprehensive evaluation of the improvements in an experimental production pipeline, from L1b to L3C level products, in two NOAA online monitoring systems: global NOAA SST Quality Monitor (SQUAM) and image-quality oriented ACSPO Regional Monitor for SST (ARMS).

#### S4-P5: BAYESIAN CLOUD DETECTION SCHEME IMPROVEMENTS FOR THE SLSTR INSTRUMENT

Agnieszka Faulkner<sup>(1)</sup>, Claire Bulgin<sup>(1)</sup>, Christopher Merchant <sup>(1)</sup>, Niall McCarroll<sup>(1)</sup>, Gary Corlett<sup>(2)</sup>

<sup>(1)</sup>Department of Meteorology, University of Reading, Reading, UK, Email: [c.e.bulgin@reading.ac.uk](mailto:c.e.bulgin@reading.ac.uk)

<sup>(2)</sup>EUMETSAT, Germany

The SLSTR instrument onboard Sentinel-3 provides Sea Surface Temperature (SST) data for climate data records. To accurately retrieve SST, clouds are screened operationally using the Bayesian Cloud Detection Scheme (BCDS). Coastal regions offer more challenging regimes for cloud detection than open oceans with an increased frequency of turbid waters, changing ocean colour and SST fronts, leading to some failures in the operational cloud masking. These are in part related to the mapping of higher resolution reflectance imagery to the infrared imagery grid, for use in the cloud detection. Poorly matched observations can result in both false flagging and failures to detect cloud. In order to establish an improved cloud-screening algorithm, modifications to the BCDS have been made by introducing a pre-processor to optimise the visible imagery re-gridding for joint use with the infrared data.

SLSTR channels making observations at reflectance wavelengths (S1-S6, Table 1) are at 0.5 km resolution at nadir. There are two detectors (stripe A and B), both of which make observations for channels S4-S6. For channels S1-S3 observations are made only with detector A. Thermal infrared observations (channels S7-9, Table 1) are made at 1 km resolution.

Channel	Central Wavelength ( $\mu\text{m}$ )	Band Width ( $\mu\text{m}$ )
S1	0.555	0.02
S2	0.659	0.02
S3	0.865	0.02
S4	1.375	0.015
S5	1.61	0.06
S6	2.25	0.05
S7	3.74	0.38
S8	10.85	0.9
S9	12.0	1.0

Table 1: SLSTR channel characteristics.

Figure 1 is a schematic illustrating the different spatial resolutions of SLSTR observations. The two detectors at reflectance wavelengths (stripes A and B) are represented by the beige and purple colours, with the infrared channel resolution indicated by a red dashed line. The thermal and reflectance channel observations are not co-registered.

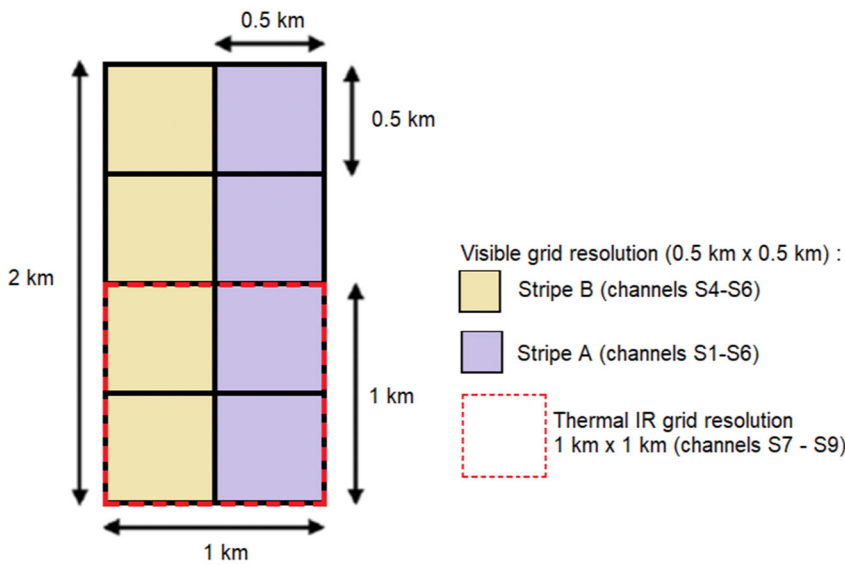


Figure 1: Schematic for visible and infrared image grids. The thermal and reflectance pixels are not co-registered (see Figure 2).

Operational cloud masking relies on re-gridding the reflectance channel data to the thermal channel resolution. This is done using a simple 2x2 extract from the reflectance channel grid for each infrared pixel and considers only stripe A observations. This method of matching also ignores both cosmetically filled and orphan pixels. Figure 2 shows an example of the reflectance and infrared channel footprints obtained using this simple methodology. We see that often the reflectance channel footprints (orange lines) are a poor representation of the full geographical coverage of the infrared pixel (blue line). There is also relevant data available from the B stripe detector (green dots), which are currently unused. This figure highlights the need for improved consistency between the reflectance and infrared channel for the purpose of cloud detection, which relies on good collocation of observations at different wavelengths.

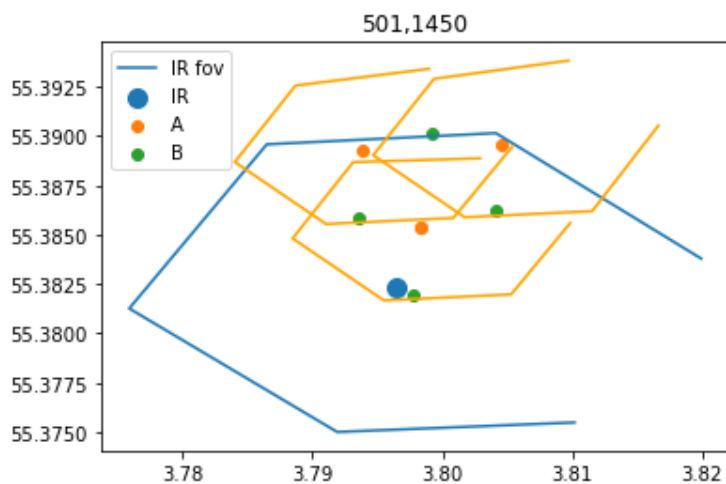


Figure 2: Field of view (FOV) for an example infrared (IR) pixel (blue) with corresponding FOVs for the reflectance channel pixels from a 2x2 re-gridding using stripe A only. Green dots show stripe B observations, which are also of relevance but currently unused operationally.

We present here a new pre-processor to co-register the reflectance and infrared channel observations. This takes the location of each infrared pixel and uses 'n' nearest neighbours based on Cartesian distance from the pixel centre to identify the closest matching reflectance channel observations. B stripe data can be included where available (channels S4-S6), and orphan pixels, excluded when placing observations on the imagery grid, are also interrogated.

Figure 3 shows the benefit of the new pre-processor in improving the co-registration of the reflectance channels with the infrared observations. The figure shows the infrared data (right) compared with re-gridded reflectance data using the operational method (left) and our pre-processor (centre). In the boxes highlighted in red, we see that the pre-processor gives improved consistency between the re-gridded reflectance observations and the infrared. This improved collocation is particularly important for cloud detection along boundaries such as coasts and cloud edges.

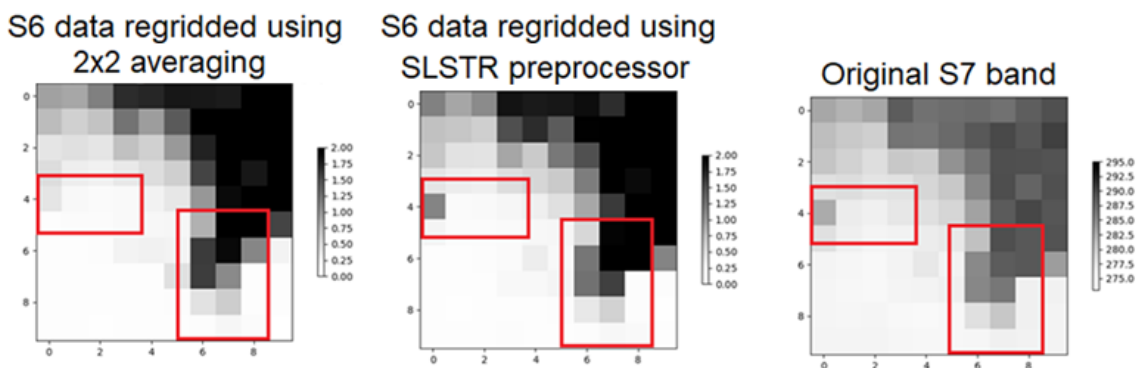


Figure 3: Comparison of reflectance channel re-gridding using the operation 2x2 extraction method and the new pre-processor. The comparison shows stripe A only matches with five nearest neighbours.

Finally we demonstrate the improved performance of the Bayesian cloud detection when using the pre-processor to collocate the reflectance and infrared imagery. Figure 4 shows data from two infrared channels (S7 and S8) in the top panel, and the cloud detection output using the operational collocation (top right) and three versions of the new pre-processor (bottom panels). The S7 image clearly shows the difference between cloud and clear-sky in this example. Cloudy observations are warmer in S7 in this scene (black) whilst clear-sky is cooler (grey colour). In the clear-sky probabilities, cloudy observations are yellow (clear-sky probability close to zero) and obviously clear regions are black. Blue colours denote cases where the classifier is less certain of whether the pixel is clear or cloud. Several features are highlighted with red ellipses, and careful study of the images shows that cloud shapes seen in the imagery are better represented by the cloud detection using the pre-processor, particularly when using the configuration of  $n=10$  with both detector stripes.

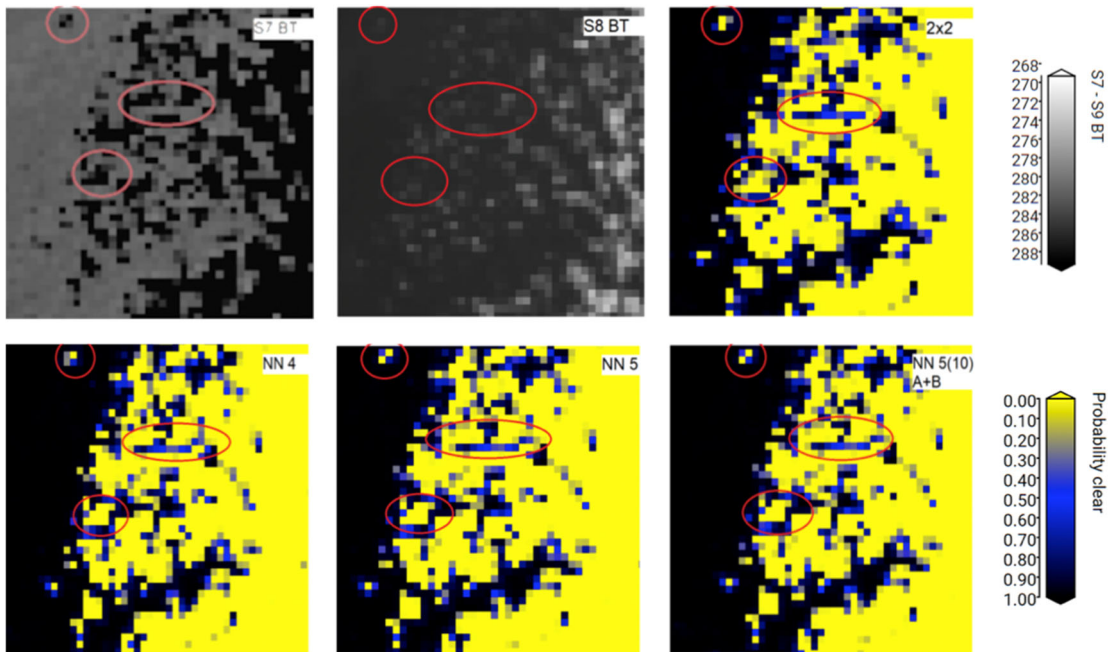


Figure 4: Probability of clear-sky in a region of scattered cloud using the operation re-gridding (top right) compared with several different configurations of the pre-processor:  $n = 4$ , stripe A only (bottom left),  $n = 5$ , stripe A only (bottom centre), and  $n = 10$ , stripe A and B (bottom right). Cloud features in the reflectance channels most closely correspond to the infrared imagery for the  $n = 10$  case.

**SCIENCE SESSION 5**  
**COMPUTING AND PRODUCTS**



## S5 - SESSION REPORT

**Chair: Prasanjit Dash<sup>(2)</sup>, Rapporteur: Chunxue Yang<sup>(2)</sup>**

(1) NOAA NESDIS STAR; CSU CIRA, USA, Email: [prasanjit.dash@noaa.gov](mailto:prasanjit.dash@noaa.gov)

(2) ISMAR-CNR UOS Roma, Italy, Email: [chunxue.yang@artov.ismar.cnr.it](mailto:chunxue.yang@artov.ismar.cnr.it)

### HIGHLIGHTS

- Opportunity to identify and consider new practises due to increasing amounts of data and computational power in the cloud which are unlocking new approaches for data-driven discovery
- GHRSSST for Analysis Ready Data (ARD) SST
- New version of HadISST also uses ESA CCI AVHRR data to complement the data record
- Multi-band SST, high-resolution Sea Ice Concentration and all-weather sea surface wind speed to be standard products for AMSR3
- New L4 reprocessed foundation SST using OSTIA, from 1981-2020

### INTRODUCTION

This report summarizes the outcome and discussions related to each oral and poster presentation in session 5. There are five oral and eight poster presentations focusing on newly developed technologies and products from different agencies and their applications.

### RESOURCES

- View presentations (recordings): <https://training.eumetsat.int/mod/book/view.php?id=14071&chapterid=627>
- Discussion forum for recordings: <https://training.eumetsat.int/mod/forum/view.php?id=14088>
- Download the slides: <https://training.eumetsat.int/mod/folder/view.php?id=14089>
- Posters padlet: <https://padlet.com/TrainingEUMETSAT/46oseukzvpio7s0m>

**ORAL PRESENTATIONS**

### **Olafur Jonasson et al., First evaluation of the diurnal cycle in the ACSPO global super-collated SST from Low Earth Orbiting Satellites (L3S-LEO)**

NOAA has developed a new ACSPO 0.02 gridded super-collated SST product from Low Earth Orbit satellites to provide both day and night data. Nighttime observations from three VIIRSs overpasses are used to improve the coverage. A new algorithm has been developed to retrieve SST. Currently this new SST is available at the NOAA Coastwatch website and will be available in PO.DAAC soon. The new algorithm improves L3U SST images by reducing residual cloud leakages.

The validation shows substantial improvements for daytime SST. More sensors will be included in future development, and consistency checks will be carried out to ensure synergy.

Discussion: Chris Merchant has highlighted that this work has shown significant and innovative progress and would like to understand more about the approach (available now at <https://doi.org/10.1117/12.2551819>, <https://doi.org/10.1117/12.2585819>, [ftp://ftp.star.nesdis.noaa.gov/pub/socd/osb/aignatov/SPIE/2019/Papers/GladkovaEtAl\\_Towards\\_Hi-Res\\_L3S\\_110140L.pdf](ftp://ftp.star.nesdis.noaa.gov/pub/socd/osb/aignatov/SPIE/2019/Papers/GladkovaEtAl_Towards_Hi-Res_L3S_110140L.pdf)).

### **Xu Li, The sea surface temperature analysis in the NCEP GFS and the future NCEP UFS**

NOAA/NCEP has updated the NCEP SST products recently, and validation shows that satellite radiances bias is significantly reduced as well as the bias against drifting buoys. The SST in the Gulf Stream area is much improved after the update by using clear AVHRR radiances only. Currently, the NOAA/NCEP team has been using NOAA SST to improve their coupled models, showing more realistic diurnal variability and improved MJO, for instance.

Discussion: Helen Beggs commented that the NSST diurnal warming tends to be too strong even though the presentation mentioned that including the NSST model in the UFS leads to a more realistic diurnal variation in the coupled model. Helen has asked the following question to the presenter (verbatim):

*"Is the updated exp NSST model providing the UFS coupled model with an hourly (or 6-hourly) skin SST based on some diurnal variation model, via the simulated NSST T-Profile." If yes, then which diurnal variation model do you use?"*

### **Wen-Hao Li, PODAAC milestone: GHRSSST data migrating to AWS Cloud**

To provide easy access and reduce heavy downloading, the NASA team has been working on the migration of PO.DAAC data to Earthdata cloud hosted in Amazon Web Services Cloud to provide great flexibility for data analysis and data sharing. The new platform offers the same high level of services as before but with easy access to large datasets and across data centers. GHRSSST data will be available in the Earthdata cloud after June 2021.

Discussion: Jean-Francois has asked what service will be free of charge and will require payment and the answer from the presenter is that "all the services of searching, accessing, and downloading the datasets from the cloud are free, including using the data services for subsetting, reformatting, regridding, and notebook recipes. If users want to do the computation with the dataset in the cloud, they will have to pay for those CPU cycles and any storage they might need for intermediate results. Again, for NASA data egress (download or subsetting, whether full granules or subsetted/regridded data), there is no charge". Alexander Ignatov was pleased with his initial testing of the system for NOAA L3S-LEO products.

### **Ed Armstrong, Analysis Ready Data applications for GHRSSST and related data**

Ed presented the concept of Analysis Ready Data (ARD) and the potential applications for GHRSSST data. Original L4 SST NetCDF occupies around 3TB space, and the ARD version of this data is in Zarr format that could be accessed in a few seconds. The ARD stored in the Amazon Web Service also improves efficient analysis. ARD is an evolving concept that has immense potential in the future, and the well-established satellite-based ARD content in CEOS enables the growth of the ARD concept.

Discussion: Helen Beggs mentioned an Australian application of the "Open Data Cube" used by Geosciences Australia for their Digital Earth Australia (DEA) portal at [www.ga.gov.au/dea](http://www.ga.gov.au/dea). This DEA portal initially presents Landsat data but shows images of high and low tide composites.

She has also commented that "Also, it occurred to me that the data cube approach Chelle used for MUR might be applied to the IMOS 0.02 deg L3S data sets over the Australian domain for 1992 to present. I frequently get complaints from users that they want just one whole aggregate dataset, rather than individual daily NetCDF files, that they can interrogate themselves to extract the information they need. Currently, the Australian Ocean Data Network (<https://portal.aodn.org.au/>) has an aggregation option to produce a time series from gridded level 3 or level 4 SST data over a specified area and period, but this is quite cumbersome."

**Alexander Ignatov commented that the ARD is an interesting and promising concept and practical way forward.**

Prasanjit commented that it's tough to get such compiled information, and the YouTube link will be helpful as a helpful pointer.

**Chelle Gentemann, Science Storms the Cloud**

The increasing data size and keeping updated data version, data storage and maintenance cost, and the difficulty to share and access data ask for an open data policy. Advanced technology enables us to remove barriers to collaborate extensively. The open data (cloud-based) and open science are in urgent need to advance science. Gentemann et al. promoted this idea in this presentation.

Discussion: Prasanjit liked the approach and commented that "Scalable solutions (use of Dask etc.) is the future given the exploding amount of satellite data expected shortly, and open science and open data will shape the future of earth science".

**POSTER PRESENTATIONS**

### **Dorina Surcel Colan, Recent Updates of CMC SST**

Dorina presented the newly developed SST data from CMC. Compared to the previous version, NOAA20 VIIRS, AVHRR from Metop-C, and additional ship data are added, showing small improvements.

Future work plans have been presented that include transition to a new internal format for observation data and use a variational data assimilation scheme instead of optimal interpolation, and CMC will produce a reanalysis SST from 1990 to 2020.

Discussion: Xu Li (NOAA) asked: How the analysis bias and standard deviation are calculated with your analysis scheme?

### **Misako Kachi, Updates of AMSR3 on GOSAT-GW and its Ocean products**

Kachi et al. have updated AMSR3 development onboard GOSAT-GW, currently scheduled for launch in 2023. Compared to AMSR-2, there will be additional 10.25, 165.5, 183+-7, 183+-3 GHz channels. In addition, the specification of the Ka-band is changed to reduce the future risk of radio frequency interference from the 5G mobile communications system. Misako also briefed on the possibility of high-resolution SST and sea ice products.

### **John Kennedy, Use of ESA SST CCI data in HadISST 2.3.0c**

Kennedy et al. presented the new version of HadISST version 2.3.0, in which they have integrated ESA-CCI SST, which has relatively small biases. ESA-CCI satellite data SST is used to estimate high-resolution spatial patterns and mid-scale variability residual.

Discussion: John Kennedy has provided additional information for the presentation in terms of feature fidelity (verbatim).

"I found the talk about feature fidelity very interesting because we have a related difficulty in making HadISST2. We can easily identify large-scale structures in SST fields, by which I mean really large scale: things like El Ninos and global warming. Being statistical, they may not have a straightforward physical meaning, but we don't easily confuse them for measurement errors.

At smaller scales, however, the covariance functions that we use are typically "local," i.e., they are simple exponentially decaying functions for which the covariance depends on the distance between two points. The characteristic length scales run from 100s to 1000s of kilometers. At the lower end of this range, there is potential for confusion with locally-correlated error terms in the observational uncertainty from satellites, particularly if we don't have a good idea of what small-scale errors and SST structures actually look like."

### **Pallavi Govekar, Himawari-8 and Multi-sensor sea surface temperature products and their applications**

Govekar et al. presented near-real-time SST based on the Himawari-8 geostationary satellite and high resolution, gap-free multi-sensor L3S SST.

The newly developed multi-sensor SST products have used data from Himawari-8, NOAA-20 and Suomi NPP VIIRS files, OSISAF from Metop-B, and NOAA-18 AVHRR-18 L2P files. Users could potentially use this multi-sensor SST to monitor marine heatwaves, identify coastal upwelling, study diurnal warming, verify the coastal model and monitor coral bleaching risk.

### **Lars Hunger, Towards ACSPO super-collated gridded SST product from Multiple Geostationary Satellite (L3S-GEO)**

A suite of multi-sensor gridded super-collated SST data developed in NOAA has been presented by using the Advanced Clear Sky Processor for Ocean (ACSPO) enterprise SST system. The current status is that an end-to-end infrastructure for super-collating individual-sensor GEO L3C SSTs and its global monitoring in SQUAM has been created.

### **Anne O'Carroll, Copernicus Sentinel-3 SLSTR Sea (and sea-ice) Surface Temperature: product status, evolutions and projects**

Copernicus Sentinel-3A and 3B have been launched in 2016 and 2018 to deliver sea surface temperature data, and S3A-SLSTR SST has been operationally provided since 2017 and S3B since 2019. This poster

presents the status of the product and future plan. The poster also highlighted other related activities, such as fiducial reference measurements through the TRUSTED project and a Bayesian cloud detection approach for coastal areas scheduled for June 2021 end. Newer projects were also listed, such as SST/IST (Noveltis, Meteo-France, Ifremer, Met. No, DMI, Univ of Reading; Mar 2021) and intercomparison and validation of FRM radiometers (Karlsruhe Inst. of Technology and University of Southampton).

**Mark Worsfold, A new OSTIA product for late-1981 to present**

A new version of OSTIA SST from late 1981-present has been introduced. The updated version will be near-real-time with a 6-month delay mode. The latest version has included an increased variety of input datasets and used a new analysis system. The mean and standard deviation has been improved with the new system and more data integrated.

**Boris Petrenko, Filtering cold outliers in NOAA AVHRR SST for ACSPO GAC RAN2**

A new SST product based on NOAA AVHRR 2/3 GAC data is developed by filtering cold SST outliers. Warm and cold SST biases have been identified in the historical AVHRR SST products. The AVHRR series is occasionally exposed to direct sunlight when the satellite approaches the terminator from the dark side of the Earth. Sun impingement on the Earth view sector of the sensor field-of-view causes warm SST outliers, whereas the exposure of the black body calibration target gives rise to cold outliers. The volcanic aerosols also caused cold biases in earlier AVHRS SST records following significant volcanic eruptions of Mt. El Chichon (1982), Mt. Pinatubo, and Mt. Hudson (1991). Petrenko et al. have developed two methods to mitigate the cold SST bias by using corrected calibration coefficients and a modified clear-sky mask. The method of filtering cold outliers, which exploits the latitudinal structure of their concentration, has been tested in RAN2 B02. The method of correcting the nighttime L1B calibration coefficients is being developed for RAN2 B03 to mitigate the effects of Sun impingement on the black body calibration target.

## **S5 - ORAL PRESENTATIONS - ABSTRACTS**

## S5-1: SCIENCE STORMS THE CLOUD

**Chelle L. Gentemann<sup>(1,2)</sup>, Chris Holdgraf<sup>(3,4)</sup>, Ryan Abernathey<sup>(3,5)</sup>, Daniel Crichton<sup>(6)</sup>, James Colliander<sup>(3,7,8)</sup>, Edward Joseph Kearns<sup>(9)</sup>, Yuvi Panda<sup>(3)</sup>, Richard P. Signell<sup>(10)</sup>**

- (1) Farallon Institute, USA [cgentemann@faralloninstitute.org](mailto:cgentemann@faralloninstitute.org)
- (2) Earth and Space Research, USA
- (3) 2i2c, USA
- (4) International Computer Science Institute, USA
- (5) Lamont Doherty Earth Observatory of Columbia University, USA
- (6) Jet Propulsion Laboratory, California Institute of Technology, USA
- (7) Pacific Institute for the Mathematical Sciences, Vancouver, Canada,
- (8) University of British Columbia, Vancouver, Canada,
- (9) First Street Foundation, Brooklyn, NY, 10US Geological Survey, USA

The core tools of science (data, software, and computers) are undergoing a rapid and historic evolution, changing what questions scientists ask and how they find answers. Earth science data are being transformed into new formats optimized for cloud storage that enable rapid analysis of multi-petabyte datasets. Datasets are moving from archive centers to vast cloud data storage, adjacent to massive server farms. Open source cloud-based data science platforms, accessed through a web-browser window, are enabling advanced, collaborative, interdisciplinary science to be performed wherever scientists can connect to the internet. Specialized software and hardware for machine learning and artificial intelligence (AI/ML) are being integrated into data science platforms, making them more accessible to average scientists. Increasing amounts of data and computational power in the cloud are unlocking new approaches for data-driven discovery. For the first time, it is truly feasible for scientists to bring their analysis to data in the cloud without specialized cloud computing knowledge. This shift in paradigm has the potential to lower the threshold for entry, expand the science community, and increase opportunities for collaboration while promoting scientific innovation, transparency, and reproducibility. Yet, we have all witnessed promising new tools which seem harmless and beneficial at the outset become damaging or limiting. What do we need to consider as this new way of doing science is evolving?

Please see <https://agupubs.onlinelibrary.wiley.com/doi/full/10.1029/2020AV000354>.

## S5-2: ANALYSIS READY DATA APPLICATIONS FOR GHRSSST DATA AND APPLICATIONS

**Edward M. Armstrong<sup>(1)</sup>, Christo Whittle<sup>(2)</sup>, Chelle Gentemann<sup>(3)</sup>, Chris Lynnes<sup>(4)</sup>, Steve Labahn<sup>(5)</sup>, Adam Lewis<sup>(6)</sup>, Amie Baciauskas<sup>(7)</sup>**

- (1) Jet Propulsion Laboratory, California Institute of Technology, Pasadena, CA, 91109 USA, Email: [edward.m.armstrong@jpl.nasa.gov](mailto:edward.m.armstrong@jpl.nasa.gov)
- (2) SANSa, Email: [CWhittle@csir.co.za](mailto:CWhittle@csir.co.za)
- (3) Farallon Institute, Petaluma CA 94952, Email: [cgentemann@faralloninstitute.org](mailto:cgentemann@faralloninstitute.org)
- (4) NASA, Email: [christopher.s.lynnes@nasa.gov](mailto:christopher.s.lynnes@nasa.gov)
- (5) USGS, Email: [labahn@usgs.gov](mailto:labahn@usgs.gov)
- (6) Geosciences Australia, Email: [Adam.lewis@ga.gov.au](mailto:Adam.lewis@ga.gov.au)
- (7) Development Seed, Email: [aimee@developmentseed.org](mailto:aimee@developmentseed.org)

### INTRODUCTION

Analysis Ready Data (ARD), a broad term to describe the readiness of data for scientific analysis, has been challenging to precisely define because its utility and context often depend on various combinations of the science application, compute environment and the science discipline needs. It could be argued that all GHRSSST datasets are ARD due to the prescribed self-describing netCDF data containers containing well-structured metadata, coordinate systems and importantly SST measurement uncertainty and quality information of which the GHRSSST Project was among of the first remote sensing communities to require of all its datasets since 2006.

The Committee on Earth Observation Satellites (CEOS) has taken a pioneering role in providing a foundational definition and specification for ARD for remote sensing products. This work, initiated in the Land Surface Imaging Virtual Constellation (LSI-VC) in 2017 has resulted in a formal CEOS approved governance structure (known as the CEOS ARD Framework) for evaluating data for ARD status and adoption, and several datasets such as Landsat collection 2 that have gone through the process now have a CEOS ARD seal of approval and recognition. In the context of this CEOS ARD Framework, the GHRSSST data model was evaluated from the perspective of the MODIS L2P Aqua SST dataset.

In this evolving landscape of ARD, other perspectives on ARD are also presented with regard to data containers, data services, environmental applications and community interests.

### CEOS ARD

#### CEOS ARD Definition and Framework

Analysis Ready Data as publicized by CEOS starts with this succinct definition:

“Analysis ready data are satellite data that have been processed to a **minimum set of requirements** and organized into a form that allows **immediate analysis** with a minimum of additional user effort and **interoperability** both **through time and with other datasets**.”

The key bolded text in the definition stresses a set of data requirements that supports both immediate time series analysis and as well as interoperability with other related datasets. Fundamentally, this definition sets the foundational requirements for constructing and evaluating ARDs that is the core part of the CEOS ARD Framework.

The CEOS established ARD Framework exists as three distinct parts.

1. A governance model that represents the workflow of the ARD peer review/acceptance process, and roles and responsibilities of stakeholders
2. The Product Family Specification (PFS); the thematic list of ~30-40 acceptance criteria with “Threshold” and “Target” levels used to assess candidate products
3. The list of approved CEOS ARD products (e.g., Landsat collection 2)

These components are described in more detail on the CEOS ARD website (<https://ceos.org/ard>).

## CEOS ARD “Beyond Land”

As specified in the Introduction, the CEOS ARD activities were initiated by representatives in the LSI-VC beginning around 2017. Thus the existing PFSs have emphasized the land remote sensing discipline and include PFSs for evaluating Land Surface Reflectance, Land Surface Temperature, and Radar Backscatter datasets. In fact, the CEOS ARD Framework is colloquially known as “CEOS Analysis Ready Data for Land” (CARD4L). The closest supported ocean discipline PFS is the Aquatic Surface Reflectance PFS that is near completion but only suitable for remote sensing datasets at the immediate land/coastal ocean interface.

Recognizing this bias toward land in the existing Framework, the CEOS has undertaken a “CEOS ARD Beyond Land” initiative that strives to improve the overall Framework and develop recommendations to both streamline the governance process and importantly adapt the PFS specifications to accommodate other earth science disciplines including the ocean community. The SST-VC has been actively participating and co-leading this effort. A set of recommendations is expected by September 2021 to be presented at the upcoming CEOS SIT Technical Workshop.

## EVALUATING MODIS L2P AS ARD

### MODIS L2P Assessment

As an experiment, an existing GHRSSST dataset was evaluated against the most appropriate existing PFS. The dataset chosen was the MODIS Aqua L2P SST dataset (<https://doi.org/10.5067/GHMDA-2PJ19>) using the Land Surface Temperature (LST) PFS. As expected not all of the 30+ assessment factors for the LST PFS were appropriate for SST measurements. But of the ones that were, the MODIS dataset fared quite well meeting at least the “Threshold” level in categories representing the general metadata and pixel level quality and uncertainty information. For this dataset, pixel geo-location is specified in a well-described coordinate system using CF metadata conventions and netCDF data model.

However, the existing PFS stipulates that satellite observed pixels should “line up” and be spatially coincident through time, a requirement that cannot be met with typical Level 2 polar orbiting wide swath, moderate resolution SST data such as from MODIS. Other findings point to the need to develop a SST focused PFS as well.

### ARD Data Services

Another approach to the ARD concept is an “on demand” creation capability through web services. In this model a user invokes a data service to “tune” or transform existing data to meet the requirements or format of ARD whatever they may be. In the case of MODIS L2P SST, since the primary failure of the existing MODIS L2 ARD assessment was the pixel non-coincidence, the service would transform the netCDF L2 swath data to a L3 common mapped grid. An example of this use case was developed as a Jupyter python notebook that leveraged NASA Harmony web services for discovery and subsetting of cloud data in conjunction with the GDAL and NCO toolkits to:

1. Discover granules (and cloud storage endpoints) using a space/time search
2. Perform subsetting in a region of interest
3. Execute GDAL/NCO commands to transform and regrid subsets
4. “Stack” the outputs in an aggregated data cube

As shown in Figure 1, this data cube now essentially functions as the ARD container where pixels are coincident and “line up” making further time series analysis relatively straightforward. Of course, there are further challenges in this approach to document and quantify the information loss and effect on measurement uncertainty from the regridding and transformation methodology.

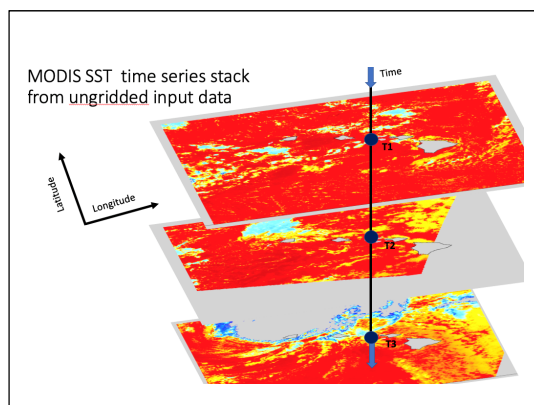


Figure 1: “Data cube” of gridded co-located 1 km MODIS Aqua SST subsets over the Hawaiian Islands region. Created “on demand” via web services and scripts. Only first three time steps shown with no cloud masking applied.

### AN ARD OF 19 YEARS OF GLOBAL DAILY 1 KM SST

An existing example of an ARD is the MUR 1 km dataset that was transformed into the Zarr format for the Amazon Open Data Registry (<https://registry.opendata.aws/mur/>). This is an AWS demonstration service with open access and compute capability to a number of large earth science and societal datasets. In case of MUR, this 3 TB dataset in the AWS cloud allows for data proximate scalable computations, and the cloud optimized Zarr format allows a user to specify the exact space/time portions of the time series to access and load into memory.

In comparison to single file netCDF, the Zarr format has shown be more flexible and significantly faster for data access and compute in a cloud storage and compute environment.

### OTHER ARD INTERESTS

In addition to CEOS other ARD interests and stakeholders are emerging in the commercial and geospatial communities such as from small satellite providers (e.g., Planet), GIS interests (e.g., ESRI) and from other non-profit organizations (e.g., Pangeo, ARD Zone). In January 2021 a session called “ARD in Science and Industry” (<https://2021esipwintermeeting.sched.com/event/g49Q/analysis-ready-data-in-science-and-industry>) was organized at the 2021 ESIP Winter Meeting to explore this landscape. A word poll conducted among the 80 participants on the meaning of ARD revealed some pertinent findings (Figure 2).



Figure 2: Word cloud from the ESIP Winter Meeting session regarding the participants impressions on the ARD concept and definition.

Key findings from this session included:

- The ARD definition/approach (or use case) is often community/discipline/application dependent (e.g., Research/Applications, Space/Earth, Satellite/GIS/Model).

- ARDs are linked to data formats, services, and metadata. Metadata and web services play important roles for cloud-optimized formats and fulfilling requirements for services for “on-demand” ARDs derived from L1/L2 data

### **USER NEEDS ARD**

A practical example of a user needs driven ARD ecosystem in support of active marine environmental management is under development in South Africa in support of the National Oceans and Coastal Information System (OCIMS). This application will require the implementation of a marine analysis ready data (ARD) structure to facilitate the ingestion of diverse marine-relevant remote sensing geophysical products into an open data cube (ODC) for rapid comparative time series data analysis and decision support. The project has implemented and tested the CEOS ODC framework using docker containers to manage the application with the next steps to transform locally produced products to conform to the CEOS ARD Framework and Product Family Specifications.

### **CONCLUSIONS**

For the earth science community, the CEOS ARD Framework presents a well-defined and attractive roadmap and methodology for ARD evaluation and creation. However, it has primarily focused on land based remote sensing products and is now being evaluated and extended (CEOS ARD “Beyond Land”) to meet the needs of other earth science thematic disciplines including for ocean parameters such sea surface temperature. For example, an ARD assessment of the MODIS Aqua L2P SST dataset, while overall very positive, identified some limitations due to pixel geolocation factors and requirements (that could be overcome with web service based data transformations). An improved ARD Framework with revised governance structure and a “bare bones” ARD assessment template is expected later in 2021. For ocean products, in general, it will best to focus on high resolution L3/L4 datasets as future ARD candidates.

There are certainly other examples of ARD in larger earth science community. The AWS Open Data Registry contains the MUR L4 1km SST dataset that has been refactored into the Zarr format in the Pangeo ecosystem, and a recent ESIP Winter meeting session on ARD stressed the nature of its evolving definition, and other approaches and understanding of ARD. For example, the cloud “friendlessness” of an ARD is an important access/compute/cost factor, and there is a role for “on demand” web-based data transformations for ARD creation.

### **Acknowledgements**

These activities were carried out at the Jet Propulsion Laboratory, California Institute of Technology, under a contract with the National Aeronautics and Space Administration (80NM0018F0848). Dedicated funding for PO.DAAC activities is through a grant from NASA’s ESDIS Project.

©2021 California Institute of Technology. Government Sponsorship Acknowledged.

### **S5-3: PODAAC MILESTONE: GHRSSST DATA MIGRATING TO AWS CLOUD**

**Wen-Hao Li<sup>(1)</sup>, Edward M Armstrong<sup>(1)</sup>, David Moroni<sup>(1)</sup>, Jorge Vazquez<sup>(1)</sup>**

(1) Jet Propulsion Laboratory, California Institute of Technology, Pasadena, CA,  
Email: wen-hao.li@jpl.nasa.gov

NASA's Physical Oceanography Distributed Active Archive Center (PO.DAAC) is the Global Data Assembly Center (GDAC) for the Group of High Resolution Sea Surface Temperature (GHRSSST) project. Recently, PO.DAAC has made revolutionary changes to its data publication, access, distribution systems through NASA's Earthdata Cloud, powered by Amazon Web Service (AWS). A recent update to the PO.DAAC web-portal provides direct synchronization of dataset content via the Earthdata Search API, providing seamless integration and distribution of data distributed both in the cloud and on premise. A growing number of PO.DAAC datasets, including GHRSSST, are already available in the cloud. This is a big step forward for PO.DAAC to enhance and promote the GHRSSST data discoverability, usability and services. All of the 95 GHRSSST datasets currently archived at the PO.DAAC have been or will be moved to the AWS Cloud by February 2022 with the MUR, MODIS, and VIIRS SST datasets as the pioneer group. Such efforts enable the GHRSSST datasets to be available to a much broader SST and interdisciplinary user community, and further promote open science and data fusion research. The traditional data access and service tools are being transitioned into the Earthdata Cloud system, but availability will vary due to the configuration steps required for cloud-based integration. An enterprise-level web service API, known as NASA Harmony, for data discovery, download, subsetting and reformatting will be described, including some Jupyter notebook recipes developed by the PO.DAAC. In parallel to the cloud-migration effort, PO.DAAC has also reformed the metadata management and archiving infrastructure by switching the local management service to NASA's Common Metadata Repository (CMR), which is an enterprise-level data and metadata management system. CMR integrates metadata from all 12 NASA DAACS, providing the capability to make data search and extraction through the cloud more efficient than ever before.

## **S5-4: THE SEA SURFACE TEMPERATURE ANALYSIS IN THE NCEP GFS AND THE FUTURE NCEP UFS**

**Xu Li<sup>(1)</sup>, John Derber<sup>(1)</sup>, Andrew Collard<sup>(1)</sup>, Daryl Kleist<sup>(2)</sup>**

(1) IMSG at EMC/NCEP/NOAA, USA

(2) EMC/NCEP/NOAA, USA

### **INTRODUCTION**

At National Centers for Environmental Prediction (NCEP), the Sea Surface Temperature (SST) is analyzed in the Global Forecast System (GFS), referred to as NSST (Near-Surface Sea Temperature), and will be in the Unified Forecast System (UFS), Medium-Range Weather and Subseasonal to Seasonal Application, a coupled data assimilation and weather prediction system.

The NSST has undergone several upgrades since becoming operational in the NCEP GFS in 2017.

The evaluation results of an NSST update package developed recently is reported here. This package includes three updates, inclusion of two more AVHRR and two VIIRS radiances, new background error correlation length scales and a smaller thinning box size for AVHRR and VIIRS radiances, which are developed to address the issue that small-scale spatial features are not well resolved in the operational NSST analysis. Another update, the exclusion of AVHRR partly-clear radiances is included in the package as well.

The effort to produce SST analysis in the future UFS is underway. The near surface sea water temperature simulated by the coupled model, with the 2-m top layer thickness oceanic model (MOM6), has been verified against the buoy observations. It has shown the fit to drifting buoy is encouraging, but the diurnal variability is too weak, which means an explicit diurnal warming model is still needed in the coupled system. The results to evaluate the impact of the NSST model, including a diurnal warming and a skin-layer cooling parameterization, on the coupled model performance, with a scheme to determine the foundation temperature with the NSST and MOM6 T-Profiles, is presented as well.

### **THE EVALUATION OF THE NSST PACKAGE**

The NSST update package includes 4 updates, (1) inclusion of two more avhrr, NOAA-19 and Metop-b, two VIIRS satellites, npp and j1. (2) Change of the background error correlation length scales from a constant 100 km to the first baroclinic Rossby radius of deformation in the ocean. (3) Reduction of the thinning box size from a constant 145 km to 25 to 75 km for AVHRR and VIIRS radiances. (4) Exclusion of the partly-clear AVHRR radiances.

This package has been tested by a 33-day cycling run with GFSv15.2 at C768, which is the operational version at that time, starting from 00Z, November 10, 2019.

Figure 1 shows the fit to drifting buoy observations. We can see the RMS has been improved slightly for O – B, and significantly for O - A. This is a positive sign since it can be expected that the fit to in situ observation system degrades due to the much more satellite observations, from another platform, are assimilated.

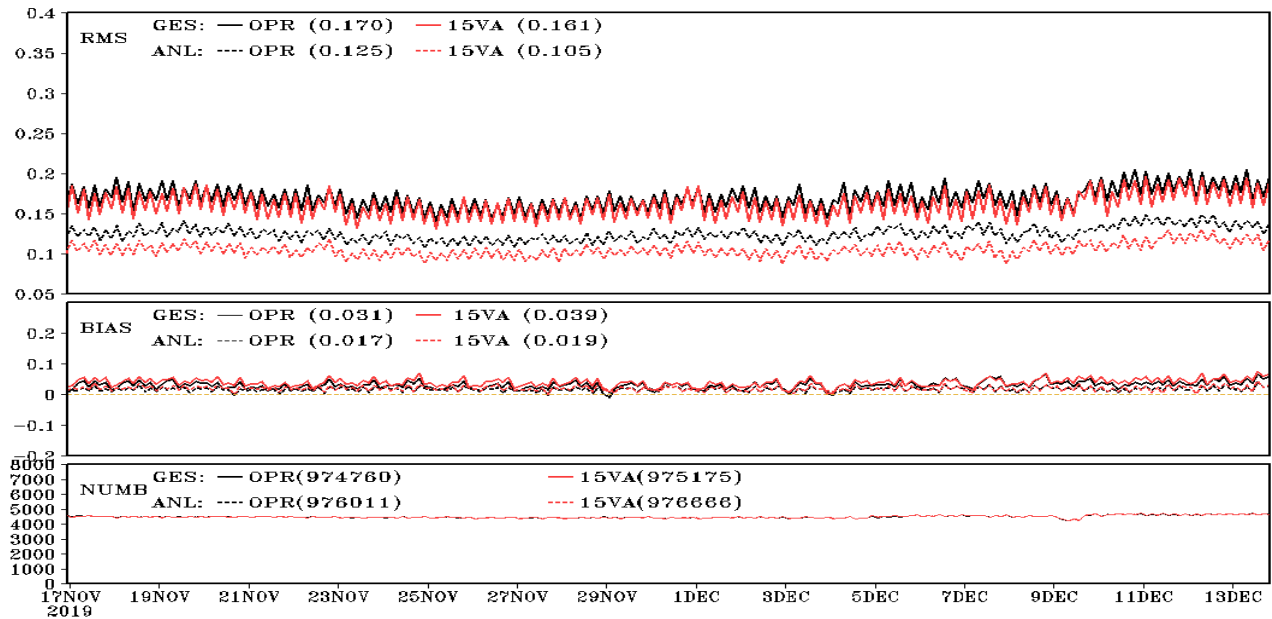


Figure 1. Verification of the NSST analysis with O – B & O – A of Dbuoy. OPR and EXP (15VA). Global.

Figure 2 shows the fit to AVHRR channel-4 radiance observations. We can see that the counts of the assimilated radiances increases by about 9 times, mainly due to the thinning update. It is positive that the RMS of both O – B and O – A are reduced significantly.

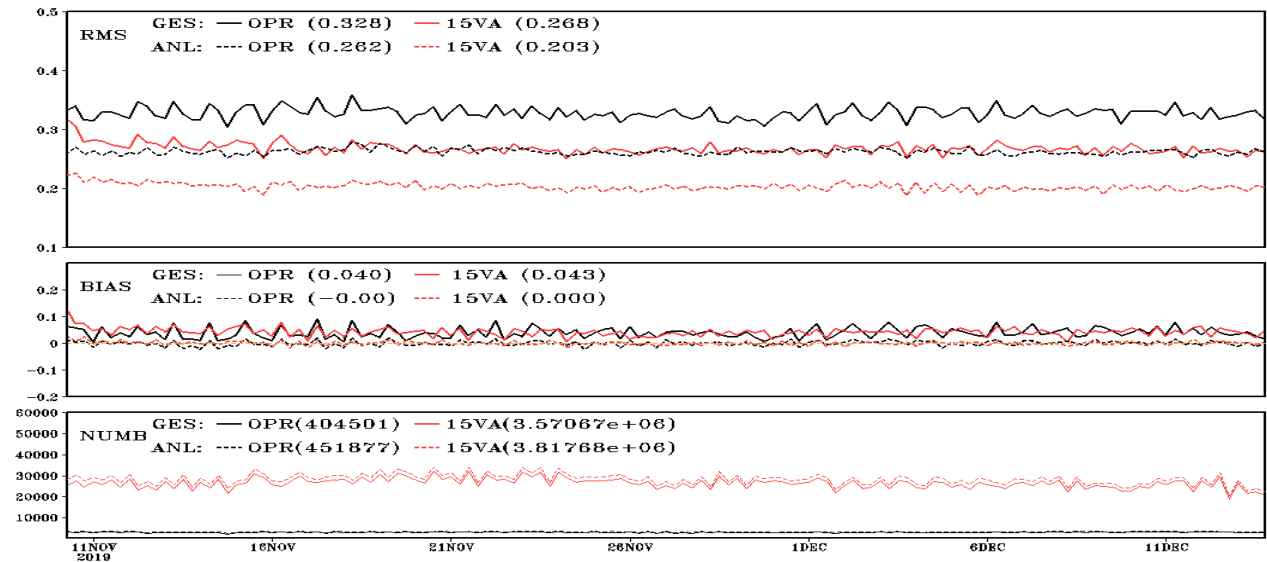


Figure 2. Verification of the NSST analysis with O – B & O – A of AVHRR Ch-4 radiance. OPR and EXP (15VA). Global.

Figure 3 shows the improvement of the Gulf Stream, a small-scale spatial feature, with the package. We can see that the Gulf Stream is too weak in the operational NSST (OPR), it is improved a lot with 3 updates (15VT). And is improved even more with the 4<sup>th</sup> update (15VA).

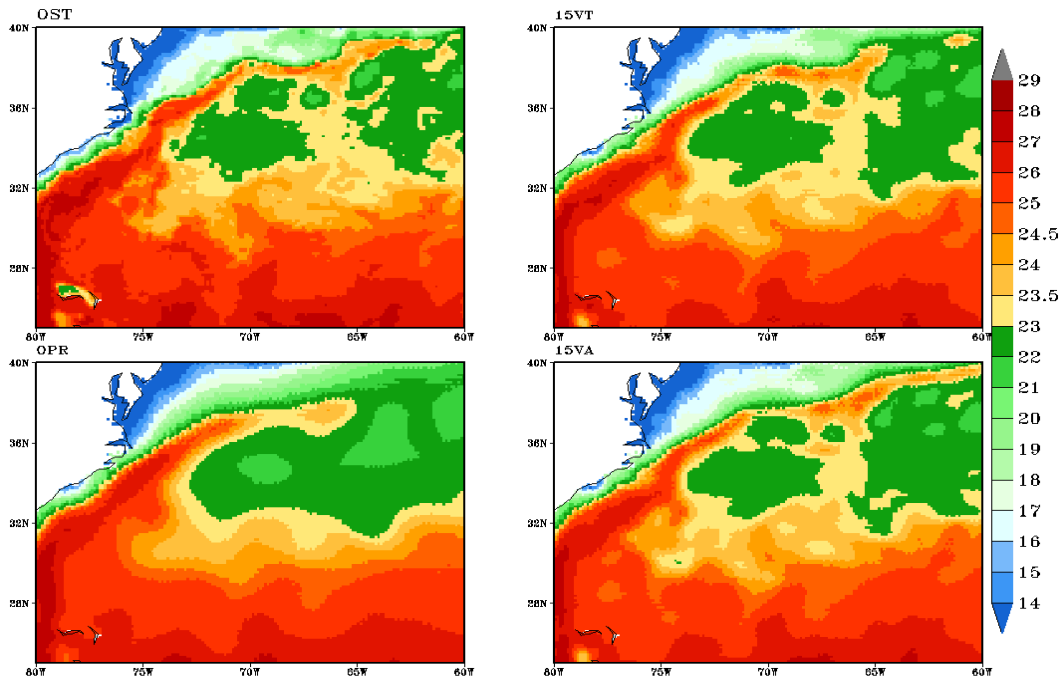


Figure 3. The Gulf Stream in the foundation temperature analyses. 18Z, Nov. 20, 2019. 19 days after starting from the operational initial conditions (at 00Z, Nov. 10, 2019).

### THE IMPACT OF THE NSST MODEL ON THE COUPLED MODEL

In order to evaluate the impact of the NSST model, including a diurnal model and a skin layer parameterization, 56 (2 x 28), 35-day coupled model (MRW/S2S) runs, with (NST run) or without (CTL run) the NSST model, have been done. The verification of the simulated near-surface temperature against the drifting buoys is presented for one 35-day run, starting from 00Z, October 1, 2011, here. The O – F is calculated as follows:  $T^{ob}(z_{ob}) - [T_f^{fcst}(z_w) + T_w^{fcst}(z_{ob})]$ , here,  $T^{ob}(z_{ob})$  is the temperature observed by the drifting buoys ( $z_{ob} = 0.2$  m, currently, no cooling effect therefore),  $T_f^{fcst}(z_w)$  is the foundation temperature at the depth  $z_w$ , the base of the warm layer. And the foundation temperature is determined by the NSST T-Profile,  $T^{nst}(z, t) = T_f(z_w, t) + T'_w(z, t)$ , and MOM6 top layer temperature,  $T_1(t)$ , with Scheme-A.1,  $T_f(t) = T_1(t) - (1/z_1) \int_0^{z_1} [T'_w(z, t)] dz$ . The verification is done for different drifting buoy groups, which are grouped with the diurnal warming amount at 0.2 m simulated by the NSST model.

Figure 4 shows the time series of RMS, Bias of (O – F) defined above and the counts of the used drifting buoys. We can see that the NSST diurnal warming model improves both RMS and Bias overall. Particularly, in the initial time period (about 6 days), reduces RMS significantly (roughly from 0.45 to 0.35) and the cold Bias (~ 0.4 K) to nearly zero. It is also noticed that NSST diurnal warming is too strong after about 6 days. The similar results can be seen for the other groups of the drifting buoys with different diurnal warming amount (not shown).

### CONCLUSIONS

With the initial implementation of the GFS NSST, it was found that small-scale spatial features are not well resolved due to two major reasons: too broad horizontal background error correlation length and observation coverage. It was found also that the cloud contamination of the partly clear AVHRR radiance cannot be discriminated well with the available GSI cloud detection scheme. To address these issues, an NSST update package have been developed and tested. Experimental results have shown the NSST analysis can be improved significantly with this package.

The impact of the NSST model, including a diurnal warming and a skin-layer cooling parameterization, on the coupled model performance is positive, particularly in the initial simulation period. This is positive to have the NSST model included in the future NCEP UFS.

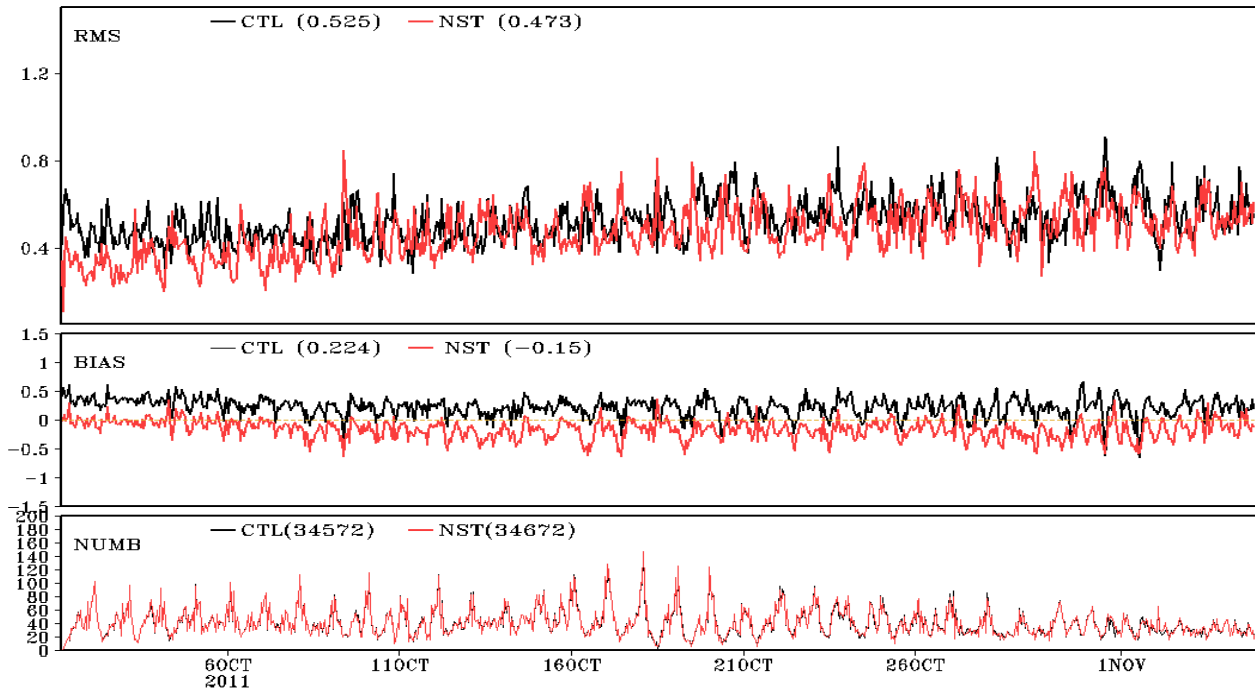


Figure 4: Observation minus Forecasting (O-F) time series of RMS, BIAS and the number of used data, Global, 35-day coupled model run starting from 10/01/2011. For Drifting buoys with dTw: [0.25, 0.50), 3.8% of the total count.

## REFERENCES

Derber, J., and X. Li, 2018: Assimilating SST with an atmospheric DA system. ECMWF Workshop on Sea Surface Temperature and Sea Ice Analysis and Forecast, Reading, United Kingdom, ECMWF, 27 pp., <https://www.ecmwf.int/node/17984>.

NCEP EMC web site on the NSST introduction:

[https://www.emc.ncep.noaa.gov/emc/pages/numerical\\_forecast\\_systems/sst.php](https://www.emc.ncep.noaa.gov/emc/pages/numerical_forecast_systems/sst.php)

## **S5-5: FIRST EVALUATION OF THE DIURNAL CYCLE IN THE ACSPO GLOBAL SUPER-COLLATED SST FROM LOW EARTH ORBITING SATELLITES (L3S-LEO)**

**Olafur Jonasson**<sup>(1,2)</sup>, **Irina Gladkova**<sup>(1,2,3)</sup>, **Alexander Ignatov**<sup>(1)</sup>, **Yury Kihai**<sup>(1,2)</sup>

(1) STAR, NOAA Center for Weather and Climate Prediction (NCWCP), USA, Email: olafur.jonasson@noaa.gov

(2) Global Science and Technology, Inc., USA

(3) City College of New York, USA

SST products from geostationary (GEO) and low-earth-orbit (LEO) satellites are provided by NOAA using the Advanced Clear Sky Processor for Ocean (ACSPO) system. Up until recently, LEO SST products have been available in L2P and L3U formats, organized into 10-minute granules. The number of high-resolution LEO satellites processed in ACSPO reached seven (2 VIIRSs aboard NPP/N20, three AVHRR FRACs aboard Metop-A/B/C, and two MODISs aboard Terra/Aqua). In conjunction with two planned launches of N21 VIIRS, and Metop-SG METimage, the numerous L2P/3U data are becoming progressively more challenging to manage by users.

In response, NOAA is developing a new suite of super-collated (L3S) products, separately from low-earth (L3S-LEO) and geostationary (L3S-GEO) satellites. The ACSPO L3S-LEO family comprises two lines: PM, from “afternoon” (currently, NPP/N20) and AM, “mid-morning” (currently, Metop-A/B/C). Both AM and PM L3S-LEO products are publicly available in near-real-time on the NOAA CoastWatch website and continuously validated in NOAA SQUAM and ARMS systems.

Both AM and PM lines are reported twice-daily, night and day, sampling the diurnal cycle at four points around 01:30, 9:30, 13:30 and 21:30 local time. Keeping the four L3S-LEO products can potentially capture the diurnal cycle. In this work we analyse this potential by comparing L3S-LEO diurnal signal to the quality-controlled in situ data from the NOAA iQuam system. We also discuss recent L3S-LEO algorithm improvements, which were aimed at improving spatial continuity of SST imagery and reducing impact of cloud leakages from individual sensor L3U data.

**S5 - POSTER PRESENTATIONS – ABSTRACTS**

## **S5-P1: TOWARDS ACSPO SUPER-COLLATED GRIDDED SST PRODUCT FROM MULTIPLE GEOSTATIONARY SATELLITES (L3S-GEO)**

**Lars Hunger**<sup>(1,2)</sup>, **Irina Gladkova**<sup>(1,2,3)</sup>, **Alexander Ignatov**<sup>(1)</sup>, **Yury Kihai**<sup>(1,2)</sup>, **Olafur Jonasson**<sup>(1,2)</sup>

(1) STAR, NOAA Center for Weather and Climate Prediction (NCWCP), USA

(2) Global Science and Technology, Inc., USA

(3) City College Of New York, 160 Convent Ave., New York, NY, USA 10031

Email: [lars.hunger@noaa.gov](mailto:lars.hunger@noaa.gov)

NOAA users increasingly state the need for reduced-volume, high information content SST products from multiple satellites. In response, NOAA is developing a suite of Advanced Clear Sky Processor for Ocean (ACSPO) multi-sensor 0.02° gridded super-collated (L3S) SST products, which aim to maximally preserve temporal and spatial resolution of the original satellite data, without reliance on modeled data. Two ACSPO L3S-LEO products have been produced from two Low Earth Observing families (the afternoon JPSS and mid-morning Metop) since 2020. L3S-LEO data are reported 4 times daily: L3S-PM/AM, day/night, to capture the diurnal cycle (at approximately 1:30am, 9:30am, 1:30pm, and 9:30pm local time). This presentation focuses on its geostationary counterpart, L3S-GEO, which reports 24 files per day, in 1hr UTC increments. Initial L3S-GEO implementation super-collates data from 3 GEO sensors (2 ABIs onboard G16/17, and one AHI onboard H08). Data from the future FCI onboard the EUMETSAT MTG will be added after its launch (expected in 2023). The L3S-GEO algorithm comprises 3 major steps: 1) creating satellite-based SST reference; 2) its use to debias individual-satellite products; 3) aggregating the debiased individual SSTs into L3S-GEO. We demonstrate that the debiasing makes the individual GEO products more consistent and reduces collation artifacts. Initial qualitative evaluation of the L3S-GEO SST imagery and its quantitative global validation against iQuam in situ data is performed in the NOAA monitoring systems ARMS and SQUAM. We discuss the remaining issues and potential improvements.

## S5-P2: USE OF ESA SST CCI DATA IN HADISST.2.3.0.C

**John Kennedy**<sup>(1)</sup>, **Nick Rayner**<sup>(1)</sup>, **Holly Titchner**<sup>(1)</sup>

(1) Met Office Hadley Centre, UK Email: [john.kennedy@metoffice.gov.uk](mailto:john.kennedy@metoffice.gov.uk)

### INTRODUCTION

The Met Office Hadley Centre Sea Ice and Sea-Surface Temperature data set, HadISST2, combines 170+ years of in situ measurements of sea surface temperature with over 35 years of satellite data. In the latest version of HadISST2 we use SST retrievals from the ESA SST CCI AVHRR v2.1 data set together with SSTs from the AATSR Reanalysis for Climate (ARC) data set. Minimal bias adjustments are required to homogenise the satellite records so that they can be combined seamlessly with the in situ SSTs. As in previous versions of HadISST2, data with near-global coverage from satellite SSTs over the past 35 years is combined with the much longer, yet sparser records from in situ data to estimate large-scale and local covariance structures in the data. These, together with SST inferred from sea ice concentration are used to produce a globally complete and consistent analysis of SST and sea ice with homogeneous mean and variance. HadISST2 is presented as a set of ensemble members the spread of which indicates uncertainty associated with: residual bias in the data, measurement error more generally, and sparse sampling.

### SOME BASICS

HadISST data sets (Rayner et al. 2003) have been widely used for a variety of purposes. Chiefly designed to provide a globally-complete and consistent boundary condition for reanalyses and atmosphere-only runs of GCMs, they have found a much wider range of applications. For many of these purposes, it is important to have a data set that is homogeneous in its mean and variance and which has realistic variability and meaningful uncertainty information. This requirement presents some difficulties when combining sparse and noisy in situ data with more copious satellite data.

HadISST.2.3.0.c combines in situ data from ICOADS release 3 (Freeman et al. 2017) with satellite SST retrievals from ESA SST CCI (Merchant et al. 2020) and the ATSR Reanalysis for Climate (Merchant et al. 2012). A schematic of the processing chain is shown in Figure 1. Each of the different data sources is assessed for relative biases (Kennedy et al. 2019), assuming the target SST is whatever drifting buoys measure. The Satellite sources are then blended with each other and then any gaps are filled using in situ data. SST is also inferred from estimated sea-ice concentrations (Titchner and Rayner 2014) in the marginal ice zone (MIZT).

A large-scale reconstruction is performed using an iterative PCA-based algorithm (VBPCA) at low (5° monthly) resolution. Each monthly field is represented by a weighted sum of spatial patterns. The time series of the weights are then projected onto the high resolution combined in situ and satellite data and then smoothed to create high-resolution patterns. The time series of weights are also smoothed in time using Gaussian Process regression to ensure consistent temporal variance and auto correlation.

The large-scale reconstruction is subtracted from the combined in situ and satellite data and a mid-scale reconstruction is performed (from scales of around 1° in latitude upwards). The mid-scale reconstruction is a Gaussian Process reconstruction using a non-stationary covariance with two length scales, variance and local rotation specified at each grid location. Samples are drawn from the posterior of the mid-scale reconstruction and combined to give the final reconstruction.

At each step we use the data source, or combination of data sources that best serves the end goal. The following sections detail where SST CCI data was of particular use in this process.

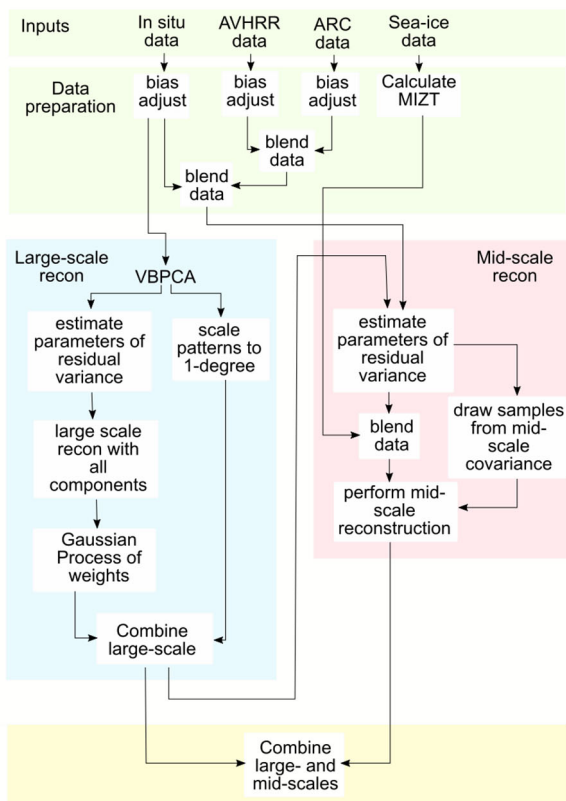


Figure 1: Schematic of the HadISST.2.3.0.c processing

### ESA SST CCI AVHRR DATA HAVE A RELATIVELY SMALL BIAS

The AVHRR data from phase 2 of the ESA SST CCI project have a relatively small bias when compared to earlier versions of the data set and other AVHRR products previously used in HadISST2. Bias adjustment was done at low spatial resolution (5°) so the full in situ uncertainty model could be used. This allows for better use of ship data in the 1980s and early 1990s when there were few drifters.

Bias-adjustments were estimated monthly using a Gaussian Process, with a fixed standard deviation and length scale. This also allowed us to expand the low-resolution bias estimates to higher resolution (1°). Globally biases were small even before adjustment, in the range 0.0-0.5K, and after adjustment, they were less than 0.1K. Divergences were larger locally.

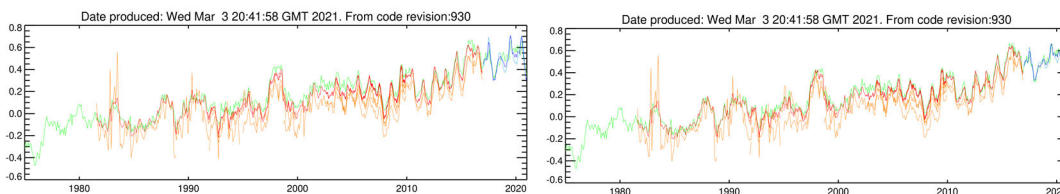


Figure 2: Global mean SST anomalies (relative to 1961-1990) for non-collocated (left) and collocated (right) time series: HadSST.4.0.1.0 (green), SST CCI AVHRR (orange), bias adjusted SST CCI AVHRR (red), METOP AVHRR (light blue) and bias-adjusted METOP AVHRR (dark blue).

### SATELLITE DATA USED TO ESTIMATE HIGH-RESOLUTION SPATIAL PATTERNS

An initial reconstruction was performed at low resolution using only the in situ data. This gives an initial estimate of the EOFs and the full uncertainty model can be used to estimate the principal component series. Once the principal component series are calculated, these can then be projected onto the blended high-

resolution data to get high-resolution patterns for the reconstruction (Figure 3 left). Because early in situ data is patchy, the EOFs were smoothed using a Gaussian filter. This removed the ship tracks that were apparent in some of the EOFs and which would otherwise get baked into the reconstruction. The smoothing means that some small scale features are potentially lost. However, small scale features are recovered in the next step of the reconstruction which uses a local optimal interpolation scheme to recover features down to 1° resolution.

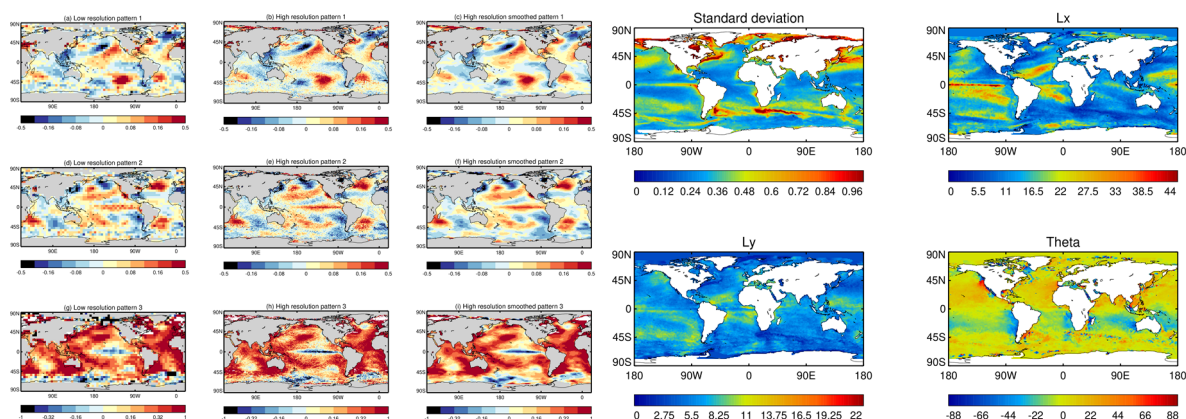


Figure 3: (left panel) Patterns used in the reconstruction of HadISST.2.3.0.c. The first three patterns are shown (rows one to three) for the initial low-resolution pattern estimation (left column), the projection to high-resolution (centre column) and the final, smoothed, high-resolution pattern (right column). (right panel) Parameters of the mid-scale reconstruction: standard deviation (top left); longer length scale, Lx (top right); the shorter length scale, Ly (bottom left); and the local angle of rotation of the longer axis, theta (negative is clockwise, bottom right)

### SATELLITE DATA CAN BE USED TO ESTIMATE RESIDUAL MID-SCALE VARIABILITY

The high-resolution satellite patterns data can be used to estimate a non-stationary covariance kernel for the second step of the reconstruction which uses a Gaussian Process to reconstruct mid-scale variability (features down to 1° resolution). The method is based on Karspeck et al. 2012 but expanded to the whole ocean. The covariance at each location is parameterised using four parameters (Figure 3, right): standard deviation, an east-west length scale (Lx), a north-south length scale (Ly), and an angle (theta) by which the two length scales are rotated away from the N-S and E-W directions.

This allows the reconstruction to produce features that have different spatial scales and also to produce features that have a preferred orientation. Smaller spatial scales are seen in frontal regions and in western boundary currents. The theta parameter allows for features that follow coastlines e.g. the California and Humboldt currents or the Mozambique Channel.

### PULLING IT ALL TOGETHER

The reconstruction (an example is shown in Figure 4) starts with the available observations. Large scale patterns are projected onto the observations (b) and then filled (c) to be globally complete. The filled large-scale reconstruction is subtracted from the observations and the (d) local optimal interpolation is performed. Note that there is a lack of variability in data voids as the reconstruction reverts to the prior mean of zero. The local OI and large scale are combined (e) and then the marginal ice zone temperatures (inferred from sea-ice concentrations) are added (f). Next, a sample of the mid-scale variability is drawn from the posterior distribution of the mid-scale reconstruction (g). This has realistic variability in regions that are sparsely observed or completely unobserved, i.e. those areas where the prior dominates. Where observations are plentiful, such as the North Atlantic, the sample will have little variability. The sample is combined (h) with the large and mid-scale reconstructions and the marginal ice zone temperature is added back in (i).

The multi-step reconstruction allows us to use the different components of the observing system according to their strengths and provides more consistent variability through time. The SST CCI data with its relatively small biases and high resolution extending over 30 years is an excellent complement to the longer but sparser in situ record.

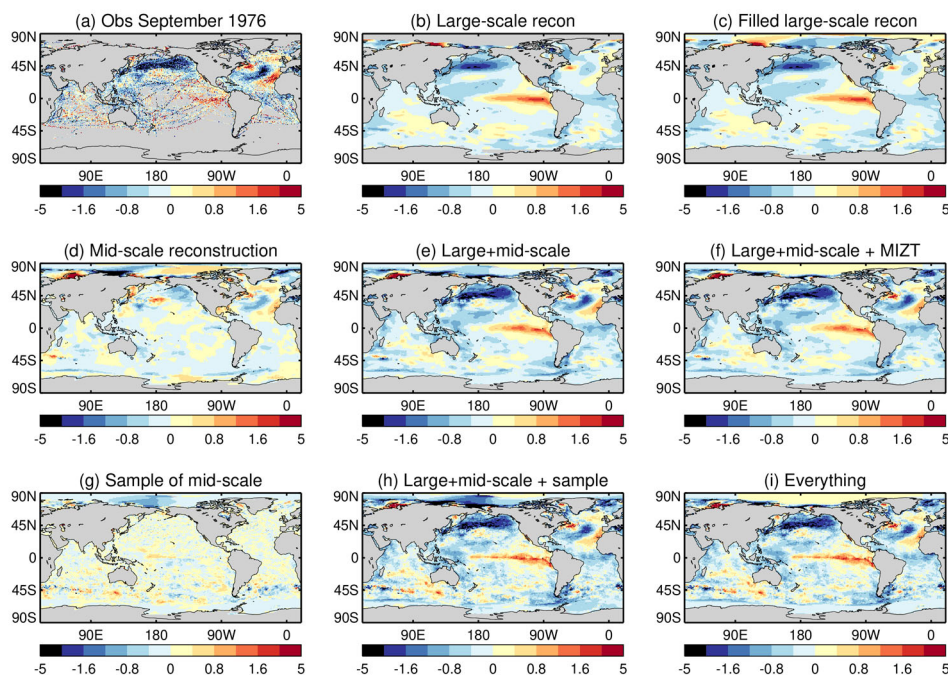


Figure 4: (a) SST anomalies calculated from available observations, September 1976. Grey areas indicate missing data. (b) Large scale reconstruction. (c) Large scale reconstruction filled to be globally complete. (d) Mid-scale reconstruction. (e) combined large and mid-scale reconstructions. (f) Combined large and mid-scale reconstructions including SST inferred from sea-ice concentration in the Marginal Ice Zone (MIZT). (g) Sample of the residual mid-scale variability. (h) Combined large scale and mid-scale reconstruction with the sample of the residual variability. (i) The final reconstructed field for one ensemble member.

## REFERENCES

- Ingleby, N. B. and A. C. Lorenc, Bayesian Quality-Control Using Multivariate Normal-Distributions, *Quart. J. Roy. Met. Soc.* **119** (513), 1195-1225 Part B, 1993.
- Freeman, E., S. D. Woodruff, S. J. Worley, S. J. Lubker, E. C. Kent, W. E. Angel, D. I. Berry, P. Brohan, R. Eastman, L. Gates, W. Gloeden, Z. Ji, J. Lawrimore, N. A. Rayner, G. Rosenhagen and S. R. Smith (2017), ICOADS Release 3.0: a major update to the historical marine climate record. *Int. J. Climatol.*, **37**: 2211-2232. doi:10.1002/joc.4775
- Karspeck, A. R., A. Kaplan and S. R. Sain, Bayesian modelling and ensemble reconstruction of mid-scale spatial variability in North Atlantic sea-surface temperatures for 1850–2008. *Q.J.R. Meteorol. Soc.*, **138**: 234-248. <https://doi.org/10.1002/qj.900>, 2012
- Kennedy, J. J., Rayner, N. A., Atkinson, C. P., & Killick, R. E. (2019). An ensemble data set of sea-surface temperature change from 1850: the Met Office Hadley Centre HadSST.4.0.0.0 data set. *Journal of Geophysical Research: Atmospheres*, **124**. <https://doi.org/10.1029/2018JD029867>
- Merchant, C. J., Embury, O., Bulgin, C. E. et al. Satellite-based time-series of sea-surface temperature since 1981 for climate applications. *Sci Data* **6**, 223 (2019). <https://doi.org/10.1038/s41597-019-0236-x>
- Merchant, C. J., Embury, O., Rayner, N. A., Berry, D. I., Corlett, G., Lean, K., Veal, K. L., Kent, E. C., Llewellyn-Jones, D., Remedios, J. J. and Saunders, R. (2012) A twenty-year independent record of sea surface temperature for climate from Along-track Scanning Radiometers. *Journal of Geophysical Research*, **117**. C12013. ISSN 0148-0227 doi: 10.1029/2012JC008400
- Rayner, N. A., Parker, D. E., Horton, E. B., Folland, C. K., Alexander, L. V., Rowell, D. P., Kent, E. C. and Kaplan, A. (2003), Global analyses of sea surface temperature, sea ice, and night marine air temperature since the late nineteenth century, *J. Geophys. Res.*, **108**, 4407, doi: 10.1029/2002JD002670, D14
- Titchner, H. A., and N. A. Rayner (2014), The Met Office Hadley Centre sea ice and sea surface temperature data set, version 2: 1. Sea ice concentrations, *J. Geophys. Res. Atmos.*, **119**, 2864-2889, doi: 10.1002/2013JD020316.

### **S5-P3: HIMAWARI-8 AND MULTI-SENSOR SEA SURFACE TEMPERATURE PRODUCTS AND THEIR APPLICATIONS**

**Pallavi Govekar<sup>(1)</sup>, Christopher Griffin<sup>(1)</sup>, Helen Beggs<sup>(1)</sup> and Leon Majewski<sup>(1)</sup>**

(1) Bureau of Meteorology, Docklands, Vic 3008, Australia

Sea surface temperature (SST) products within a few kilometres of coasts that can resolve fine-scale features, such as ocean upwelling, are increasingly in demand. The Australian Bureau of Meteorology (Bureau) currently produces operational, real-time SST from the Himawari-8 geostationary satellite every 10 minutes at ~2 km spatial resolution. These native resolution SST data have been composited to experimental hourly, 4-hourly and daily SST products and projected onto the rectangular Integrated Marine Observing System (IMOS) grid at 0.02 x 0.02 degrees. In response to user requirements for gap-free, highest spatial resolution and highest accuracy SST data, the Bureau is experimenting with compositing geostationary Himawari-8 data with data from the Visible Infrared Imaging Radiometer Suite (VIIRS) and Advanced Very High-Resolution Radiometer (AVHRR) satellite sensors installed on polar-orbiting satellites to construct new "Multi-sensor L3S" products. The compositing reduces data gaps due to clouds and presents an opportunity for easy-to-use, more gap-free SST data. The new Himawari-8 and Multi-sensor L3S SST products are expected to provide improved data for applications such as IMOS OceanCurrent, FISHTRACK and the Bureau's ReefTemp Coral Risk Monitoring service. The improved coverage will also provide useful insight into the study of marine heatwaves and ocean upwelling in near-coastal regions. We will discuss our method to combine data from different sensors and present validation of the Multi-sensor L3S SST against in-situ SST data.

For more information, please refer to Helen Beggs' Report in Agency News.

## **S5-P4: RECENT UPDATES OF CMC SST ANALYSIS**

**Dorina Surcel Colan<sup>(1)</sup>, Audrey-Anne Gauthier<sup>(1)</sup>, Kamel Chikhar<sup>(1)</sup> and Gregory Smith<sup>(2)</sup>**

(1) Canadian Center for Meteorological and Environmental Prediction, Meteorological Service of Canada, Environment and Climate Change Canada

(2) Research Meteorological Division, Environment and Climate Change Canada

Email: [Dorina.surcel-colan@canada.ca](mailto:Dorina.surcel-colan@canada.ca)

As part of its operational prediction program, the Canadian Meteorological Centre (CMC) produces a daily sea surface temperature (SST) analysis on a global 0.1° latitude-longitude grid. This analysis assimilates satellite data from AVHRR, AMSR2 and VIIRS instruments, in situ observations from fixed and drifting buoys and from ships and it uses ice information from CCMEP global ice concentration analysis.

Recent updates of the system include assimilation of AVHRR data from Metop-C, VIIRS data from NOAA 20 and the addition of ships data available on GTS in BUFR format.

This study reviews the SST analysis with emphasis on the later implementations. It assesses the impact of assimilating different satellite datasets to the quality of global SST analysis. Verification against independent data and against GMPE product are also presented.

## **S5-P5: COPERNICUS SENTINEL-3 SLSTR SEA (AND SEA-ICE) SURFACE TEMPERATURE: PRODUCT STATUS, EVOLUTIONS AND PROJECTS**

**Anne O'Carroll, Gary Corlett, Igor Tomazic**

EUMETSAT, Eumetsat-Allee 1, 64295 Darmstadt (Germany), Email: [Anne.Ocarroll@eumetsat.int](mailto:Anne.Ocarroll@eumetsat.int)

### **ABSTRACT**

The first Copernicus Sentinel-3 satellite was launched on 16<sup>th</sup> February 2016 and the second on 25<sup>th</sup> April 2018. One of its main objectives is to observe very accurate Sea Surface Temperature (SST) from the Sea and Land Surface Temperature Radiometer (SLSTR). These highly accurate SSTs provide a reference satellite SST dataset and time-series for other satellite SST missions and are important for climate monitoring.

Operational SLSTR SST products have been distributed from the EUMETSAT marine centre since 5<sup>th</sup> July 2017. EUMETSAT performs ongoing validation activities for SLSTR SST, together in coordination with the Sentinel-3 validation team, and real time monitoring is shown from the link to [metis.eumetsat.int](http://metis.eumetsat.int). Validation results show the products performing extremely well, and dual-view SSTs are recommended to be able to be used as a reference SST source.

The ongoing validation activities are important for assessing and maintaining SLSTR SST product quality. In addition to inter-comparisons with other satellite SST, key components are collocations and analyses with drifting buoy SSTs. A Copernicus-funded EUMETSAT project called 'Towards Fiducial Reference Measurements (FRM) of Sea-Surface Temperature by European Drifters' (TRUSTED) is now in its fourth year. Over 100 high-resolution drifting buoys (HRSST) with the design of SVP-BRST have so far been deployed. Activities continue to assess and validate these reference buoys as FRM for SLSTR together in coordination with the HRSST Task Team of the Group for High Resolution Sea-Surface Temperature (GHRSSST). The status of these assessments, together with the outcomes from a science review workshop in March 2021 on HRSST and TRUSTED for SLSTR SST validation are described.

EUMETSAT are beginning activities in 2021 towards a revised and improved algorithm for SLSTR SST with the intention of the operational implementation of SLSTR day-2 SST in early 2023. This will include improvements to the Bayesian cloud-screening in coastal zones. In addition, activities continue towards an operational implementation of sea-Ice Surface Temperature from SLSTR, and the evolutions and initial results from the prototype processor deployed in the EUMETSAT offline environment are described.

Further ongoing projects and evolutions relating to marine Surface Temperature at EUMETSAT are described.

### **INTRODUCTION**

The Sea and Land Surface Temperature Radiometer (SLSTR) flies onboard the European Commission's Copernicus Sentinel-3A and Sentinel-3B satellites, which were successfully launched on 16<sup>th</sup> February 2016, and 25<sup>th</sup> April 2018 respectively, with the mission to deliver high quality sea (and land) surface temperature (SST) data. S3A SLSTR SST products have been provided operationally since 5<sup>th</sup> July 2017, and S3B SLSTR SST products since 12<sup>th</sup> March 2019.

To ensure continued product quality, validation and monitoring activities are ongoing, and continually being updated to address (emerging) user needs and requirements. The report summarises the current product status, overviews ongoing and upcoming projects, and describes planned evolutions.

### **SEA SURFACE TEMPERATURE FROM SLSTR**

SLSTR skin SSTs [1] are designed to be accurate to 0.3K over the dual-view swath. The design of the SLSTR instrument [2] allows for dual-view skin SST retrievals in the central (offset) part of the swath (740km) and nadir-view only SST over the wide swath (1400km), at 1km spatial resolution [2].

S3 SLSTR SST product has the following status:

- Level-2 SST Processing Baseline i2r71-MARINE.

- Latest update on 14<sup>th</sup> December 2020 to resolve an issue in the calculation of the aerosol dynamic indicator (ADI) resulting in a small increase in the amount of pixels of quality level 5, as well as an update to the SLSTR-A SSES to compensate for an increase of the SLSTR-A Cold Finger Temperature that occurred on 14<sup>th</sup> October 2020.
- Information, including product notices, are available online from: <https://slstr.eumetsat.int>.

## ONGOING COPERNICUS SST PROJECTS AT EUMETSAT

**Towards Fiducial Reference Measurements (FRM) drifting buoy SST** nearly 150 drifting buoys for SST have been deployed as part of the TRUSTED project since 2019 with upgraded calibration and a higher specification towards SI-traceable standards. These improved drifting buoy SST measurements, plus additional measurements such as near-surface water pressure, contribute to the necessary FRM needed for the validation of high resolution, high accuracy satellite SST, such as from SLSTR. SLSTR validation activities are used to assess and establish the benefit of improved capability of HRSST-2 drifting buoys for satellite SST validation, in coordination with the international community including the Data Buoy Cooperation Panel (DBCP). Information is available online from: <https://www.eumetsat.int/TRUSTED>. For access to the TRUSTED dataset and matchup dataset with SLSTR SST this link can be followed: <https://s3calval.eumetsat.int/ma/sst/trusted/>. Information on the HRSST Task Team can be found from the GHRSSST Task Team moodle.

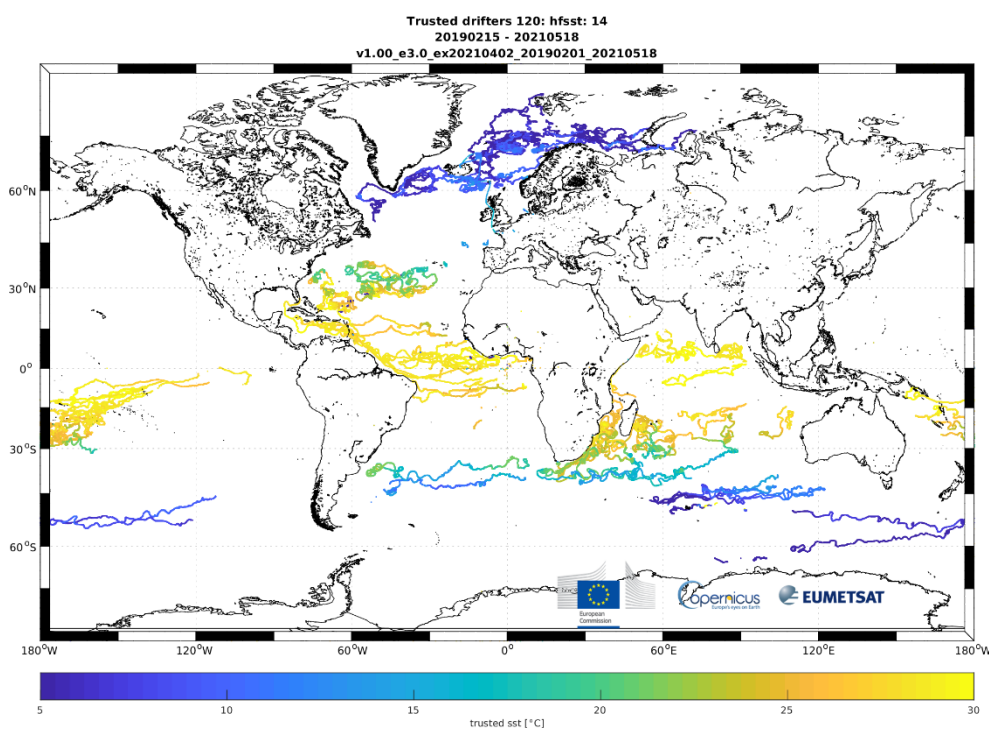


Figure 1. TRUSTED drifters Sea Surface Temperature

**GHRSSST Project Office** From August 2017-July 2021, the Copernicus funded GHRSSST Project Office was coordinated by the University of Leicester, continuing the era of supporting operational oceanography SST products. The activities will continue with the Danish Meteorological Institute (DMI) and Noveltis from July 2021 onwards [www.ghrsst.org](http://www.ghrsst.org).

**Evolution of a Bayesian Cloud Detection Scheme (BCDS):** A project with the University of Reading is due to end in summer 2021 on improving cloud detection in coastal regions for SLSTR Sea Surface Temperature <https://www.eumetsat.int/BCDS>.

## COMPLETED COPERNICUS SST PROJECTS

**SLSTR L0/1 monitoring and uncertainties** documentation, python tools and Look Up Tables (LUTs) to enable users to extract pixel level-1 thermal infrared and visible / Short-wave infrared uncertainties. <https://www.eumetsat.int/S3-TIR-uncertainties> (Rutherford Appleton Laboratory).

**SLSTR validation cloud processor** The incorrect identification of cloud is a significant source of uncertainty in SST products derived from infrared data. This project developed a cloud processing module at EUMETSAT to operate directly on the SLSTR matchup dataset, to enable further analysis of the efficiency of the cloud tests, enabling updates and evolutions contributing to improved user products (Deimos).

**SLSTR sea-ice surface temperature retrieval and validation** Accurate knowledge of the surface temperature is crucial information for surface and atmosphere energy balances and as input to operational forecasting models, however, the derivation and use of ice surface temperature from satellites is relatively new. The project derived and described the theoretical description of SLSTR sea-ice and marginal ice zone temperature (hereafter sea-IST) algorithms, provides a validation and quantitative assessment of the algorithms, documentation and prototype processor. A demonstrational SLSTR sea-IST processor is being implemented at EUMETSAT in 2021, with an operational version under preparation for 2023/2024. (DMI, Ifremer, Met.no, University of Leicester). Further information can be found here: <https://www.eumetsat.int/S3-SLSTR-SIST> and <https://www.eumetsat.int/prototype-processor-sea-ice-surface-temperature>.

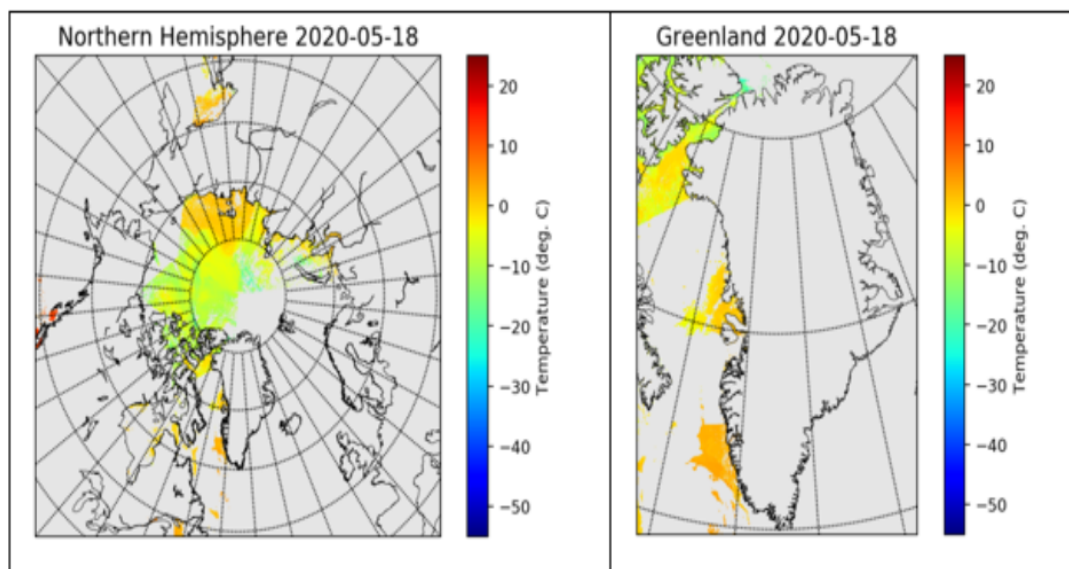


Figure 2 Level-3 plots of 6 hours of SLSTR IST data from May 18, 2020, showing the Arctic ocean and more (left) and Greenland and surrounding seas (right). SLSTR IST data are quality levels 2-5.

## SLSTR SST VALIDATION

**METIS-SST:** Validation activities include daily comparisons (<http://metis.eumetsat.int>) against Met Office Operational SST and sea ice analysis and Canadian Met Centre SST. The step change in the METIS time-series for SLSTR is due to the introduction of SLSTR SST as a reference sensor in OSTIA.

**SLSTR matchup dataset (MDB):** Validation of SLSTR SST against drifting buoys continue from assessment of the SLSTR matchup dataset and GHRSSST Task Team on MDBs <https://www.ghrsst.org/about-ghrsst/task-teams/>

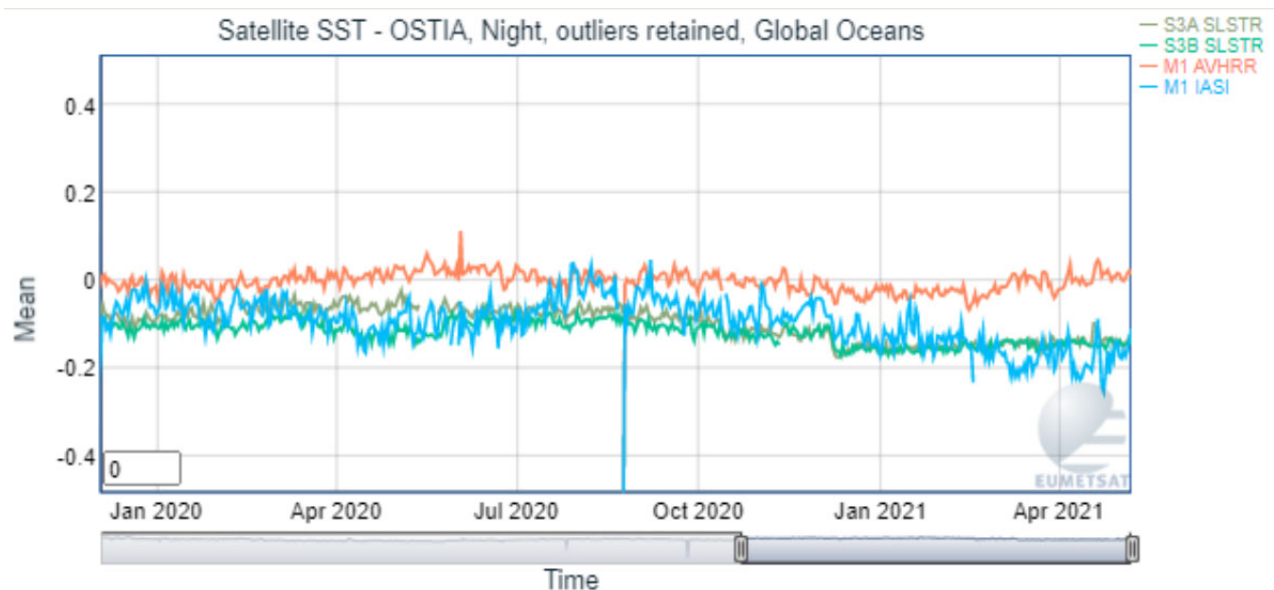


Figure 3. SLSTR L2P SST compared to OSTIA

### NEW COPERNICUS PROJECTS

**SST / IST project** (Noveltis, Meteo-France, Ifremer, Met.no, DMI, University of Reading) began in March 2021. Main activities are:

- day-2 SLSTR SST algorithm
- Evolution of Cal/Val tools and matchup datasets (MDB)
- GHRSSST Project Office

The operational implementation of the day-2 SLSTR SST algorithm and product is expected in 2023/2024. Activities will also be included on sea-IST algorithms and validation. Mechanisms for funding sea-IST Fiducial Reference Measurements are also being considered and planned.

**TIR inter-comparisons and validation with FRM radiometers** (KIT, University of Southampton) Inter-comparison of infrared satellite surface temperature products over Lake Constance with FRM from KIT and ISAR. An experiment took place in September 2020 and the analysis and project is due to end in 2021. <https://www.eumetsat.int/TIR-radiometer-inter-comparison>.

### SUMMARY

Operational Copernicus Sentinel-3 SLSTR SST products continue to be produced and distributed by EUMETSAT and are of very good quality with the dual-view SSTs able to be used as a reference sensor. The product notices should be read by users and are available from <https://slstr.eumetsat.int>. Developments are in progress towards sea-ice surface temperature from SLSTR. Validation activities continue to ensure product quality and several projects are ongoing and beginning to develop improvements for the products.

### REFERENCES

- [1] O'Carroll, A.G., H. Bonekamp, F. Montagner, V. Santacesaria, I. Tomazic, 2015: Sea Surface Temperature from EUMETSAT including Sentinel-3 SLSTR, Proceedings of Sentinel-3 for Science Workshop, Venice, June 2015, ESA SP-734, ISBN 978-92-9221-298-8
- [2] Donlon, C.J., B. Berruti, A. Buongiorno et al, The Global Monitoring for Environment and Security (GMES) Sentinel-3 mission, RSE, 120 (2012), 37-57

## S5-P6: UPDATES OF AMSR3 ON GOSAT-GW AND ITS OCEAN PRODUCTS

**Misako Kachi<sup>(1)</sup>, Naoto Ebuchi (1)(2), Akira Shibata (3), Rigen Shimada (1), Takashi Maeda (1), Hideyuki Fujii (1), Kenichi Ohara (1), Eri Yoshizawa (1), Marehito Kasahara (4), Kazuya Inaoka (4), and Yoasushi Kojima (4)**

(1) JAXA Earth Observation Research Center, Tsukuba, Japan, Email: [kachi.misako@jaxa.jp](mailto:kachi.misako@jaxa.jp)

(2) Hokkaido University, Sapporo, Japan

(3) Remote Sensing Technology Center of Japan, Tsukuba, Japan

### INTRODUCTION

The 3rd generation of Advanced Microwave Scanning Radiometer (AMSR) series, called AMSR3, will be carried on the Global Observation SATellite for Green-house gases and Water cycle (GOSAT-GW) and is currently under development to be launched in Japanese Fiscal Year (JFY) of 2023. The Preliminary Design Review (PDR) of satellite system including AMSR3 was completed in March 2021. Sensor characteristics and channel set of AMSR3 will be almost equivalent to that of AMSR2 except additional channels in X- and G-band and some change in Ka-band to avoid possible future risk caused by the new 5G communication. Additional channels in X-band (10.25-GHz) will have wider bandwidth with finer NEDT than original 10.65-GHz channels for more robust SST in higher resolution. New G-band channels will contribute to snowfall retrievals and numerical weather prediction. Two ocean products, multi-band SST and all-weather sea surface wind speed, was upgraded to standard product while they are research products in AMSR2. The recent status in development of AMSR3 hardware and algorithms are introduced

### HISTORY OF AMSR SERIES

JAXA has operated a series of passive microwave imagers shown in Table 1. With experience of development and operation of MSR, JAXA developed the 1st generation of AMSR (AMSR and AMSR-E) with large antenna size and C-band channels. AMSR-E continuous its science observation about 9.5-year, and its high capabilities enable to expand utilizations in operational and research areas. The 2nd generation of AMSR (AMSR2) was launched in 2012 and succeeds AMSR-E observations to establish its data utilization in various areas. The 3rd generation of AMSR (AMSR3) is being developed and to be launched in JFY2023.

Sensor	MOS-1/ MSR	ADEOS-II/ AMSR	Aqua/ AMSR-E	GCOM-W/ AMSR2	GOSAT-GW/ AMSR3
Launch	1987	2002	2002	2012	JFY2023
Coverage	Direct receive only	Global			
Swath	317km	1600km	1450km	1617km	> 1530km
Frequencies (GHz)	2 (23,31)	9 (6.9,10,18,23, 36,50,52,89)	6 (6.9,10,18,23,36, 89)	6 (6.9/7.3,10.65,18, 23,36, 89)	8 (6.9/7.3, 10.25/10.65,18,23,36 ,89,166,183)
Polarization	Mixed V and H	V and H	V and H	V and H	V and H (166/183 are V only)
Antenna Size	0.5m	2.0m	1.6m	2.0m	2.0m
Spatial Res.	23km@31GHz	8x14km@36GHz	8x14km@36GHz	7x12km@36GHz	7kmx11km@36GHz

Table 1: Improvements of Sensor Specifications of JAXA's Passive Microwave Imagers

### AMSR2 SENSOR DEVELOPMENT

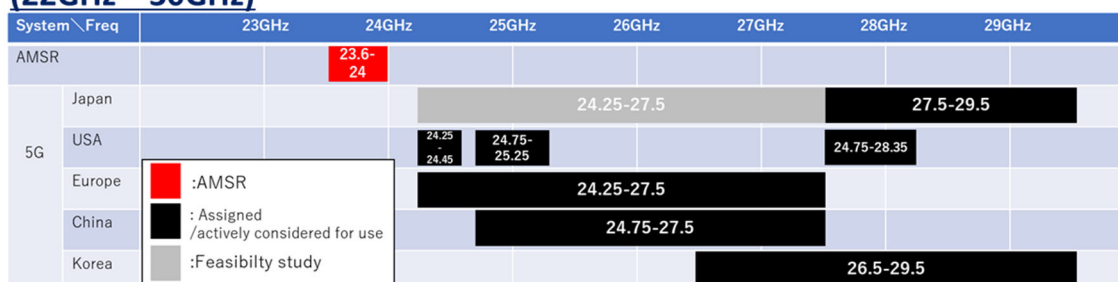
The Preliminary Design Review (PDR) of GOSAT-GW satellite system including AMSR3 was completed in Mar. 2021. Currently, JAXA is being coordinated major characteristics and performances of new G-band and conducted manufacture and test of engineering models of AMSR3 component, for example, G-band antenna sub-system, Receivers.

Sensor specification of AMSR3 is slightly changed from that of AMSR2 (Table 2). Channels of 10.25, 165.5, 183+7, 183+3 GHz are newly added to AMSR2 channels.

Center frequency [GHz]	Polarization	Band width [MHz]	NEDT (1σ)	Beam width (spatial resolution)
6.925 / 7.3	H/V	350	< 0.34 K	1.8° (34km x 58km)
<b>10.25</b>	<b>H/V</b>	<b>500</b>	<b>&lt; 0.34 K</b>	<b>1.2° (22km x 39km)</b>
10.65	H/V	100	< 0.70 K	1.2° (22km x 39km)
18.7	H/V	200	< 0.70 K	0.65° (12km x 21km)
23.8	H/V	400	< 0.60 K	0.75° (14km x 24km)
<b>36.42</b>	<b>H/V</b>	<b>840</b>	< 0.70 K <b>(TBD)</b>	0.35° (7km x 11km)
89.0 A/B	H/V	3000	< 1.20 K	0.15° (3km x 5km)
<b>165.5</b>	<b>V</b>	<b>4000</b>	<b>&lt; 1.50 K</b>	<b>0.3° (6km×10km)</b>
<b>183.31±7</b>	<b>V</b>	<b>2000×2</b>	<b>&lt; 1.50 K</b>	<b>0.28° (5km×9km)</b>
<b>183.31±3</b>	<b>V</b>	<b>2000×2</b>	<b>&lt; 1.50 K</b>	<b>0.28° (5km×9km)</b>

Table 2: AMSR3 Channel Sets (as of Mar. 2021). Bold indicates changes from AMSR2.

#### (22GHz ~ 30GHz)



#### (33GHz ~ 41GHz)



Figure 1: AMSR3 and 5G Allocated Frequencies. For 24.0-24.25 GHz, AMSR3 and 5G frequencies have a buffer band of 250 MHz. On the other hand, AMSR3 and 5G frequencies are adjacent to each other with no buffer band for 36-37 GHz. Its impact cannot be avoided by improving the out-of-band frequency characteristics while maintain the bandwidth.

As shown in Table 2, we will also modify specification of Ka-band (36 GHz) passband to reduce the future risk of RFIs from the 5th Generation Mobile Communications System (5G) to reduce possible impacts on 36 GHz channels. As a result of the allocation of new frequency bands for 5G at WRC-19, the frequencies used in the 23 GHz and 36 GHz bands of the AMSR series were close or adjacent to those of 5G. Figure 1 is a schematic view of frequency allocations for AMSR3 and 5G.

After impact evaluation, the bandwidth, which will affect NE $\Delta$ T of 36 GHz band needed to be narrowed to avoid the influence of 5G. Its impact on 23 GHz will be negligible by improving the out-of-band frequency characteristics. Under the study to minimize the reduced bandwidth, that of 36 GHz was changed from 1000MHz to 840 MHz with confirmation of algorithm developers and related users. Value of temperature resolution will remain unchanged, but with TBD, and will be fixed with critical design results.

We plan to hold the Critical Design Review (CDR) of AMSR3 in the first half of JFY2021, and completion of AMSR3 development is scheduled in the second half of JFY2022 for launch of the GOSAT-GW satellite in JFY2023.

### NEW OCEAN PRODUCTS TOWARD AMSR3

The GCOM-W project has released several ocean research products recently.

New multi-band SST using 6.9, 7.3 and 10.65 GHz channels to retrieve SST was released in Oct. 2020. Figure 2 is an example of multiband SST in comparison with standard SST. It is stored in the same HDF5 file of standard SST product distributed from the JAXA G-Portal (<https://gportal.jaxa.jp/gpr/>), and also available in GDS2.0 format via the JAXA GHRSSST server (<https://suzaku.eorc.jaxa.jp/GHRSSST/>). Missing pixels due to RFIs are reduced in multi-band SST and missing areas around the coast are also reduced by combining different channels. So, multi-band SST can be estimated more closer to the coast. It will be standard product in AMSR3 era.

Figure 3 is an example of new sea ice concentration product. High-resolution sea ice concentration using 89-GHz channel with 5-km resolution over the Northern Hemisphere was also released in Apr. 2021 via the GCOM-W Research Product Distribution Service ([https://suzaku.eorc.jaxa.jp/GCOM\\_W/research/resdist.html](https://suzaku.eorc.jaxa.jp/GCOM_W/research/resdist.html)). Standard sea ice concentration product is using 18 and 36 GHz channels and spatial resolution is about 15-km. Though 89 GHz channels are more affected by clouds and rain, high-resolution sea ice concentration is expected to contribute in ship navigation especially near the ice edge. The product for the Southern Hemisphere is under development for future release. This product will be standard product in AMSR3 era.

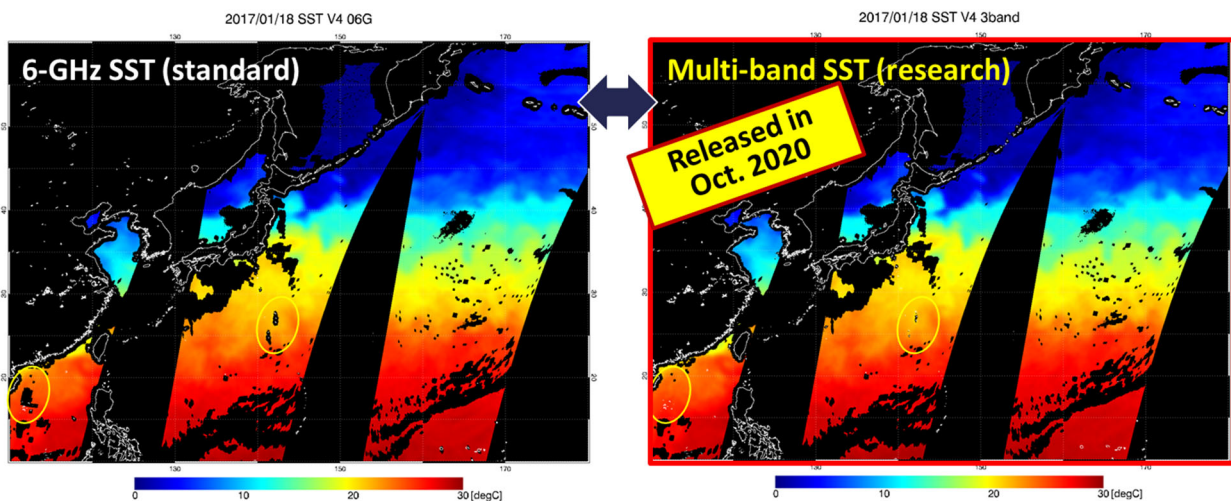


Figure 2: AMSR2 Multi-band SST Ver.1. (Right) Example of AMSR2 6-GHz (standard) SST Ver.4 around Japan on Jan. 18, 2017. (Left) Same as right but for AMSR2 Multi-band SST Ver.1.

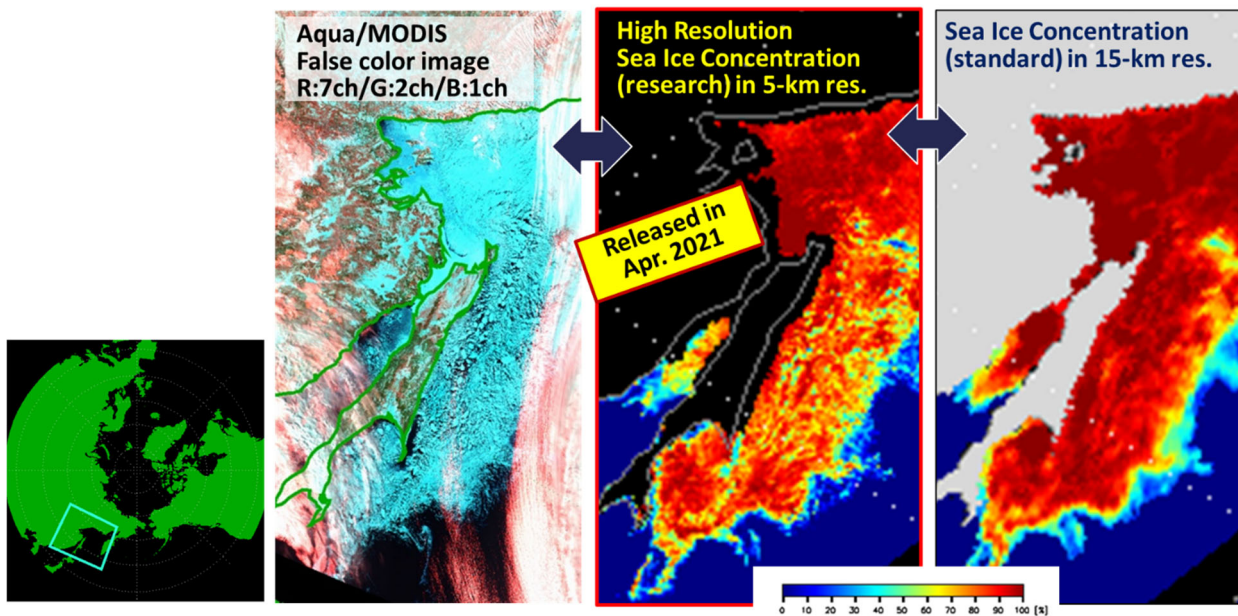


Figure 3: AMSR2 High Resolution Sea Ice Concentration Ver.1. From right to left, target area (blue box) in the Arctic, close-up of target area by Aqua/MODIS false color image using Ch7, Ch2, and Ch1 for RGB, AMSR2 high-resolution sea ice concentration Ver.1 and AMSR2 standard sea ice concentration Ver.3 on Mar. 16, 2016.

### DEVELOPMENT OF NEW HIGH-RESOLUTION SST (HST)

To produce SST in higher spatial resolution in AMSR3, spatial resolution enhancement algorithm (Maeda, 2019) was developed to produce high-resolution brightness temperature product (L1H) that is used as input to produce High-resolution SST (HST). Figure 4 is a processing flow of standard SST and HST (Maeda et al., 2021).

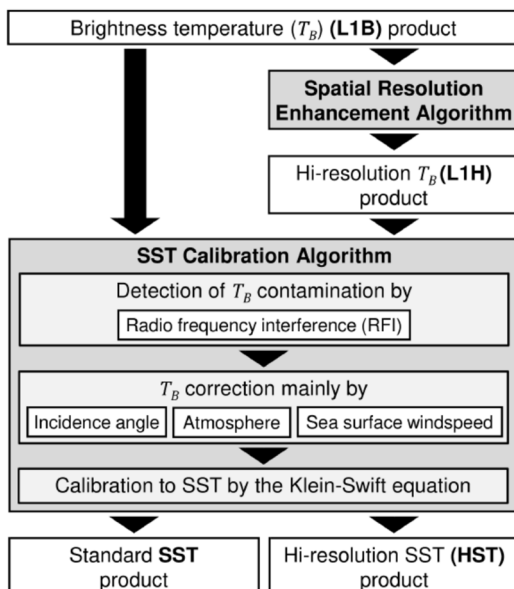


Figure 4: Processing flow chart of standard SST and high-resolution SST (HST) (Maeda et al., 2021).

Figure 5 is an example of HST product in comparison with standard SST for 6 GHz channels. When we use AMSR2 6 GHz brightness temperature from L1H, we can produce HST at 30 km resolution where original resolution of 6-GHz is 35x62 km. HST can estimate SST closer to the coast less than 30 km, while validation with iQuam buoys shows equivalent accuracy to standard SST less than 0.5 degC (Maeda et al., 2021).

The same algorithm will be applied to 10 GHz channels to produce 20-km resolution SST.

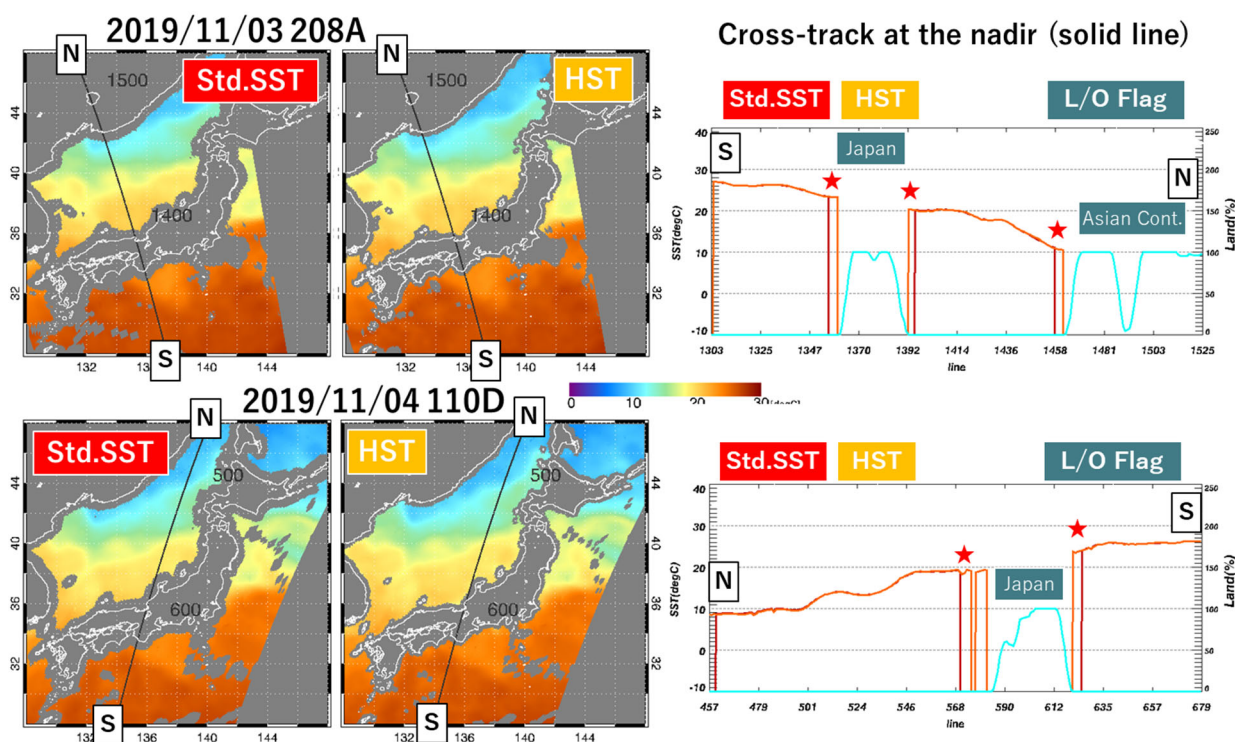


Figure 5: Comparison of standard SST and high-resolution SST (HST) around Japan. (Upper) Case for path No. 208/Ascending on Nov. 3, 2019. (Lower) Case for path No. 110/Descending on Nov. 4, 2019. Modified from Maeda et al. (2021).

## CONCLUSION

Recent status of development of AMSR3 instrument and ocean algorithms are introduced. In AMSR3, several ocean related products, multi-band SST, high-resolution sea ice concentration, and all-weather sea surface wind speed, which are research products in AMSR2, are defined as standard products. In addition, development of high-resolution brightness temperature and SST products in 20-km spatial resolution are underway for AMSR3. Addition of 10.25 GHz in AMSR3 will provide robustness in retrieval and RFI impact to produce high-resolution SST. Updates of algorithms are ongoing to be ready for the launch of the GOSAT-GW satellite in JFY2023.

## REFERENCES

- Maeda, T., Spatial Resolution Enhancement Algorithm Based on the Backus–Gilbert Method and Its Application to GCOM-W AMSR2 Data, *IEEE Trans. Geoscience Remote Sens.* **58** (4), 2809-2816, doi:10.1109/TGRS.2019.2955967, 2019.
- Maeda, T., N. Tomii, M. Seki, K. Sekiya, Y. Taniguchi, and A. Shibata, Validation of Hi-Resolution Sea Surface Temperature Algorithm Toward the Satellite-Borne Microwave Radiometer AMSR3 Mission, *IEEE Geoscience Remote. Sens. Letters.* doi:10.1109/LGRS.2021.3066534, 2021.

## S5-P7: PRESENTING A NEW HIGH-RESOLUTION CLIMATE DATA RECORD PRODUCT

**Mark Worsfold<sup>(1)</sup>, Simon Good<sup>(2)</sup>, Owen Embury<sup>(3)</sup>**

(1) UK Met Office FitzRoy Road, Exeter, Devon, EX1 3PB, UK, Email: [mark.worsfold@metoffice.gov.uk](mailto:mark.worsfold@metoffice.gov.uk)

(2) UK Met Office FitzRoy Road, Exeter, Devon, EX1 3PB, UK, Email: [simon.good@metoffice.gov.uk](mailto:simon.good@metoffice.gov.uk)

(3) University of Reading, Department of Meteorology, Meteorology Building, Earley Gate, Reading, RG6 6ET, UK. Email: [o.embury@reading.ac.uk](mailto:o.embury@reading.ac.uk)

### INTRODUCTION

The near real time OSTIA SST production system is continuously upgraded, and therefore historical data will not be consistent with newer data. To address this, we announce a new level 4 reprocessed foundation SST product generated using the OSTIA system as part of the Copernicus Marine Environment Monitoring Service.

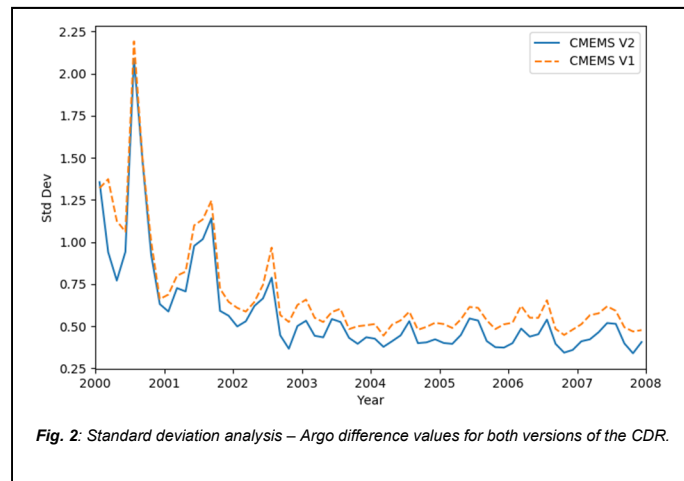
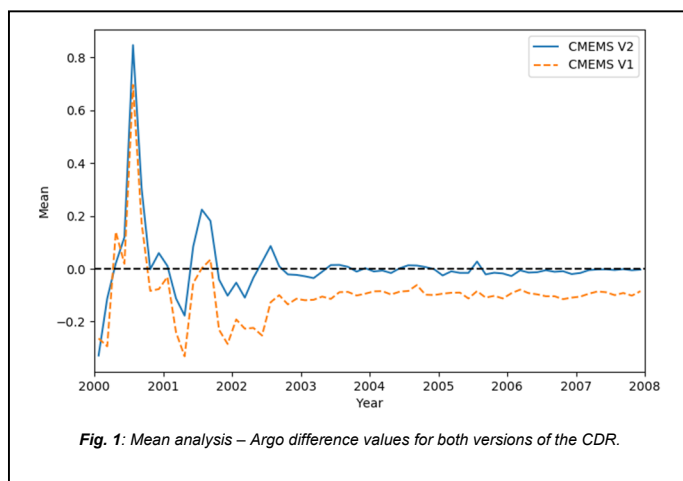
This reprocessed product aims to serve users of the near real time OSTIA data who want a consistently processed dataset going back in time. This second version of the CMEMS OSTIA reprocessing replaces the previous version which spanned the period 1985-2007 (Robert-Jones 2012). V2.0 spans 1981-2020 and will be updated twice-yearly with 6-month delay. It also incorporates data from a wider range of instruments than previously, and uses the data recently generated by the ESA SST CCI and C3S projects.

We discuss the accuracy and feature resolution of the new product compared to the previous dataset.

### VALIDATION AND COMPARING THE TWO VERSIONS.

Both analyses were compared to Argo float data which are only available from 2000 onwards. The V1 dataset extends to 2007, therefore our validation is for the period 2000-2007.

The time series plot of the mean analysis – Argo differences (**Fig. 1**) indicate that V1 has a colder bias. V2 has lower standard deviation and bias values (**Fig. 2**).



### CONCLUSION

The increased variety of input datasets and upgrades to the analysis system have allowed V2 to demonstrate a clear improvement over V1 in terms of the mean and standard deviation of differences to Argo data. The low bias values also indicate the V2 provides an accurate representation of SST values. This dataset and its documentation is readily available for download from CMEMS:

[https://resources.marine.copernicus.eu/?option=com\\_csw&view=details&product\\_id=SST\\_GLO\\_SST\\_L4\\_REP\\_OBSERVATIONS\\_010\\_011](https://resources.marine.copernicus.eu/?option=com_csw&view=details&product_id=SST_GLO_SST_L4_REP_OBSERVATIONS_010_011)

## REFERENCES

J. Roberts-Jones, K. Fiedler, M. Martin (2012). Daily, Global, High-Resolution SST and Sea Ice Reanalysis for 1985–2007 using the OSTIA System. *Journal of Climate*, 6215–6232, DOI: <https://doi.org/10.1175/JCLI-D-11-00648.1>

## S5-P8: FILTERING COLD OUTLIERS IN NOAA AVHRR SST FOR ACSPO GAC RAN2

**Boris Petrenko<sup>(1)</sup>, Victor Pryamitsyn<sup>(2)</sup> and Alex Ignatov<sup>(3)</sup>**

- (1) NOAA STAR, GST, Inc., USA, Email: boris.petrenko@noaa.gov  
(2) NOAA STAR, GST, Inc., USA, Email: victor.pryamitsyn@noaa.gov  
(3) NOAA STAR, USA, Email: alex.ignatov@noaa.gov

### INTRODUCTION

A quality record of global SST since 1981-present is being created from 4 km NOAA AVHRR/2 and /3 GAC data under the NOAA AVHRR GAC Reanalysis (RANs) project [1-3]. The initial reprocessing of the AVHRR data (RAN2 Beta01; RAN2 B01, for short) had revealed periodic contaminations of retrieved SST with cold and warm outliers, originating from two sources.

- The AVHRR sensors of all satellites are occasionally exposed to the direct sunlight when the satellite approaches the terminator from the dark side of the Earth. The Sun impingements on the Earth view sensor causes warm SST outliers, whereas the exposures on the black body calibration target gives rise to cold outliers.
- Massive cold outliers also appeared in NOAA-07, -11 and -12 SSTs when the atmosphere was contaminated with the volcanic aerosol after major volcanic eruptions of Mt. El Chichon (1982), Mt. Pinatubo and Mt. Hudson (1991).

During the earlier phase of the project (RAN2 B01), a set of sensor-specific filters was implemented in the NOAA Advanced Clear Sky Processor for Ocean (ACSPO) Clear-Sky Mask (ACSM) to screen out warm SST outliers [2]. This documents describes the methods developed during RAN2 B02 to mitigate cold SST outliers:

- Accounting for the latitudinal structure of the concentration of cold SST outliers.
- Correction of the nighttime L1B calibration coefficients, which mitigates the effects of Sun impingement on the black body calibration target.

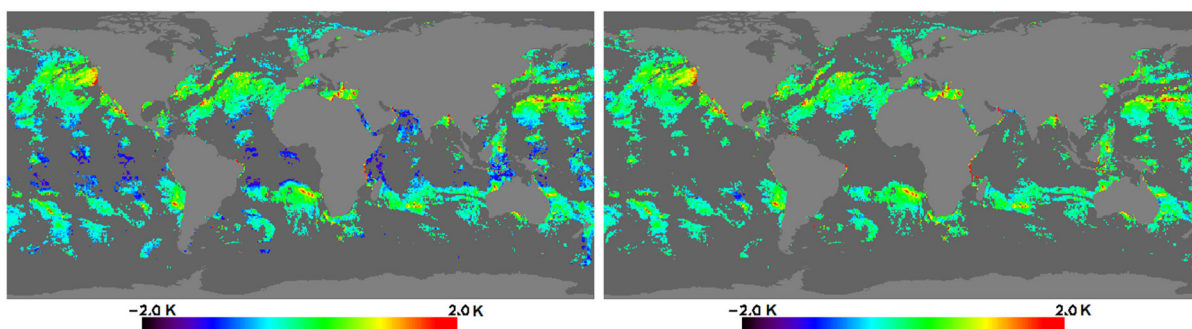


Figure 1: Daytime GR - CMC SST retrieved from NOAA-11 on 30 Sep 1991, after the Mt. Pinatubo and Mt. Hudson eruptions, with (left panel) the initial ACSM and (right panel) the latitude-dependent ACSM.

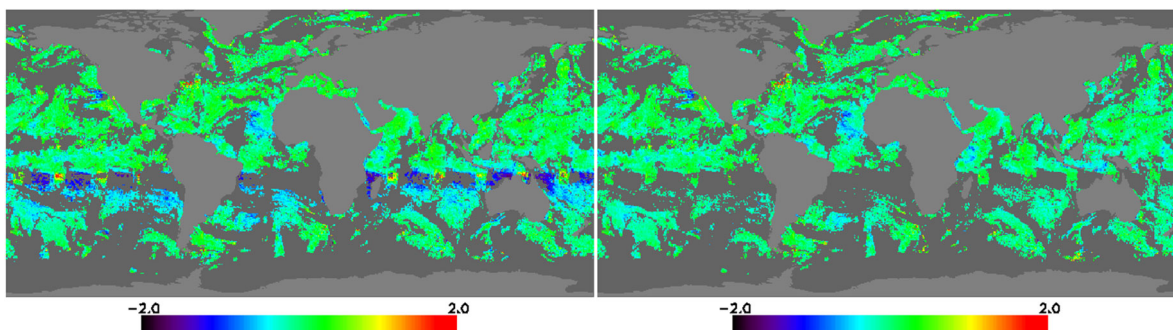


Figure 2: Nighttime GR - CMC SST retrieved from NOAA-16 on 14 Nov 2006, with (left panel) the initial ACSM and (right panel) the latitude-dependent ACSM.

### RAN2 B02: ACCOUNTING FOR THE LATITUDINAL STRUCTURE OF COLD SST OUTLIERS

A common feature of the cold SST outliers, both originating from the calibration issues and caused by the volcanic aerosol, is that they concentrate in specific latitudinal bands. The RAN2 B02 mitigation algorithm works as follows:

- All-sky histograms of Global Regression (GR) SST – Analysis L4 SST are accumulated within 5° latitudinal bands and the locations of their maxima,  $T_M$ , are estimated.
- Contaminated latitudinal bands are identified by colder  $T_M$ 's.
- Based on  $T_M$ 's, the ACSPO clear-sky mask (ACSM) [4] is adjusted more conservatively in the contaminated latitudinal band.

Figure 1 shows the deviations of the ACSPO GR SST, produced with the initial and the latitude-dependent ACSMs, from the L4 SST by the Canadian Meteorology Center (CMC) [5]. Data are from NOAA-11 on 30 Sep 1991, when the atmosphere was contaminated with volcanic aerosol from eruptions of Mt. Pinatubo and Mt. Hudson. Figure 2 additionally compares results of applying the two ACSMs to the GR SST retrieved from NOAA-16 on 14 Nov 2006. In both cases, the latitude-dependent ACSM significantly improves filtering of massive cold SST outliers in the contaminated latitudinal bands, while preserving a low false cloud detection rate in the unaffected areas.

### TOWARDS RAN2 B03: CORRECTION OF L1B CALIBRATION COEFFICIENTS

The most prominent calibration errors in the thermal AVHRR bands are caused by Sun impingement on the black body calibration target at night [6,7]. The areas where the AVHRR black body can be exposed to sunlight are identified by the increased signal in the AVHRR reflectance bands, as shown in Figure 3. The radiances in the AVHRR/3 thermal channels,  $R$ 's, are calculated from the following equation:

$$R = a + b\Delta + c\Delta^2$$

Here,  $\Delta$  is Earth view count minus the space view count,  $a$ ,  $b$  and  $c$  are band-specific calibration coefficients. Sun impingement on the black body causes abnormal variations in L1B calibration coefficients, as shown in Figure 4, which, in turn, results in erroneous  $R$ 's and retrieved SSTs (as shown in the left panel of Figure 2). We mitigate the artifacts by interpolating the calibration coefficients between the closest unaffected (or least affected) parts of the orbit. As shown in Figure 3 (right panel), the replacement of the erroneous calibration coefficients with interpolated values eliminates cold SST outliers, even without applying the latitude-dependent ACSM.

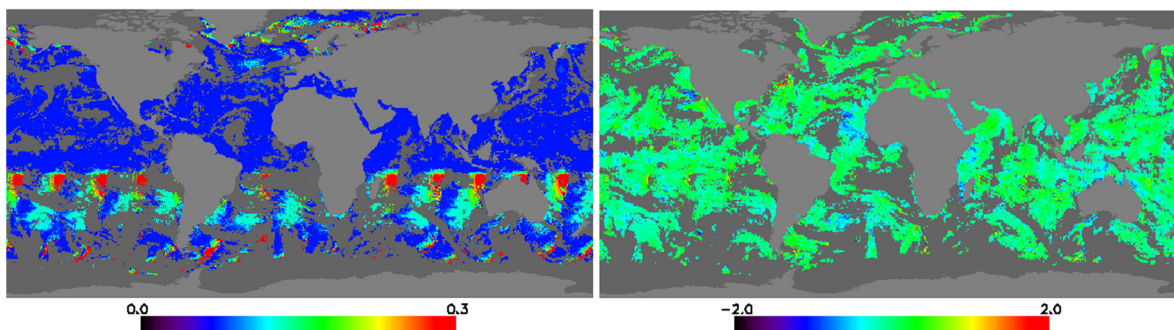


Figure 3. Left panel: Nighttime signal in NOAA-16 AVHRR Ch2 (0.85  $\mu\text{m}$ ) on 14 Nov 2006, identifies areas where Sun impinges on the AVHRR Earth view, and on the black body calibration target. These two factors offset each other, and

their relative contribution determines the net effect on the BTs in thermal AVHRR bands, and the signs of the corresponding SST outliers (cf. left panel in Figure 2). Right panel: Daytime GR - CMC SST retrieved from NOAA-16 on 14 Nov 2006, with the initial ACSM after correction of calibration coefficients.

By present, we have explored the correction of the L1B calibration coefficients for the AVHRR/3 sensors onboard NOAA-15, -16, -17 -18 and -19. Figs. 5 and 6 demonstrate the effect of this correction with the fragments of daily latitudinal Hovmöller diagrams of deviations of the ACSPO GR SST from in situ SST, produced from NOAA-16 and -18 AVHRRs. For comparison, Figs. 5 also shows the result of applying the latitude-dependent ACSM to the GR SST retrievals from the original L1B data.

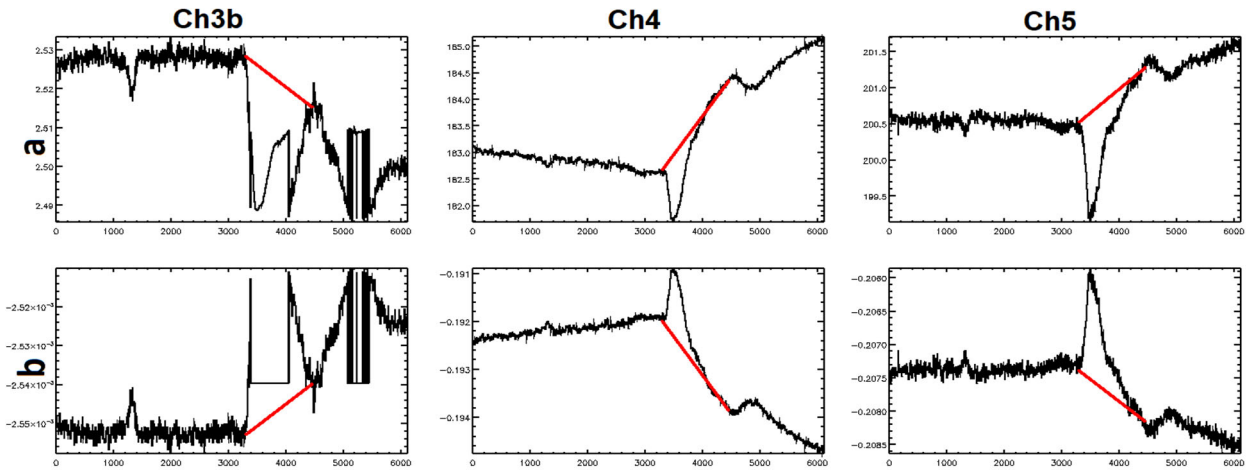


Figure 4. **Black:** Original L1b calibration coefficients in the NOAA-16 AVHRR thermal bands as a function of scan line on one descending half-orbits on 14 Nov 2006. **Red:** The interpolation mitigates the abnormal variations in the calibration coefficients.

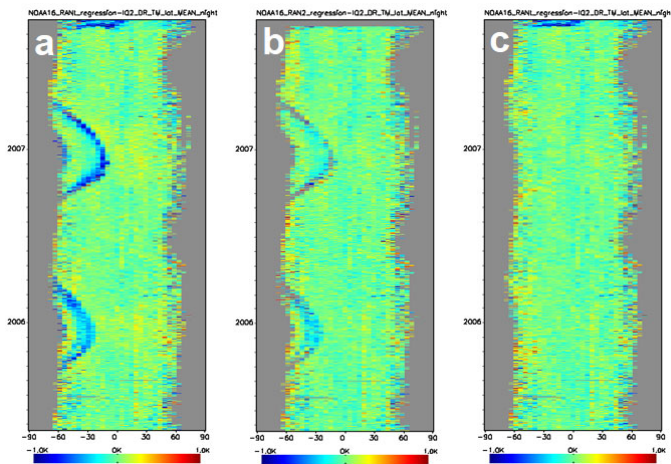


Figure 5. Daily latitudinal Hovmöller diagrams of NOAA-16 ACSPO GR – in situ SST, produced from: (a) original AVHRR L1B data with the original ACSM; (b) original L1B and latitude-dependent ACSM; (c) re-calibrated L1B data and original ACSM.

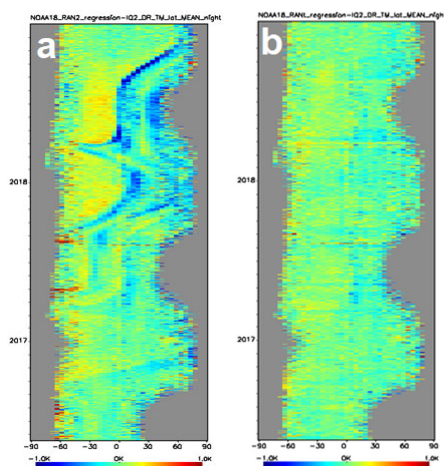


Figure 6. Daily latitudinal Hovmöller diagrams of NOAA-18 ACSPO GR – in situ SST in 2016-2018, produced from: (a) original AVHRR L1B data with the original ACSM; and (b) re-calibrated L1B data with original ACSM.

In 2005-2007, the orbit of the NOAA-16 satellite periodically approached the terminator from the dark side of the Earth. In those cases, the cold SST outliers took shapes of arches covering certain latitudinal bands during specific periods on the Hovmöller diagram, as shown in Figure 5a. The latitude-dependent ACSM filtered the cold SST outliers, thus reducing the clear-sky domain within the affected latitudinal bands (Figure 5b). In Figure 5c, the correction of the calibration coefficients completely eliminated the cold outliers without reducing the clear-sky domain.

In 2016-2018, the NOAA-18 satellite flew practically along the terminator, which is why the cold SST outliers formed irregular curves in the Hovmöller diagram (Figure 6a). In Figure 6b, the correction of L1B calibration coefficients efficiently mitigated the manifestations of cold SST outliers without reducing the clear-sky domain.

## SUMMARY AND FUTURE WORK

We have developed two efficient methods for mitigation of massive cold outliers in SST retrieved from the AVHRR data and applied them during historical reprocessing of AVHRR GAC (RAN2 B02):

- Modification of the ACSPO clear-sky mask based on the latitudinal dependency of the concentration of cold outliers
- Correction of L1B calibration coefficients

The future work will include:

- Correction of the AVHRR/2 L1B calibration coefficients and reprocessing of NOAA-7/-9/-11/-12/-14 data
- The release of the final RAN2 AVHRR GAC record for 1981-present is planned by the end of 2021
- Correction of METOP-A/-B/-C AVHRR FRAC L1B calibration coefficients and creating the next iteration of the Metop FRAC RAN data set [8]

## REFERENCES

- [1] Ignatov, A., Zhou, X., Petrenko, B., Liang, X., Kihai, Y., Dash, P., Stroup, J., Sapper, J. and DiGiacomo, P., *Remote Sensing*, **8**, 315 (2016), doi: 10.3390/rs8040315.
- [2] Petrenko, B., Pryamitsyn, V., Ignatov, A., and Kihai, Y., *Proc. SPIE 11420, Ocean Sensing and Monitoring XII*, 1142004 (30 June 2020); doi: 10.1117/12.2558660.

- [3] Pryamitsyn, V., Petrenko, B., Ignatov, A., Jonasson, O., and Kihai, Y. Proc. SPIE 11420, Ocean Sensing and Monitoring XII, 1142005 (18 May 2020); doi:10.1117/12.2558751.
- [4] Petrenko, B., Ignatov, A., Kihai, Y., and Heidinger, A., JTECH, **27**, 1609–1623 (2010), doi: 10.1175/2010JTECHA1413.1.
- [5] Brasnett, B. and Surcel Colan, D., JTECH, **33**, 361-375, doi: 10.1175/JTECH-D-15-0093.1 (2016).
- [6] Cao, C., Weinreb, M., and Sullivan, J., JGR, **106**, D24, 33,483-33,469 (2001).
- [7] Trishchenko, A.P., Fedoseevs, G., Li, Z., and Cihlar, J., JGR, **107**, D24, 4778, doi: 10.1029/2002JD002353 (2002).
- [8] Pryamitsyn, V., Petrenko, B., Ignatov, A., Jonasson, O., and Kihai, Y., Proc. SPIE 11752, Ocean Sensing and Monitoring XIII, 1175204 (12 April 2021); doi: 10.1117/12.2585893.



**GHRSSST**  
GROUP FOR HIGH RESOLUTION  
SEA SURFACE TEMPERATURE

The GHRSSST Project Office is funded by the European Union Copernicus Programme and is hosted by the Danish Meteorological Institute, Lyngbyvej 100, 2100 Copenhagen (DK)

E-mail:

Chiara Bearzotti, Project Coordinator, [gpc@ghrsst.org](mailto:gpc@ghrsst.org)

Pia Wind, Project Administrator, [gpa@ghrsst.org](mailto:gpa@ghrsst.org)



Follow us on Twitter: <https://twitter.com/ghrsst>

Website: <https://www.ghrsst.org/>

Zenodo: <https://zenodo.org/communities/ghrsst>



**Copyright 2021© Group for High Resolution Sea Surface Temperature (GHRSSST)**

This report has been edited by the GHRSSST Project Office.

This copyright notice applies only to the overall collection of papers: authors retain their individual rights and should be contacted directly for permission to use their material separately. Editorial correspondence and requests for permission to publish, reproduce or translate this publication in part or in whole should be addressed to the GHRSSST Project Office. The papers included comprise the proceedings of the meeting and reflect the authors' opinions and are published as presented. Their inclusion in this publication does not necessarily constitute endorsement by GHRSSST or the co-organisers.

AGENCY NEWS



## Agency News

**Chair** : Toshiyuki Sakurai, Office of Marine Prediction, Atmosphere and Ocean Department, Japan  
Meteorological Agency  
Email: [tsakurai@met.kishou.go.jp](mailto:tsakurai@met.kishou.go.jp)

**Rapporteur** : Dorina Surcel-Colan, Canadian Centre for Meteorological and Environmental Prediction,  
Canada  
Email: [dorina.surcel-colan@ec.gc.ca](mailto:dorina.surcel-colan@ec.gc.ca)

The 22<sup>nd</sup> GHRSSST meeting included a session where representatives of 20 participating agencies have contributed with reports of their agency's activities over the last year. This report contains a brief overview of each report and the questions and discussions arising during the forum session.

### Highlights

- Migration of all GHRSSST data from PODAAC on the cloud using Amazon Web Services (AWS) - final by 2025.
- iQUAM improvements underway, increased number of products monitored in SQUAM.
- AMSR2 high-resolution sea ice concentration data available from July 2012 to present for the Arctic.
- Representatives of 20 participating agencies demonstrated wealth of available GHRSSST data with continuous and ongoing improvements.

### Resources

---

The discussion forum on the agency reports can be found on the EUMETSAT Moodle  
<https://training.eumetsat.int/mod/forum/view.php?id=14066>

Armstrong, Ed, Huai-Min Zhang, John, Ignatov, Alexander, Beggs, Helen, Wang, Sujuan, Surce-Colan, Dorina, Buongiorno Nardelli, Bruno, O'Carroll, Anne, Piolle, Jean-Francois, Kachi, Misako, Sakurai, Toshiyuki, Good, Slmon, McKenzie, Bruce, Maturi, Eileen, Shi, Lijian, Saux-Picart, Stephane, & Donlon, Craig. (2021, September 29). News from GHRSSST contributing Agencies: Report to the GHRSSST 22nd Science Team Meeting. Zenodo. <https://doi.org/10.5281/zenodo.5537084> (full slide deck with inputs of all agencies)

### GHRSSST system Components: GDAC

---

Ed Armstrong presented the statistics for the last five years in term of number of user, volume of data and number of files accessed and used from different platforms of GDAC. The main point is the migration of all data to the cloud.

Alexander Ignatov asked about the number of unique users which declined in 2019, while the number of files and GB have increased. This happened in the same time with the retire of ftp and the introduction of PO.DAAC Drive. The PO.DAAC Drive allows the better accounting of independent users?

Bruce McKenzie said that NAVO is currently acquiring from the PO.DAAC the OSISAF MSG 1/4 SEVIRI L3C. Is there a cutoff date that they have to move the data access to the cloud?

During the live session Ed Armstrong mentioned October 2025 as date when all data will be available only on Cloud.

### **GHRSSST system Components: LTSRF**

Huai-Min Zhang presented the list of new products achieved since G21 and statistics for the last five years in term of number of unique IP addresses, volume of data and number of files served. Updates and future work regarding the data acquisition and data access were also presented.

### **GHRSSST system Components: SST Quality Monitor (SQUAM) and in situ SST Quality Monitor (iQUAM)**

Alexander Ignatov mentioned in the report that work is underway to improve iQUAM. There is an increased number of products monitored in SQUAM which requires redesigning the back end which means a transition from old IDL scripts to Python, C++ and SQL database. Transitions of Polar SQUAM completed in 2020. The thermal fronts were added in ARMS.

After mentioning the nice updates to SQUAM and ARMS, Hellen Beggs asked about the plan in SQUAM to update the L4 time series plots to present (currently 25 Dec 2020). A. Ignatov answered apologizing for the incomplete series, but he mentioned they are overwhelmed with the coming 4 new launches in 2021-23 (G18, N21/J2, MTG and Metop-SG). He also said they will do the update depending on resources but without promising or having a deadline.

### **Australian Bureau of Meteorology, ABoM**



Helen Beggs presented the updates for GAMSSA and RAMSSA L4 analyses and for the L3U and L3S SST products from Bureau of Meteorology. The presentation also contains news from ISAR SST from RV Investigator and plans for the future.

Yukio Kurihara commented that he could not make any progress over the last year but he would like to compare SGLI SST v3 with ISAR and he will share the results when comparison is finished.

Helen Beggs replied that would be very nice if he could use the ISAR data to verify SGLI. She also suggested using other shipborne radiometer SST skin data available in L2R format from ships4sst.org. Hellen mentioned the possibility to use the ships4sst ship skin SST data for verifying SGLI and to look at the report of Werenfrid Wimmer during the Tuesday Task Team 2 session.

### **National Satellite Meteorological Center, CMA**



Sujuan Wang, representing CMA presented the modifications done to operational products and the plan for the next launches in 2021. The presentation also included the reprocessed SST for VIRR, the experimental products and evaluations against OSTIA and CMC.

Anne O'Carroll recognized the progress on activities and asked about the progress with the tests on FY3/VIRR and FY3D/MERSI in GHRSSST specification. The second question was about the launch period for FY3E and when the first test products are expected to be ready.

Sujuan Yang responded that only preliminary tests on FY3/VIRR reprocessing SST in GHRSSST specification have been done. FY3E is due for launch in July 2021 and the first test products are depended on the Post Launch Test.

## Canadian Meteorological Centre, CMC



---

Dorina Surcel Colan made a short presentation of CMC SST, summarized the CMC last year updates and the performance of the analysis against GMPE and OSTIA for 2020. The presentation contains also the plans for the next year.

## Copernicus Marine Environment Monitoring Service, CMEMS



---

Buongiono Nardelli presented the report for CMEMS SST TAC. They completed the integration of Sentinel 3B data in all processing chains and integrated new L4 products for the European Seas and Mediterranean/Black Seas. The ESA-CCI/C3S data was integrated in all processing chains and they updated the Ocean monitoring Indicators (OMI).

## EUMETSAT



---

Anne O'Carroll presented the updates for SLSTR data including the resolution of an issue in the calculation of the aerosol dynamic indicator and update of SSES for SLSTR S3A. The reprocessing of IASI L2P data will be ready by the end of 2021. The last part focused on the projects conducted by EUMETSAT and Copernicus Surface Temperature.

## Ifremer



---

Jean-Francois Piollé delivered the report from Ifremer. There were changes to the production line and changes in the distribution and collection of data as GDAC. The presentation contained also the upgrade of different datasets and new services for Metop data.

## Japan Aerospace Exploration Agency, JAXA



---

Misako Kashi presented the last updates for GCOM-C/SGLI, Himawari-8/AHI, GCOM-W/AMSR2 and the preparation work for GOSAT-GW/AMSR3 to be launched in JFY2023 (Apr. 2023 - Mar. 2024).

Toshiyuki Sakurai asked about the availability of high-resolution sea ice concentration data (5 km): for AMSR2 observation period, the high-resolution sea ice concentration data are available from July 2012 to present; the AMSR-E data were not processed yet.

The second question was about both 10GHz bands to be used in AMSR3 retrievals: the multi-band SST of AMSR3 will use 4 channels (6.9, 7.3, 10.25, 10.65 GHz), so the importance of 10 GHz SST becomes higher in retrievals, especially in coastal area.

An additional question from Helen Beggs was about the new high resolution AMSR2 ice concentration product over the Arctic. BoM is interested for a similar product but for the Antarctic. JAXA plans to extend the algorithm to the Antarctic region in future. The algorithm developer (Dr. Georg Heygster and his team) tuned parameters only for the Arctic region, the algorithm has been tested for the Antarctic region at JAXA. Validation results were not good (more than 35%), so the decision was to release the Arctic region as first step. The developer will do further tuning for the Antarctic region to achieve release accuracy of 15%. Validation results of the Arctic are available from here. Current accuracy is ~15%.  
[https://suzaku.eorc.jaxa.jp/GCOM\\_W/data/product/210421\\_AMSR2\\_HSI\\_Validation\\_result\\_e.pdf](https://suzaku.eorc.jaxa.jp/GCOM_W/data/product/210421_AMSR2_HSI_Validation_result_e.pdf)  
The data from the research product are available on the ftp server after simple registration.  
[https://suzaku.eorc.jaxa.jp/GCOM\\_W/research/resdist.html](https://suzaku.eorc.jaxa.jp/GCOM_W/research/resdist.html)

## Japan Meteorological Agency, JMA



---

Toshiyuki Sakurai presented the news from the reorganization of JMA. A summary of JMA products and the updates for global and regional SST analysis followed and the presentation was completed by the work in progress and plans for the future (addition of VIIRS/NOAA20, SGLI/GCOM-C).

## Met Office



---

Simon Good showed all available GHRSSST products and the last updates of OSTIA foundation temperature analysis including the impact of the addition of SLSTR as reference sensor together with VIIRS. Comparison of different analyses against GMPE are also presented.

Toshiyuki Sakurai asked about using SLSTR in satellite bias correction: this reduces the negative bias of OSTIA in global average, but is there a difference depending on the sea area? Simon replied that the reduction in negative bias occurs in all regions and it is particularly noticeable in the Arabian Sea and in the tropical Atlantic Ocean west of Africa.

## NASA



---

Edward Armstrong presented the news from NASA with reference to MODIS and VIIRS L2P and to MUR analysis. There was mentioned the availability of data on cloud and different recipes to access the data using Jupiter notebooks. News about MISST and CEOS Coverage Project were also presented.

## Naval Oceanographic Office, NAVO



Bruce McKenzie reported the status of different SST datasets provided to PO.DAAC, the new data assimilated in the Navy Global Ocean Forecast System and plans for new datasets processing. The summary of last year updates included the restoring of MetOp-B processing 21 days after loss of HIRS sensor, the release of MetOp-C data and an improved version for VIIRS SST. To note that MetOp-A dataset will be discontinued in Oct. 2021.

## NOAA/NESDIS/STAR 2



Eileen Maturi mentioned all available NOAA/NESDIS products for GHRSSST and the changes done to the algorithm retrievals. Some examples of these changes were also presented. The work in progress includes a blended SST using SLSTR, VIIRS and in situ data and an Ocean Heat Content product.

## NOAA/NCEI



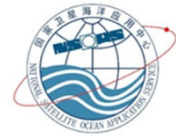
Huai-Min Zang started with the presentation of all available GHRSSST products. For each product a short description and the last improvements were also presented. For example, the last version of ICOADS including TAC and BUFR data was compared to the previous version, showing that the decrease in number of data was recovered. The evaluation of different GHRSSST L4 analyses was done against buoys and against ARGO data.

## NOAA/ACSP0



Alexander Ignatov presented the status of different NOAA/ACSP0 datasets. All products are using ACSP0 v2.80 which in addition to SST also report thermal fronts. The priorities for next year include the completion of AVHRR GAC SST RAN2 (1981-pr) and the release of new satellites/sensors in L3S-LEO and L3S-GEO format.

## National Satellite Ocean Application Service, NSOAS



---

Lijian Shi reported the status of satellites launched in 2020 and the changes in the SST products. The validation of different datasets retrievals against other satellites or against in situ data were also presented.

## Satellite Application Facility on Ocean and Sea Ice, OSI-SAF



---

Stéphane Saux-Picard presented the main activities of OSI-SAF. These include the revision of bias correction for geostationary satellites, the release of Metop-C data and the preparation of NOAA20 products. The work is in progress to improve the cloud mask and to produce an L2 ice concentration using AMSR2 and SSMIS sensors.

Regarding the question from Toshiyuki Sakurai about the status of Meteosat-8 as “demonstrational”, Stéphane answered that "demonstrational" refers to the fact that it was not initially planned to process both Meteosat satellites therefore the production of Meteosat-8 is not "operational", meaning there is no obligation in terms of timeliness and so on. However, everything is done to keep a NRT production and to avoid interruptions.

Bruce McKenzie mentioned that NAVO uses Met-11 and Met-8 GHRSSST products for operational assimilation in their models. He asked if Met-9 is moved to the IO, then OSI-SAF are going to produce datasets similar with those from Met-8? The answer from was positive.

## European Space Agency, ESA



---

Craig Donlon mentioned that ESA continues to support SST activities. The Sentinel 3C/D are in final stage of preparation. Copernicus LSTM and CIMR missions are now in Phase-B2. ESA is also preparing the next CEOS shipborne radiometer intercalibration experiment.

## **AGENCY PRESENTATIONS – ABSTRACTS**

## REPORT FROM THE AUSTRALIAN RDAC TO GHRSSST-XXII

**Helen Beggs<sup>(1)</sup>, Pallavi Govekar<sup>(2)</sup>, Lixin Qi<sup>(3)</sup>, Christopher Griffin<sup>(4)</sup>, Janice Sisson<sup>(5)</sup>, Nicole Morgan<sup>(6)</sup>**

- (1) Bureau of Meteorology, Melbourne, Australia, Email: [helen.beggs@bom.gov.au](mailto:helen.beggs@bom.gov.au)  
(2) Bureau of Meteorology, Melbourne, Australia, Email: [pallavi.govekar@bom.gov.au](mailto:pallavi.govekar@bom.gov.au)  
(3) Bureau of Meteorology, Melbourne, Australia, Email: [lixin.qi@bom.gov.au](mailto:lixin.qi@bom.gov.au)  
(4) Bureau of Meteorology, Melbourne, Australia, Email: [christopher.griffin@bom.gov.au](mailto:christopher.griffin@bom.gov.au)  
(5) Bureau of Meteorology, Melbourne, Australia, Email: [janice.sisson@bom.gov.au](mailto:janice.sisson@bom.gov.au)  
(6) CSIRO Oceans and Atmosphere, Hobart, Australia, Email: [nicole.morgan@csiro.au](mailto:nicole.morgan@csiro.au)

### ABSTRACT

This is a report of progress during the past 12 months in the Australian Regional Data Assembly Centre (RDAC) at the Bureau of Meteorology (BoM), relating to the provision and validation of Group for High Resolution Sea Surface Temperature (GHRSSST) products, and related SST research.

### OVERVIEW

As a contribution to the Integrated Marine Observing System (IMOS), the Australian Bureau of Meteorology produces several real-time and delayed mode (reprocessed), GHRSSST format products (GHRSSST Science Team, 2012) for a range of operational and research applications, using locally received and overseas sea surface temperature (SST) data sets obtained from polar-orbiting and geostationary satellites (Beggs, 2021). These products are listed in Sections 1.1, 1.2 and 1.3 with data access listed in Section 2. Recent updates to the operational and experimental GHRSSST products are described in Section 3 and future plans in Section 4.

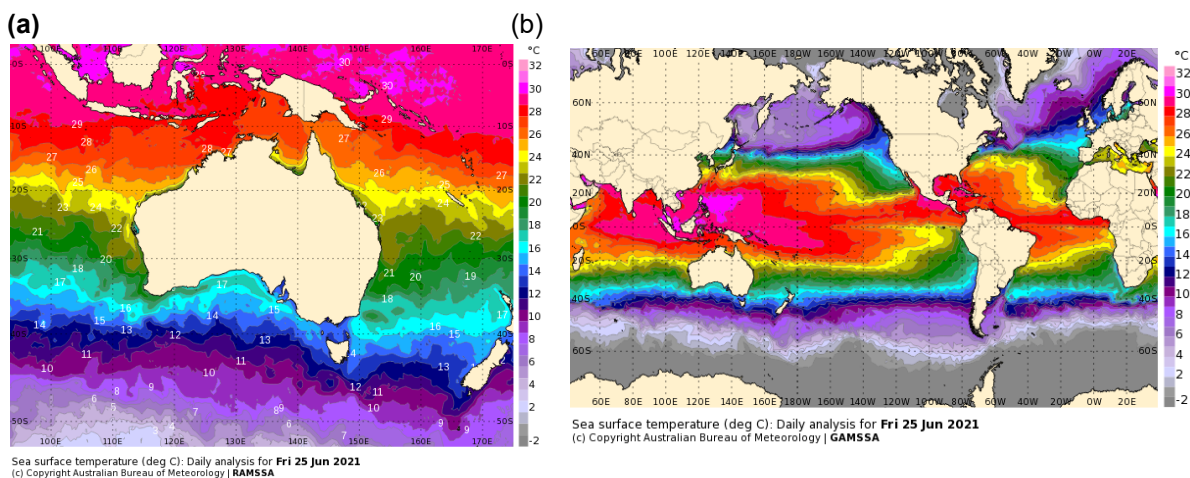


Figure 1: Example of foundation SST for 26<sup>th</sup> June 2021 from BoM Daily L4 analyses (a) RAMSSA and (b) GAMSSA, formed from NAVOCEANO GAC AVHRR L2P (MetOp-B), JAXA AMSR-2 L2P (GCOM-W), NOAA ACSPO VIIRS L3U (Suomi-NPP, NOAA-20) and in situ SST (ships, buoys).

#### Operational Real-time GDS2.0

- Daily Regional 1/12° SSTfnd L4 ("RAMSSA") over 60°E to 190°E, 70°S to 20°N (Figure 1a)
- Daily Global 0.25° SSTfnd L4 ("GAMSSA") (Figure 1b)
- km SSTskin L2P from High Resolution Picture Transmission (HRPT) Advanced Very High Resolution Radiometer (AVHRR) data (NOAA18, NOAA-19)
- 0.02° SSTskin L3U and day/night L3C over Australia (70°E to 190°E, 70°S to 20°N) and Southern Ocean (2.5°E to 202.5°E, 77.5°S to 27.5°S) from HRPT AVHRR data (NOAA-18, NOAA-19),

- EUMETSAT OSI-SAF Full Resolution Area Coverage (FRAC) AVHRR L2P data (MetOp-B) and ACSPO Visible Infrared Imaging Radiometer Suite (VIIRS) L3U data (Suomi-NPP and NOAA-20)
- 0.02° day/night SSTskin and day+night SSTfnd L3S over Australia (70°E to 190°E, 70°S to 20°N) and Southern Ocean (2.5°E to 202.5°E, 77.5°S to 27.5°S) from
  - AVHRR-only: HRPT AVHRR (NOAA-18) L3C
  - Multi-sensor: HRPT AVHRR (NOAA-18) L3C, FRAC AVHRR (MetOp-B) L3C and VIIRS (Suomi-NPP and NOAA-20) L3C
- 2 km 10-minute v1 Himawari-8 AHI SSTskin L2P

#### Experimental Real-Time GDS2.0

- 0.02° SSTskin L3U and day/night L3C over Australia (70°E to 190°E, 70°S to 20°N) and Southern Ocean (2.5°E to 202.5°E, 77.5°S to 27.5°S) from EUMETSAT OSI-SAF Full Resolution Area Coverage (FRAC) AVHRR L2P (MetOp-C) and EUMETSAT SLSTR L2P (Sentinel-3A, Sentinel-3B)
- 0.02° day/night SSTskin and day+night SSTfnd L3S over Australia (70°E to 190°E, 70°S to 20°N) and Southern Ocean (2.5°E to 202.5°E, 77.5°S to 27.5°S) from
  - Multi-sensor: IMOS v2 AHI L2P (Himawari-8), IMOS v1 HRPT AVHRR data (NOAA-18), IMOS FRAC AVHRR (MetOp-B) L3C, IMOS VIIRS (Suomi-NPP, NOAA-20) L3C (Figure 2a)

#### Reprocessed GDS2.0

- HRPT AVHRR L2P/L3U/L3C/L3S from 1992 to 2018 (NOAA-11 to NOAA-19 satellites)
- AVHRR and VIIRS L3U/L3C/L3S from 2012 to 2018 (NOAA-18, NOAA-19, MetOp-A, MetOp-B, Suomi-NPP)
- MTSAT-1R Hourly 0.05° L3U (2006 to 2010)
- Experimental 2 km 10-minute v2 Himawari-8 AHI SSTskin L2P
- Experimental 0.02° Hourly, 4-hourly and Daily night-only SSTskin L3C over Australia (70°E to 190°E, 70°S to 20°N) from v2 Himawari-8 AHI L2P

## DATA AVAILABILITY

#### Real-time GDS2.0

- Operational daily L4 (RAMSSA/GAMSSA) are available within 6 hours of final observation back to 2006/2008 from JPL PO.DAAC Drive and Thredds server ([https://podaac.jpl.nasa.gov/dataset/RAMSSA\\_09km-ABOM-L4-AUS-v01](https://podaac.jpl.nasa.gov/dataset/RAMSSA_09km-ABOM-L4-AUS-v01) and [https://podaac.jpl.nasa.gov/dataset/GAMSSA\\_28km-ABOM-L4-GLOB-v01](https://podaac.jpl.nasa.gov/dataset/GAMSSA_28km-ABOM-L4-GLOB-v01)) and the Australian Ocean Data Network (AODN) Thredds Server at <http://thredds.aodn.org.au/thredds/catalog/IMOS/SRS/SST/ghrsst/L4/catalog.html>
- Operational IMOS fv01 HRPT AVHRR (available 2015 to present)
  - L2P: OPeNDAP server (contact [ghrsst@bom.gov.au](mailto:ghrsst@bom.gov.au))
- Operational IMOS fv01 HRPT AVHRR L3U/L3C/L3S, fv01 NPP VIIRS L3U/L3C and fv01 Multi-sensor L3S: <http://thredds.aodn.org.au/thredds/catalog/IMOS/SRS/SST/ghrsst/catalog.html>
- BoM AHI Himawari-8
  - v1 L2P: (available 24 March 2016 to present) Contact [ghrsst@bom.gov.au](mailto:ghrsst@bom.gov.au)
  - v1 L3C: (available 1 October 2017 to present) Contact [ghrsst@bom.gov.au](mailto:ghrsst@bom.gov.au)

#### Reprocessed GDS2.0

- IMOS fv02 HRPT AVHRR (available 1992 to 2018)
  - L2P: <http://dapds00.nci.org.au/thredds/catalog/rr5/satellite/GHRSSST/v02.0fv02/L2P/catalog.html>
  - L3U/L3C/L3S: <http://portal.aodn.org.au> and <http://dapds00.nci.org.au/thredds/catalog/rr5/satellite/GHRSSST/v02.0fv02/Continental/catalog.html>
- IMOS AVHRR and VIIRS L3U/L3C/L3S (available 2012 to 2018): Contact [ghrsst@bom.gov.au](mailto:ghrsst@bom.gov.au)
- IMOS MTSAT-1R L3U (available Jun 2006 to Jun 2010): IMOS Thredds server at <http://rs-data1-mel.csiro.au/thredds/catalog/imos-srs/sst/ghrsst/L3U/mts1r/catalog.html>
- Experimental v2 L3C: (available 1<sup>st</sup> March to 31<sup>st</sup> May 2021) Contact [ghrsst@bom.gov.au](mailto:ghrsst@bom.gov.au)

### PROGRESS SINCE GHRSSST-XXI

#### Operational SST Analyses

##### Overview

BoM produces regional 1/12° (“RAMSSA”, Figure 1a) and global 1/4° (“GAMSSA”; Figure 1b) operational daily foundation L4 SST analyses in near real-time based on an optimal interpolation method. For more information on RAMSSA see Beggs et al. (2011) and for GAMSSA see Zhong and Beggs (2009) and Beggs et al (2011). As reported at GHRSSST-XXI and in Beggs et al. (2020), RAMSSA was updated on 17<sup>th</sup> November 2019 and GAMSSA on 29<sup>th</sup> April 2020 to ingest VIIRS SST data. RAMSSA and GAMSSA are available for internal use only in GHRSSST GDS1.6 (Beggs and Pugh, 2009) (no longer supplied to PO.DAAC) and externally in GDS2.0 L4 format (GHRSSST Science Team, 2012; Section 2).

#### Current SST inputs (27<sup>th</sup> June 2021):

- 9 km NAVOCEANO GAC AVHRR GHRSSST-L2P SST1m (currently MetOp-B only) (NOAA-18 stopped 22<sup>nd</sup> May 2018, NOAA-19 stopped 24<sup>th</sup> October 2018, MetOp-A stopped 7<sup>th</sup> July 2020) – SSES Bias is subtracted
- 2 km NOAA/OSPO ACSPO VIIRS L3U SST(0.2 m) (Suomi-NPP, NOAA-20) - SSES Bias is subtracted
- ~50 km JAXA AMSR-2 (GCOM-W) L2P SSTsubskin (since 1<sup>st</sup> December 2014) - no SSES used
- GTS Buoy and ship in situ SSTdepth (with additional Argo and CTD SSTdepth ingested into RAMSSA)

**Sea Ice inputs:** NOAA/NCEP Daily 1/12° sea-ice concentration analysis (Grumbine, 1996)

#### Background Field:

- RAMSSA: Formed from a combination of previous day's RAMSSA analysis and BoM Global Weekly 1° SST analysis (Smith et al., 1999).
- GAMSSA: Formed from a combination of previous day's GAMSSA analysis and BoM Global Weekly 1° SST analysis (Smith et al., 1999) (since 29<sup>th</sup> April 2020).

**Applications:** Boundary condition for BoM NWP models, validating ocean forecasts, SST and SST anomaly maps (<http://www.bom.gov.au/marine/sst.shtml> and <http://www.bom.gov.au/australia/meteye>). In addition, GAMSSA contributes to the GHRSSST Multi-Product Ensemble (<https://ghrsst-pp.metoffice.gov.uk/ostia-website/gmpe-monitoring.html>) and provides initial conditions for the new BoM seasonal prediction model, ACCESS-S2.

### Progress

On 27<sup>th</sup> May 2020 the HIRS sensor failed on MetOp-B, preventing valid version 1 (v1) MetOp-B 8.8 km GAC AVHRR SST data to be produced by NAVOCEANO. With the release by NAVOCEANO of version 2 (v2) 4.4 km GAC AVHRR L2P data, MetOp-B GAC AVHRR L2P SSTs were again ingested into RAMSSA and GAMSSA from 7<sup>th</sup> July 2020, but v2 MetOp-A GAC AVHRR L2P SSTs were not, due to its reduced accuracy caused by a drifting orbit. With the imminent de-orbiting of MetOp-A in December 2021, work is underway to ingest NAVOCEANO v2 MetOp-C GAC AVHRR L2P SST data into RAMSSA and GAMSSA.

On 13<sup>th</sup> October 2020, JAXA updated their near real-time AMSR-2 L2P SST files from version 3.0 to version 4.0, so from this date near real-time v4.0 Standard AMSR-2 L2P SSTs were ingested into RAMSSA and GAMSSA. Filenames are of the form \*JAXA-L2P-GHRSSST-SSTsubskin-AMSR2\_NRT-{version}\*.nc.gz.

Work is underway to ingest BUFR format ship SST observations from the Global Telecommunications System (GTS) into RAMSSA and GAMSSA, becoming more important due to the steady increase in BUFR - only format ship observations being uploaded on the GTS, and the decrease in TAC (SHIP and Trackob) format observations, particularly from March 2020.

From January 2020, NOAA/NCEP is no longer making any code changes to its operational daily 1/12° sea ice analysis system (see <https://polar.ncep.noaa.gov/seaice/Analyses.shtml>), so work is underway to assess the UK Met Office's CMEMS OSTIA daily 0.25° sea ice fraction field as a replacement for the Bureau's NWP models (e.g., ACCESS-G) and SST analyses (RAMSSA, GAMSSA, Weekly, Monthly).

### IMOS GHRSSST AVHRR and VIIRS Composite Products

#### AVHRR

As part of the Integrated Marine Observing System (IMOS: [www.imos.org](http://www.imos.org)), BoM in collaboration with CSIRO, produces a range of HRPT AVHRR GDS2.0 L2P, L3U, L3C and L3S products from the series of NOAA Polar Orbiting Environmental Satellites (NOAA-11 to NOAA-19). Following methods documented in Paltoglou et al. (2010), Griffin et al. (2017) and Wijffels et al. (2019), SST values are derived by regressing brightness temperatures against regional drifting buoy SST observations at ~0.2 m depth, error estimates obtained using matchups with buoy data, and quality levels defined from proximity to detected cloud. The 0.02° resolution level 3 products are available in a range of averaging periods from single orbit to 1 month to suit different applications (Beggs, 2021). All products are available in real-time "fv01" files (within 3 to 24 hours of final observation) (Paltoglou et al., 2010) and have also been reprocessed to "fv02" files to cover the period from 1992 to 2018 (Griffin et al., 2017). For more information see IMOS (2018) and AODN (2019).

**Applications:** BoM operational coral bleaching nowcasting service (ReefTemp NextGen: <http://www.bom.gov.au/environment/activities/reeftemp/reeftemp.shtml> until 20th November 2018), regional maps of ocean currents and SST (<http://oceancurrent.imos.org.au/> until 20<sup>th</sup> November 2018), SST climatologies (Wijffels et al., 2018), and research/monitoring SST diurnal variation, Marine Heat Waves and coastal upwelling (Beggs, 2019).

#### VIIRS + AVHRR

From 2018, NOAA officially replaced the AVHRR sensor program with the Visible Infrared Imaging Radiometer Suite (VIIRS) sensor program, after a long trial which began with the first VIIRS sensor launched in 2012 aboard the Suomi National Polar-Orbiting Partnership (NPP) platform. The VIIRS sensor provides higher spatial resolution (0.75 km at nadir) and lower noise than AVHRR, and has better orbital stability, with daily global SST coverage in cloud-free conditions at around 01:20 and 13:20 local time. The NOAA Office of Satellite and Product Operations (OSPO) produce real-time Suomi-NPP and NOAA-20 VIIRS L3U SST on the IMOS 0.02° x 0.02° grid (NOAA CoastWatch, 2018). The Bureau of Meteorology (BoM) have composited the NOAA ACSP0 VIIRS L3U data, following the method in Griffin et al. (2017), to produce daily day/night L3C composites of VIIRS data on the IMOS grid and domain. The VIIRS L3U data are composited based on quality and uncertainty estimates with AVHRR SST data to construct the new IMOS "Multi-sensor L3S"

product suite (Griffin et al., 2017; Govekar et al., 2020), resulting in improvements to overall quality, accuracy and coverage (Beggs et al., 2019a). These products, produced operationally at BoM from 16<sup>th</sup> November 2018 using NPP VIIRS L3U and IMOS NOAA-18 HRPT AVHRR L2P data, and updated on 21<sup>st</sup> November 2019 to ingest EUMETSAT OSI-SAF MetOp-B FRAC AVHRR L2P and NOAA ACSPO NOAA-20 VIIRS L3U data (e.g., Figure 3(a)), are intended to be drop-in replacements for the existing AVHRR-only L3S product set, with similar file formats. Validation of the night-time 1-day Multi-sensor L3S SST against in situ SST indicates incorporating VIIRS data significantly reduces the standard deviation of the 30-day differences from typically 0.4-0.7°C to 0.2-0.5°C for highest quality level L3S SSTs (Beggs et al., 2019c).

Real-time, operational, "fv01" Multi-Sensor L3S netCDF files containing average SSTs over periods of 1, 3, 6 days and 1 month are available back to 1<sup>st</sup> January 2018 from the AODN Thredds server at <http://thredds.aodn.org.au/thredds/catalog/IMOS/SRS/SST/ghrsst/catalog.html> in the L3SM-1d, L3SM-3d, L3SM-6d and L3SM-1m sub-directories, and from the AODN portal (<http://portal.aodn.org.au>). The "fv02" Multi-sensor L3S products have been reprocessed from 2012 to 2018 to incorporate all available OSI SAF FRAC AVHRR L2P data (from MetOp-A and MetOp-B), IMOS fv02 HRPT AVHRR L2P (from NOAA-15, NOAA-18 and NOAA-19) and NOAA ACSPO VIIRS L3U data (from Suomi-NPP and NOAA-20). These fv02 files are available for the period 1<sup>st</sup> January 2012 to 31<sup>st</sup> December 2018 from the AODN Thredds server at <http://thredds.aodn.org.au/thredds/catalog/IMOS/SRS/SST/ghrsst/catalog.html> in the L3SM-1d, L3SM-3d, L3SM-6d and L3SM-1m sub-directories, and from the AODN portal (<http://portal.aodn.org.au>).

### Applications:

Maps of these Multi-sensor composite SSTs are available for various Australian regions from IMOS OceanCurrent (<http://oceancurrent.imos.org.au/index.php>) back to 1<sup>st</sup> January 2018. Since 21<sup>st</sup> November 2018, the IMOS Multi-sensor 1-day nighttime L3S SSTs have been ingested into the Bureau of Meteorology's ReefTemp NextGen coral bleaching risk monitoring system (<http://www.bom.gov.au/environment/activities/reeftemp/reeftemp.shtml>). Maps of the 1-day night-only Multi-sensor L3S SSTskin can be viewed in the NOAA/NESDIS ACSPO Regional Monitor (<https://www.star.nesdis.noaa.gov/sod/sst/arms/>).

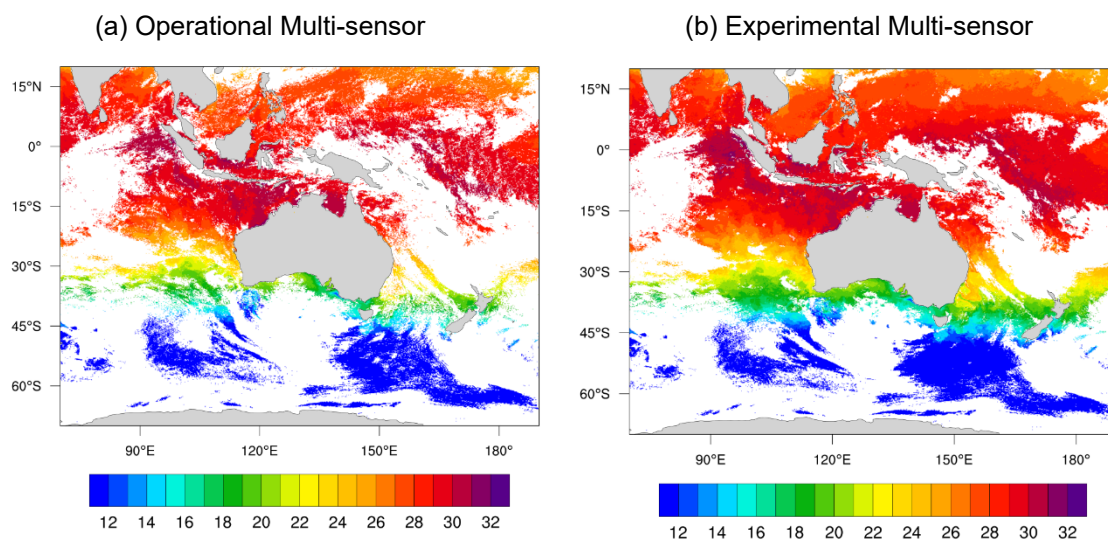


Figure 2: Examples of remapped quality level  $\geq 3$  skin SST for 15<sup>th</sup> March 2020 from IMOS 1-day night-time Multi-sensor L3S products formed from (a) NOAA-18/AVHRR, MetOp-B/AVHRR, Suomi-NPP/VIIRS and NOAA-20/VIIRS L3C SST, and (b) v2 Himawari-8/AHI, NOAA-18/AVHRR, MetOp-B/AVHRR, Suomi-NPP/VIIRS and NOAA-20/VIIRS L3C SST.

### Himawari-8 L3C SST

#### Operational Version 1 Himawari-8 Products

BoM, in collaboration with JMA and NOAA/NESDIS/STAR, have since 8<sup>th</sup> March 2016 produced operational real-time Himawari-8 L2P skin SSTs on the GEO grid, by regressing against ACSPO VIIRS L3U SSTsubskin measurements for a single date (21<sup>st</sup> July 2015), followed by subtracting 0.17 K to convert from subskin to skin SST. Currently, the operational Sensor Specific Error Statistics (SSES) values are estimated using a function based on AHI brightness temperature variability on 21<sup>st</sup> July 2015, and do not adjust for sensor changes over time. Quality level values are derived for each SST value based on the Griffin et al. (2017) method, using a combination of proximity to cloud, identified using the GEOCAT method (<http://cimss.ssec.wisc.edu/csppgeo/geocat.html>), and size of the estimated error, estimated on "local SST variability". Possible quality levels are 0 to 5, with 5 identifying the most cloud-free pixels.

The 10 minute v1 Himawari-8 L2P SST values are composited in real-time to hourly L3C files on the GEO projection by selecting the best quality spatially and temporally consistent SST. For the daily, night-time L3C composition, the retrieval is selected from the hourly retrievals, such that it is the best quality, closest in time to local sunrise. The hourly, 4-hourly or daily L3C data on the GEO projection is further mapped to the IMOS 0.02° x 0.02° grid using sub-pixel area weighted averaging of any overlapping pixels. The Himawari-8 SST composition method involves no smoothing or interpolation.

The v1 Himawari-8 L3C GDS2.0 files from 1<sup>st</sup> October 2017 to present are available via OPeNDAP on request.

**Applications:** Himawari-8 L2P files are ingested into IMOS 4-hourly SST composite maps (<http://oceancurrent.imos.org.au/product.php?product=fourhour>), L3C files have been used for research into coastal upwelling (Beggs et al., 2019b).

#### Experimental Version 3 Himawari-8 Products

In order to reduce cloud contamination and SST biases in the operational v1 Himawari-8 SST products, BoM, in collaboration with Jonathan Mittaz (University of Reading), have produced a new version 3 ("fv03") Himawari-8 L2P skin SST product on the GEO grid, employing the Radiative Transfer Model (RTTOV12.3) and Bayesian cloud clearing method based on the ESA CCI SST code developed at the University of Reading (Merchant et al., 2019), with inputs of BoM Numerical Weather Prediction forecast meteorological profile data from ACCESS-G3 (BoM, 2019). Possible quality levels are 0 to 5, with 5 identifying the highest quality pixels. An example of single scene fv03 Himawari-8 L2P skin SSTs is shown in Figure 3a.

Following the method used for the reprocessed IMOS fv02 HRPT AVHRR L2P products, SSES bias and SSES standard deviation values are estimated using the empirical model developed at BoM, based on the number of degrees of freedom, median bias and standard deviation of matchups with drifting buoy and tropical mooring SST observations, separated into swath and geographical components (see Section 2.3 in Griffin et al., 2017).

The 10 minute fv03 Himawari-8 L2P SST values on native coordinates are composited to 1-hour and 4-hourly L3C on the native GEO projection by selecting the closest temperatures to a warm piecewise linear diurnal trend, then projected using the equal area weighted averaging method based on quality level and SSES (Griffin et al., 2017). For the daily, night-time L3C composition, the retrieval is selected from the hourly retrievals, such that it is the best quality, closest in time to local sunrise. The hourly, 4-hourly or daily L3C data on the GEO projection are further mapped to the IMOS 0.02° x 0.02° grid using sub-pixel area weighted averaging of any overlapping pixels. The Himawari-8 SST composition method involves no smoothing or interpolation. Examples of the fv03 Himawari-8 1-hour, 4-hour and 1-day night-time L3C SSTskin over the IMOS domain (70°S to 20°N, 70°E to 190°E) are shown in Figures 3b to 3d.

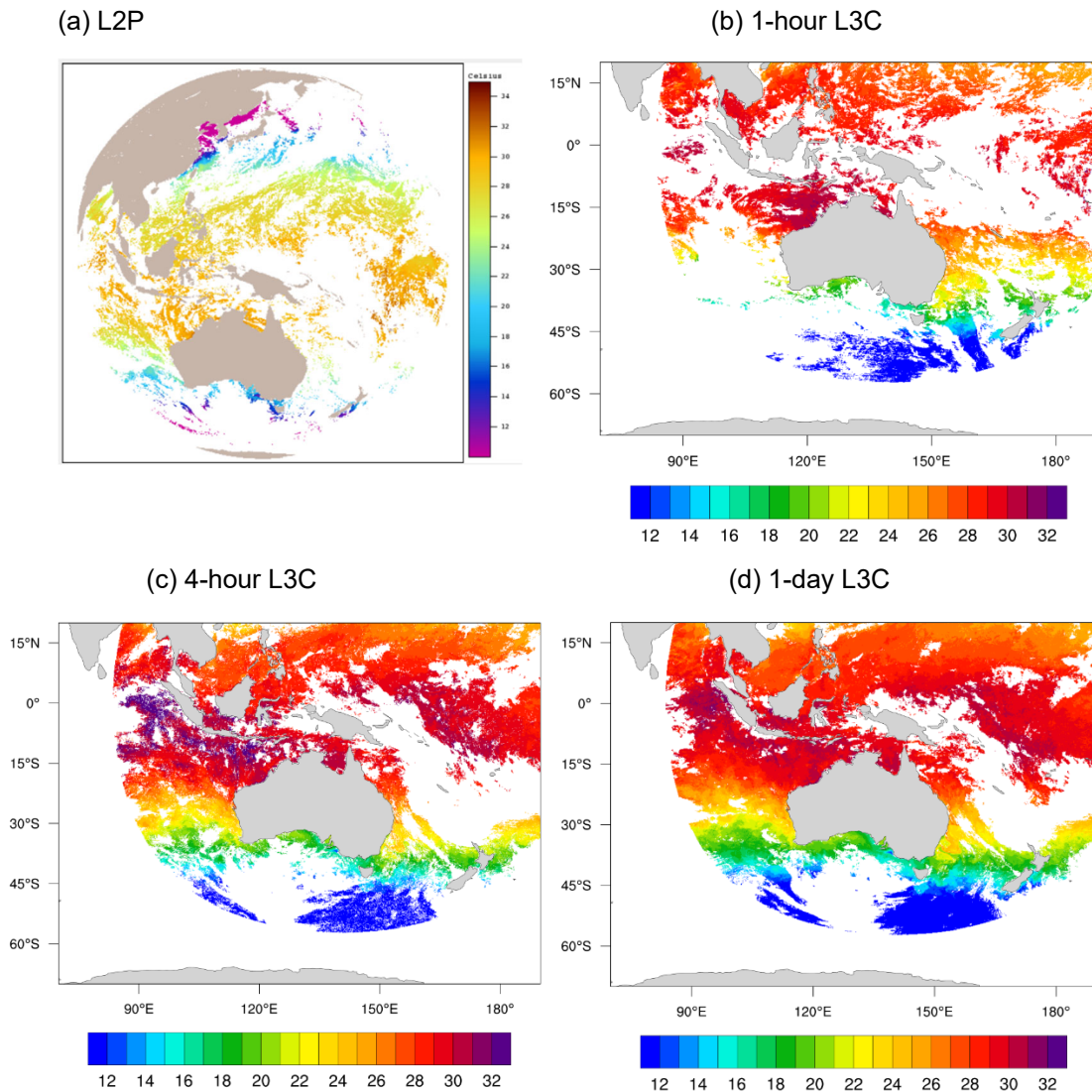


Figure 3: Examples of remapped quality level  $\geq 3$  skin SST for 15<sup>th</sup> March 2021 from experimental fv03 IMOS Himawari-8 AHI products (a) L2P, (b) 1-hour L3C, (c) 4-hour L3C and (d) 1-day night-time L3C.

In response to user requirements for gap-free, highest spatial resolution and highest accuracy SST data, BoM is experimenting with compositing fv03 Himawari-8 L3C data with fv01 VIIRS L3C and fv01 AVHRR L3C to construct new version 3 ("fv03") Multi-sensor L3S products. In order to merge data from different satellite sensors, the quality level (QL) of each dataset to be merged is redefined as the minimum of the original quality level provided by the data provider and remapped quality level calculated using SSES (Appendix A in Griffin et al., 2017). The latter is calculated using SSES bias ( $\mu_{sses}$ ) and SSES standard deviation ( $\sigma_{sses}$ ) estimates, thus:

$$q_{sses} = \frac{1}{\sqrt{2}} \sqrt{\max \left( \left( \frac{\sigma_{sses}}{\sigma_0} \right)^2 + \left( \frac{\mu_{sses} - \mu_0}{\sigma_{sses}} \right)^2 - 1, 0 \right)}$$

$$q_s = \lfloor 5 \exp^{\eta q_{sses}} \rfloor$$

Different data sources can then be combined using  $q_s$ , provided that  $\eta/\sigma_0 = \text{constant}$ , where  $\eta$  is a scaling parameter and the half square brackets in the  $q_s$  equation represent the "nearest integer" function. The addition of Himawari-8 SST to existing data streams for the operational fv01 Multi-sensor L3S product (NOAA-18/AVHRR, MetOp-B/AVHRR, Suomi-NPP/VIIRS and NOAA-20/VIIRS, Figure 2a and 4a) reduces data gaps due to clouds and shows significant improvement in spatial coverage for remapped quality level 4 (Figure 2b and 4b), and similar bias and standard deviation values to operational Multi-sensor L3S for remapped QL  $\geq 4$  (Figure 5). Further tuning of QL remapping may be required before we reprocess the entire fv03 Himawari-8 L3C and fv03 Multi-sensor L3S data set from 1<sup>st</sup> January 2015 to present.

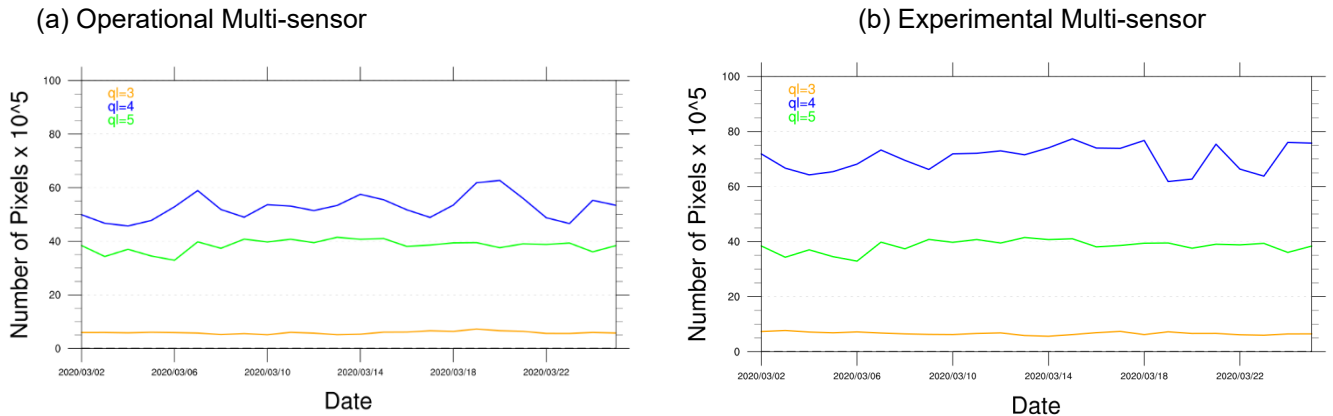


Figure 4: Number of pixels in L3S 1-day night files for March 2020 from (a) operational fv01 Multi-sensor and (b) experimental fv03 Multi-sensor for remapped QL = 3 (orange), QL = 4 (blue) and QL = 5 (green).

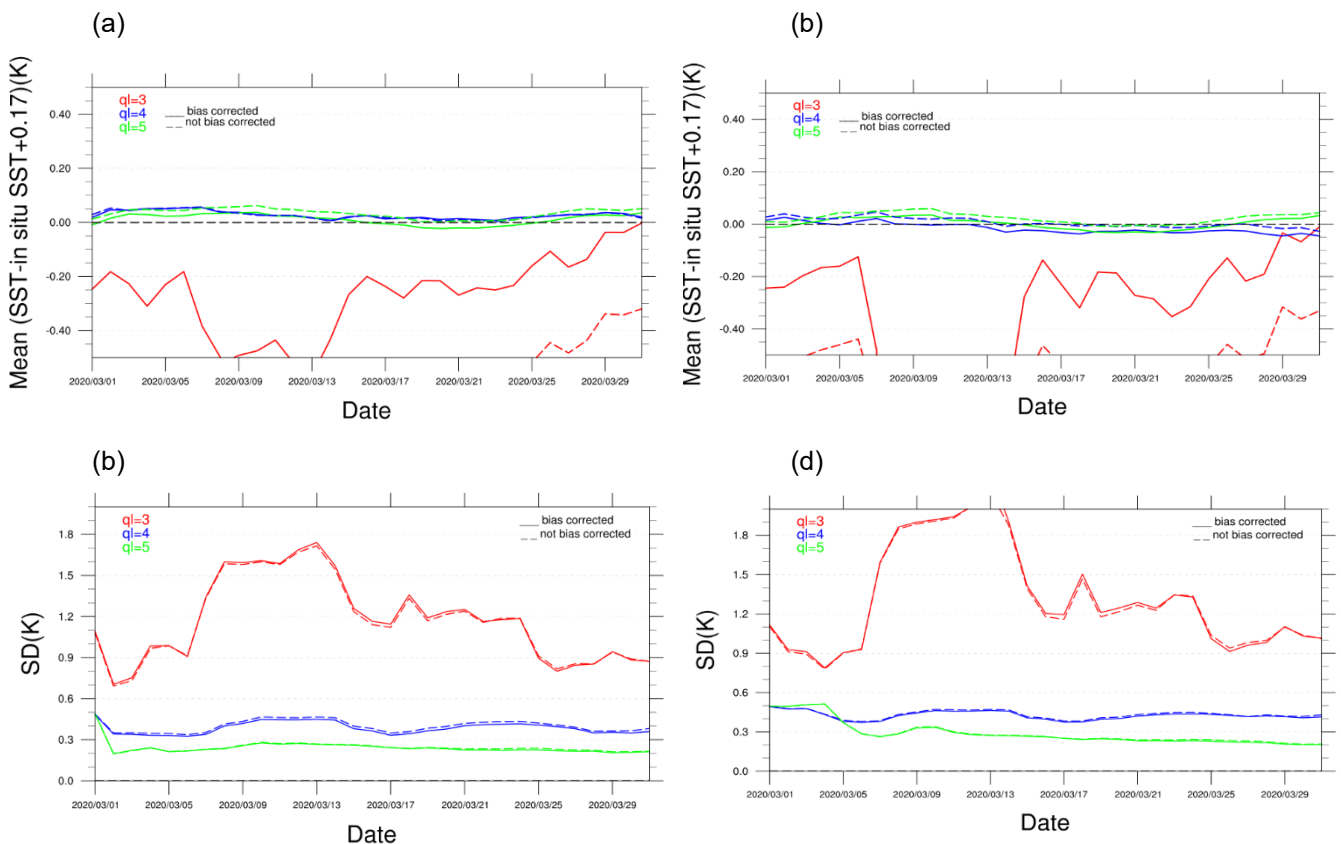


Figure 6: Validation statistics of the 1-day night operational fv01 Multi-sensor L3S (a) mean bias (c) standard deviation and experimental fv03 Multi-sensor L3S (b) mean bias (d) standard deviation SSTs over a 7-day moving window for March 2020. Note: Mean bias = SST - in situ SST + 0.17 (in Kelvin), Matchup thresholds: < 10 km and < 6 hours.

## PLANS FOR 2021/2022

During the coming 12 months, the Bureau of Meteorology plans to:

- Add NAVOCEANO MetOp-C GAC AVHRR L2P to BoM operational L4 SST analyses and ocean models
- Add BUFR format ship SST observations from the GTS to RAMSSA and GAMSSA L4
- Assess CMEMS OSTIA L4 daily 0.05° sea ice fraction to replace NOAA/NCEP daily 1/12° sea ice analysis sea ice concentration ingested into RAMSSA and GAMSSA
- In collaboration with Jonathan Mittaz (Uni. of Reading), validate the new BoM/IMOS fv03 Himawari-8 SST and reprocess to GHRSSST GDS2.0 format L2P and L3C products over the period 1<sup>st</sup> January 2015 to present, prior to ingesting into reprocessed 4-hourly, 1-day, 3-day, 6-day and 1-month IMOS Multi-sensor L3S.

## REFERENCES

AODN (2019). Australian Ocean Data Network Satellite SST Products Help Page:

<https://help.aodn.org.au/satellite-sst-data/>

Beggs, H. and Pugh T. (2009) Format Specification for the Australian Bureau of Meteorology's SST Analysis L4 files. Bureau of Meteorology Technical Document, 12 March 2009, Version 7, 12 pp.

Beggs H., A. Zhong, G. Warren, O. Alves, G. Brassington and T. Pugh (2011). RAMSSA – An Operational, High-Resolution, Multi-Sensor Sea Surface Temperature Analysis over the Australian Region, Australian Meteorological and Oceanographic Journal, **61**, 1-22, 2011

<http://www.bom.gov.au/jshess/papers.php?year=2011>

Beggs, H., Griffin, C. and Govekar, P. (2019a). New IMOS multi-sensor sea surface temperature composites provide better coverage and accuracy, IMOS web article, 21 February 2019,

[http://imos.org.au/fileadmin/user\\_upload/shared/SRS/SST/Beggs\\_2019\\_IMOS\\_Multi-sensor\\_L3S\\_article\\_21Feb2018.pdf](http://imos.org.au/fileadmin/user_upload/shared/SRS/SST/Beggs_2019_IMOS_Multi-sensor_L3S_article_21Feb2018.pdf)

Beggs, Helen, Christopher Griffin, Gary Brassington and Pallavi Govekar (2019b) Measuring coastal upwelling using IMOS Himawari-8 and Multi-Sensor SST. Presented as a poster presentation at the 20<sup>th</sup> GHRSSST Science Team Meeting, Frascati, Italy, 3<sup>rd</sup> – 7<sup>th</sup> June, 2019. DOI: 10.13140/RG.2.2.22966.45129

Beggs H, P. Govekar, C. Griffin, L. Majewski, L. Qi, A. Zhong and P. Sakov (2019c) Report from the Australian RDAC to GHRSSST-XX, In: Proceedings of the GHRSSST XX Science Team Meeting, Frascati, Italy, 3<sup>rd</sup> – 7<sup>th</sup> June, 2019. p. 40 – 49. <https://www.ghrsst.org/meetings/20th-ghrsst-international-science-team-meeting-g-xx>

Beggs, Helen, Lixin Qi, Pallavi Govekar and Christopher Griffin (2020) Ingesting VIIRS SST into the Bureau of Meteorology's Operational SST Analyses, In: Proceedings of the 21<sup>st</sup> GHRSSST Science Team Meeting, Virtual Meeting hosted by EUMETSAT, 1<sup>st</sup> – 4<sup>th</sup> June 2020. p. 104-110.

<https://www.ghrsst.org/meetings/21st-ghrsst-international-science-team-meeting-g-xxi/>

Beggs, Helen M. (2021) Temperature. Ch 14 in Earth Observation: Data, Processing and Applications. Volume 3B: Applications – Surface Waters (Eds. Harrison, B.A., Anstee, J.A., Dekker, A., Phinn, S., Mueller, N., and Byrne, G.) CRC SI, Melbourne. <https://www.eoa.org.au/earth-observation-textbooks> (in press)

BoM (2019) National Operations Centre Operations Bulletin Number 125: APS3 upgrade of the ACCESS-G/GE Numerical Weather Prediction System, Australian Bureau of Meteorology, pp 68, [NMOC Operations Bulletin Number 93 \(bom.gov.au\)](https://www.bom.gov.au/operations/bulletin/93)

GHRSSST Science Team (2012). The Recommended GHRSSST Data Specification (GDS) 2.0, document revision 5, available from the GHRSSST International Project Office, 2012, pp 123.

<https://www.ghrsst.org/wp-content/uploads/2016/10/GDS20r5.pdf>

Govekar, Pallavi, Christopher Griffin and Helen Beggs (2020) Ingesting SLSTR SST into IMOS Multi-sensor SST Composites, In: Proceedings of the 21<sup>st</sup> GHRSSST Science Team Meeting, Virtual Meeting hosted by EUMETSAT, 1<sup>st</sup> – 4<sup>th</sup> June 2020. p.127-132. <https://www.ghrsst.org/meetings/21st-ghrsst-international-science-team-meeting-g-xxi/>

Griffin, C., H. Beggs and L. Majewski (2017). GHRSSST compliant AVHRR SST products over the Australian region – Version 1, Technical Report, Bureau of Meteorology, Melbourne, Australia, 151 pp.

[http://imos.org.au/fileadmin/user\\_upload/shared/SRS/SST/GHRSSST-DOC-basic-v1.0r1.pdf](http://imos.org.au/fileadmin/user_upload/shared/SRS/SST/GHRSSST-DOC-basic-v1.0r1.pdf)

Grumbine, R.W. 1996. Automated Passive Microwave Sea Ice Concentration Analysis at NCEP. Tech. Note, NOAA/NCEP, 13 pp.

IMOS (2018). IMOS Satellite Remote Sensing SST Data Web Page:

<http://imos.org.au/facilities/srs/sstproducts/ssdata0/>

Merchant, C. J., O. Embury, C. E. Bulgin, T. Block, G. K. Corlett, E. Fiedler, Si. A. Good, J. Mittaz, N. A. Rayner, D. Berry, S. Eastwood, M. Taylor, Y. Tsushima, A. Waterfall, R. Wilson and C. Donlon (2019) Satellite-based time-series of sea-surface temperature since 1981 for climate applications, Nature Scientific Data, 6:223, <https://doi.org/10.1038/s41597-019-0236-x>

NOAA CoastWatch (2018). ACSPO Global SST from VIIRS Web Page:

<https://coastwatch.noaa.gov/cw/satellite-data-products/sea-surface-temperature/acspo-viirs.html>

Paltoglou, G, H. Beggs and L. Majewski (2010) New Australian High Resolution AVHRR SST Products from the Integrated Marine Observing System, In: Extended Abstracts of the 15<sup>th</sup> Australian Remote Sensing and Photogrammetry Conference, Alice Springs, 13-17 September, 2010.

[http://imos.org.au/ssdata\\_references.html](http://imos.org.au/ssdata_references.html)

Smith, N.S., Ebert, B. and Warren, G. 1999. The Bureau of Meteorology SST Analysis System. An informal paper produced as background for the OOPC/AOPC Workshop on SST Analyses for Climate, International Research Institute, LDEO, Palisades NY USA, Nov 10–12, 1998.

Wijffels, Susan E., Helen Beggs, Christopher Griffin, John F. Middleton, Madeleine Cahill, Edward King, Emlyn Jones, Ming Feng, Jessica A. Benthuisen, Craig R. Steinberg and Phil Sutton (2018). A fine spatial scale sea surface temperature atlas of the Australian regional seas (SSTAARS): seasonal variability and trends around Australasia and New Zealand revisited, J. Marine Systems, **187**, 156-196.

<https://doi.org/10.1016/j.jmarsys.2018.07.005>

Zhong, Aihong and Helen Beggs (2008). Analysis and Prediction Operations Bulletin No. 77 - Operational Implementation of Global Australian Multi-Sensor Sea Surface Temperature Analysis, Bureau of Meteorology Web Document. <http://www.bom.gov.au/australia/charts/bulletins/apob77.pdf>

## MET OFFICE PRODUCTION UPDATE

**Simon Good**<sup>(1)</sup>

(1) Met Office, FitzRoy Road, Exeter, Devon EX1 3PB, UK, Email: [simon.good@metoffice.gov.uk](mailto:simon.good@metoffice.gov.uk)

### INTRODUCTION

The Met Office produces a number of level 4 GHRSSST datasets, mostly as part of the Copernicus Marine Environment Monitoring Service (CMEMS). The Operational Sea Surface Temperature and Ice Analysis (OSTIA) foundation SST (Good et al., 2020), the OSTIA diurnal skin SST (While et al., 2017) and the GHRSSST Multi-Product Ensemble (GMPE; Martin et al., 2012) are produced in near real time. A reprocessed version of OSTIA foundation SST is also available. A climate dataset of the daily average 20cm depth SST is produced as part of the European Space Agency (ESA) Climate Change Initiative (CCI) (Merchant et al., 2019) and the Copernicus Climate Change Service (C3S). These are listed, along with recent updates and links to where they can be obtained, in Table 1.

Product	Updates	Availability
OSTIA foundation SST near real time	Now using SLSTR in addition to VIIRS and in situ data to bias correct other satellite data (see Section 2)	<a href="#">CMEMS</a> <a href="#">PO.DAAC</a>
OSTIA foundation SST reprocessed product for late 1981 – present	Now updated every 6 months to 6 months behind real time	<a href="#">CMEMS</a>
OSTIA diurnal skin SST near real time		<a href="#">CMEMS</a>
GHRSSST multi-product ensemble (GMPE)	Updated webpages showing ensemble monitoring and validation against Argo data ( <a href="https://ghrsst-pp.metoffice.gov.uk/ostia-website/index.html">https://ghrsst-pp.metoffice.gov.uk/ostia-website/index.html</a> )	<a href="#">CMEMS</a>
ESA CCI and C3S daily average 20cm depth SST for late 1981 - present	Now updated daily and is available at a month behind real time from C3S	<a href="#">CCI</a> (to 2016) <a href="#">C3S</a> <a href="#">CMEMS</a>

Table 1: L4 GHRSSST data sets produced at the Met Office, recent updates to them, and download links.

### USE OF SLSTR IN THE OSTIA FOUNDATION SST BIAS CORRECTION REFERENCE DATASET

In December 2020 the OSTIA foundation SST near real time production system was updated to add SSTs from the Sea and Land Surface Temperature Radiometers (SLSTRs) on Sentinel-3A and -3B to its reference dataset used to bias correct other sensors. This was in addition to the SSTs from the two Visible Infrared Imaging Radiometer Suite (VIIRS) sensors and in situ data that were already in use.

The impact of the changes is described in the CMEMS Quality Information Document ([link](#)). The result was to warm the analyses, improving the mean difference to Argo validation data globally from -0.08K to -0.04K in statistics for the month of June 2020. The warming occurred over all regions, but was particularly pronounced in the Arabian Sea and in the tropical Atlantic Ocean west of Africa. However, the standard deviation of differences to Argo data were not impacted by the change.

### REFERENCES

- Good, S., Fiedler, E., Mao, C., Martin, M.J., Maycock, A., Reid, R., Roberts-Jones, J., Searle, T., Waters, J., While, J., Worsfold, M. The Current Configuration of the OSTIA System for Operational Production of Foundation Sea Surface Temperature and Ice Concentration Analyses. *Remote Sens.* 2020, 12, 720. <https://doi.org/10.3390/rs12040720>
- Martin, M., Dash, P., Ignatov, A., Banzon, V., Beggs, H., Brashett, B., Cayula, J.F., Cummings, J., Donlon, C., Gentemann, C., et al. Group for High Resolution Sea Surface temperature (GHRSSST) analysis fields inter-

comparisons. Part 1: A GHRSSST multi-product ensemble (GMPE). *Deep. Sea Res. Part II Top. Stud. Oceanogr.* 2012, 77–80, 21–30. <https://doi.org/10.1016/j.dsr2.2012.04.013>

Merchant, C.J., Embury, O., Bulgin, C.E. et al., Satellite-based time-series of sea-surface temperature since 1981 for climate applications. *Sci Data* 6, 2019, 223. <https://doi.org/10.1038/s41597-019-0236-x>

While, J., Mao, C., Martin, M.J., Roberts-Jones, J., Sykes, P.A., Good, S.A. and McLaren, A.J., An operational analysis system for the global diurnal cycle of sea surface temperature: implementation and validation. *Q.J.R. Meteorol. Soc.*, 2017, 143: 1787-1803. <https://doi.org/10.1002/qj.3036>

## NAVAL OCEANOGRAPHIC OFFICE (NAVOCEANO) REGIONAL DATA ASSEMBLY CENTER (RDAC) UPDATE

**Bruce McKenzie, Danielle Carpenter, Harron Wise, Valinda Kirkland, Michelle Little**

Naval Oceanographic Office, Stennis Space Center, MS (US)

### ABSTRACT

NAVOCEANO is a GHRSSST RDAC providing operational near real time L2P and L4 products made available to the global application community by the Physical Oceanography Distributed Active Archive Center at NASA's Jet Propulsion Laboratory in Pasadena, CA.

### INTRODUCTION

Details on the GHRSSST products generated and acquired by NAVOCEANO are presented along with SST matchup statistics that are calculated using satellite specific drifting buoy matchup databases.

### L2P AND L4 PRODUCTS PRODUCED

The current set of NAVOCEANO L2P GDSV2.0 products are MetOp-A, MetOp-B, and MetOp-C AVHRR 8.8km, and S-NPP VIIRS 750m. The NAVOCEANO L4 product is a 1/10<sup>th</sup> degree composite updated daily from operational SST retrievals generated by NAVOCEANO (MetOp-A FRAC, MetOp-B FRAC, S-NPP and NOAA-20 VIIRS, GOES-E, GOES-W, and Himawari-8), OSI-SAF (MSG1 and MSG4), and JAXA (AMSR-2) along with NCEI OISST 1/4° Climatology and the National Ice Center's daily ice edge. Figures 1 and 2 are plots of the polar orbiting NAVO and GHRSSST buoy SST matchup statistics. The buoy and satellite SST matchup thresholds are 1 hour and 10 km, except for AMSR2 which is 4 hours and 25 km.

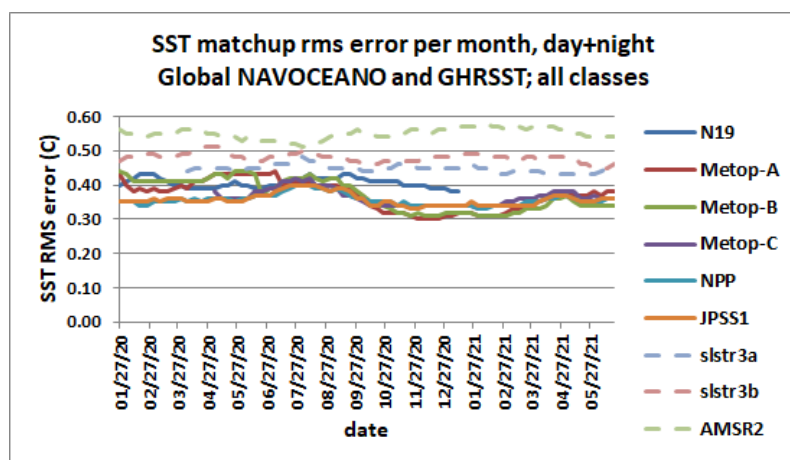


Figure 1. Polar orbiting L2P buoy matchup statistics (RMS)

### PLANS

Plans for 2021 are to discontinue MetOp-A SST processing due to the satellite being de-orbited, implement high latitude SST processing improvements developed by the Naval Research Lab at Stennis Space Center under the ONR MISST project, and to provide GOES-13 Indian Ocean coverage GHRSSST L2P products.

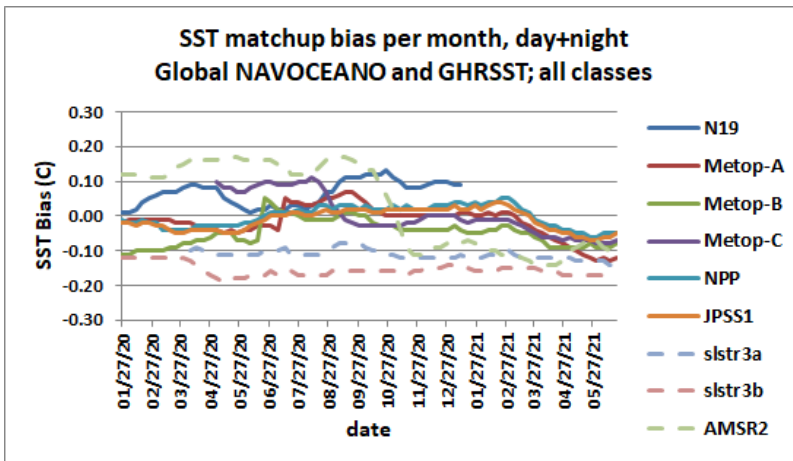


Figure 2. Polar orbiting buoy matchup statistics (bias)

**GHRSSST PRODUCTS USED BY NAVO**

NAVOCEANO operationally retrieves OSI-SAF MSG1 and MSG4 SEVIRI L3C data from the JPL PO.DAAC, GCOM-W AMSR2\_NRT from JAXA, and EUMETSAT Sentinel-3A/B SLSTR L2P from NOAA/NESDIS Center for Satellite Applications and Research (STAR), which has a terrestrial EUMETCAST feed of Sentinel-3 data. Figures 3 and 4 are plots of the buoy matchup statistics for the geostationary NAVO and GHRSSST SST data. The buoy and satellite SST matchup thresholds are 1 hour and 10 km, except for MSG1 and MSG4 which are 1 hour and 18 km. Please note that NAVO does not distribute to the PODAAC the GOES-16, GOES-17, and Himawari-8 SST data it generates.

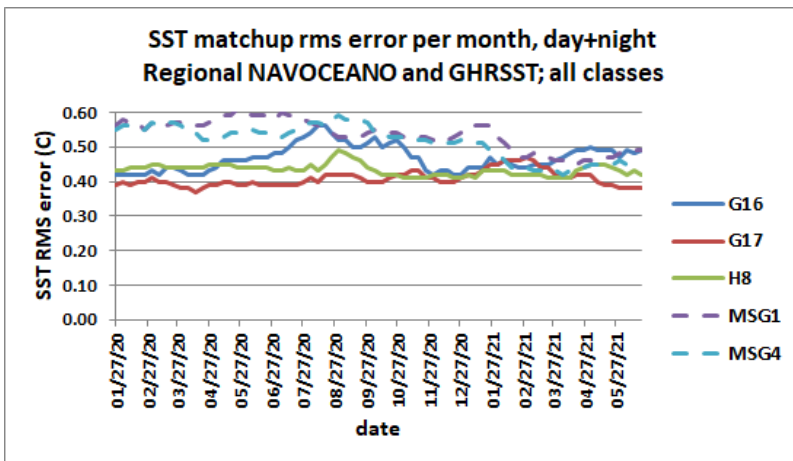


Figure 3. Geostationary buoy matchup statistics (RMS)

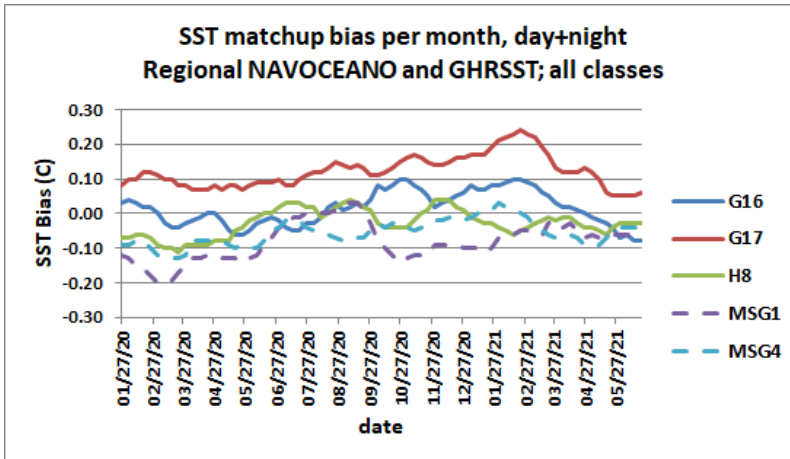


Figure 4. Geostationary buoy matchup statistics (bias)

### CONCLUSION

GHRSSST is a valuable source of SST data for NAVOCEANO and a collaborative group to work on issues that affect all aspects of SST.

Approved for public release; distribution unlimited



**GHRSSST**  
GROUP FOR HIGH RESOLUTION  
SEA SURFACE TEMPERATURE

The GHRSSST Project Office is funded by the European Union Copernicus Programme and is hosted by the Danish Meteorological Institute, Lyngbyvej 100, 2100 Copenhagen (DK)

E-mail:

Chiara Bearzotti, Project Coordinator, [gpc@ghrsst.org](mailto:gpc@ghrsst.org)

Pia Wind, Project Administrator, [gpa@ghrsst.org](mailto:gpa@ghrsst.org)



Follow us on Twitter: <https://twitter.com/ghrsst>

Website: <https://www.ghrsst.org/>

Zenodo: <https://zenodo.org/communities/ghrsst>



**Copyright 2021© Group for High Resolution Sea Surface Temperature (GHRSSST)**

This report has been edited by the GHRSSST Project Office.

This copyright notice applies only to the overall collection of papers: authors retain their individual rights and should be contacted directly for permission to use their material separately. Editorial correspondence and requests for permission to publish, reproduce or translate this publication in part or in whole should be addressed to the GHRSSST Project Office. The papers included comprise the proceedings of the meeting and reflect the authors' opinions and are published as presented. Their inclusion in this publication does not necessarily constitute endorsement by GHRSSST or the co-organisers.

GHR SST PRIORITIES



## **GHRSSST PRIORITIES: PANEL DISCUSSION**

### **SESSION REPORT**

**Anne O'Carroll**<sup>(1)</sup>, **Gary Corlett**<sup>(2)</sup>

(1) EUMETSAT, Darmstadt, Germany, Email: [anne.ocarroll@eumetsat.int](mailto:anne.ocarroll@eumetsat.int)

(2) EUMETSAT, Darmstadt, Germany, Email: [gary.corlett@eumetsat.int](mailto:gary.corlett@eumetsat.int)

### **INTRODUCTION**

This report summarises the GHRSSST Priorities panel discussion, which took place on Wednesday 9<sup>th</sup> June 2021 from 13:00 to 14:30 UTC.

The discussion comprised three groups of invited panellists who were asked to give their views in three main areas.

- Panel discussion 1: Regional SSTs
- Panel discussion 2: Coupled assimilation
- Panel discussion 3: Data access and usage

Participants were then able to directly ask questions to the presenters or post comments in the chat function.

*Link to recording available to participants:* <https://training.eumetsat.int/mod/page/view.php?id=14678>

## PANEL DISCUSSION 1 – REGIONAL SSTS

### Seed question

What progress is GHRSSST making with regard to the user priorities on Observational Needs for SST as set out in the Ocean Obs 19 white paper e.g. Arctic, coastal, feature resolution? What still needs to be done?

### Panellists

- Jacob Hoeyer (DMI)
- Christo Whittle (CSIR)
- Chris Merchant (University of Reading)
- Marouan Bouali (University of Sao Paulo)

### Highlights

- GHRSSST should update the GDS specification to accommodate sea-ice ST
- GHRSSST should consider dedicated coastal SST products
- GHRSSST should use AI and new generation algorithms to improve features in L4 analyses

### Summary of feedback from panel and discussion

- GHRSSST has made good progress on the Arctic, especially securing future passive microwave (PMW) data (CIMR, AMSR3). However, some challenges remain.
- Improved exploitation of PMW data is needed in L4 analyses as many have issues in regions of persistent cloudiness.
- Improvements are needed in tying infrared (IR) and PMW data in general and not just in the Arctic.
- Knowledge of how SST varies around the ice edge is needed, especially for climate models.
- Merging of PMW data with IR data is needed for CDRs to investigate potential clear-sky biases.
- Better quality in situ data, including FRM, are needed.
- Future field campaigns should also focus on the next generation of PMW sensors.
- Progress is still needed on coastal zone SSTs.
- Coastal zones are complicated as their orientation and bathymetry mean most coastal areas are unique. A specialise interest group is needed.
- There are obvious benefits from hi-res imagery but how does GHRSSST take advantage when most products are global.
- Dedicated case studies linked to operational products are needed.
- Improvements needed to retrievals and masking owing to higher variability in coasts.
- Additional challenges arise in accounting for nearshore versus estuarine SSTs.
- How good are coastal in situ for assessing CDRs?
- Other developments have a focus on coastal zones, e.g., the CEOS COASTS project, and it is noted that UN recently announced a decadal focus on coasts.
- Users not always using the most appropriate data – better guidance is needed.
- Interdisciplinary approach needed – need other data, e.g., winds, chlorophyll.

- Useful for cloud application as internet connections are limited in some countries
- Are we fully exploiting capabilities of GEO sensors?
- Some progress has been made on feature resolution
- GHRSSST should provide a metric on how well features are preserved; this is usually done using spectral analysis but new methods are needed.
- Improvements in cloud masking, especially over-flagging at fronts.
- Consistency between L2 and L4 needs to be improved

**Priorities actions for GHRSSST**

- GHRSSST should update the GDS specification to accommodate sea-ice ST
- GHRSSST should consider dedicated coastal SST products
- GHRSSST should use AI and new generation algorithms to improve features in L4 analyses

## PANEL DISCUSSION 2 – COUPLED ASSIMILATION

### Seed question

What are the needs of coupled ocean atmosphere NWP for satellite SST and how can GHRSSST contribute to this?

### Panellists

- Tony McNally (ECMWF)
- Xu Li (NOAA NCEP)
- Helen Beggs (BoM)
- Simon Good (Met Office)

### Highlights

- GHRSSST should evaluate options for provide SSES-type adjustments or observation errors for radiances.
- GHRSSST RDACs should provide a pre-operational data stream for a minimum of 3 months when implementing evolutions.
- GHRSSST should continue coordination with NWP teams and those involved with direct assimilation, particularly on verification, validation, skin effect, diurnal variability model, and evolving L2 to L4 needs.

### Summary of feedback from panel and discussion

- Developments in coupled model assimilation are focussed in two areas: (1) direct IR radiance assimilation and (2) assimilation of retrieved SST fields.
- Direct IR radiance assimilation requires access to high quality radiances in real time.
- Users need guidance on how to use IR radiances, how well IR radiances are calibrated, and how to cloud screen IR radiances.
- Direct assimilation also requires observation, understanding and modelling of key processes, e.g. the skin effect, diurnal variability, and how to better quantify the meteorological variability of such processes
- Studies are needed on how to calibrate data assimilation systems (e.g. NEMOVAR) for high spatial resolution measurements.
- Is there scope for using SSES with radiances? This is possible but they would need to be RTM dependent, which would need to be the same as used in the NWP system.
- Assimilation of Level 2 SST fields into coupled models is similar to how Level 4 analyses are generated, but with a different treatment of uncertainties. Are the current SSES relevant for coupled NWP?
- Important to have testing if GHRSSST format products change. This is straight forward for Level 4 analyses but is much more challenging for coupled assimilation systems.
- Timeliness is important for coupled assimilation, especially in the Tropics. Most L4 analyses have a wide window, which is not true for NWP systems that are run multiple times daily.
- Important to carry out inter-comparisons between coupled model outputs and dedicated SST analyses/retrievals.
- Coupled assimilation has stricter requirements on  $SST_{skin}$  measurements – 3 hourly, < 5 km resolution, < 0.1 K uncertainty. This level of accuracy will require improved harmonisation across the constellation.

- Residual data artefacts will be an issue, especially at small scales (< 10 km). Better to use a global DA system to remove e.g. atmospheric effects, although such effects will still be present in a DA system, especially where tightly coupled.
- Also, there are issues at fronts when representing heat fluxes as the atmosphere will usually have a scale length not seen in the ocean front.

#### **Priorities actions for GHRSSST**

- GHRSSST should evaluate options for provide SSES-type adjustments or observation errors for radiances.
- GHRSSST RDACs should provide a pre-operational data stream for a minimum of 3 months when implementing evolutions.
- GHRSSST should continue coordination with NWP teams and those involved with direct assimilation, particularly on verification, validation, skin effect, diurnal variability model, and evolving L2 to L4 needs.

## PANEL DISCUSSION 3 – DATA ACCESS AND USAGE

### Seed question

- What progress has been made in GHRSSST to consider Artificial Intelligence / Machine Learning techniques and applications, and what more can be done?
- How can GHRSSST better promote open science and open data not only in the SST community but also for related ocean and atmospheric measurements? Are there things we can do in our community to improve the sharing of results besides publications?

### Panellists

- Ken Casey (NOAA)
- Chunxue Yang (CNR)
- Jean-Francois Piolle (Ifremer)
- Ed Armstrong (NASA)
- Misako Kachi (JAXA)

### Highlights

- GHRSSST should engage more with computational experts to develop new explainable AI methods and increase beneficial activities using machine learning
- GHRSSST should take steps to ensure GDS format products are cloud-ready and available via cloud services
- GHRSSST should provide simple guides and open access tools for exploiting SST data available via cloud services

### Summary of feedback from panel and discussion

- Progress is not good in using AI/ML methods.
- AI/ML is not a panacea and appropriate conditioning of the data is required.
- GHRSSST format data held by the PO.DAAC moving to the cloud. What about data from other agencies?
- Guidance is needed for users on how to access GHRSSST format data in the cloud.
- Best practices are needed for data sharing in cloud environments, especially for PI provided science data.
- The SST community needs to get more computational experts involved in its activities
- Some groups are now incorporating physical constraints into AI schemes, called explainable AI.
- Progress on open science and open data access is slow.
- GHRSSST should engage with CEOS on ARD and open data cubes to get better exploitation of data amongst other communities.
- GHRSSST should ensure its data catalogues link to data stored in the cloud.
- GHRSSST should exploit new image processing techniques.
- GHRSSST should address data format issues, especially with the current GHRSSST data format, and consider ARD and ZARR formats.
- Need to ensure consistency between different platforms – cannot end up with inconsistencies between different approaches to cloud storage and access.
- Cloud processing is a steep learning curve for users and GHRSSST needs to help them with using new capabilities.

- Sharing tools and methods using open source environments is essential.
- Current project funding is not used to pay per use and not necessarily set-up for these type of projects. Funding bodies and agencies need to adapt to these new approaches.
- GHRSSST should ensure there are people with specific skills to interact with users by providing simple guides for use by intermediaries.
- GHRSSST should make sure GHRSSST format data is searchable via Google and other search engines/
- GHRSSST needs to ensure traceability as new platforms mean data is further away from the producers.
- GHRSSST should consider usage based discovery.

#### **Priorities actions for GHRSSST**

- GHRSSST should engage more with computational experts to develop new explainable AI methods and increase beneficial activities using machine learning
- GHRSSST should take steps to ensure GDS format products are cloud-ready and available via cloud services
- GHRSSST should provide simple guides and open access tools for exploiting SST data available via cloud services



**GHRSSST**  
GROUP FOR HIGH RESOLUTION  
SEA SURFACE TEMPERATURE

The GHRSSST Project Office is funded by the European Union Copernicus Programme and is hosted by the Danish Meteorological Institute, Lyngbyvej 100, 2100 Copenhagen (DK)

E-mail:

Chiara Bearzotti, Project Coordinator, [gpc@ghrsst.org](mailto:gpc@ghrsst.org)

Pia Wind, Project Administrator, [gpa@ghrsst.org](mailto:gpa@ghrsst.org)



Follow us on Twitter: <https://twitter.com/ghrsst>

Website: <https://www.ghrsst.org/>

Zenodo: <https://zenodo.org/communities/ghrsst>

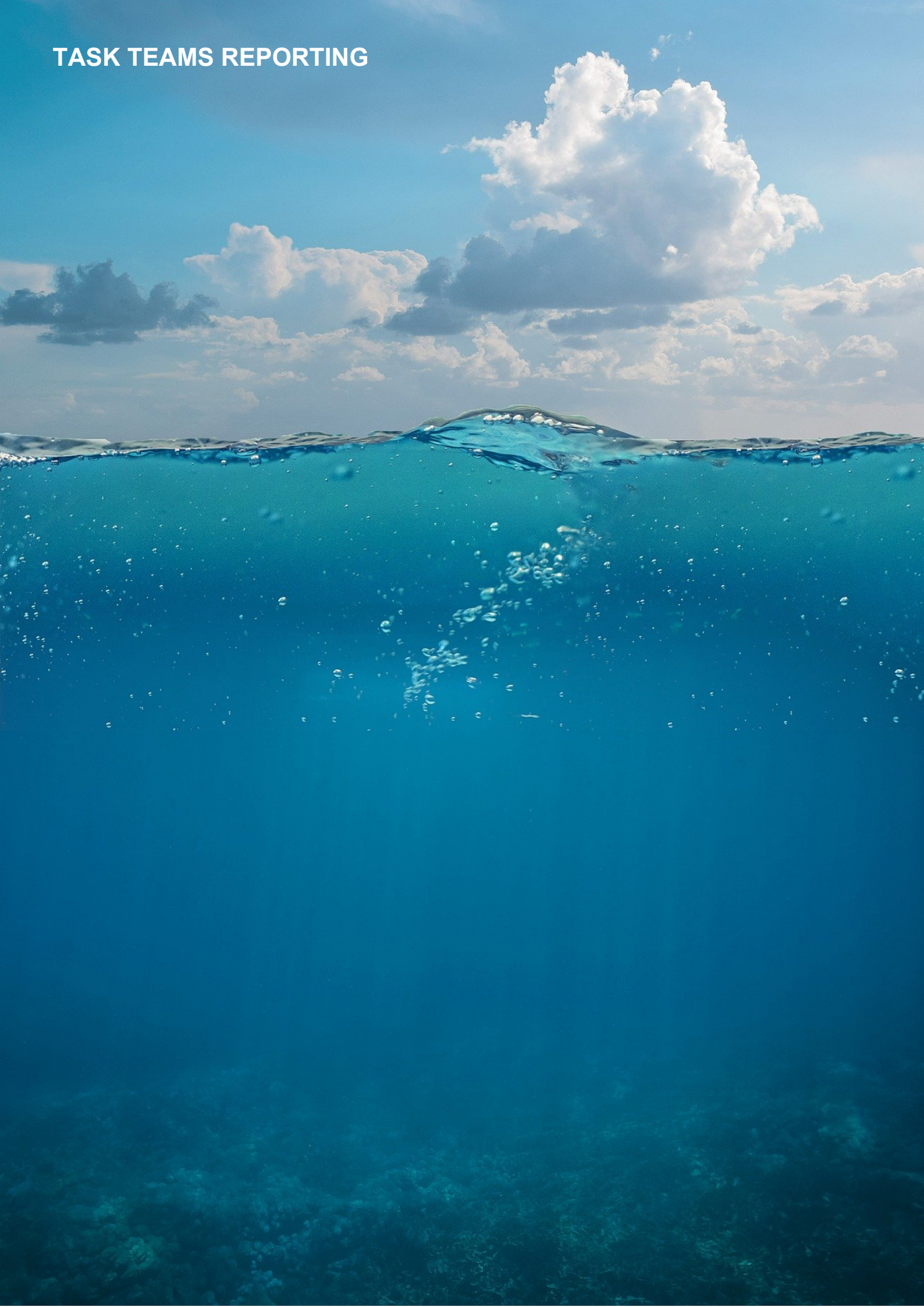


**Copyright 2021© Group for High Resolution Sea Surface Temperature (GHRSSST)**

This report has been edited by the GHRSSST Project Office.

This copyright notice applies only to the overall collection of papers: authors retain their individual rights and should be contacted directly for permission to use their material separately. Editorial correspondence and requests for permission to publish, reproduce or translate this publication in part or in whole should be addressed to the GHRSSST Project Office. The papers included comprise the proceedings of the meeting and reflect the authors' opinions and are published as presented. Their inclusion in this publication does not necessarily constitute endorsement by GHRSSST or the co-organisers.

# TASK TEAMS REPORTING



## **HIGHLIGHTS OF THIS SESSION**

- Development of Climate Data Assessment Framework (CDAF) in progress, Felyx stand-alone Match-Up Database (MDB). Assessment of existing MDB methodologies as a way forward for homogenisation.
- Inter-comparison activity for shipborne radiometers being planned. Ongoing effort to share good practises and create new methods for optimal cloud masking. Efforts to understand and characterise Single Sensor Error Statistics (SSES). Focus on improving High Latitude SST (in situ data collection, dry atmosphere corrections).

**TASK TEAM REPORTING 1**

**CLIMATE DATA ASSESSMENT FRAMEWORK**

**GHR SST MDB**

**FEATURE RESOLUTION**

## TASK TEAM REPORTING 1 - SESSION REPORT

**Chair: Werenfrid Wimmer<sup>(1)</sup>, Rapporteur: Rosalia Santoleri<sup>(2)</sup>**

(1) University of Southampton, Southampton, UK, Email: [w.wimmer@soton.ac.uk](mailto:w.wimmer@soton.ac.uk)

(2) Consiglio Nazionale delle Ricerche – Istituto di Scienze Marine, Venice, Italy , Email: [rosalia.santoleri@cnr.it](mailto:rosalia.santoleri@cnr.it)

The Task Team Reporting 1 session was held on Monday 7th June 2021, between 13.30 and 15.00 UTC.

### RESOURCES

Link to recording available to participants: <https://training.eumetsat.int/mod/page/view.php?id=14678>

### INTRODUCTION

Sea surface temperature (SST) is an “essential climate variable”. The accuracy of SST data is crucial to evaluation of climate and ocean models, observational quantification of climate change and variability. The Task Teams 1 Section was devoted to the three GHRSSST Task teams reports aiming to assess the accuracy of SST and provide information on the SST data quality. In GHRSSST Task Teams are established by the GHRSSST Science Team to address particular crucial issues which requires collaboration among the GHRSSST members. Each Task Team reports at the GHRSSST meeting on the activities carried out during the year and the results achieved. In particular, the Task Teams 1 Section of GHRSSST 2021 there were three the GHRSSST Task teams presentations:

- Climate Data Assessment Framework Task Team, presented by Jon Mittaz
- GHRSSST Matchup Database Task Team, presented by Igor Tomazic
- Feature Fidelity Task Team, presented by Peter Cornillon

### CLIMATE DATA ASSESSMENT FRAMEWORK (CDAF) TASK TEAM

Dr. Jonathan Mittaz from University of Reading opened the section reporting the activity carried out by CDAF Task Team. This task team has been established several years ago with the aim to support users of sea surface temperature (SST) datasets to understand the suitability of GHRSSST datasets for use as Climate Data Records. This year a preliminary step to develop a CDAF Tool Workflow has been achieved, the felyx MMDB generation system has been being upgraded to run both in distributed mode or in an easily installable standalone single machine. The system has been tested with success. JF Pilot then presented tool based on FELIX showing the resulting matchup database produced, After the presentation on the tool Charles Brown asked details how the matchup has been created. At the end it was decided to maintain this task team.

### GHRSSST MATCHUP DATABASE (MDB) TASK TEAM

The report on MDB Task Team was presented by Dr. Igor Tomazic from Eumetsat. He recalled that this task Team was recently established at GHRSSST XX, 2019, and sees the participation of researchers of several organization. The objective is to suggest the way forward towards common SST MDB production method and assessment metrics and protocols. The team decided to start with a review of the methodologies common used for MDB by: collecting relevant journal papers explaining different MDB criteria's; preparing a list of MDB tools applied by the different agencies that could be used for a intercomparison exercise and tools. The identification of metrics and protocols in SST analysis the preparation of a list of validation and referent types of data and datasets is ongoing. These will allow to define a round robin validation SST MDB intercomparison exercise to be carried out in the 2022. The Task Team proposed also to prepare a White Paper.

### **FEATURE FIDELITY TASK TEAM**

Prof Peter Cornillon from University of Rhode Island reported on the Feature Fidelity Task Team activities. The objective of this Task Team is to address the impact of artifacts and noise in satellite-derived SST fields on the faithful reproduction of mesoscale and smaller oceanographic features: fronts, eddies, gradients. The task team aims to categorize the classes of problems contributing to the uncertainty associated with mesoscale to submesoscale features and, to the extent possible, outline a methodology for quantifying these effects. To achieve this goal the Task Team identified three tasks: 1) the classification of the types of features to be considered, 2) the identification of the 'effects' important for the characterization of the uncertainties associated with these features and 3) putting it all together outlining approaches to determine the uncertainty relevant to the study of mesoscale through submesoscale features observed in SST fields. Examples of corrupted field were presented providing indication of the origin of errors could derived from L1 data to any step of the processing. To better understand the problem a study was carried out analysis the SST variance in clear sky condition. Boxes of 125 x125 pixels with cloud cover less 95% were extracted from L2 MODIS Aqua SST data at global scale and used to compute the statistics. This analysis showed a well-defined linear dependence of variance on mean SST and a the presence also of local dependence of the SST accuracy. The task Team proposed two broad categories of approaches to determine the uncertainty in satellite-derived SST fields of importance in the study of mesoscale and smaller features: 1) propagation of known errors through the processing system; 2) analysis of the retrieved SST fields. These two approach should be combine in order to produce an estimation of the error associated to feature fidelity. There was a long discussion on the possible source of errors that can created this variance dependence from SST value which requires further investigation.

### **CLIMATE DATA ASSESSMENT FRAMEWORK (CHAIR: JON MITTAZ)**

John Mittaz (JM) gave a short presentation on the envisaged Climate Data Assessment Framework (CDAF) Task Team (TT) framework. This will include a number of tools, including a tool to populate the CDAF from data, CDAF metrics and stability tools.

Discussion:

Charlie Barron (CB): The match-up number seems low.

Jean-François Piollé (JFP): Only moored buoys were used.

CB: What is the window size?

JFP: 2h and 50 km.

CB: Models / would expect more match-ups, but maybe it is because moored buoys were used.

JFP: Only half were used per match-up.

Peter Cornillon (PC): This, at the moment, only covers absolute precision, but we also need to think of precision in climate application of high gradient and low gradient regimes.

Jon Mittaz (JM): Agrees, the CDAF TT starts from the lowest denominator, simple statistics, and work from there. It should be very simple to use the framework to add more complicated statistics later.

Ed Armstrong (EA): Good progress! What about the flexibility of the system, such as open API? Running experiments through scripts?

JM: No code has been written to date. But no experience on API design in the current team. JM invites EA to join the team.

EA: Could help with requirements.

JM: EA's help would be great.

JFP: System at the moment very static, every provider makes their own match-ups. MDB sent to CDAF. CDAF has no server or website and no processing hardware at the moment. Only the results/statistics get published at CDAF web page. The tools provided can have flexibility.

Gary Corlett (GC): CDAF form code is on the CCI repository, including example.

Jorge Vazquez (JV): Has the accuracy increased with the number of match-ups?

JM: No analysis has been carried out on that.

GC: THE GMTBA array is for stability not for coverage. Drifting buoys are used for coverage.

Andy Harris (AH): Window on Argo floats approx. 100 / day, but 5m depth SST won't change much over time. Argo is maintained at approx. 4000 floats globally.

JM, GC: No information on that, Matches in the tropics mainly at night, but even with a 6h time window not enough data.

**GHRSSST MDB (CO-CHAIRS: IGOR TOMAŽIĆ AND JEAN-FRANÇOIS PIOLLÉ)**

Igor Tomažić (IT) gave a presentation summing up the progress in the last year. This included a spreadsheet with the currently in use MDB's and the metrics and protocols used. He suggest a MDB match-up methods analysis form the GHRSSST ST, and functionality of MDB tools. The timeline for development is to have match-up metrics by the end of 2021 and a MDB round robin in 2020.

Discussion:

Where can the MDB data be accessed?

IT: We do not produce the MDB data, so no central access point. Additional data produced on the existing MDB will be available next year as will be a test data set.

Chris Merchant (CM): One of the big differences of the MDB's is the quality control (QC) on the in-situ data, any thoughts on this by the TT?

IT: We propose to us input data without any QC and then use different QC methods to see the effect on the MDB.

## FEATURE FIDELITY (CHAIR: PETER CORNILLON)

Peter Cornillon (PC) gave a presentation on how to assess the precision of features rather than absolute precision. He also showed an example of MODIS data where the along scan SST has a temperature dependence affects the feature precision. He followed this up by suggestion to improve SST products feature precision by adding information on the precision of the cloud function to the data products and asked for user to identify and report feature fidelity issues.

Discussion:

Charlie Barron (CB): The plot around Africa; is this an aerosol/dust effect?

PC: Can it be dust if it is east of Africa?

Andy Harris (AH): There is lots of dust on the Arabian Peninsula.

PC: Why would dust reduce  $\sigma_s$  with high SST? This is feature precision not absolute SST. See also Chris Merchants talking in cloud TT.

AH: IT is an algorithm feature, which product was used?

PC: MODIS L2 Goddard R29 NLSST / split widow algorithm.

AH: It is an effect of the gamma function in NLSST.

PC: Specific to that: Gradients resolve better in mid high latitudes.

AH: Algorithm sensitivity issue: split window algorithm in high water vapour region has low SST sensitivity. Have you used other products?

PC: No.

Peter Minnett (PM): Agrees with aerosol/ uncorrected aerosol issue; should use smaller length scale SST function?

PC: We just used one product to show issues; there is no indicator to data users on these issues.

PM: Just commenting on what can contribute to the issues.

Jorge Vazquez (JV): Have you tried using Saildrone data to validate structures?

PC: Used shipborne data; MDB needs to focus on feature precision on just absolute SST.

?: Hints that NLSST in high temperature issues.

PC: Interesting, shows SST dependence plots with outliers. SST standard deviation goes from 0.03K to 0.25K

CB: Wind speed effect?

PC: Should be taken care of.

Rosalía: What is the impact on finding fronts?

PC: Big impact, especially on finding weak fronts.

JV: Would it be helpful to have information on that in the data?

PC: would be great.

Nicolás Weidberg (NW): What is the impact on products, new product with 70m resolution?

PC: Problem is the retrievals. Higher resolution retrieval should be better, see more of the front.

CM: SST sensitivity will show you fronts. Linear variable in MDB, tracks the aerosol front.

IT Not yet in MDB

JM: SST sensitivity use the CDAF, needs to be provided by the data producers, not yet in GDAC.

PC: Sensitivity not noise on gradient.

CM: uncertainty in algorithm; DP + Noise in SST + sensitivity of SST. Under/over correction of water vapour will do exactly what PC has shown. PC: The information is there but not in L2 data.

CM: Not on the GDS (not a standard variable) but as optional variables in the CCI product.

Helen Beggs (HB): All TT seem to talk about the same issue. SST sensitivity seems important; do we need an update to the GDS with a new field and the algorithm used? Needs to be propagated from L2, L3 and L4.

CM: Need to use it in a user community first. Maybe CDAF TT?

Owen Embury: It is in the CCI product as an optional variable.

[https://climate.esa.int/media/documents/SST\\_CCI-PSD-UKMO-201-Issue-2-signed.pdf](https://climate.esa.int/media/documents/SST_CCI-PSD-UKMO-201-Issue-2-signed.pdf)

Veronica Lance - NOAA: We have a "split" in users: Some of our "power" users are very interested in robust data characterizations (uncertainties, sensitivities) while others have no interest and basically "trust" the measurement as presented.

AH: To clarify - the methodology outlined in the Merchant et al. GRL requires Jacobean information (dB<sub>T</sub>/dSST) for each pixel. So if you're not running RTM as part of your processing, it will be difficult

Also, for algorithm sensitivity, see <https://agupubs.onlinelibrary.wiley.com/doi/full/10.1029/2009GL039843>.

**Chat questions:**

From Jorge Vazquez: Is there any evidence that the accuracy of the SSTs improve with the number of matchups?

From Chris Merchant: There is only one match per day per place because it is L4

From Chris Merchant: That would be right.

From Charlie Barron : So when I said "the number of matchups seems low", that would be from a level 2 frame of mind and using fixed and drifting buoys; for Metop, NAVOCEANO gets over 20K matchups per month; 40000 per month for VIIRS

From Jim Carton: does the temporal variability correspond to dust outbreaks?

From Marouan Bouali: With respect to Andy's question and for anyone interested on the linear dependency of sigma (SST) on SST, the following paper addresses this issue when using NLSST:

<https://www.tandfonline.com/doi/abs/10.1080/2150704X.2019.1666312?journalCode=trsl20>

From Charlie Barron: I agree that the fidelity in representing gradients and features is a useful area for understanding the limits of using these data for assimilation into and validation of ocean and coupled models

From c : @peter I suspect the aerosol is leading to the smoothed signals in the Sst plot (there be are huge aerosol loads in the Arabian Peninsula) I would also suggest you consider the impact of stratification that will.

Mask surface features in summer time. In the Gulf Stream salinity provides a better measure of structures (see papers of Reul et al on SMOS salinity in N Atlantic)

From Andy Harris: Also, for algorithm sensitivity, see

<https://agupubs.onlinelibrary.wiley.com/doi/full/10.1029/2009GL039843>

From Andy Harris: If you've removed the geophysical SST structure, then I'm sure it's the NLSST "gamma" term, which is directly dependent on SST. The 2-d histogram even shows the different gradients for the "low-to-mid" and "mid-to-high" water vapour retrieval conditions

From Ed Armstrong: SST sensitivity could be added as an experimental variable if the producer can provide it.

From John Kennedy : Do you have info about the error correlations to go with the pixel by pixel uncertainty info that you'd need for assessing spatial gradients and more complex features?

From Owen Embury: The SST-CCI products include SST sensitivity and per-pixel uncertainty estimates as additional fields. Product Specification is available here: [https://climate.esa.int/media/documents/SST\\_CCI-PSD-UKMO-201-Issue-2-signed.pdf](https://climate.esa.int/media/documents/SST_CCI-PSD-UKMO-201-Issue-2-signed.pdf)

From Chris Merchant: @John. Yes, we understand which components of uncertainty are independent between adjacent pixels and which are shared.

From Veronica Lance - NOAA : We have a "split" in users: Some of our "power" users are very interested in robust data characterizations (uncertainties, sensitivities) while others have no interest and basically "trust" the measurement as presented.

From Andy Harris: To clarify - the methodology outlined in the Merchant et al. GRL requires Jacobean information (dB<sub>T</sub>/dSST) for each pixel. So if you're not running RTM as part of your processing, it will be difficult.

## CDAF TOOL TASK TEAM

**Jonathan Mittaz**<sup>(1)</sup>, **Prasanjit Dash**<sup>(2)</sup>, **Jean-Francois Piolle**<sup>(3)</sup>

(1) University of Reading, Reading, UK, Email: [j.mittaz@reading.ac.uk](mailto:j.mittaz@reading.ac.uk)

(2) NOAA, NCWCP, College Park, MD, USA, Email: [prasanjit.dash@noaa.gov](mailto:prasanjit.dash@noaa.gov)

(3) Ifremer, Brest, France, Email: [jean.francois.piolle@ifremer.fr](mailto:jean.francois.piolle@ifremer.fr)

## INTRODUCTION

One of the primary documents of the GHRSSST Climate Data Record Technical Advisory Group (CDR TAG) is the Climate Data Assessment Framework or CDAF (<https://zenodo.org/record/4700356>). The CDAF outlines a proposed set of metrics to support users of sea surface temperature (SST) datasets in understanding the suitability of GHRSSST datasets for use as Climate Data Records (CDRs). It aims to provide authoritative, comparable information about GHRSSST datasets that will allow users to make their own judgment about use of the datasets as CDRs for their application and is currently aimed at datasets in GHRSSST GDS2.0 format. The proposed metrics include checks on basic information such as the length of the record and if the data is GDS2 compliant to statistical tests looking at different aspects of the dataset including standard global statistics as well as regional statistics on a ~1000km scale. Information regarding SST trends are also included. As a summary the CDAF defines a 2 page form to be filled out which is then used as the basis for review by the CDR TAG.

Since the release of the CDAF there has only been minimal uptake of the CDAF process by GHRSSST dataset producers, in part because of the logistics of calculating the required statistics. The CDAF tool task team was therefore set up to design and implement a tool to support different GHRSSST dataset producers in generating the required statistics using a consistent reference dataset.

## PROGRESS TO GHRSSST XXII

Some progress has been made towards developing the CDAF tool in the past year. First, we have begun to setup processes to provide the required matchup datasets from which the statistics are derived. This is based on the felyx system (<http://hrdds.ifremer.fr>) which is being updated to support two modes of operation

- 1. in distributed mode (as currently): runs on a cluster, intended for large scale and operational processing**
- 2. as an easily installable standalone running on a single machine: for local processing, testing and evaluation => easier to run and use in the context of the CDAF toolbox (but slower as using less computing resources)**

In terms of the CDAF tool we are working on the premise that the second mode (standalone operations) would be the one utilized by most users. This assumption will, of course, be tested as part of our project.

Using the felyx system we have already created two matchup datasets. One used the AVHRR L3C from the CCI Project and the other used the OSTIA L4 from CMEMS. Both were matched with the GTMBA moored buoy dataset from the CCI SST project. These two matchup datasets will then be used to start testing the next steps in the tool development. An example of the number of matches in one of the datasets is shown in Figure 1.

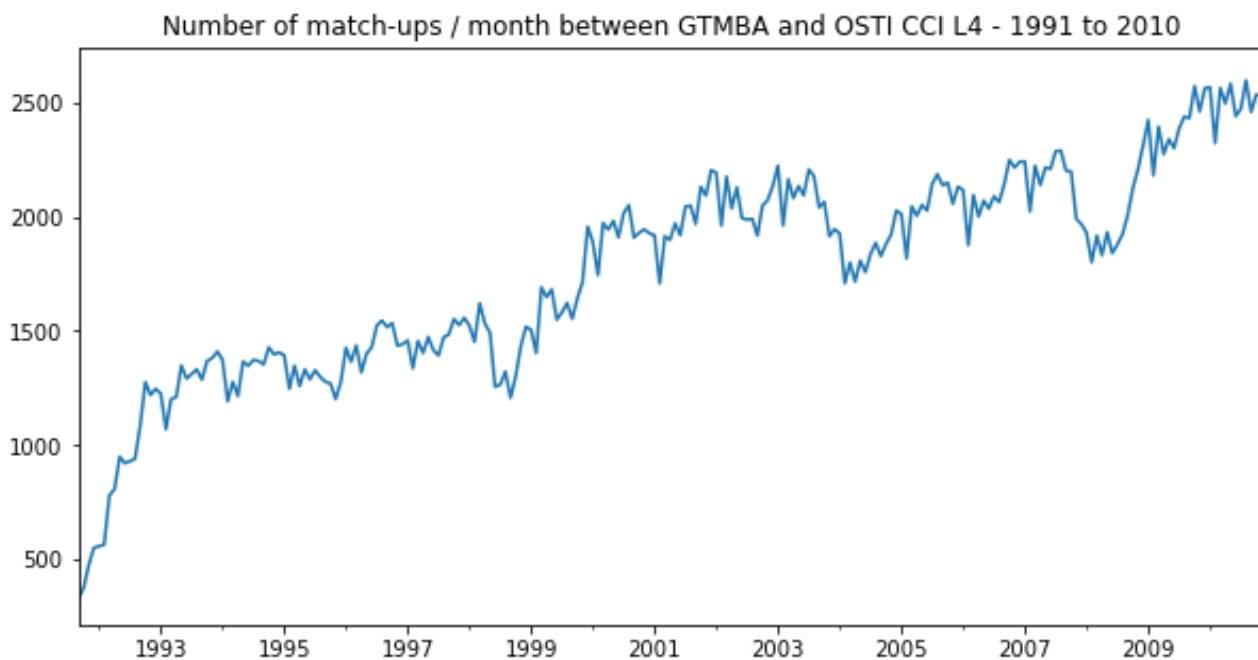


Figure 1 Time series of number of matches in one of the matchup datasets derived using the felix scripts setup for the CDAF tool.

In terms of the tool development, we have also started to investigate different code bases and algorithms that will be needed. To begin with the SST team at Meteo-France kindly provided some of their python code for us to look at which has helped kick-start our thoughts on the software design. Further, after the discussion session from the GHRSSST XXII meeting we will try and design the statistical modules to be flexible regarding the exact statistics/maps that can be created. To help with this we will leverage of the experience of Ed. Armstrong (who has agreed to join the team) from the NASA PO.DAAC at JPL. In the next year we will therefore be designing and writing the code to generate the statistics.

We have also started thinking about the user interface for the tool. There will, of course, be a number of steps in running the tool including running the matchup scripts on a user's particular GHRSSST dataset (which has to be GDS2.0 compliant) and running code to generate the raw statistical information. Once the statistics have been generated and stored the values/trends etc. will then be viewed through a bespoke interface which will both provide the information to fill out the CDAF assessment table. It is also planned that it will also provide an interactive interface to delve in more depth into the data which may be used to further improve the CDAF process. Some initial design concepts for this interface have been made and are shown in the following figures. Figure 2 shows our initial thoughts on the overall design of the interface including help sections, tutorials and interfaces into the analysis and CDAF statistics sections. Figure 3 shows a possible design for drop down menus which would drive the interactive analysis. And Figure 4 shows an example of a plotting pane with associated dropdown menus. As we progress we will, of course, update such designs as needed.

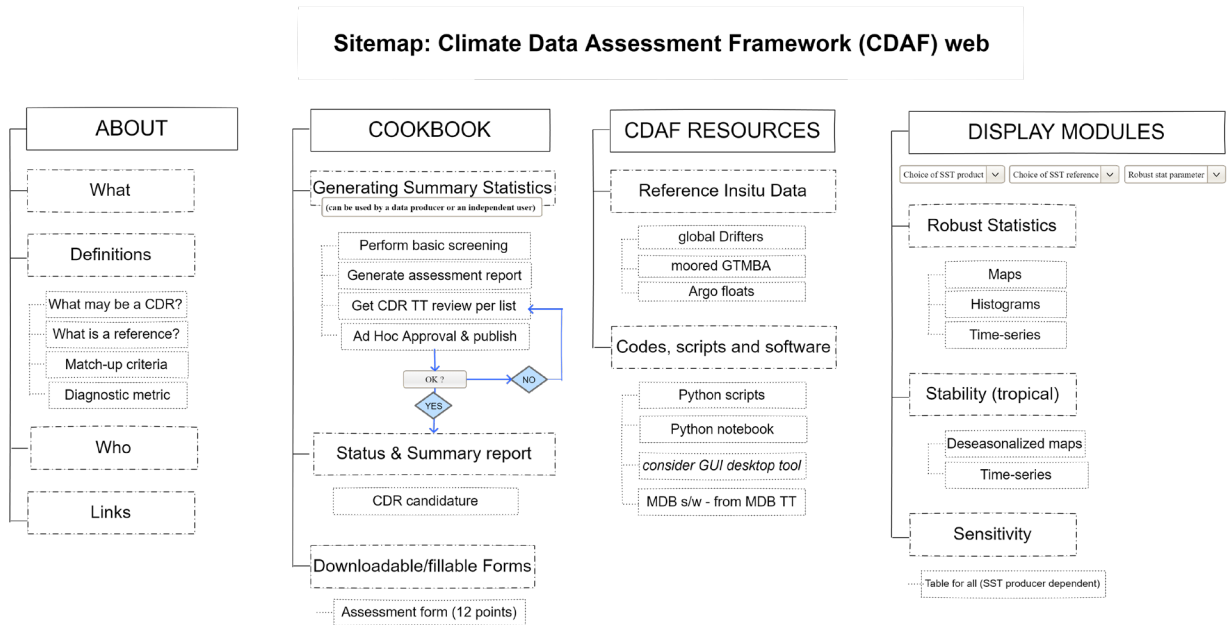


Figure 2 Overall design concept for the user interface into the interactive analysis tool for the CDAF

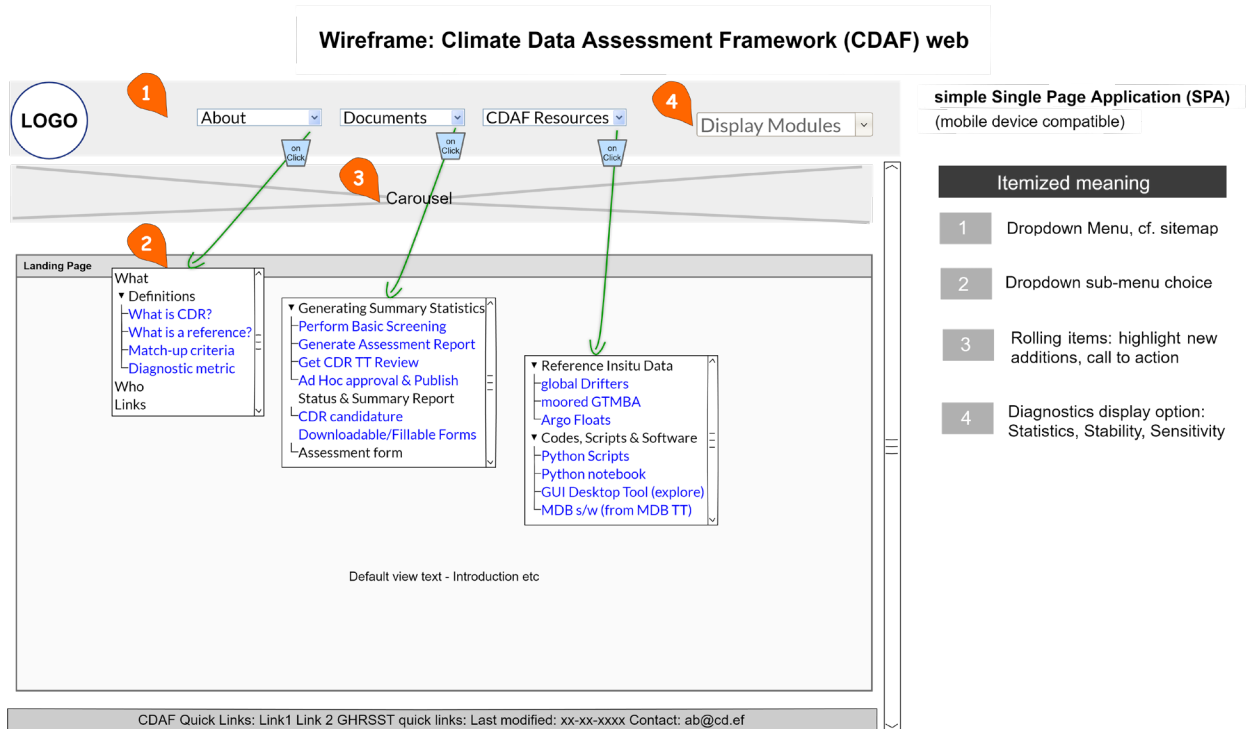


Figure 3 Potential design of dropdown menus of the CDAF analysis tool interface

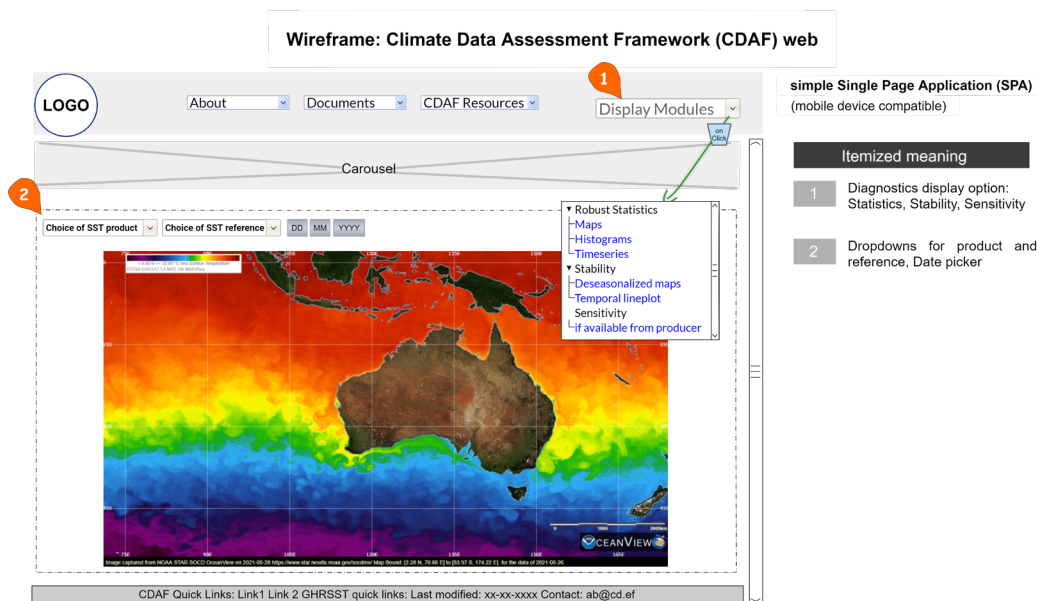


Figure 4 Showing an example of a plotting pane for the user interface

## NEXT STEPS

In the next year we will be tracking and incorporating developments in the felyx system liaising with the GHRSSST Matchup Database Standards task team of which Jean-Francois is also a member. We will also start developing the statistical code in earnest leveraging again where possible on extant code bases. For example, along with the Meteo-France code we are already aware of IDL code available from Gary Corlett from EUMETSAT which was an initial attempt at code to generate CDAF statistics which was shown at GHRSSST XV. Finally, we will also start a more detailed design for the interface based on Prasanjit's extensive experience in user interfaces into SST and associated products at NOAA. This work will be reported at the next GHRSSST meeting (GHRSSST XXIII).

**TASK TEAM REPORTING 2**

**SHIPBORNE RADIOMETRY**

**CLOUD MASKING SSES AND L4**

**HIGH LATITUDE SST**

## TASK TEAM REPORTING 2 - SESSION REPORT

**Chair: Owen Embury<sup>(1)</sup>, Rapporteur : Jean-François Piollé<sup>(2)</sup>**

(1) University of Reading, UK, Email: [o.embury@reading.ac.uk](mailto:o.embury@reading.ac.uk)

(2) IFREMER, France, Email: [Jean.Francois.Piolle@ifremer.fr](mailto:Jean.Francois.Piolle@ifremer.fr)

The Task Team Reporting 2 session was held on Tuesday 8th June 2021, between 13.30 and 15.00 UTC

### RESOURCES

Link to the recording available to participants: <https://training.eumetsat.int/mod/page/view.php?id=14678>

### SHIPBORNE RADIOMETRY (WERENFRID WIMMER)

Objective of task team is to setup network of data providers and users to define data formats and standards for inter-comparison etc.

- Website: <https://www.ships4sst.org/>
- Data available from IFREMER FTP site (access instructions on ships4sst website).
- Data format L2R (similar to L2P but focused on in situ radiometer measurements).
- Covid-19 pandemic caused significant disruption data collection as most instruments carried on cruise ships.
- An intercomparison activity is being planned. Location is currently under discussion and should be defined by 2022. Feasibility will also depend on future travel restrictions.

#### Discussions:

- Are data available via GTS? No – data are not available in real-time so are not suited for distribution via GTS.
- What are the requirements for the inter-comparison location? Basically, the longer the pier the better so long as the site has electricity and is accessible. In addition, site should be quiet (summer leisure activities on water would interfere with work) and with low currents.
- Charlie Baron suggested a bridge (destroyed by Hurricane Katrina and repurposed as a fishing pier - <http://www.sttammanyfishingpier.com/index.php/about>). Could be a useful comparison to some lake-based observations made by DMI.
- Could the locations / times of observations be supplied more rapidly to allow timely generation of the MDB (EUMETSAT has a 1 month rolling archive of SLSTR data held online)? Maybe – some ships could be reporting locations within 24 hours, but not possible on others. Would need to agree a subset of the L2R format.

### CLOUD MASKING (CHRIS MERCHANT)

Objective is to share good practice for cloud masking methods and generate new ideas for improved cloud masking in GHRSSST products. Current priority areas are over-flagging of frontal features and coastal zone cloud detection.

- Co-operation with Feature Fidelity Task Team (F2T2) including joint meeting.
- Over flagging frequently occurs in frontal regions due to the use of IR spatial variability tests (these can also trigger due to instrument issues like stripe noise).
- Daytime only solution would be to disable IR variability tests and rely on Vis/NIR instead.
- Cloud and fronts can be distinguished in imagery by human experts – so can we use the larger scale context to automatically classify, or unflag frontal pixels? (see F2T2 for more details).
- Coastal zones are difficult for several reasons: clear-sky reflectance is higher (turbidity and bottom reflectance), high thermal spatial variability, land contamination.

- An SLSTR-specific issue due to the different Vis/NIR and IR resolutions means that the two are not co-registered.

Discussion:

- How will this information on over-flagging / unflagging be communicated to users? This is not a simple question, unlikely to be a single final approach suitable for all instruments. Different instruments may require different approaches. Objective is to investigate and share best practices.
- Cloud (or “bad-pixel”) masking is still a major problem in use of SST data. Over flagging is not only an issue for frontal regions but can also affect larger areas (cold core eddies, upwelling regions etc.) in some products. At the same time, under flagging (or failure to detect clouds) remains an issue.
- Systematic cloud masking failures, particularly masking of colder waters is an issue for climate studies.
- What about the use of machine learning methods? ML-methods have potential and are used in some cases. Physically based methods still have the advantage of being based on our understanding of the physics, so would prefer to combine these with further information on the large-scale context.
- Stripping is actually a calibration issue (not a retrieval or cloud detection). However, it is still a masking problem from the user perspective. There are methods to de-stripe images without addressing the underlying calibration.

### **SSES AND L4 (ANDY HARRIS)**

Current objective of the task team is to understand the different L2/3 SSES methodologies in use

- Requesting updated L2/3 SSES methodologies from data providers.
- Aim to start investigating impact of SSES methods in L4 data production with experiments to be defined in an intersessional virtual meeting.
- Showed example of ACSPO SSES method. Applying ACSPO SSES bias converts SST from “simple” linear regression to piece-wise regression (PWR – Petrenko et al. 2016).

Discussion:

- What is the difference between SSES and uncertainties? The SSES are a bias and standard deviation relative to in situ measurements. The ACSPO SSES bias can be added to the retrieval to give a different retrieval with reduced standard deviation but also reducing diurnal warming amplitudes (reduced sensitivity). These SSES is a measure of discrepancy between two datasets so incorporates different effects and does not provide an estimate of the uncertainty.
- Algorithms which are trained against in situ (both simple linear retrieval and PWR as used in ACSPO SSES) will always suppress the diurnal cycle as the cycle is weaker in in situ buoy measurements.
- What about other SSES schemes? These are all different and need to be documented on the GHRSSST website.

## HIGH LATITUDE SST (MIKE STEELE)

The high latitude task team is focussing on polar regions to provide consistent retrievals for both SST and IST.

- Surface can be sea-ice so should be retrieving IST. However, IST is very noisy as it is actually a mixture of both snow and ice and snow is very spatially variable. So, we need many more in situ observations.
- Presented comparison of L4 and two saildrones sent into the Arctic during 2019.
- Polar atmospheres are very dry so use of spatial averaging to reduce instrument (nedt) noise.
- Can real time Saildrone SST & SSS be used to avoid ice edge? No – see Chiodi et al. 2021.
- Plans for coming year: coordinate in situ observation collection, improve dry atmosphere corrections, coordination of ocean and ice fields (what SST field does an ice product use, what ice fields does a SST product use etc.)

### Discussion:

- Agree that improved communication between sea-ice and SST producers is very important.
- Should this group be working with other groups working on in situ sea ice. Yes – we want to work with groups like the IABP. Getting suitable in situ measurements is a challenge due to the conditions. DMI have put weather stations on the ice which had simple radiometers.
- Where can the Saildrone data be obtained? Validated and QC controlled data are available in netCDF format from PO.DAAC
- How reliable is the Saildrone skin SST? The skin temperature is problematic, the difference between skin and depth (CTD) measurements is very noisy and does not always follow expectations and maybe related to measurement of the sky radiance. This is still under investigation.
- Need to be aware that there is not a clean distinction between water and ice especially as the ice thins. The ice breaks into smaller fragments, so there will be both ice spreading into water pixels and islands of SST within an ice field.
- Is there any IST data in the Antarctic? Yes, there is the International Programme for Antarctic Buoys (IPAB), but data are far fewer than the Arctic.
- CIMR may improve knowledge in marginal ice zones too.
- EUMETSAT [TRUSTED](#) project is starting to think about FRM measurements in marginal and sea ice zones.

## REFERENCES

Chiodi, A. M. et al., **2021**, Exploring the Pacific Arctic Seasonal Ice Zone With Saildrone USVs, *Frontiers in Marine Science*, **8**, [doi:10.3389/fmars.2021.640697](https://doi.org/10.3389/fmars.2021.640697)

Petrenko, B., Ignatov, A., Kihai, Y., & Dash, P., **2016**, Sensor-Specific Error Statistics for SST in the Advanced Clear-Sky Processor for Oceans, *Journal of Atmospheric and Oceanic Technology*, **33**(2), 345-359. [doi:10.1175/JTECH-D-15-0166.1](https://doi.org/10.1175/JTECH-D-15-0166.1)

**TASK TEAM REPORTING 3**

**CLIMATOLOGY AND L4 INTERCOMPARISON**

**CORAL HEAT STRESS**

**USER SST REQUIREMENTS**

**HRSST FOR SATELLITE SST**

## TASK TEAM REPORTING 3 - SESSION REPORT

**Chair: Ioanna Karagali<sup>(1)</sup>, Rapporteur: Igor Tomazic<sup>(2)</sup>**

(1) DMI - Danish Meteorological Institute, Copenhagen-Ø, Denmark. Email: [ika@dmi.dk](mailto:ika@dmi.dk)

(2) EUMETSAT, Darmstadt, Germany, Email: [Igor.Tomazic@eumetsat.int](mailto:Igor.Tomazic@eumetsat.int)

The Task Team Reporting 3 session was held on Thursday 10th June 2021, between 13.00 and 14.30 UTC.

### RESOURCES

Link to recording available to participants: <https://training.eumetsat.int/mod/page/view.php?id=14678>

### INTRODUCTION

This report summarises the main points from the third session on reporting from the Task Teams (TT), which took place on Thursday June 10th using the online zoom platform, recording available using the link <https://training.eumetsat.int/mod/page/view.php?id=14678>. The three Task Teams (TT) scheduled were the GHRSSST Climatology and Inter-comparison TT, the Coral Heat Stress User SST Requirements TT and the HRSST for Satellite SST Validation TT. All presenters were given a 30-minute time slot, where 10 minutes were assigned to a summarising presentation and 20 minutes were allocated for discussion. Participants were able to directly ask questions to the presenters or post comments in the chat function. This report summarises the main points raised during the presentations along with the relevant comments during the discussion.

### GHRSSST CLIMATOLOGY AND INTER-COMPARISON TASK TEAM (ICTT, PRESENTER: HELEN BEGGS)

#### **Task 1: Inter-comparison of SST analysis for climate studies (led by Chunxue Yang, CNR/ISMAR)**

Contribution to C3S\_511 (C3S) project with plans for next phase.

Progress since last GHRSSST: a) using multi-product median SST, b) NOAA/NCEI daily OISSTv2.0 and Daily OISSTv2.1 replaced by NOAA/NCEP Monthly OISSTv2, c) added CMEMS OSTIA-based repro SST analysis, d) Yang et al. published paper in J. Climate comparing various long-term SST analyses for climate applications within C3S framework showing trends and recommended 8 products for climate applications.

#### **Task 2: Understand differences among SST analysis products and find ways for improvement (led by Xu Li, NOAA/NCEP)**

Ongoing, no new activities. - Suggested task 2.2 during GXXI to understand contribution (through assimilation, quality control or bias correction) of all types of in-situ SST data in operational SST analysis, no progress.

#### **Task 3: Feature inter-comparison of SST analysis (led by Jorge Vazquez, NASA/JPL)**

Status ongoing and active. –

Task 3.1: Validate L2, L3 and L4 SST gradients in variable regions using Saildrone SST data, status ongoing with several posters (Jorge and Marouan) presented.

Task 3.2.: produce on line visualisation tool for L4 SST gradients using OceanView from Prasanjit Dash, very powerful tool to show magnitude and length of SST gradients and profiler to see the values of SST gradients

Task 3.3: Develop the science to calculate SST fronts and compare, status ongoing; OceanView, based on the Sobel filter, include other L4 products, CMC, OSTIA, etc. and Saildrones.

Task 3.4: Validate SST gradients/fronts with other data, SSS, OC, SSH and altimetry currents, status ongoing, based on OceanView

Task 3.5: Compare feature resolution of various SST analysis (Jorge Vasquez), status ongoing. Concept is to explore methods other than spectral analysis to define resolution metric; focus on L4 products and check what features are persevered from L2.

Discussion:

- The methods used to define resolution metric in Task 3, are for all products or only for L4? Because if focus is on L2, the task should be part of the Feature Fidelity (FF) Task Team. But not if the focus is on climate related issues or long term trends, generally overlapping should be avoided.

Response: Focus was on L4, and L2 products, to understand how much resolution is preserved. Yet, the focus is to examine fronts over longer periods of time. Therefore there is an overlap with FF TT also with the work from Peter and Xavier on automatic extraction of SST anomalies which could be reused in this work with the focus of comparison between L4 and L2.

- It was pointed out that this task team seems related to the Feature Fidelity Task Team (F2T2), yet there were some further clarifications on this since F2T2 is looking at preservation of features in the SST L2 fields while if features that do appear in L2 are preserved in L4 is a different task - as the reasons for features failing to be represented in L2 are quite different to the reasons for them not appearing in L4. In summary, this TT focuses on L4 and how features are well preserved in L4 compared to L2. The general recommendation is to avoid adding too many tasks in the TT, but collaboration is OK.
- One VIIRS L2 snapshot is not the same as a 24-hours composite and it is not yet discussed how to resolve this in terms of metrics, and combine with tidal motion, and what can be resolved in 24h analysis. This is more important for near-shore regions due to tides, visible in geostationary data. Could be new activities for TT.
- Inter-comparison of SST gradients, if tasks 1 and 3 can be combined together. Within C3S has been discussed how to improve user engagement. For Task 3 the focus is also on Saildrones to have validation of SST gradients. For now only couple of years of data.
- -Many ship data available from sbe38 and thermosalinograph on science vessels going back to several years that could be used. Jorge is working together with Marouan and prof. Gomez on similar dataset but not examined carefully. (not clear the name of the institute and the name of the call 30:30)

### **CORAL HEAT STRESS USER SST REQUIREMENTS (PRESENTER: WILLIAM SKIRVING)**

The GHRSSST Coral Heat Stress Task Team (TT) was setup to provide expert advice to the community on satellite SST requirements for monitoring the effect of heat stress on coral health due to the importance of coral reefs as number one source of new medicines. Globally, between 0.5 and 1 billion people depend on healthy reefs, with a combined value of \$10 trillion per year. Climate change is a big problem due to increased temperature (satellite SST is important). There are other uses of satellite SST in coral reefs such as downscaling techniques, predicting outbreaks, reef restoration, using temperature range as indicator for different species. User Requirements should also be extended to novice users for understanding the use of satellite SST.

Summary of requirements:

L3 vs L4 SST: there is a need for continuous (gap-free) data, L4 is the main product of choice.

Diurnal variability vs daily average: becoming more important, with products providing daily min/max or full diurnal variation will be useful. Work on diurnal variability in coastal regions as it is challenging.

Radiometric accuracy/spatial resolution: accuracy of 0.2 K still applicable, for heat stress SST > 25 °C but for general coral use > 15 °C. Spatial resolution of 0.05 deg ok for now.

NRT vs reprocessed SST: there is a need for one continuous dataset, e.g. in OSTIA there is difference. If possible to combine both reprocessed and NRT into single dataset.

Regional analysis: reefs are smaller than the pixel scale, which is a mix of different classes of water in and around the reefs. Use other parametrizations on bathymetry, tides, winds and solar radiation to improve estimate of the reef temperature and combine with the use of high resolution SST (e.g. Landsat). Could be improved through reprocessed SST data with improved spatial resolution.

New categories added:

- Need for the preservation of oceanographic features such as upwelling, fronts, currents, eddies. Maybe combine L2 and L4 products to achieve better understanding of such features.
- Measure effective spatial resolution: need for “transparency” regarding the effective spatial resolution of products. The majority of coral reef users expect that mentioned grid resolution is also the effective resolution and that the information from the gridded pixel comes from the satellite measurement. Suggestion to include information in the product about the effective spatial and temporal resolution and conditions that can degrade them.

Discussion:

- The importance to accurately describe differences between grid and feature resolution is clear, e.g. the MUR SST product consists of different effective resolutions.
- The tasks for the next 12 months focus on extending the requirements to include all marine organisms and all oceans, including high latitude and Polar Regions and include Polar Watch NOAA, thus effectively extending the TT with other members.
- BoM has HRPT data over the Antarctic/Southern Ocean from mid 90s, reprocessed and archived, but still patchy. Such data should ideally be turned to L4.
- Are the requirements for satellite SST community feasible, e.g. one consistent, high resolution product with reprocessed and NRT. One size fits all will not work, e.g. example for feature resolution between L2 and L4. What is important is to produce range of products. They are using blended product, but there is always limitation.
- ECOSTRESS, is on the Space Station thus overpasses happen at all times of day with repeat intervals from sub-daily and up to ~5 days. Although primarily a terrestrial mission, ECOSTRESS does capture ocean scenes and can be a source of higher resolution SST (compared to Landsat). Temperatures are generated for both land and water surfaces in all scenes. Coverage can be found using [search.earthdata.nasa.gov](https://search.earthdata.nasa.gov) and there will be plenty of interest in the marine biological community for expanding access to GHRSSST products at higher latitudes.
- It was pointed out that only models, i.e. GFD with forcing and observational input, can provide data that continually resolve at the grid scale. “New” focus, in the context of this task team, should be given in resolving ocean eddies, fronts, upwelling dynamics using SST and other satellite products as current products are daily and are spatial and temporal averages thus smaller scale oceanographic processes aren't well resolved.

### **HIGH RESOLUTION SST FOR SATELLITE SST VALIDATION (PRESENTER: GARY CORLETT)**

The HRSST Task Team (TT) is new and refers to in situ data. GHRSSST and JCOMM DBCP established a project to define standards for SST measurements from drifting buoys - known as HRSST (maybe the name is not the best as it only differs from GHRSSST by 1 letter - open question on a better name). Currently, the majority of buoys are HRSST compliant. TT aim is to analyse the quality and performance of current drifter network with focus on HRSST, revise HRSST specifications and propose initial standards for Fiducial Reference Measurement (FRM) drifters, add traceability to SI. The main work is related to the TRUSTED project, there is access to the TRUSTED Matchup Data Base (MDB) and information while T1 and T2 are of main/initial focus.

Task1: Initial assessment of current drifters.

- Most drifters are HRSST-2, with SST accuracy below 0.05K, reporting to 0.01 K + HRSST-1 + reduced uncertainty below 0.05 K.
- HRSST-1: position accuracy to 0.01 deg.
- Clarification between HRSST vs FRM: drifter metadata important source for assessment. AOML metadata used to have deployment data, manufactured, type, drogue-off.
- Small difference between Non-HRSST and HRSST, similar coverage and statistics, still with larger robust standard deviation in the order of 0.2 K, but not on the expected order of 0.05 K.
- Analysis between drogues off and on: no change, positive results with the current results.
- Separating by manufacturer does not show significant difference, but for some manufacturers there is limited number of matchups.

- Separating by drifter type shows bigger differences likely due to the campaigns and number of measurements.
- Suggestion to keep only couple of drifter types with the highest number of measurements.

Task 2: propose uncertainty model

Status: Recently started, led by Chris Merchant, from climate perspective look at the uncertainty of the drifter ensemble.

Other tasks:

- Task 3: Self quality control of the data.
- Task 4: revise HRSST specification.
- Task 5: propose initial FRP specification.

Discussion:

GDP proposed the minimal list of metadata, e.g. date of production and deployment is important to understand shelf time due to the degradation.

Open discussion on additional metadata:

- SST sensor depth (also for other measured variables - although sensor depth is referring to the nominal depth when the sensor is manufactured, not the actual depth), pre-launch calibration date and method (could be related to SST calibration traceability), spatial bounds of deployment, drogue depth, parameter to add network to simplify extraction of network (programme identification).
- An issue with drifters is biofouling, as it will make them sink while rate of accumulation is difficult to predict. Nonetheless, it is not yet clear if the life time of the drifters is an issue or not. To be investigated in the future.
- In summary, most drifters conform to HRSST-2, as it is going through NOAA GDP defined initial classification, iridium drifters but not from DBI (only as calibration, not confirmed). There is an ongoing revision together with the GDP community to select several drifter types with metadata availability.
- Points raised during the discussion:
- At the Bureau of Meteorology it has been found that the only way to identify HRSST drifters on the GTS is to check if they have higher resolution data in the data record; this is very frustrating. Nonetheless, it was pointed out that metadata can be used, if transmitted through Iridium but not through DBI manufacturer. The source of metadata is an open question, and AOML currently have this information, and work in progress with GDP to provide better sources. Currently it is not operational, and in the future should be together with the data. Important to clarify that HRSST drifters are subset of all drifters available in GTS, and TRUSTED drifters are subset of HRSST drifters.
- Pressure sensors from TRUSTED, yet not possible to see the impact in the analysis, although for calm seas with no wind it should be possible. The nominal drifter mean measurement depth is 20 cm, but it could depend on the manufacturer. It can be added in metadata. Still difficult to know actual depth in the ocean.
- Beyond NOAA GDP there are many more drifters with temperature sensors being deployed. So some effort needs to be made to ingest these extra initiatives into the GTS.
- MOAA/NCEI ICOADS team collects GTS on daily basis, and produce BUFR+TAC merged dataset.
- Regarding TRUSTED, from the workshop it was reported that most drifters from 2015 have 0.05 K accuracy. Three-way analysis (and 0.2 K accuracy) could be revised in the future and perform the split between intrinsic accuracy of the drifters and point-space issues.
- The standard deviation for SLSTR is below 0.2 K and the retrieval is the limiting factor. To achieve the 0.05 K accuracy, retrievals with the lowest uncertainty and high quality are required. The drifter network is improved and the point-space issue should be covered in MDB TT.

**TASK TEAM REPORTING 4**  
**REGIONAL AND GLOBAL TASK SHARING**

## TASK TEAM REPORTING 4 - SESSION REPORT

**Huai-Min Zhang (Session Chair)**<sup>(1)</sup>, **Alexander Ignatov (Session Rapporteur)**<sup>(2)</sup>, **Jean-François Piollé (TT Chair)**<sup>(3)</sup>

- (1) US NOAA National Centers for Environmental Information, Asheville, NC, USA,  
Email: [huai-min.zhang@noaa.gov](mailto:huai-min.zhang@noaa.gov)
- (2) US NOAA Center for Satellite Applications and Research, College Park, MD, USA,  
Email: [alex.ignatov@noaa.gov](mailto:alex.ignatov@noaa.gov)
- (3) Ifremer, Brest, France, Email: [Jean.Francois.Piolle@ifremer.fr](mailto:Jean.Francois.Piolle@ifremer.fr)

The Task Team Reporting 4 session was held on Friday 11th June 2021, between 13.00 and 13.30 UTC as a zoom video call (link to recording available to participants:

### RESOURCES

Link to recording available to participants: <https://training.eumetsat.int/mod/page/view.php?id=14678>

### INTRODUCTION

This document reports the presentation and discussions of the Task Team Report, Session 4, “GHRSSST Regional/Global Task Sharing” (R/G TS).

### EXTENDED ABSTRACTS

The Task Team Chair, Jean-François Piollé, gave a [14-slide presentation](#) of about 20 minutes, reviewing the last year’s activities and outlining planned works for next year, followed by discussions of about 10 minutes.

During the last year, active TT members/participants were: Jean-François Piollé (Ifremer), Ed Armstrong (NASA PO.DAAC), Wen-Hao Li (NASA PO.DAAC), Yongsheng Zhang (NOAA/NCEI), Huai-Min Zhang (NOAA/NCEI), and Korak Saha (NOAA/NCEI). Last year’s major activities and progresses included:

#### **Specifying and releasing the new R/G TS framework- Supporting its implementation**

Specifically, the TT held semi-regular teleconference meetings; refined the R/G TS’s data discovery, search and access system; conducted pilot project demonstrating the central catalogue and federated query system based on OpenSearch; released [system architecture document](#); conducted survey of DACs and producers on [R/G TS readiness](#); updated list of DAC and GDP contacts; defined content of central catalogue’s dataset metadata profile; secured Copernicus/EUMETSAT funding for the R/G TS Central Catalogue and Inventory Search service (OpenSearch); and started TS system implementation.

In summary and looking forward to next year, activities include the following:

- Implementation of central catalogue and federated OpenSearch service is now on its way and will be completed by next GHRSSST workshop
- Engagement of GHRSSST data producers will start early next year to populate and update the GHRSSST catalogue
- Engagement of GHRSSST DACs will start this year to interconnect the existing open-search endpoints
- Challenge for the next two years is to have a comprehensive GHRSSST catalogue and all DACs interconnected





**GHRSSST**  
GROUP FOR HIGH RESOLUTION  
SEA SURFACE TEMPERATURE

The GHRSSST Project Office is funded by the European Union Copernicus Programme and is hosted by the Danish Meteorological Institute, Lyngbyvej 100, 2100 Copenhagen (DK)

E-mail:

Chiara Bearzotti, Project Coordinator, [gpc@ghrsst.org](mailto:gpc@ghrsst.org)

Pia Wind, Project Administrator, [gpa@ghrsst.org](mailto:gpa@ghrsst.org)



Follow us on Twitter: <https://twitter.com/ghrsst>

Website: <https://www.ghrsst.org/>

Zenodo: <https://zenodo.org/communities/ghrsst>

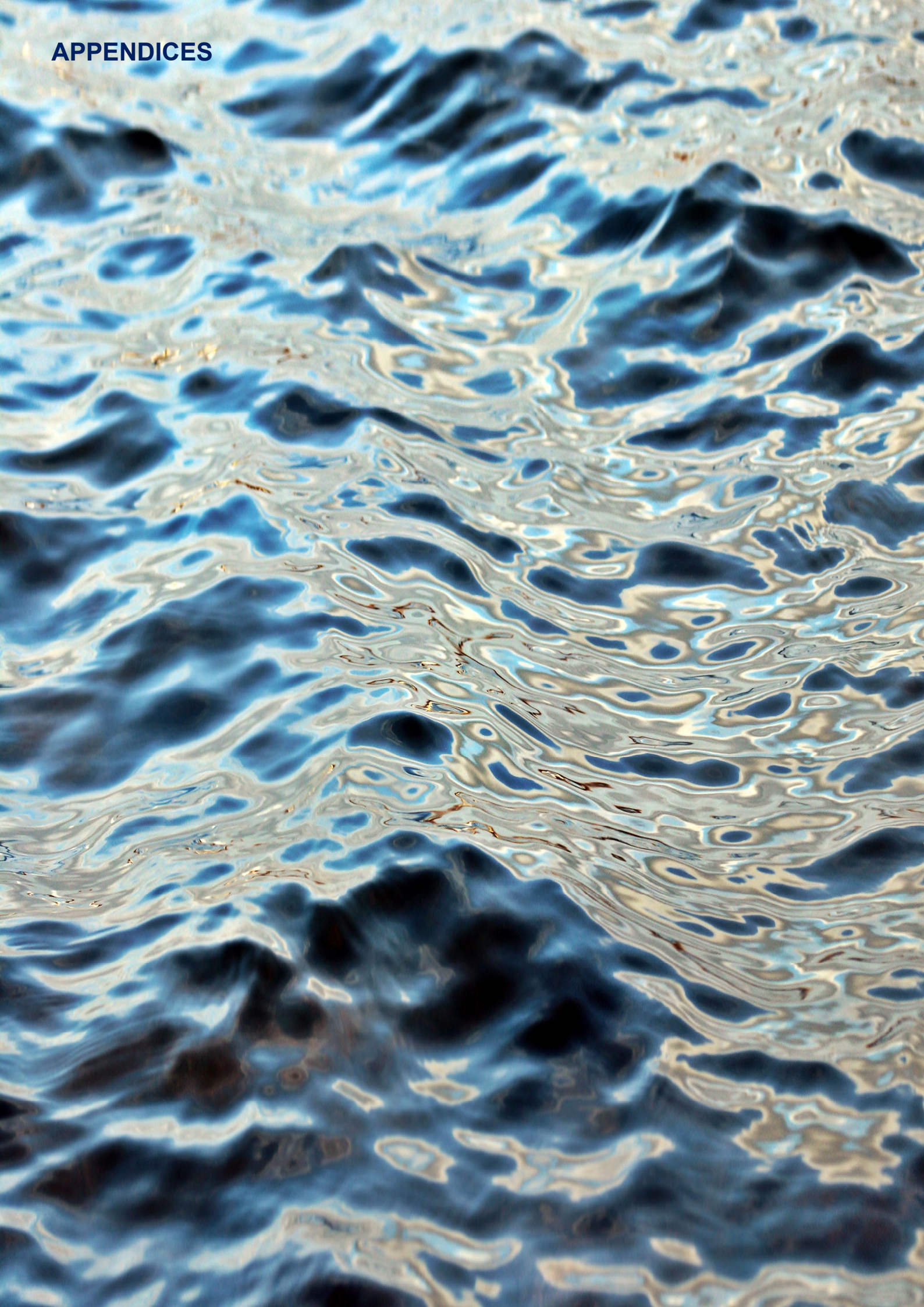


**Copyright 2021© Group for High Resolution Sea Surface Temperature (GHRSSST)**

This report has been edited by the GHRSSST Project Office.

This copyright notice applies only to the overall collection of papers: authors retain their individual rights and should be contacted directly for permission to use their material separately. Editorial correspondence and requests for permission to publish, reproduce or translate this publication in part or in whole should be addressed to the GHRSSST Project Office. The papers included comprise the proceedings of the meeting and reflect the authors' opinions and are published as presented. Their inclusion in this publication does not necessarily constitute endorsement by GHRSSST or the co-organisers.

# APPENDICES



## Agenda

LIVE SESSION	
Monday	<p><b>GXXII Welcome: Welcome and Logistics</b>            Chair: Anne O'Carroll            Rapporteur: Karen Veal</p>
	<p><b>Task Team Reporting 1</b>  <b>Climate Data Assessment Framework</b>  <b>GHRSSST MDB</b>  <b>Feature Resolution</b>            Chair: Werenfrid Wimmer            Rapporteur: Rosalia Santoleri</p>
	<p><b>Remembering Tim Liu</b>            Led by Jorge Vazquez            All welcome</p>
Tuesday	<p><b>Task Team Reporting 2</b>  <b>Shipborne Radiometry</b>  <b>Cloud masking</b>  <b>SSES and L4</b>  <b>High Latitude SST</b>            Chair: Owen Embury            Rapporteur: Jean-François Piollé</p>
Wednesday	<p><b>GHRSSST Priorities (Panel discussions)</b>            Chair: Anne O'Carroll            Rapporteur: Gary Corlett</p>
Thursday	<p><b>Task Team Reporting 3</b>  <b>Climatology and L4 Intercomparison</b>  <b>Coral Heat Stress User SST Requirements</b>  <b>HRSST for Satellite SST</b>            Chair: Ioanna Karagali            Rapporteur: Igor Tomazic</p>
Friday	<p><b>Task Team Reporting 4</b>  <b>Regional and Global Task Sharing</b>            Chair: Huai-min Zhang            Rapporteur: Alex Ignatov</p>
	<p><b>Closing Session</b>            Report from the GHRSSST Advisory Council – Igor Tomazic            Task Team Planning, Review of actions and A.O.B.,            Closing Remarks.            Close of Meeting            Chair: Anne O'Carroll            Rapporteur: Karen Veal</p>

<b>SCIENCE SESSIONS - ORAL AND POSTER PRESENTATIONS</b>	
<b>Science Session 1: Challenging Regions: The Coastal Margin and The Arctic</b>	
Chair: Andy Harris	
Rapporteur: Steinar Eastwood	
S1-ORAL PRESENTATIONS	
S1-1-ID-034 - Introducing the ISRO-CNES TRISHNA mission for high resolution SST observations in coastal ocean and continental waters	Emmanuelle Autret
S1-2-ID-012 - SST at 70-m scale from ecostress on the space station: application to complex coasts and intertidal flats	David S.Wethey
S1-3-ID-040 - Development of consistent surface temperature retrieval algorithms for the sea surface, marginal ice zone and sea ice in the polar regions	Jacob Høyer
S1-4-ID-025 - Status and plans for the sea-ice concentration data records from the EUMETSAT OSI SAF and ESA CCI: possibilities for polar SST products	Thomas Lavergne
S1-POSTER PRESENTATIONS	
S1-P1-ID-013 - Ultra high-resolution SST from NASA ECOSTRESS resolves fine structure of upwelling zones	Nicolás Weidberg
S1-P2-ID-021 - Validation of satellite sea surface temperatures and long-term trends in Korean coastal regions (1982–2018)	Kyung-Ae Park
S1-P3-ID-039 - A CMEMS level 4 SST and IST climate data set for the Arctic	Pia Nielsen-Englyst
S1-P4-ID-006 - Using Saildrones to Validate Sea Surface Temperatures in the Arctic	Jorge Vazquez
<b>Science Session 2: Applying The Data: Spatio-temporal Variation; Extreme Events</b>	
Chair: Gary Wick	
Rapporteur: Christo Whittle	
S2-ORAL PRESENTATIONS	
S2-1-ID-046 - Detection and Characterisation of Marine Heat Waves in the Mediterranean Sea in the past 40 years	Francesca E Leonelli
S2-2-ID-036 - Deep Learning of Sea Surface Temperature Patterns to Identify Ocean Extremes	J. Xavier Prochaska
S2-3-ID-038 - Instrument Noise, Retrieval Issues or Geophysical Signal?	Peter Cornillon

S2-4-ID-028 - Studying the thermal skin layer using thermofluorescent dyes	Peter Minnett
<b>S2-POSTER PRESENTATIONS</b>	
S2-P1-ID-041 - The NOAA STAR SOCD OceanView (OV): An application for integrated visualization of satellite, in situ, and model data & ocean events – the v1.0 release	Prasanjit Dash
S2-P2-ID-015 - The intermittency of Sea Surface Temperature: a global perspective	Jordi Isern-Fontanet
S2-P3-ID-022 - Is there a need for yet another model to account for SST diurnal variability?	Ioanna Karagali
S2-P4-ID-020 - Observations of Infrared SST Autonomous Radiometer (ISAR) Skin Temperatures in the Seas around Korean Peninsula, Indian Ocean, and Northwest Pacific	Kyung-ae Park
S2-P5-ID-037 - Revealing Fundamental SST Patterns with Deep Learning	J. Xavier Prochaska
<p><b>Science Session 3: Calibration, Validation and Product Assessment</b></p> <p>Chair: Sandra Castro</p> <p>Rapporteur: Yukio Kurihara</p>	
<b>S3-ORAL PRESENTATIONS</b>	
S3-1-ID-042 - Uncertainty validation of shipborne radiometers	Werenfrid Wimmer
S3-2-ID-009 - A completeness and complementarity analysis of the data sources in iQuam	Haifeng Zhang
S3-3-ID-001 - Saharan dust effects on North Atlantic sea surface skin temperatures	Bingkun Luo
S3-4-ID-048 - Use of ESA CCI SST analysis to validate sampling and measurement error models for SST from ships	Alexey Kaplan
<b>S3-POSTER PRESENTATIONS</b>	
S3-P1-ID-003 - Evaluation of AIRS and CrIS SST measurements relative to three globally gridded SST products between 2013 and 2019	Jorge Vazquez
S3-P2-ID-004 - Assessment and intercomparison of NOAA Daily Optimum Interpolation Sea Surface Temperature (DOISST), version 2.1	Boyin Huang
S3-P3-ID-032 - Using SAILDRONE Campaigns to assess the accuracy of SST gradients in Level 2 SST datasets	Marouan Bouali
S3-P4-ID-035 - EUMETSAT SLSTR SST multi-mission matchup database: ongoing work, TRUSTED MDB and evolutions	Igor Tomazic
S3-P5-ID-019 - Validation of SGLI SST	Yukio Kurihara

<b>Science Session 4: Algorithms</b>	
Chair: Jacob Hoeyer	
Rapporteur: Simon Good	
S4-ORAL PRESENTATIONS	
S4-1-ID-018 - Optimal Estimation of SST from INSAT-3D/3DR Imagers	Rishi K Gangwar
S4-2-ID-033 - A New Operational Mediterranean Diurnal Optimally Interpolated SST Product within the Copernicus Marine Service	Andrea Pisano
S4-3-ID-014 - Bias-aware optimal estimation for sea surface temperatures from historic AVHRRs	Chris Merchant
S4-4-ID-027 - Developments towards a 40-year climate data record from the ESA Climate Change Initiative	Owen Embury
S4-POSTER PRESENTATIONS	
S4-P1-ID-045 - Open source algorithms for AMSR3	Chelle Gentemann
S4-P2-ID-008 - Historical and Near-real Time SST retrievals from Metop AVHRR FRAC with ACSPO 1	Victor Pryamitsyn
S4-P3-ID-030 - USE of ERA-5 Sea Surface Temperature Fields as prior in Optimal Estimation retrieval of SST from MODIS	Goshka Szczodrak
S4-P4-ID-029 - Towards Improved ACSPO Clear-Sky Mask for SST from Geostationary Satellites	Alexander Semenov
S4-P5-ID-047 - Bayesian Cloud Detection Scheme improvements for the SLSTR instrument	Claire Bulgin
<b>Science Session 5: Computing and Products</b>	
Chair: Prasanjit Dash	
Rapporteur: Chunxue Yang	
S5-ORAL PRESENTATIONS	
S5-1-ID-044 - Science Storms the Cloud	Chelle Gentemann
S5-2-ID-024 - Analysis Ready Data applications for GHRSSST and related data	Ed Armstrong
S5-3-ID-016 - PODAAC milestone: GHRSSST data migrating to AWS Cloud	Wen-Hao Li
S5-4-ID-026 - The Sea Surface Temperature analysis in the NCEP GFS and the future NCEP UFS	Xu Li
S5-5-ID-010 - First Evaluation of the Diurnal Cycle in the ACSPO Global Super-Collated SST from Low Earth Orbiting Satellites (L3S-LEO)	Olafur Jonasson
S5-POSTER PRESENTATIONS	

S5-P1-ID-011 - Towards ACSPO Super-Collated Gridded SST Product from Multiple Geostationary Satellites (L3S-GEO)	Lars Hunger
S5-P2-ID-023 - Use of ESA SST CCI data in HadISST2	John Kennedy
S5-P3-ID-017 - Himawari-8 and Multi-sensor sea surface temperature products and their applications	Pallavi Govekar
S5-P4-ID-031 - Recent Updates Of CMC SST Analysis	Dorina Surcel-Colan
S5-P5-ID-005 - Copernicus Sentinel-3 SLSTR Sea (and sea-Ice) Surface Temperature: product status, evolutions and projects	Anne O'Carroll
S5-P6-ID-043 - Updates of AMSR3 on GOSAT-GW and its Ocean Products	Misako Kachi
S5-P7-ID-002 - Presenting a new high-resolution Climate Data Record product	Mark Worsfold
S5-P8-ID-007 - Filtering cold outliers in NOAA AVHRR SST for ACSPO GAC RAN2	Boris Petrenko
<b>AGENCY NEWS</b>	
<i>Agency reporting will be by slide deck and online forum</i>	
Chair: Toshiyuki Sakurai	
Rapporteur: Dorina Surcel-Colan	
GHRSSST connections with CEOS SST-VC (slide presentation)	
Ed Armstrong and Christo Whittle	

---

**List of participants**

First name	Surname	Email address
Melanie	Abecassis	melanie.abecassis@noaa.gov
Aida	Alvera Azcarate	a.alvera@ulg.ac.be
Ed	Armstrong	edward.m.armstrong@jpl.nasa.gov
Emmanuelle	Autret	emmanuelle.autret@ifremer.fr
Sheekela	Baker-Yeboah	Sheekela.Baker-Yeboah@noaa.gov
Charlie	Barron	charlie.barron@nrlssc.navy.mil
Chiara	Bearzotti	chb@dmi.dk
Helen	Beggs	helen.beggs@bom.gov.au
Marouan	Bouali	marouanbouali@gmail.com
Silvia	Bragaglia-Pike	gpa@ghrsst.org
Dominique	Briand	dominique.briand@ifremer.fr
Claire	Bulgin	c.e.bulgin@reading.ac.uk
Bruno	Buongiorno Nardelli	bruno.buongiornonardelli@cnr.it
Danielle	Carpenter	danielle.carpenter@navy.mil
Matthew	Carr	matt@saeon.ac.za
James	Carton	carton@atmos.umd.edu
Kenneth	Casey	kenneth.casey@noaa.gov
Sandra	Castro	sandrac@colorado.edu
Jean-François	Cayula	jf_cayula@yahoo.com
Julio	Ceniceros	julio.ceniceros@noaa.gov
T. Mike	Chin	mike.chin@jpl.nasa.gov
Daniele	Ciani	daniele.ciani@artov.ismar.cnr.it
Gary	Corlett	gary.corlett@eumetsat.int
Peter	Cornillon	pcornillon@me.com
Peng	Cui	cuipeng@cma.gov.cn
Prasanjit	Dash	prasanjit.dash@noaa.gov
Yuanxu	Dong	Yuanxu.Dong@uea.ac.uk
Craig	Donlon	craig.donlon@esa.int
Steinar	Eastwood	s.eastwood@met.no
Owen	Embury	o.embury@reading.ac.uk
William (Bill)	Emery	emery@colorado.edu
Claudia	Fanelli	claudia.fanelli@artov.ismar.cnr.it
Bertrand	Forestier	bertrand.forestier@gmail.com

First name	Surname	Email address
Rishi Kumar	Gangwar	rgphybhu@gmail.com
Chelle	Gentemann	cgentemann@gmail.com
Irina	Gladkova	irina.gladkova@gmail.com
Cristina	Gonzalez-Haro	cgharo@icm.csic.es
Simon	Good	simon.good@metoffice.gov.uk
Pallavi	Govekar	pallavi.govekar@bom.gov.au
Chris	Griffin	pe_chris@hotmail.com
Lei	Guan	leiguan@ouc.edu.cn
Andrew	Harris	andy.harris@noaa.gov
Jacob	Hoeyer	jlh@dmi.dk
Yuwei	Hu	yuwei.hu2@student.adfa.edu.au
Boyin	Huang	boyin.huang@noaa.gov
Lars	Hunger	lars.hunger@noaa.gov
Alexander	Ignatov	alex.ignatov@noaa.gov
Jordi	Isern-Fontanet	jiser@icm.csic.es
Andrew	Jessup	jessup@uw.edu
Chong	Jia	cxj363@miami.edu
Olafur	Jonasson	olafur.jonasson@noaa.gov
Misako	Kachi	kachi.misako@jaxa.jp
Alexey	Kaplan	alexeyk@ldeo.columbia.edu
Ioanna	Karagali	ika@dmi.dk
Hugh	Kelliher	hugh.kelliher@spaceconnexions.com
John	Kennedy	john.kennedy@metoffice.gov.uk
Hee-Young	Kim	heeyoungkim@snu.ac.kr
Fumiaki	Kobashi	kobashi@kaiyodai.ac.jp
Yukio	Kurihara	ykuri.kiyo@gmail.com
Veronica	Lance	veronica.lance@noaa.gov
Martin	Lange	martin.lange@dwd.de
Albert	Larson	albertl@uri.edu
Thomas	Lavergne	thomas.lavergne@met.no
Arrow	Lee	arrow.lee@stfc.ac.uk
Eun-Young	Lee	eunyounglee@snu.ac.kr
Francesca Elisa	Leonelli	francesca.leonelli@artov.ismar.cnr.it
Ninghui	Li	925966258@qq.com
Wen-Hao	Li	wenhaoli@jpl.nasa.gov

First name	Surname	Email address
Xu	Li	xu.li@noaa.gov
Zhuomin	Li	lizhuomin@stu.ouc.edu.cn
Michelle	Little	michelle.c.little1@navy.mil
Bailu	Liu	bailu_0126@163.com
Chunying	Liu	chunying.liu@noaa.gov
Gang	Liu	gang.liu@noaa.gov
Mingkun	Liu	liumingkun@ouc.edu.cn
Bingkun	Luo	lbk@rsmas.miami.edu
Gaston	Manta	gastonmanta@gmail.com
Justino	Martinez	justino@icm.csic.es
Salvatore	Marullo	salvatore.marullo@enea.it
Eileen	Maturi	eileen.maturi@noaa.gov
Jackie	May	jackie.may@nrlssc.navy.mil
Niall	McCarroll	n.f.mccarroll@reading.ac.uk
Bruce	McKenzie	bruce.mckenzie@navy.mil
Christopher	Merchant	c.j.merchant@reading.ac.uk
Peter	Minnett	pminnett@rsmas.miami.edu
Jonathan	Mittaz	j.mittaz@reading.ac.uk
Kohei	Mizobata	kmizobata@gmail.com
Nolwenn	Nano-Ascione	nolwenn.nano-ascione@meteo.fr
Pia	Nielsen-Englyst	pne@dmi.dk
Tim	Nightingale	tim.nightingale@stfc.ac.uk
Estelle	Obligis	estelle.obligis@eumetsat.int
Anne	O'Carroll	anne.ocarroll@eumetsat.int
Keiichi	Ohara	ohara.keiichi@jaxa.jp
Ana	Oliveira	ana.oliveira@colabatlantic.com
Françoise	Orain	francoise.orain@meteo.fr
Pierdomenico	Paolino	ppaolino@gmail.com
Kyung-Ae	Park	kapark@snu.ac.kr
Francisco	Pastor	paco@ceam.es
Boris	Petrenko	boris.petrenko@noaa.gov
Gabriela	Pilo	gabriela.semolinipilo@csiro.au
Sam	Pimentel	sam.pimentel@twu.ca
Jean-François	Piollé	jfpiolle@ifremer.fr
Andrea	Pisano	andrea.pisano@cnr.it

First name	Surname	Email address
Caroline	Poulsen	caroline.poulsen@bom.gov.au
J. Xavier	Prochaska	jxp@ucsc.edu
Victor	Pryamitsyn	victor.pryamitsyn@noaa.gov
Louise	Ruchon	louise.ruchon@ensta-paris.fr
Korak	Saha	korak.saha@noaa.gov
Toshiyuki	Sakurai	tsakurai@met.kishou.go.jp
Rosalia	Santoleri	rosalia.santoleri@cnr.it
Stéphane	Saux Picart	stephane.sauxpicart@meteo.fr
Alexander V	Semenov	alexvladsemenov@gmail.com
Sergey	Skachko	sergey.skachko@canada.ca
William	Skirving	william.skirving@noaa.gov
Blake	Spady	blake.spady@reefsense.com.au
Michael	Steele	mas@apl.washington.edu
Craig	Steinberg	c.steinberg@aims.gov.au
Susan	Sun	susan.sun@metoffice.gov.uk
Dorina	Surcel Colan	dorina.surcel-colan@canada.ca
Goshka	Szczodrak	gszczodrak@miami.edu
Pradeep	Thapliyal	pkthapliyal@gmail.com
Igor	Tomazic	igor.tomazic@eumetsat.int
Jorge	Vazquez	jorge.vazquez@jpl.nasa.gov
Karen	Veal	klv3@le.ac.uk
Sujuan	Wang	wangsj@cma.gov.cn
Brian	Ward	bward@nuigalway.ie
Katharine	Weathers	katharine.weathers@perspecta.com
Nicolas	Weidberg	j_weidberg@hotmail.com
David	Wethey	wethey@biol.sc.edu
Christo Peter	Whittle	cwhittle@csir.co.za
Gary	Wick	gary.a.wick@noaa.gov
Ruth	Wilson	ruth.wilson@spaceconnexions.com
Werenfrid	Wimmer	w.wimmer@soton.ac.uk
Pia	Wind	pwi@dmi.dk
Hye-Jin	Woo	hyejinwoo@snu.ac.kr
Mark	Worsfold	mark.worsfold@metoffice.gov.uk
Chunxue	Yang	chunxue.yang@cnr.it
Haifeng	Zhang	haifeng.zhang@noaa.gov

<b>First name</b>	<b>Surname</b>	<b>Email address</b>
Huaimin	Zhang	huai-min.zhang@noaa.gov
Yongsheng	Zhang	yongsheng.zhang@noaa.gov
Xuepeng	Zhao	Xuepeng.Zhao@NOAA.gov

## Group photo

The link to view the Padlet is: <https://padlet.com/TrainingEUMETSAT/29pc7csqqw17d8ki>

If you participated in the meeting and did not yet add your photo, you can still do so by accessing the Padlet and clicking on the pink blob (with a plus sign) at the bottom of the screen on the right (see below).



## Science team members 2021-22

O'Carroll	Anne	(Chair) EUMETSAT, Darmstadt, Germany
Armstrong	Ed	NASA JPL PO.DAAC, USA
Barron	Charlie	US Naval Research Laboratory, Stennis Center, USA
Beggs	Helen	Bureau of Meteorology, Melbourne, Australia
Bouali	Maouan	Institute of Oceanography of the University of Sao Paulo, Brazil
Casey	Kenneth S	NOAA/NESDIS NODC, USA
Castro	Sandra	University of Colorado, Boulder, USA
Cayula	Jean-François	Vencore, Inc, Stennis Space Center, Mississippi, USA
Chin	Mike	NASA JPL, USA
Cipollini	Paolo	ESA ESTEC, Noordwijk, The Netherlands
Clayson	Carol Anne	WHOI, USA
Corlett	Gary	EUMETSAT, Darmstadt, Germany
Cornillon	Peter	University of Rhode Island, USA
Dash	Prasanjit	NOAA, USA
Donlon	Craig J	European Space Agency, The Netherlands
Eastwood	Steinar	Met.no, Norway
Embury	Owen	University of Reading, UK
Gentemann	Chelle	Earth and Space Research, USA
Good	Simon	Met Office, UK
Guan	Lei	Ocean University of China, China
Harris	Andrew	NOAA/NESDIS ORA, USA
Høyer	Jacob	Danish Meteorological Institute, Denmark
Huan	Boyin	NCEI, NOAA, USA
Ignatov	Alexander	NOAA/NESDIS/STAR, USA
Kachi	Misako	Japan Aerospace Exploration Agency (JAXA), Japan

Kaplan	Alexey	Columbia University, USA
Karagali	Ioanna	Technical University of Denmark, Denmark
Kurihara	Yukio	Japan Aerospace Exploration Agency (JAXA), Japan
Luo	Bingkun	Columbia University, LDEO, USA
Mao	Chongyan	Met Office, UK
Marullo	Salvatore	ENEA, Italy
Maturi	Eileen	NOAA/NESDIS/STAR/SOCD/MECB, USA
May	Jackie	US Naval Research Laboratory, Stennis Center, USA
Merchant	Christopher	University of Reading, UK
Minnett	Peter	RSMAS, University of Miami, USA
Mittaz	Jonathan	University of Reading, UK
Nightingale	Tim	Rutherford Appleton Laboratory, UK
Park	Kyung-Ae	Seoul National University, Korea
Piollé	Jean-François	IFREMER, France
Santoleri	Rosalia	ARTOV.ISAC.CNR, Italy
Saux Picart	Stéphane	Météo-France, France
Surcel Colan	Dorina	CMC - Environment Canada
Thapliyal	Pradeep	Indian Space Research Organisation (ISRO)
Tomazic	Igor	EUMESTAT, Darmstadt, Germany
Vazquez	Jorge	NASA JPL PO.DAAC, USA
Wang	Sujuan	National Satellite Meteorological Center, Met Adm, China
Whittle	Christo	CISR, South Africa
Wick	Gary	NOAA/OAR/PSL, USA
Wimmer	Werenfrid	University of Southampton, UK
Yang	Chunxue	ISMAR-CNR, Italy
Zhang	Huai-min	NOAA National Center for Environmental Information, USA

**Credits pictures**

Cover page: Hermann Richter, Pixabay

Session 1 cover picture: by Mynzman, Pixabay

Session 2 cover picture: by Goubik, Pixabay

Session 3 cover picture: by Stux, Pixabay

Session 4 cover picture: by Gerd Altman, Pixabay

Session 5 cover picture: by Felix Mittermeier, Pixabay



**GHRSSST**  
GROUP FOR HIGH RESOLUTION  
SEA SURFACE TEMPERATURE

The GHRSSST Project Office is funded by the European Union Copernicus Programme and is hosted by the Danish Meteorological Institute, Lyngbyvej 100, 2100 Copenhagen (DK)

E-mail:

Chiara Bearzotti, Project Coordinator, [gpc@ghrsst.org](mailto:gpc@ghrsst.org)

Pia Wind, Project Administrator, [gpa@ghrsst.org](mailto:gpa@ghrsst.org)



Follow us on Twitter: <https://twitter.com/ghrsst>

Website: <https://www.ghrsst.org/>

Zenodo: <https://zenodo.org/communities/ghrsst>



**Copyright 2021© Group for High Resolution Sea Surface Temperature (GHRSSST)**

This report has been edited by the GHRSSST Project Office.

This copyright notice applies only to the overall collection of papers: authors retain their individual rights and should be contacted directly for permission to use their material separately. Editorial correspondence and requests for permission to publish, reproduce or translate this publication in part or in whole should be addressed to the GHRSSST Project Office. The papers included comprise the proceedings of the meeting and reflect the authors' opinions and are published as presented. Their inclusion in this publication does not necessarily constitute endorsement by GHRSSST or the co-organisers.